

**Characterization of the polo-like kinase, Cdc5p, and its influence on mitosis
and morphogenesis in *Candida albicans***

Amandeep K. Randhawa Glory

A Thesis
in
The Department
of
Biology

Presented in Partial Fulfillment of the Requirements
For the Degree of Doctorate of Philosophy at
Concordia University,
Montreal, Quebec, Canada

July 2016

©Amandeep Glory, 2016

CONCORDIA UNIVERSITY
School of Graduate Studies

This is to certify that the thesis prepared

By: Amandeep Kaur Randhawa Glory

Entitled: Characterization of the polo-like kinase Cdc5p and its influence on mitosis and morphogenesis in *Candida albicans*

and submitted in partial fulfillment of the requirements for the degree of

DOCTOR OF PHILOSOPHY (Biology)

complies with the regulations of the University and meets the accepted standards with respect to originality and quality.

Signed by the final examining committee:

_____	Joanne Turnbull	_____	Chair
_____	Culne Wu	_____	External Examiner
_____	Paul Joyce	_____	External to program
_____	Vladimir Titorenko	_____	Examiner
_____	William Zerges	_____	Examiner
_____	Catherine Bachewich	_____	Thesis Supervisor

Approved by _____ Patrick Gulick _____ Chair
Chair of Department or Graduate Program Director

____ July 27, 2016 _____
Date André Roy
Dean, Faculty of Arts and Science

Abstract

Characterization of the polo-like kinase Cdc5p and its influence on mitosis and morphogenesis in *Candida albicans*.

Amandeep Kaur Randhawa Glory, Ph.D.

Concordia University, 2016

Candida albicans is a commensal fungus in humans, but can cause infections with high mortality rates. Cell proliferation and differentiation between yeast and hyphae are important for virulence and survival in the host. An understanding of their regulation may reveal new targets for therapeutic strategies. My work aimed to elucidate the regulation of mitosis in *C. albicans*, a poorly understood process, and focussed on characterizing the roles of a Polo-like kinase (Plk), Cdc5p. Plks are critical regulators of many aspects of mitosis in diverse organisms. Previous work demonstrated that depleting Cdc5p in *C. albicans* yeast resulted in a block in spindle elongation and mitosis, followed by formation of filaments and expression of hyphal-specific virulence genes, under yeast growth conditions. However, the mechanisms underlying Cdc5p function, mitotic progression, formation of novel filaments and expression of virulence genes, remained unclear.

In order to address these questions, I first investigated a putative Cdc5p target, the Anaphase-Promoting Complex/Cyclosome (APC/C). In Chapter 2, I showed that APC/C co-activators Cdc20p and Cdh1p had some conservation in mitotic function, and may lie downstream of Cdc5p. However, additional novel features suggest variations in the mitotic circuitry.

I next investigated the identity of the Cdc5p-depleted filaments, since this was controversial. We hypothesized that the cells were elongated yeast buds that failed to switch from polar to isometric growth, but adapted a hyphal fate over time due to maintenance of polarized growth. In Chapter 3, time course assays demonstrated that hyphal-diagnostic features

emerged in Cdc5p-depleted filaments at only later growth stages, in agreement with our hypothesis. Our results expand on the strategies that *C. albicans* can utilize to modulate growth and virulence determinants.

I further addressed the mechanisms of Cdc5p function during mitosis and morphogenesis in Chapter 4 by screening for interacting factors. I discovered a novel, *Candida*-specific factor, *CP11* (*C. albicans* Plk-interacting protein), which was not essential for growth but required to maintain mitotic arrest and may interact with the spliceosome. Collectively, the work enhances our knowledge of mitotic regulation in *C. albicans*, and underscores variations in the regulatory circuitry that have important implications for controlling growth.

Acknowledgements

I would like to thank my supervisor Dr. Catherine Bachewich for her support, and guidance throughout my degree. Her enthusiasm, knowledge, never to give up attitude, positive and critical thinking, push for the results and unique way to get the answers of her questions from students is highly remarkable. I have gained a wealth of knowledge from her expertise. In these years, I have developed a special bonding with her in my professional as well as personal life. I would also like to thank the members of my committee, Dr. Vladimir Titorenko and Dr. William Zerges, for their valuable suggestions during the course of my graduate research.

I am grateful for the funding I have received during my graduate studies from Concordia University and NSERC. I would also like to extend my thanks to all the members of Biology department who were always ready to help with reagents, suggestions, instruments and microscopy. Many thanks to former and current lab mates Hao Haung, Amin Osmani, Yaolin Chen, Vinitha, and Samantha. I would like to thank Centre for Microscopy and Cell Imaging (CMCI) at Concordia University and Chloë van Oostende for her expert advice on microscopy.

I would like to dedicate my thesis to my deceased father, who would have been the happiest person on my achievement. I would also like to thank my beloved husband for his unconditional support, without which this day was not possible and my mother, who has always prayed for my success. They have always encouraged and stood by me. I would like to include new arrival in my life, my son Benay, who will get more playtimes with mommy after the defence!

Contribution of Authors

The chapters of this thesis are organized in the form of manuscripts for submission to peer-reviewed journals (see below). All research was performed under the supervision of Dr. Catherine Bachewich at Concordia University. Dr. Bachewich developed the research project concepts and outlines, analyzed experimental results, and prepared all manuscripts. I contributed to the planning and execution of experiments, analyses of data, and preparation of the manuscripts.

Chapter 1: Introduction

This chapter provides an overview of background information and outstanding questions that were subsequently addressed in Chapters 2-4. The writing was completed by Amandeep Glory, and edited by Dr. Bachewich. All figures were made by Amandeep Glory except Fig 1.6, which was taken from Whiteway and Bachewich, 2007 (copyright permission was not required).

Chapter 2 (published): Chou H*, Glory A*, Bachewich C. 2011. **Orthologues of the APC/C coactivators Cdc20p and Cdh1p are important for mitotic progression and morphogenesis in *Candida albicans*. *Eukaryotic Cell*. 2011; 10(5):696-709. *Authors contributed equally to this work.**

This chapter explored APC/C activity as a possible downstream effector of Cdc5p and in order to extend our understanding of the networks regulating mitosis in *C. albicans*. All biochemical and transcript experiments including Western blots, Northern blot and the construction of associated strains were performed by Amandeep Glory. This includes Figures 2.3, and 2.6 (A and B). Strains for cell phenotype experiments were made by Hsini Chou, while microscopy for the images were processed by Amandeep Glory. Dr. Bachewich contributed to the preparation of Figures 2.1, 2.2, 2.4, 2.5, 2.7 and 2.8 and cell quantification for Tables 2.2 to 2.5. Hsini Chou contributed in part to Figure 2.7 in this thesis, and Figure 8 and Table 5 in the published manuscript. Supplementary figures were prepared by Amandeep Glory and Dr. Bachewich.

Chapter 3 (in revision; proposed submission in March 2016): Glory A, Oostende C, Geitmann A, and Bachewich C. **Depletion of the mitotic kinase Cdc5p in *C. albicans* results in the formation of elongated buds that switch to the hyphal fate over time in a Ume6p-dependent manner.**

This chapter explored the nature of the cells produced through Cdc5p depletion and the mechanisms underlying their formation and expression of hyphal-specific genes. Amandeep Glory conducted all the experiments except for the confocal microscopy imaging of Mlc1p-GFP (Fig. 3.2), which was performed by Chloë Oostende from Dr. Anja Geitmann's laboratory at the Plant Biology Research Institute (Botanical Garden), Department of Biological Sciences, Université de Montréal. All figures were prepared by Amandeep Glory and edited by Dr. Bachewich, except Figure 3.2, which was contributed by Chloë Oostende. All tables and supplementary figures were contributed by Amandeep Glory. Movie S1 was contributed by Chloë Oostende.

Chapter 4: Glory A, and Bachewich C. **Identification of a novel Polo-like kinase binding protein found specifically in the *Candida* genus of fungi that interacts with the spliceosome machinery.**

This chapter explored the interacting factors of Cdc5p using affinity purification and mass spectrometry. All of the experiments were performed by Amandeep Glory, except for the mass spectrometry analyses, which were completed by Éric Bonneil at the Proteomics Centre, Institute for Research in Immunology and Cancer, Université de Montréal. All figures, tables and supplementary data were prepared by Amandeep Glory, with editing by Dr. Bachewich.

Chapter 5: Summary

This chapter summarizes the main findings of the thesis, and provides implications for the work and future directions. The chapter was prepared by both Amandeep Glory and Dr. Bachewich.

Other contributions not included in this thesis:

1. Mogilevsky K, Glory A*, Bachewich C. 2012. **The Polo-Like Kinase PLKA in *Aspergillus nidulans* is not essential but plays important roles during vegetative growth and development.** *Eukaryotic Cell*. 2012 Feb;11(2):194-205.

Amandeep Glory completed bioinformatic and phylogeny analyses, contributed to the Northern blots and prepared associated sections of the Materials and Methods.

2. Hussein B, Huang H, Glory A, Osmani A, Kaminskyj S, Nantel A, and Bachewich C. **G1/S transcription factor orthologues Swi4p and Swi6p are important but not essential for cell proliferation and influence hyphal development in the fungal pathogen *Candida albicans*.** *Eukaryotic Cell*. 2011 Mar;10(3):384-97.

Amandeep Glory constructed numerous strains and performed microscopic analyses of phenotypes.

Table of Contents

List of Figures.....	xiv
List of Tables.....	xvii
List of Abbreviations.....	xix
Chapter 1.....	1
Ch. 1 Introduction.....	2
1.1 Eukaryotic Cell cycle.....	2
1.2 Mitosis.....	2
1.2.1 Overview.....	2
1.2.2 Regulation.....	3
a. Cyclin Dependent Kinase/Cyclin B.....	3
b. Anaphase Promoting Complex/Cyclosome.....	4
c. Cdc fourteen Early Anaphase Release and Mitotic Exit Network pathways.....	7
d. Polo like kinases.....	9
1.3 <i>Candida albicans</i>	12
1.3.1 Opportunistic fungal pathogen of humans.....	12
1.3.2 Virulence-determining trait: Cell differentiation.....	12
a. Cell types.....	12
b. Differentiation of hyphae: regulation by environmental signaling pathways....	15
c. Differentiation of hyphae: mechanisms regulating polarized growth.....	17
1.3.3 Virulence-determining trait: Cell proliferation.....	18
a. Cell cycle in <i>C. albicans</i> : Overview.....	18
b. Regulation of mitosis in <i>C. albicans</i>	18
c. The influence of a polo-like kinase, Cdc5p, on mitosis and a novel polarized growth response in <i>C. albicans</i>	19
1.4 Objectives.....	21
1.5 References.....	22
Chapter 2:	31
Ch 2: Orthologues of the APC/C coactivators Cdc20p and Cdh1p are important for mitotic progression and morphogenesis in <i>Candida albicans</i>	32

Abstract.....	33
2.1 Introduction.....	34
2.2 Materials and Methods.....	36
2.2.1 Strains, oligonucleotides, plasmids, culture conditions, RNA extraction.....	36
2.2.2 Strain construction.....	36
2.2.3 Cell staining, imaging.....	42
2.2.4 Protein extraction and Western blotting.....	43
2.2.5 Cell size measurements.....	44
2.3. Results.....	44
2.3.1 Depletion of Cdc20p results in highly polarized growth of yeast buds under yeast growth conditions.....	44
2.3.2 Cdc20p is required for early and late stages of nuclear division.....	47
2.3.3 Cdc20p-depleted cells express <i>HWP1</i> at later stages of growth.....	50
2.3.4 Cells lacking Cdh1p have a pleiotropic phenotype.....	51
2.3.5 Cdh1p is important, but not essential, for nuclear division and septation.....	54
2.3.6 Clb2p and Cdc5p are elevated in Cdc20p and Cdh1p-depleted cells.....	56
2.3.7 Absence of Cdh1p does not influence Cdc5p-depleted polarized growth.....	58
2.3.8 Cdc20p does not influence serum-induced hyphal growth, while Cdh1p has a moderate effect.....	58
2.4 Discussion.....	59
2.4.1 Cdc20p is important for the metaphase-to-anaphase transition and mitotic exit.....	59
2.4.2 Cdh1p influences mitotic exit but does not behave as a repressor of Start.....	60
2.4.3 Cdc20p and Cdh1p influence yeast morphogenesis and polar growth patterns.....	60
2.5 Acknowledgements.....	63
2.6 References.....	63
2.7 Supplementary data.....	69
Chapter 3:	71
Ch 3: Depletion of the mitotic kinase Cdc5p in <i>Candida albicans</i> results in the formation of elongated buds that switch to the hyphal fate over time in a Ume6p-dependent manner.....	72
Abstract.....	73
3.1 Introduction.....	74

3.2 Materials and Methods.....	77
3.2.1 Strains, oligonucleotides, plasmids and culture conditions.....	77
3.2.2 Strain Construction.....	82
3.2.3 Northern blotting.....	84
3.2.4 Protein extraction and Western blotting.....	84
3.2.5 Cell staining and imaging.....	85
3.3 Results.....	86
3.3.1 Enriched filipin staining is present in tips of Cdc5p-depleted filaments but also in incipient buds of yeast and pseudohyphae.....	86
3.1.2 The myosin light chain Mlc1p is localized in a hyphal-specific manner in a proportion of Cdc5p-depleted cells.....	90
3.1.3 The Cdc42p GAP Rga2p shows an increase in phosphorylation and decrease in abundance during later stages of Cdc5p depletion.....	95
3.1.4 A core regulator of hyphal growth, <i>UME6</i> , and other HSGs including <i>HGC1</i> and <i>HWPI</i> are induced in Cdc5p-depleted cells at or near hyphal-specific levels.....	96
3.1.5 Ume6p influences expression of <i>HWPI</i> and morphology of Cdc5p-depleted filaments at later stages of growth.....	98
3.1.6 Cdc5p-depleted cells do not require Hms1p for polarized growth or expression of <i>UME6</i> and <i>HWPI</i>	101
3.4 Discussion.....	103
3.4.1 Cdc5p-depleted cells are elongated buds during initial stages of polarized growth.....	103
3.4.2 Cdc5p-depleted cells may switch to the hyphal fate in a Ume6p-dependent manner.....	104
3.4.3 Induction of <i>UME6</i> in the absence of environmental cues or Hms1p suggests additional modes of regulation.....	106
3.5 Acknowledgements.....	107
3.6 References.....	107
3.7 Supplementary figures.....	112
Chapter 4:	118

Ch. 4: Identification of a novel polo-like kinase binding protein found specifically in the <i>Candida</i> genus of fungi that interacts with the spliesome machinery.....	119
Abstract.....	120
4.1 Introduction.....	121
4.2 Materials and Methods.....	125
4.2.1 Strains, oligonucleotides, plasmids and culture conditions.....	125
4.2.2 Composition of PCR reaction mixes for DNA constructs.....	129
4.2.3 Composition of PCR screening reaction mixes.....	129
4.2.4 Strain Construction.....	129
a. <i>CDC5-TAP</i>	129
b. <i>CDC5-MYC</i>	129
c. <i>ORF19.3714-HA</i>	130
d. <i>ORF19.3714-TAP</i>	130
e. <i>orf19.3714Δ/Δ</i>	131
f. Strains where <i>ORF19.3714</i> was reintroduced.....	132
4.2.5 PCR screening.....	133
4.2.6 Southern blotting	134
4.2.7 Northern blotting.....	134
4.2.8 Protein extraction and Western blotting.....	135
4.2.9 Co-Immuoprecipitation.....	135
4.2.10 One-step affinity purification for identification of phosphorylation sites.....	136
4.2.11 Two Step Affinity Purification.....	136
4.2.12 Plate growth assays.....	138
4.2.13 Cell staining and imaging.....	138
4.3 Results.....	139
4.3.1 Identification of Cdc5p-interacting factors reveal a previously uncharacterized protein, Orf19.3714p.....	139
4.3.2 Orf19.3714p is a fungal-specific protein found primarily in <i>Candida</i> species.....	147
4.3.3 Orf19.3714p is hyperphosphorylated in mitotic-arrested cells, and enriched in response to Cdc5p depletion, but reduced upon depletion of Cdc20p.....	151

4.3.4	<i>ORF19.3714</i> is not essential for yeast vegetative growth or required for yeast cellular responses to a variety of stress conditions.....	158
4.3.5	Orf19.3714p is not required for hyphal development, but influences filamentous growth in response to Cdc5p depletion.....	162
4.3.6	Identification of Orf19.3714p-interacting factors through affinity purification and mass spectrometry reveals spliceosome complex proteins.....	167
4.4	Discussion.....	178
4.4.1	Orf19.3714p is a novel interacting protein of Cdc5p.....	178
4.4.2	Orf19.3714p may be important for mitosis and mitotic checkpoints.....	179
4.4.3	Orf19.3714p may be associated with the spliceosome and potentially link Plk function to spliceosome activity.....	180
4.5	Acknowledgements.....	183
4.6	References.....	183
4.7	Supplementary data.....	193
Chapter 5:	199
Discussion:	200
5.1	The APC/C cofactors Cdc20p and Cdh1p employ conserved and novel mechanisms of action during mitosis and morphogenesis in <i>C. albicans</i> , and may mediate in part Cdc5p function....	200
5.2	Cdc5p-depleted filaments are elongated buds that transition to the hyphal fate over time in a Ume6p-dependent manner.	202
5.3	Orf19.3714p is a novel, <i>Candida</i> -specific Plk interacting factor that may be important for the mitotic checkpoints in <i>C. albicans</i>	204
5.4	Orf19.3714p is associated with the spliceosome and potentially links Plk function to RNA splicing.	205
5.5	Summary.....	206
5.6	References.....	207

List of Figures

Figure 1.1: Diagrammatic presentation for role of polo-like kinases in regulation of entry into M (mitosis) phase.....	4
Figure 1.2: Activation and targets of Anaphase Promoting Complex /Cyclosome in <i>S. cerevisiae</i>	6
Figure 1.3: Mitotic exit in <i>S. cerevisiae</i> involves release of Cdc14p through FEAR (Cdc14 Fourteen Early Anaphase Release) and MEN (Mitotic Exit Network) pathways.....	8
Figure 1.4: Functions of vertebrate Polo like kinase Plk1 in cell cycle.....	10
Figure 1.5: Polo-like kinases in cytokinesis.....	11
Figure 1.6: Different cell types of <i>C. albicans</i>	14
Figure 1.7: Environmental signaling pathways regulating the yeast-to-hyphal transition in <i>C. albicans</i>	16
Figure 1.8: The hyphal signaling pathways to maintain hyphal growth and cell-cell attachment in <i>C. albicans</i>	17
Figure 2.1: Depletion of Cdc20p results in filament formation under yeast growth conditions...45	45
Figure 2.2: Cdc20p depletion results in a delay in metaphase and telophase.....48	48
Figure 2.3: <i>HWPI</i> is expressed in Cdc20p-depleted cells at later stages of growth.....50	50
Figure 2.4: Cells lacking Cdh1p demonstrate a pleiotropic phenotype.....52	52
Figure 2.5: Absence of Cdh1p results in some defects in nuclear division and spindle formation.55	55
Figure 2.6: Clb2p and Cdc5p levels in cells lacking Cdc20p or Cdh1p.....57	57
Figure 2.7: Hyphal formation in the absence of Cdc20p or Cdh1p.....59	59
Figure S2.1: Cells depleted of Cdc20p lose viability by 24h.....69	69
Figure S2.2: Repression of <i>CDHI</i> results in a pleiotropic phenotype including some filamentous growth, while overexpression results in more moderate effects.....69	69
Figure S2.3: Length by width measurements of yeast form cells in the presence and absence of Cdh1p.....70	70
Figure 3.1: Tips of Cdc5p-depleted cells and young buds of yeast and pseudohyphae show enriched filipin staining, similar to hyphal tips.....88	88

Figure 3.2: Mlc1p-GFP localization in Cdc5p-depleted cells.....	92-93
Figure 3.3: Rga2p undergoes a phosphorylation-dependent shift in Cdc5p-depleted cells.....	96
Figure 3.4: <i>UME6</i> , <i>HWP1</i> and <i>HGCI</i> expression is induced at later time points of Cdc5p depletion.....	97
Figure 3.5: Absence of <i>UME6</i> or <i>HGCI</i> influences the shape and integrity of Cdc5p-depleted filaments at only later stages of growth.....	99
Figure 3.6: Expression levels of <i>HWP1</i> and <i>HGCI</i> are reduced in Cdc5p-depleted cells lacking <i>UME6</i>	100
Figure 3.7: Absence of <i>HMS1</i> does not prevent polarized growth or expression of <i>UME6</i> and <i>HWP1</i> in Cdc5p-depleted cells.....	102
Figure S3.1: PCR confirmation of <i>MLC1/MLC1-GFP-URA3</i> strains.....	112
Figure S3.2: Confirmation of <i>RGA2/RGA2-HA-URA3</i> strains.....	112
Figure S3.3: Rga2p-HA abundance in cells lacking vs. containing Cdc5p.....	113
Figure S3.4: Confirmation of strains lacking <i>UME6</i>	114
Figure S3.5: Confirmation of strains lacking <i>HGCI</i>	115
Figure S3.6: Propidium-iodide staining of cells lacking Cdc5p in different mutant backgrounds..	116
Figure S3.7: Confirmation of strains lacking <i>HMS1</i>	117
Figure 4.1: Confirmation of Cdc5p-TAP strains.....	140
Figure 4.2: Coomassie-stained gel of tandem affinity-purified Cdc5p and control samples.....	141
Figure 4.3: Confirmation of <i>ORF19.3714-HA</i> and <i>CDC5-MYC</i> strains.	143
Figure 4.4: Co-immunoprecipitation confirming an interaction between Cdc5p and Orf19.3714p.	146
Figure 4.5: Plk phosphorylation and Polo box domain-binding sites in Orf19.3714p, Cdc7p and Dbf4p from <i>C. albicans</i>	146
Figure 4.6: Neighbour-joining tree for Orf19.3714p using Clustal Omega.	150
Figure 4.7: Orf19.3714p undergoes a phosphorylation-dependent shift in Cdc5p-depleted cells..	151
Figure 4.8: Confirmation of Orf19.3714p-TAP strains.	153
Figure 4.9: Orf19.3714p-TAP is phosphorylated in Cdc20p and Cdc5p-depleted cells, and shows a decrease or increase in abundance, respectively.....	154

Figure 4.10: *ORF19.3714* does not show significant changes in expression during Cdc5p depletion, but is moderately reduced in serum-induced hyphae.....155

Figure 4.11: Identification of phosphorylated amino acids in Orf19.3714p in the presence and absence of Cdc5p.....158

Figure 4.12: Confirmation of an *orf19.3714Δ/Δ* and *ORF19.3714* complement strains.....159

Figure 4.13: Absence of Orf19.3714p does not influence yeast growth or morpholog.....160

Figure 4.14: Orf19. 3714p is not required for yeast growth responses to a variety of environmental and chemical conditions.....161

Figure 4.15: Orf19.3714p is not required for hyphal development under a variety of hyphae-inducing conditions.....164

Figure 4.16: Orf19.3714p is required for maintaining filamentous growth in mitotic-arrested cells depleted of Cdc5p, but not S-phase arrested cells treated with HU.....165-166

List of Tables

Table 2.1: <i>Candida albicans</i> strains used in this study.....	37
Table 2.2: Oligonucleotides used in this study.....	38-39
Table 2.3: Plasmids used in this study.....	40
Table 2.4: Number of nuclei and cell morphology in Cdc20p-depleted cells.....	46
Table 2.5: Spindle patterns in Cdc20p-depleted cells.....	49
Table 2.6: Proportion of <i>CDH1</i> -deleted cells exhibiting different morphologies.....	53
Table 3.1: Strains used in this study.....	78
Table 3.2: Oligonucleotides used in this study.....	79-81
Table 3.3: Plasmids used in this study.....	81
Table 3.4: Proportion (%) of different cell morphologies and corresponding frequency of tip-enriched filipin signal in different cell types.....	89
Table 3.5: Mlc1p-GFP localization patterns in cells depleted of Cdc5p.....	94
Table 4.1: Strains used in this study.....	126
Table 4.2: Oligonucleotides used in this study.....	127
Table 4.3: Plasmids used in this study.....	127
Table 4.4: Orbitrap LC/MS analysis of putative Cdc5p-interacting proteins in exponential-growing cells.....	142
Table 4.5: Orbitrap LC/MS analysis of putative Cdc5p-interacting proteins in cells blocked in mitosis.....	143
Table 4.6: Fungal Protein Blast (Blastp) search in Saccharomyces Genome Database (SGD) using Orf19.3714p.....	148
Table 4.7: Orbitrap LC/MS identification of phosphorylation sites in Orf19.3714p in the presence vs. absence of Cdc5p.....	157
Table 4.8: Orbitrap LC/MS analysis of putative Orf19.3714p-interacting proteins in exponentially growing cells.....	169-171
Table 4.9: Enriched functional categories of proteins that interact with Orf19.3714p.....	172-175
Table 4.10: Orbitrap LC/MS analysis of putative Orf19.3714p-interacting proteins in cells blocked in mitosis.....	176-177

Table S4.1: Spliceosomal proteins in *S. cerevisiae* and orthologs in *C. albicans*.....193
Table S4.2: Cdc5p interacting proteins in *S. cerevisiae* and orthologs in *C. albicans*.....196

List of abbreviations

APC/C	Anaphase Promoting Complex/Cyclosome
BLAST	Basic Local Alignment Search Tool
bp	base pair
BSA	Bovine Serum Albumin
CaCl ₂	Calcium Chloride
cAMP	Cyclic Adenosine Monophosphate
Cdc	Cell Division Cycle
CDK	Cyclin Dependent Kinase
CGD	Candida Genome Database
CIP	Calf Intestinal Phosphate
DAPI	4', 6' Diamidino-2-phenylindole dihydrochloride
DIC	Differential Interference Contrast
DIG	Digoxigenin
DNA	Deoxyribonucleic Acid
dNTPs	Deoxyribonucleotide Triphosphates
DTT	1,4-Dithiothreitol
<i>E. coli</i>	<i>Escherichia coli</i>
ECL	Enhanced Chemiluminescence
EDTA	Ethylenediaminetetraacetic Acid
EGTA	Ethylene Glycol Tetraacetic Acid
FBS	Fetal Bovine Serum
FEAR	Fourteen Early Anaphase Release
FSC	Forward Scatter
G1	Gap 1
G2	Gap 2
GAP	GTPase-Activating Protein
gDNA	Genomic DNA
GEF	Guanine Nucleotide Exchange Factor
GFP	Green Fluorescent Protein

GO	Gene Ontology
GTPase	Guanosine Triphosphatases
GUT	Gastrointestinally Induced Transition
h	Hour
H ₂ O ₂	Hydrogen Peroxide
HA	Hemagglutinin
HCl	Hydrogen Chloride
HIV	Human Immunodeficiency Virus
HSG(s)	Hyphal Specific Gene(s)
HU	Hydroxyurea
K ₂ HPO ₄	Potassium Phosphate Dibasic
kb	kilobase pair
kDa	Kilodaltons
L	Litre
LB	Lysogeny Broth
LC/MS	Liquid Chromatography/Mass Spectrometry
M	Mitosis
M	Molar
MAPK	Mitogen-Activated Protein Kinases
MC	Methionine Cysteine
MEN	Mitotic Exit Network
mg	Milligrams
Mg	Magnesium
MgCl ₂	Magnesium Chloride
min	Minutes
ml	Millilitres
mM	Millimolar
MMS	Methanomethy sulphate
MPF	Mitosis Promoting Factor
mRNA	Messenger RNA
MWM	Molecular Weight Marker

NaCl	Sodium Chloride
NCBI	National Centre for Biotechnology Information
ng	Nanogram
nm	Nanometers
nM	Nanomolar
NTC	NineTeen Complex
O.D.	Optical Density
PBD	Polo Box Domain
PCR	Polymerase Chain Reaction
PE	PIPES EGTA
PI	Propidium Iodide
PIPES	Piperazine-N,N'-Bis (2-Ethanesulfonic Acid)
Plk(s)	Polo-like kinase(s)
PVDF	Polyvinylidene Fluoride
rDNA	Ribosomal DNA
RES	Retention And Splicing
RNA	Ribonucleic Acid
RNA Pol	RNA Polymerase
RNP(s)	Ribonucleoprotein(s)
rRNA	Ribosomal RNA
S	Synthetic
s.e.m	Standard Error of the Mean
SAC	Spindle Assembly Checkpoint
SCF	Skp, Cullin, F-box
SD	Synthetic Medium with Dextrose
SDS	Sodium Dodecyl Sulphate
SDS	Sodium Dodecyl Sulphate Polyacrylamide Gel Electrophoresis
PAGE	
SGD	Saccharomyces Genome Database
SLAD	Synthetic Low Ammonium Dextrose
snRNP(s)	Small Nuclear Ribonucleoprotein(s)

SS	Synthetic Medium with Sodium Succinate
TAP	Tandem Affinity Purification
TBST	Tris Buffered Saline-Tween
TCA	Trichloroacetic Acid
TEV	Tobacco Etch Virus
TOR	Target Of Rapamycin
tRNA	Transfer RNA
VALAP	Vaseline:Lanolin:Paraffin
vs	Versus
X g	Gravity
YEPD	Yeast Extract, Peptone, Dextrose
μg	Micrograms
μl	Microlitres
μm	Micrometers
μM	Micromolar
%	Percent
°C	Degree Centigrade
3D	3 Dimensional

CHAPTER 1

Ch. 1: INTRODUCTION

1.1 The Eukaryotic Cell Cycle

The cell cycle comprises a series of events that allows duplication of genetic material and its separation into two daughter cells (1). In many eukaryotes, the cell cycle consists of interphase and mitosis (M), followed by cytokinesis. Interphase is further divided into G1 (Gap 1), S (synthetic) and G2 (Gap 2) sub-phases. The G1 and G2 phases are associated with cell growth in many organisms (2), while S-phase is associated with duplication of the genetic material. During mitosis, chromosomes are segregated into two daughter cells. Proper cell cycle progression is crucial for normal growth; and deregulation of this process can lead to cancer (3). The cell cycle is also coordinated with development. In systems ranging from yeast to humans, cells exit the cell cycle at particular stages in order to embark on a developmental pathway (4-7). It is thus important to have a comprehensive understanding of cell cycle circuitry and the mechanisms underlying its regulation. To this end, significant advances have been made from studies in the model yeast systems *Saccharomyces cerevisiae* and *Schizosaccharomyces pombe*. Many factors and processes associated with cell cycle progression in these organisms are conserved in humans (8, 9). However, organism with cell-type-specific features also exist (8), underscoring the complexity and evolutionary diversity in this fundamental biological process.

1.2 Mitosis

1.2.1 Overview

Mitosis is a complex multistep process consisting of four sub-phases, including prophase, metaphase, anaphase and telophase. In mammalian cells, prophase is characterized by nuclear envelope break down, chromatin condensation, and spindle formation. In metaphase, chromosomes align at the center of the cells, and are held by spindle microtubules. Sister chromatids start separating and move to opposite poles in anaphase. Finally, during telophase, chromosomes at the opposite poles uncoil and the nuclear envelope re-assembles (1). Similar features define mitotic stages in the model yeast *S. cerevisiae*, with the exception that the nuclear envelope does not fully break down, and spindle assembly is initiated earlier in S phase (10-12).

1.2.2 Regulation

a. Cyclin Dependent Kinase/Cyclin B

The regulation of mitosis is complex and involves transcriptional, post-transcriptional and post-translational mechanisms. One key regulator is Mitosis Promoting Factor (MPF). This consists of a Cyclin Dependent Kinase (CDK) associating with a mitotic cyclin. In *S. cerevisiae*, the CDK/Cyclin B complex consists of Cdc28p/Clb2p. A “Clb2” cluster of genes, which includes the B-type mitotic cyclin *CLB2*, are induced at the G2/M transition and are under control of the Mcm1p/Fkh2p/Ndd1p transcription factor complex (13). The Cdc28p/Clb2p complex is initially inactive due to inhibitory phosphorylation by the kinase Swe1p. However, when the phosphatase Mih1p removes the inhibitory phosphate, Cdc28p/Clb2p is activated and phosphorylates a number of targets to initiate entry into mitosis (Fig. 1.1), including Anaphase Promoting Complex/Cyclosome (APC/C) subunits (14) and factors required for spindle elongation (15), for example. Cdc28p/Clb2p must be down-regulated in part through targeted degradation of Clb2p in order for cells to exit mitosis (16). A similar situation exists in mammals, where Cyclin B associates with Cdk1 for entry into mitosis. Cdk1/CyclinB is initially inactive due to phosphorylation by Wee1 and Myt1 kinases, but dephosphorylation by Cdc25 phosphatase promotes M phase entry (Fig. 1.1). Once activated, Cdk1/CyclinB can boost its own activation by phosphorylating its regulatory kinases and phosphatases (17). Targets of Cdk1/CyclinB include proteins associated with the nuclear lamina and Golgi apparatus as well as factors required for spindle assembly, chromosome condensation and APC/C regulation (18, 19). Similar to the situation in yeast, the activity must be down-regulated for mitotic exit, which is achieved in part through targeted degradation of Clb2p (16).

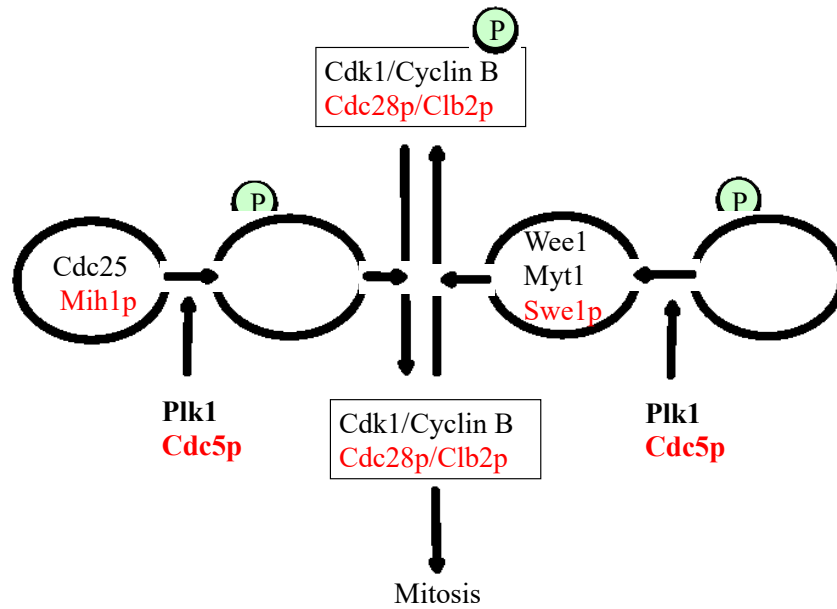


Figure 1.1: Diagrammatic presentation for role of polo-like kinases in regulation of entry into M (mitosis) phase. The polo like kinase Plk1 phosphorylates Cdc25 phosphatase, which in turn dephosphorylates Cdk1 in order to promote M phase. On the contrary, Plk1 can dephosphorylate Wee1, Myt1 kinases, which in turn phosphorylate Cdk1 to inhibit entry into M phase. *S. cerevisiae* orthologs are Cdc5p, Mih1p, Swe1p and Cdc28p/Clb2p for Plk1, Cdc25, Wee1/Myt1 and Cdk1/Cyclin B, respectively. Human proteins are shown in black while *S. cerevisiae* proteins are shown in red. Figure based on Archambault and Glover, 2009 (17).

b. Anaphase Promoting Complex/Cyclosome

Another key regulator of mitosis is the Anaphase Promoting Complex/Cyclosome (APC/C), which targets mitotic regulators for degradation, thus allowing mitotic progression and mitotic exit. The APC/C is an E3 ubiquitin ligase complex that targets degradation of proteins by addition of ubiquitin molecules. Ubiquitin is added to proteins by E1-E3 ligases.

Polyubiquitinated protein is then recognized by the 26S proteasome for degradation (20). In *S. cerevisiae*, the APC/C is activated by phosphorylation via CDK/CyclinB (21) (Fig 1.2A). It then requires association with co-activators, including Cdc20p and Cdh1p (22, 23). Initially, the APC/C is under control of Cdc20p, and APC/C^{Cdc20p} targets degradation of proteins associated with the metaphase-to-anaphase transition and mitotic exit (24, 25). A highly conserved Cdc20p target is Securin, or Pds1p in *S. cerevisiae*, which inhibits the enzyme Separase (Esp1p). Securin must be degraded in order for Separase to cleave Cohesin (Scc1p) and permit separation of chromosomes during the metaphase-to-anaphase transition (26) (Fig 1.2B).

The APC/C also targets a portion of mitotic cyclin Clb2p for degradation, thus initiating down-regulation of CDK/CyclinB activity that is necessary for mitotic exit. Towards the end of mitosis and during G1 phase, APC/C activity falls under control of the cofactor Cdh1p (Fig 1.2A). Cdh1p is held inactive by phosphorylation during most of the cell cycle. However, during late mitosis, inactivation of Cdc28p/Clb2p by APC/C^{Cdc20} as well as dephosphorylation of Cdh1p by the phosphatase Cdc14p leads to Cdh1p activation (23, 27). The APC/C^{Cdh1p} targets Cdc20p, the remainder of Clb2p and other factors for destruction, thus allowing exit from mitosis (22, 28) (Fig. 1.2B). There is strong conservation in APC/C cofactors, targets and function (24, 29, 30). Intriguingly, APC/C activity extends beyond mitotic cell cycle control (22, 31), as Cdc20p and Cdh1p function is also important for the stability of factors involved in developmental processes including axonal growth (32, 33) and maintaining the differentiated state of neurons in the mammalian brain (34).

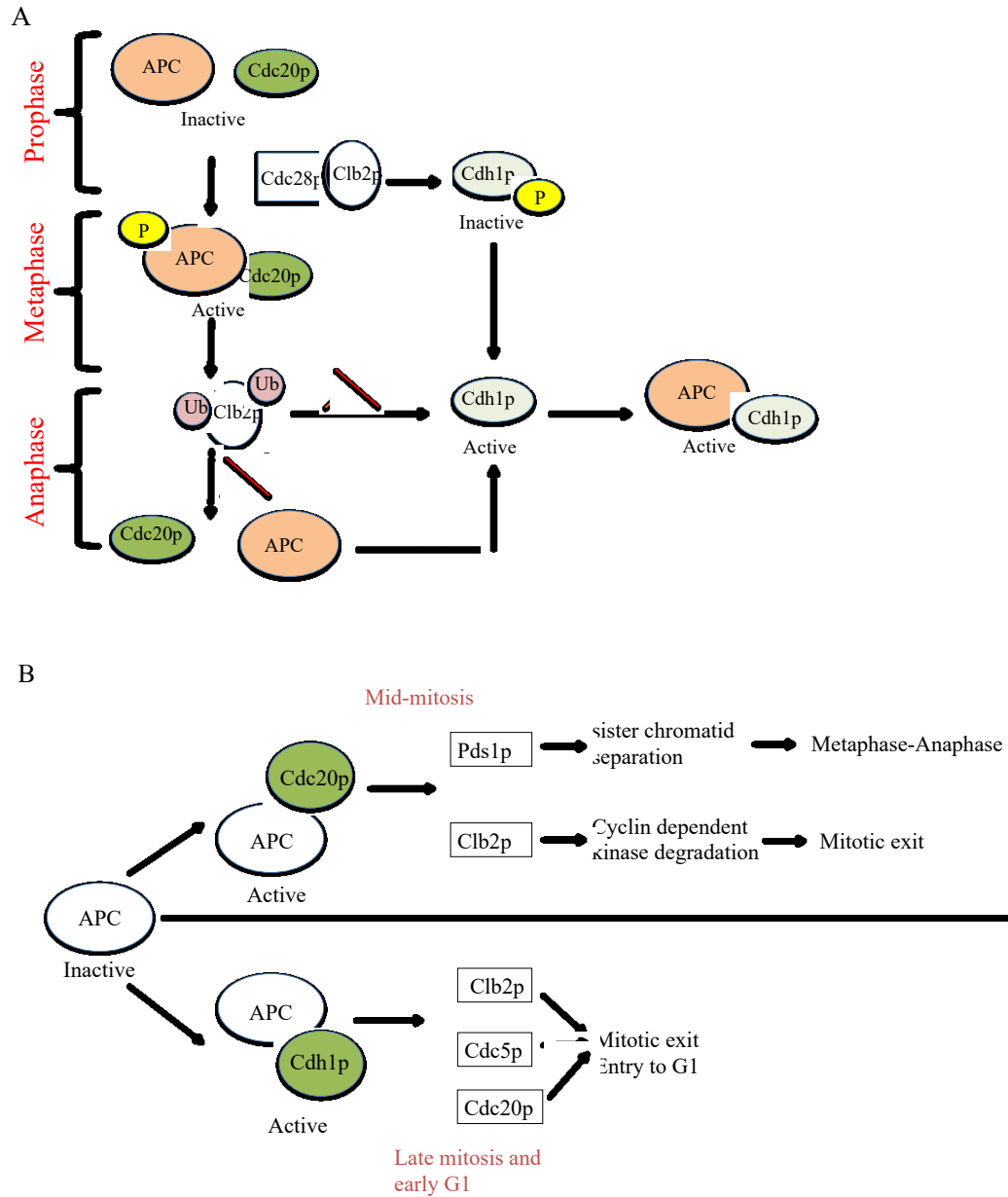


Figure 1.2: Activation and targets of Anaphase Promoting Complex /Cyclosome (APC/C) in *S. cerevisiae*. (A) During mid-mitosis (metaphase-anaphase), APC/C is phosphorylated by Cyclin dependent kinase/mitotic cyclin Cdc28p/Clb2p complex. Cdc20p binds and activates phosphorylated APC/C. Cdh1p is held inactive from mid G1 to late mitosis through phosphorylation. In late mitosis (anaphase-telophase) inhibitory phosphorylation of Cdh1p is removed due to degradation of Clb2p and it binds and thus activates APC/C. (B) During mid-mitosis, APC^{Cdc20p} targets degradation of securin Pds1p, for sister chromatid separation and mitotic cyclin Clb2p for mitotic exit. During late mitosis, APC^{Cdh1p} targets Cdc20p, polo like kinase Cdc5p and Clb2p for mitotic exit. Figure 2A is based on Castro *et al.*, 2005 (24).

c. Cdc Fourteen Early Anaphase Release and Mitotic Exit Network pathways

The Cdc Fourteen Early Anaphase Release (FEAR) pathway in *S. cerevisiae* is required for releasing the phosphatase Cdc14p from the nucleolus and mitotic exit (Fig. 1.3A). Prior to mitotic exit, Cdc14p remains sequestered in the nucleolus by Net1p. At the onset of anaphase, FEAR pathway components Esp1p, Slk19p, and Spo12p (35) (Fig. 1.3A) function to inactivate the phosphatase PP2A, which enhances phosphorylation of Net1p and contributes to release of Cdc14p from the nucleolus (36). The polo-like kinase Cdc5p is another FEAR component that directly interacts with Cdc14p and Esp1p and contributes to Cdc14p release at mid-mitosis (37, 38). A similar pathway has not been identified in mammals.

The Mitotic Exit Network pathway (MEN) consists of several components that ultimately permit the cell to exit mitosis (Fig. 1.3B). Within this pathway, Cdc5p acts to negatively regulate the GTPase-activating protein (GAP) complex Bub2p-Bfa1p. This in turn negatively regulates the Ras-like Tem1p GTPase. Tem1p is localized to the daughter spindle pole body and it is activated by Lte1p, a guanine nucleotide exchange factor (GEF) for Tem1p, once the daughter spindle pole enters the daughter cell. Tem1p activates a protein kinase signaling cascade including Cdc15p, Dbf2p and Mob1p, which functions to release the remaining Cdc14p phosphatase from the nucleolus (39). Cdc14p then dephosphorylates Sic1p, a CDK inhibitor, and Swi5p, a transcription factor for *SIC1*, resulting in down-regulation of Cdc28p/Clb2p activity. This is enhanced by Cdc14p-mediated dephosphorylation of the APC/C cofactor Cdh1p, which in turn targets the remaining Clb2p for degradation, resulting in mitotic exit (40). Inactivation of mitotic cyclins also allows the assembly of pre-replicative complexes for the next cell cycle (41). In mammals, the regulation of mitotic exit is not yet fully defined (42). Some MEN-like components exist, such as GAPCenA, a GTPase activating protein with homology to *S. cerevisiae* Bub2p (43) and Mob1 (44). While human Mob1 influences mitotic exit, the role of GAPCenA is not clear (45). Mammalian cells contain homologues of *CDC14*, but depletion does not lead to mitotic exit defects, and dephosphorylation of mitotic substrates is thought to rely on alternate phosphatases such as PP1 and PP2A (46).

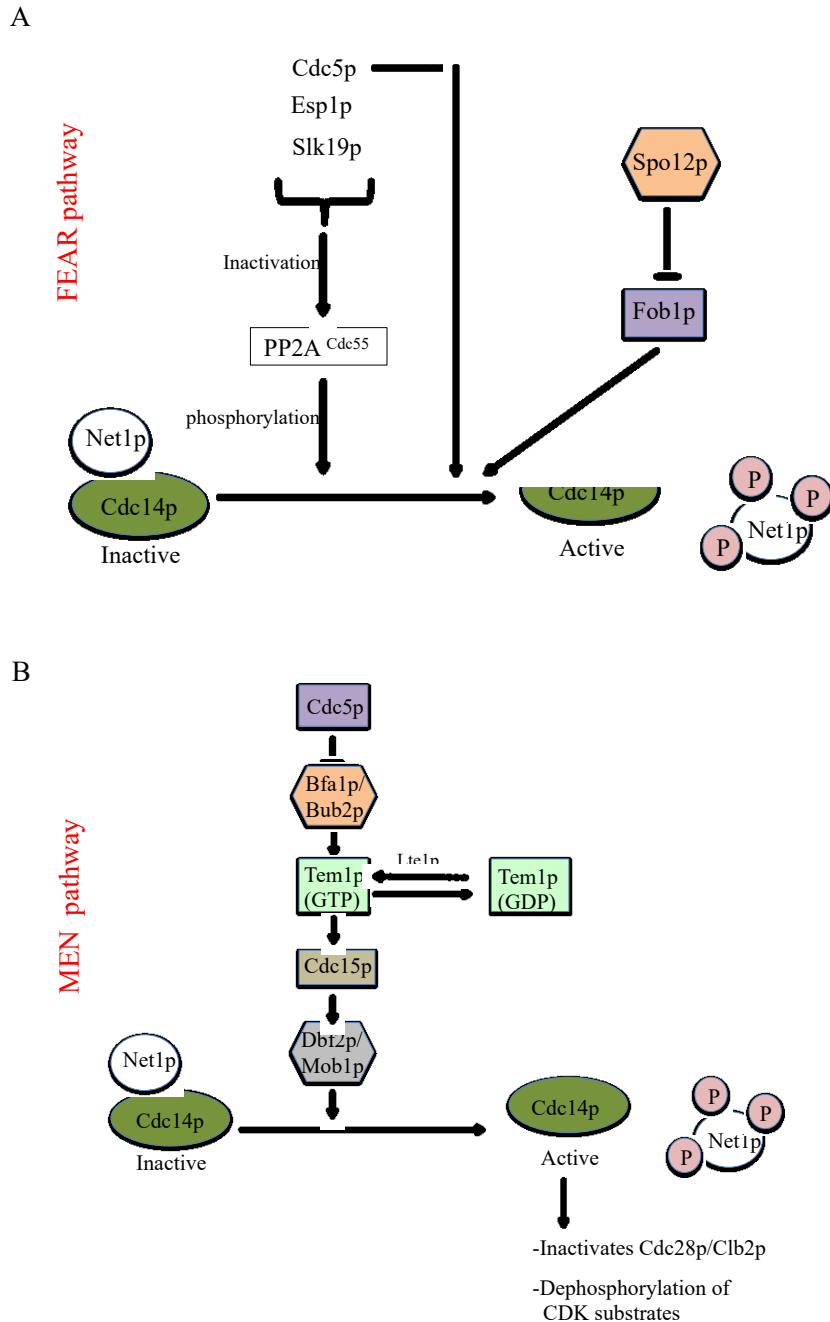


Figure 1.3: Mitotic exit in *S. cerevisiae* involves release of Cdc14p through FEAR (Cdc14 Fourteen Early Anaphase Release) and MEN (Mitotic Exit Network) pathways. Cdc14p is held inactive in the nucleolus by inhibitor Net1p. Once Net1p is phosphorylated, active Cdc14p is released from the nucleolus. Active Cdc14p inhibits cyclin dependent kinase activity to facilitate mitotic exit. (A) Cdc5p, separase Esp1p and spindle protein Slk19p inactivate phosphatase PP2A^{Cdc55}, leading to phosphorylation of Net1p. Net1p is also directly phosphorylated by Cdc5p. Nucleolar protein Spo12p inhibits FEAR inhibitor Fob1p. (B) Cdc5p inhibits GTPase activating protein complex Bfa1p/Bub2p. GTPase Tem1p is activated by guanine nucleotide exchange factor Lte1p. Active Tem1p activates Dbf2p/Mob1p complex through Cdc15p kinase, releasing Cdc14p from the nucleolus.

d. Polo-like kinases

Another important and conserved regulator of mitosis is the Polo-like kinase (Plk) family of serine/threonine kinases, including *Polo* in *Drosophila melanogaster*, *Cdc5p* in *S. cerevisiae*, *Plo1p* in *S. pombe*, *Plx1* in *Xenopus laevis* and *PLK1-5* in mammals, for example (17). Plks are defined by a kinase domain at the amino-terminus and a polo box domain (PBD) at the carboxyl terminus (47). The PBD typically contains two conserved polo boxes that function as a single unit for binding Plk targets that were previously primed via phosphorylation by CDKs or by Plks (48, 49). Plks also can interact with proteins in a phosphorylation-independent manner (50, 51). The kinase and PBD are separated by a linker domain that shows little sequence conservation but is important for localization in some cases (52).

Plks are important for many stages of mitosis, including mitotic entry, spindle formation and function, chromosome segregation, mitotic exit, as well as septation and cytokinesis (53, 54) (Fig. 1.4). For example, with respect to early mitotic events, *Cdc5p* in *S. cerevisiae* targets *Swel1p* for degradation via phosphorylation (55), leading to active *Cdc28p/C1b2p*, whereas in mammals, *PLK1* phosphorylates and activates *Cdc25C* phosphatase, leading to the G2/M transition (56) (Fig. 1.1). During spindle assembly and/or function, *Cdc5p* in *S. cerevisiae* influences microtubule growth and dynamics, and is required for the phosphorylation and proper modification of the spindle pole body components *Nud1p*, *Slk19p*, and *Stu2p* (57). However, spindles can form in the absence of *Cdc5p*. In contrast, *PLK1* from mammals is crucial for spindle formation; down-regulation results in monopolar and abnormal spindles (58). *PLK1* is also required for centrosome maturation and promotes microtubule kinetochore attachments through phosphorylation of *BubR1*, for example, and silences the spindle checkpoint until proper attachment is achieved (58, 59). *Plk1* also regulates microtubule-stabilizing proteins, such as *Asp*, for aster and spindle formation (60). During the metaphase-to-anaphase transition, Plks phosphorylate cohesin *Scc1* to permit chromosome segregation. For example, in *S. cerevisiae*, *Cdc5p* phosphorylation of *Scc1p* allows it to be further cleaved by *Separase* (61), resulting in sister chromatid separation. In mammals, *Scc1* and other cohesion subunit phosphorylation by *PLK1* results in a loosening of cohesion/chromatid associations, and the dissociation of cohesins from chromosome arms at prophase and prometaphase (62). During anaphase onset, the remaining cohesins around the centromeres are removed by *Separase* (63, 64). Other functions of

Plks during early mitosis include phosphorylating APC/C subunits, resulting in APC/C activation (65, 66). Cdc5p is also a component of the FEAR and MEN pathways described above (Fig. 1.3A).

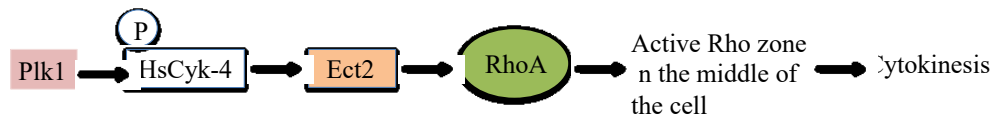
Cell cycle progression →

G2/M	Prophase	Metaphase	Anaphase	Telophase
-Mitotic entry and CDK activation	-Check-point recovery -Centrosome maturation	-Microtubule-kinetochore attachment -Spindle assembly checkpoint	-APC/C regulation -Spindle elongation -Sister chromatid separation	-Mitotic exit -Cleavage furrow formation

Figure 1.4: Functions of vertebrate Polo like kinase Plk1 in cell cycle. Plk1 regulates multiple aspects of mitosis from mitotic entry, to spindle assembly, spindle elongation, APC/C regulation, mitotic exit and cytokinesis.

During septation and cytokinesis, Plks function by phosphorylating regulators of Rho GTPases. For example, Cdc5p phosphorylates the Rho1p GEF proteins Tus1p and Rom2p, thereby recruiting and activating Rho1p locally at the bud neck to promote the formation of a contractile actin ring at the future division site (67). The polo box domain of Cdc5p also interacts with GAPs, including the Rho1p GAP Sac7p, which is involved in actin cytoskeleton organization, and the Cdc42p GAP Bem3p, a GTPase that controls establishment and maintenance of polarity and hence morphogenesis (67). Cdc5p inhibits Cdc42p activity during mitotic exit/cytokinesis, which is required for recruitment of cytokinetic proteins Iqg1p and Inn1p for normal septum formation (68). Similarly, PLK1 recruits the GEF Ect2p to the central spindle during anaphase that in turn allows accumulation of RhoA and assembly of the contractile ring (58, 69) (Fig. 1.5).

Homo sapiens:



Saccharomyces cerevisiae:

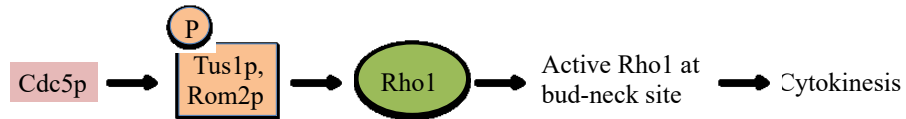


Figure 1.5: Polo-like kinases in cytokinesis. Human Plk1 and *S. cerevisiae* Cdc5p phosphorylate and activate Rho GAP or Rho GEF proteins, thereby recruiting and activating Rho locally at the middle of the cell or bud neck division site respectively to promote the formation of the contractile ring. Figure based on Petronczki *et al.*, 2008 (69).

Plks are regulated at many levels, although precise mechanisms remain elusive in many cases. *CDC5* and *PLK1* transcripts, for example, peak at the G2/M transition (70, 71), in part via the activity of forkhead transcription factors (13, 72, 73). At the post-translational level, Plks can be activated by phosphorylation in the T-loop of the kinase domain (17, 71) via Aurora kinases (74, 75) and others that remain elusive (76). Phosphorylation can also take place within the linker region. In *S. pombe*, for example, recovery from TOR (target of rapamycin) and MAPK (mitogen activated protein kinase)-dependent nutrient-induced mitotic arrest involves Plo1p phosphorylation in the linker region via the Aurora kinase Ark, leading to localization at the spindle pole bodies and mitotic entry (77). Plks can also be phosphorylated by CDK and STE20-like kinases (78, 79). Less is known about Plk dephosphorylation (17). At the level of protein stability, Plks like Cdc5p and PLK1 are ubiquitinated by APC/*C^{dhl}* and targeted for destruction during anaphase, while Plo1p is stable throughout the cell cycle (17, 80, 81). Plks are also regulated through dynamic localization, which is mediated in part by the PBD (82). Most Plks localize to the centrosome, chromatin, kinetochore, central spindle, and midbody. In yeast, they also localize to the spindle pole bodies, bud neck and medial ring (17, 83).

1.3 *Candida albicans*

1.3.1 Opportunistic fungal pathogen of humans

Candida albicans is one of the most common opportunistic fungal pathogens of humans. Although it exists as a commensal organism in the gastrointestinal or genitourinary tracts in healthy humans, an immunocompromised system can initiate pathogenesis (84, 85). *C. albicans* infections can be superficial, including oral thrush and vaginitis. However, in individuals undergoing cancer chemotherapy, organ transplant or containing HIV (86), systemic infections can occur, where *C. albicans* enters the bloodstream and invades organs such as the kidney, heart, and brain, for example (87). Candidemia, or invasive candidiasis, is the fourth most common cause of hospital-acquired infections (88, 89), associated with a 40% mortality rate, and resulted in annual Medicare costs exceeding \$1 billion in the United States alone (90). Current treatments for *C. albicans* infections include a limited number of azole, polyene, and echinocandin drugs. However, several of these have toxic side effects, and *C. albicans* is showing increasing drug resistance (91-93). Thus, there is a strong need to identify new drug targets and enhance the current repertoire of therapeutic strategies. To this end, a more comprehensive understanding of the biology of *C. albicans*, including factors that regulate growth and virulence is required.

1.3.2 Virulence determining trait: Cell differentiation

a. Cell types

One aspect of *C. albicans* biology that is important for virulence is its ability to differentiate into different cell types, including different classes of yeast, pseudohyphae, hyphae, and chlamydozoospores (94, 95) (Fig. 1.6). Yeast cells grow via budding that initiates at the G1/S transition of the cell cycle, and a ring of septins marks the future bud emergence site (Fig. 1.6). Initial bud outgrowth is polar and associated with a high concentration of actin patches, but switches to an isometric mode near mitosis, when the actin patches disperse evenly around the bud (96, 97). Tips of yeast buds also contain a polarisome, which regulates actin filament formation at growth sites (98, 99). Polarisome components, such as Spa2p, and Bud6p transiently localize to growing bud tips, then re-locate to the bud neck later in the cell cycle. Nuclear division takes place across the mother-bud neck, and cytokinesis follows the break down of the septin ring (100, 101). Yeast cells can be classified as white, opaque or GUT (gastrointestinally induced transition) cells (95, 102). White phase yeast cells are round to oval

in shape, and colonies appear creamy in color. In contrast, opaque yeast are elongated, bean-shaped cells with cell wall pimples that represent the mating-competent form of the organism, as they are homozygous at the mating-type locus. Meiosis has not been reported in *C. albicans*; mated tetraploids undergo mitotic recombination and subsequent chromosome loss to restore the normal diploid state (103). GUT cells resemble opaque cells except that they lack surface pimples and are adapted for commensal growth in the gut (102). Chlamydospores are thick walled cells formed at the tips of suspensor cells and their function in the host is not yet clear (95, 104) (Fig 1.6). Filamentous cells in *C. albicans* include pseudohyphae and hyphae.

Pseudohyphae are chains of elongated yeast cells with an extended G2 phase that do not separate after cytokinesis, and show constrictions at septation sites (101, 105). They also contain septin rings at the initial bud site, a high concentration of actin patches and a polarisome in the bud tip during polarized growth. These relocate to future septation sites near the onset of mitosis, and the nucleus divides across the bud neck (101). Hyphae are distinct in that they maintain polarized growth and a high concentration of actin patches at the tip. A transient septin band appears at the mother-germ tube neck, followed by formation of septin rings within the germ tube, where the first nuclear division takes place (88, 100, 101). Hyphae can contain a polarisome, but also possess a proposed vesicle supply center, similar to the Spitzenkörper found in tips of filamentous fungal hyphae (106, 107). The Spitzenkörper is visualized as a 3D spot at hyphal tips with FM4-64 staining, or through localization of Mlc1p (108), Sec4p (99), Sec2p (109) or Bni1p (108). These factors are maintained at the growing tip and simultaneously localize to subapical septation sites. Actin cables are oriented along the hyphal length and deliver vesicles and new cell wall/membrane material to the Spitzenkörper and growing tip (110). Additional distinct characteristics of hyphae include the absence of constrictions at septation sites, the transient appearance of a septin band at the mother-germ tube neck followed by formation of septin rings within the germ tube (111), and mitosis occurring within the germ tube as opposed to the mother cell/germ tube junction (104).

The ability to switch between cell types in different environments of the host is crucial for pathogenesis. While the yeast form of *C. albicans* is proposed to be optimal for dissemination in the blood stream and for gut colonization, the pseudohyphal and hyphal forms may be more adept at invading host tissue and escaping immune cells including macrophages and neutrophils (112).

Mixed populations of cell types are found in infected tissues (113). Mutants locked in one cell form are less virulent, supporting the notion that the ability to switch between cell types in different environments of the host is an important virulence-determining trait (114-116).

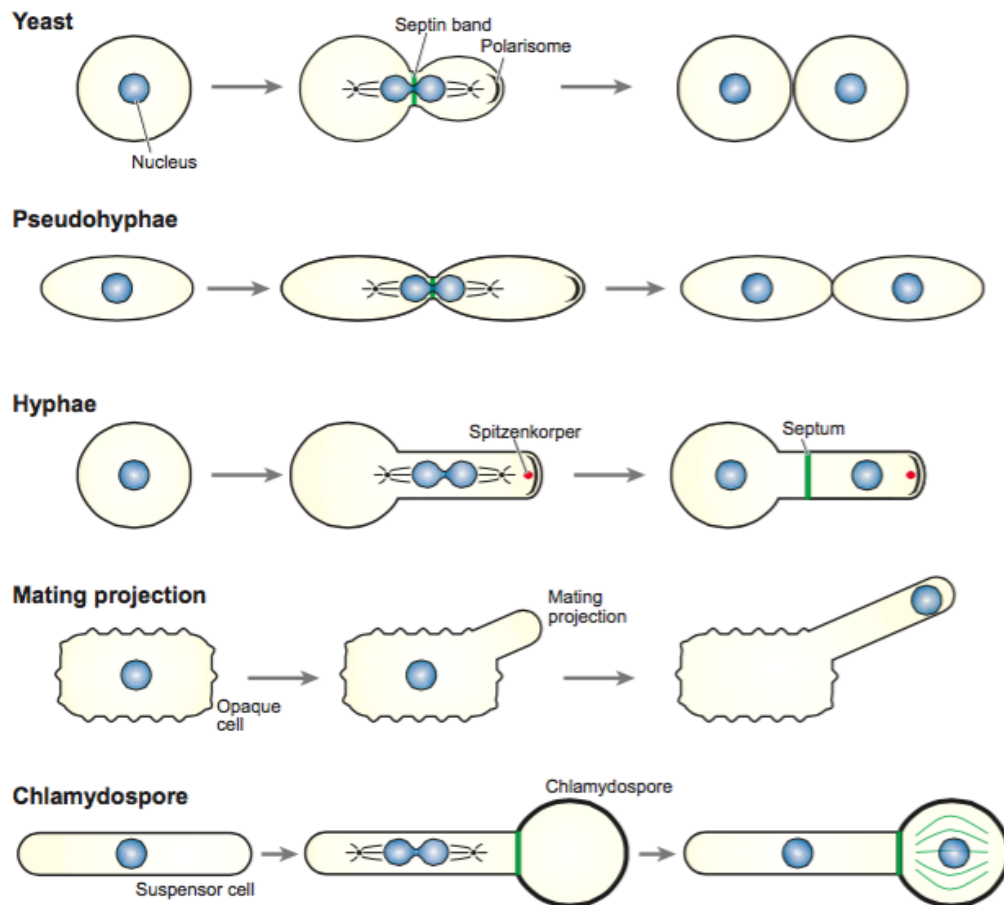


Figure 1.6: Different cell types of *C. albicans*. The yeast cells grow by budding and the nucleus divides across the septin ring, which is followed by cytokinesis resulting in two separate cells. The pseudohyphal cells also divide by budding; the nucleus divides at the septin ring but the cells do not separate resulting in chains of elongated cells. Hyphal cells form a germ tube with parallel walls in which the septum is formed. The nucleus divides in the germ tube across the septum; one nucleus moves back in the mother cell while the other remains in the germ tube. The polarized growth of buds in yeast and pseudohyphal forms is characterized by polarisome while in hyphal cells by the polarisome and Spitzenkörper. Figure source: Whiteway and Bachewich, 2007 (104).

b. Differentiation of hyphae: regulation by environmental signaling pathways

Since cell differentiation is important for virulence, an understanding of the underlying mechanisms may reveal new targets for treating infection. Cell differentiation in *C. albicans* is activated by different environmental cues (Fig. 1.7). One form of differentiation that has been well studied is the yeast-to-hyphal transition. While the yeast form is usually found under the conditions of low pH (4.0) and low temperature (30°C), slightly higher pH (6.0) and temperature (35°C) are associated with pseudohyphal growth. Hyphal growth requires high temperature (37°C) in combination with signals such as high pH (7.0), serum, or alternate carbon sources, for example. Iron deprivation, low nitrogen, high phosphate, starvation, oxidative stress and anaerobic conditions can also influence filamentation (120). High temperature is sensed by the heat shock protein Hsp90p (117), whereas other hyphal-inducing cues are mediated by a diversity of signaling pathways, including MAPK and cAMP (cyclic adenosine monophosphate), for example (Fig. 1.7). The transcription factor Efg1p is a common downstream effector of many of the pathways and considered a central regulator of hyphal formation; absence of Efg1p prevents hyphal growth under a diversity of conditions (118-120). Efg1p in turn regulates expression of several hyphal-specific genes (HSGs); it sits on their promoters and recruits factors required for nucleosomal histone H4 acetylation and transcriptional activation under hyphal-inducing conditions (121). HSGs include factors such as the cell wall adhesin protein Hwp1p, as well as other hyphal regulators including the transcription factor Ume6p (114, 122). Yeast cells lacking Ume6p initiate but do not maintain hyphal growth, and *UME6* overexpression can drive hyphal formation under yeast growth conditions (123). Ume6p in turn maintains expression of *HGCI*, a cyclin-related factor that has no known role in the cell cycle but is required for hyphal development. *HGCI* is specifically expressed in hyphal cells, and interacts with the CDK Cdc28p to regulate several processes required for maintaining hyphal growth (124, 125) (Fig. 1.8). Many HSGs are also virulence factors, emphasizing the significance of co-regulation of morphogenesis and pathogenesis (126). The yeast-to-hyphal transition is also under negative regulation, which involves the transcription factor complexes Tup1p/Nrg1p or Tup1p/Rfg1p (114, 127) (Fig. 1.7). Absence of *TUP1* or *NRG1*, for example, results in filamentous growth under yeast growth conditions, and approximately half of the known HSGs are negatively regulated by these factors. In addition, Nrg1p/Tup1p represses *UME6* (123). Despite their importance, it is still not clear how several negative regulators of the hyphal signaling pathways are in turn

controlled by environmental cues.

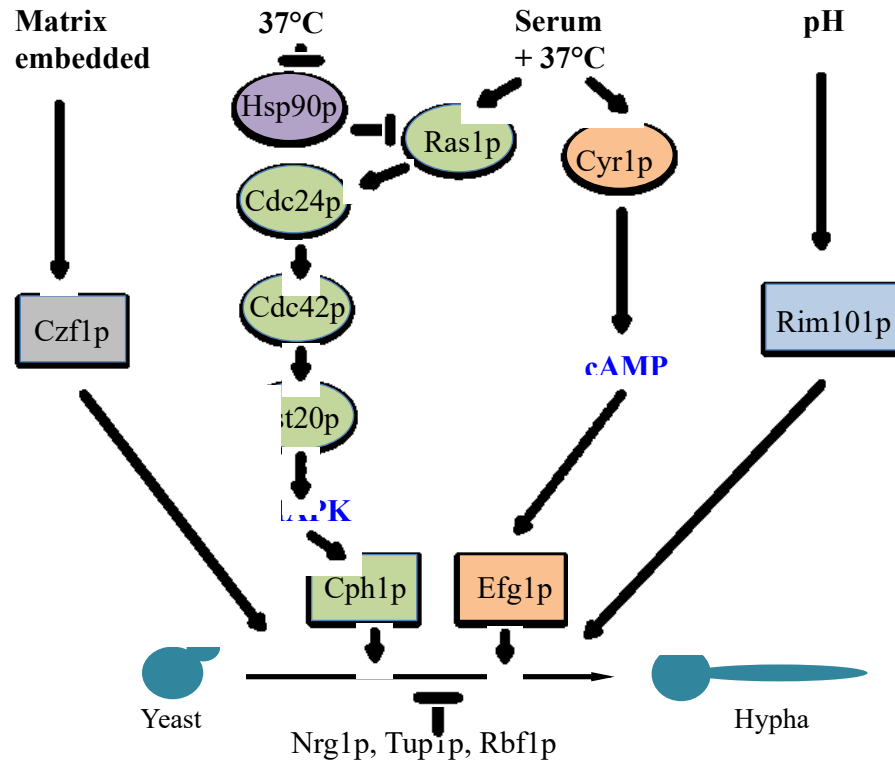


Figure 1.7: Environmental signaling pathways regulating the yeast-to-hyphal transition in *C. albicans*. The most characterized pathways are Cph1-mediated MAPK and the Efg1-mediated cAMP pathways. Ras1p lies upstream of both pathways. The pH responsive pathway is mediated through Rim101p. The matrix/embedded conditions mediate through Czf1p. Negative regulation of the yeast to hyphal switch is regulated through Tup1p, Nrg1p or Rbf1p. Transcription factors are shown in rectangular boxes. Dotted arrows indicate involvement of other additional factors, which are not in the figure. Figure based on Biswas *et al.*, 2007 (120) and Sudbery, 2011 (149).

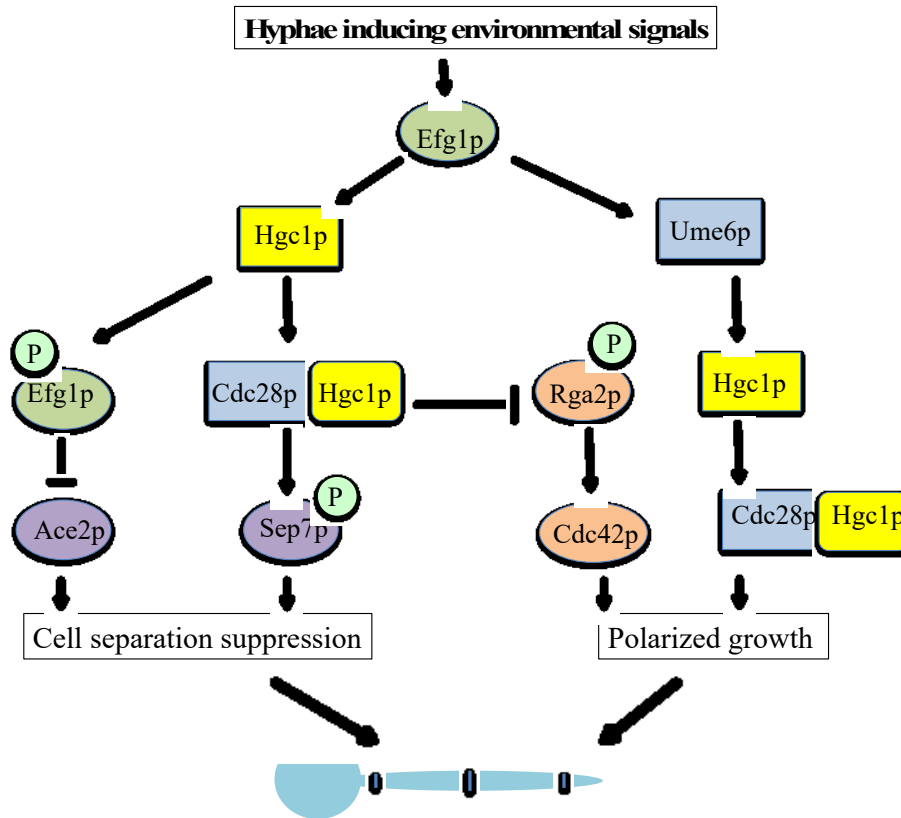


Figure 1.8: The hyphal signaling pathways to maintain hyphal growth and cell-cell attachment in *C. albicans*. Hyphal germ tube evagination occurs in the absence of G1 cyclin Hgc1p and when cyclin dependent kinase Cdc28p is inhibited. After germ tube evagination, Cdc28p/Hgc1p are required for polarized growth. Long-term maintenance of polarized growth requires Ume6p. The Cdc28p/Hgc1p complex inhibits Rga2p and thus activates master polarity regulator Cdc42p. Cdc28p/Hgc1p also phosphorylates septin Sep7p inhibiting cell separation. Figure based on: Sudbery, 2011 (149) and Patricia *et al.*, 2010 ().

c. Differentiation of hyphae: mechanisms regulating polarized growth

The multiple signaling pathways that mediate differentiation of yeast to hyphae must ultimately converge to control the mechanics of polarized hyphal growth, but our understanding of this level of the circuitry is not fully comprehended. The Rho-GTPase Cdc42p is associated with regulating actin organization and is thus a master regulator of polarization (128-130). In *C. albicans*, both *CDC42* and its activating GEF, *CDC24*, are essential for hyphal growth (100, 101). Intriguingly, the Cdc42p inhibitory GAP Rga2p is prevented from localizing to hyphal tips via phosphorylation by Cdc28p/Hgc1p under hyphal-inducing conditions, thus permitting hyphal growth (125). Cdc28p/Hgc1p also phosphorylates Efg1p, which targets it to promoters of genes

that repress cell separation in hyphae (124) (Fig. 1.8), as well as Sec2p, a secretory vesicle-associated protein that is specifically localized to the Spitzenkörper in *C. albicans* hyphae (109). More recently, the transcription factor Fkh2p was shown to be phosphorylated in a specific manner by the kinase Cbk1p as well as Cdc28p in combination with a known G1 cyclin, Ccn1p, upon hyphal induction. This is required for Fkh2p induction of genes associated with pathogenesis, host cell interaction and biofilm formation (131). Thus, several aspects of the polar growth machinery in hyphae have been identified. Their regulation, as well as that of several virulence-related processes, requires an important cell cycle regulator, Cdc28p, which is functioning outside of a cell cycle context. However, the upstream regulation of Cdc28p in response to hyphal-inducing conditions is not yet clear.

1.3.3 Virulence-determining trait: Cell proliferation

a. Cell cycle in *C. albicans*: Overview

Another aspect of the biology of *C. albicans* that is important for pathogenesis and allows survival in the host is cell proliferation, which is under control of the cell cycle. However, our current understanding of the cell cycle in *C. albicans* is poor relative to model yeast systems including *S. cerevisiae* and *S. pombe*, due in part to difficulty in synchronizing the cells. However, Cote *et al.*, 2009 (8) were able to synchronize opaque phase yeast cells through various manipulations, and obtained transcription profiles of cells as they passed through different cell cycle phases. The expression patterns showed similarity to but also many differences from the situations in *S. cerevisiae* and *S. pombe*. Importantly, several genes of unknown function were modulated at each cell cycle stage, suggesting the possibility of novel features and regulation. Such factors could be exploited for the purposes of controlling growth of *C. albicans*.

b. Regulation of mitosis in *C. albicans*

C. albicans contains homologues of many important mitotic regulators, but we currently have a poor understanding of their functions and the overall networks controlling mitosis. For example, the regulation of the G2/M transition, FEAR and MEN pathways are not fully defined. Of the few conserved mitotic factors that have been characterized, mechanisms of action are not completely clear, and in some cases, differences in function compared to orthologues in *S. cerevisiae* are apparent, suggesting variations in the mitotic circuitry of *C. albicans*. For

example, depletion of orthologues of the B-type cyclins Clb2p and Clb4p results in a block in mitosis during telophase, in contrast to earlier mitotic stages in *S. cerevisiae* (106). *C. albicans* Clb4p is also important as an S-phase cyclin (132), in contrast to Clb5p in *S. cerevisiae*. With respect to orthologues of MEN components, *CDC14* is not essential in *C. albicans*; its absence does not interfere with late mitosis or septation, but results in defective cell separation (133). In contrast, *CDC14* is essential in *S. cerevisiae*, and *cdc14Δ* cells are arrested in late anaphase (134). *DBF2* in *C. albicans* is an essential serine/threonine protein kinase involved in mitotic spindle formation, cytokinesis, septum formation, and exit from mitosis in *C. albicans* (135), while *S. cerevisiae* *DBF2* is not essential and required only for mitotic exit and cytokinesis (136). On the other hand, the GTPase Tem1p is essential for mitotic exit, cytokinesis and cell separation in both *S. cerevisiae* and *C. albicans*, (137, 138). At the time that I started my thesis work, there were no reports on APC/C function or regulation in *C. albicans*.

c. The influence of a Polo-like kinase, Cdc5p, on mitosis and a novel polarized growth response in *C. albicans*

C. albicans contains a homologue of another important regulator of mitosis, a Plk, called *CDC5*. Previous work demonstrated that Cdc5p may have some conservation in governing mitosis in *C. albicans*, but also variations in function. For example, *C. albicans* Cdc5p localized to the spindle pole bodies and chromatin, and its depletion resulted in an arrest in mitosis, similar to that reported for *S. cerevisiae* Cdc5p and other Plks. However, the cells were arrested with short spindles (97), as opposed to a late telophase arrest in *cdc5Δ* cells of *S. cerevisiae* (139), suggesting some differences in function and mechanisms of action.

Depletion of Cdc5p in *C. albicans* also resulted in a novel influence on morphogenesis in *C. albicans*. Following repression of *CDC5* and an arrest in mitosis, the yeast bud grew in a polarized manner, resulting in highly elongated filaments. In contrast, absence of Plks in other systems results in a cessation of cell growth and proliferation. For example, *S. cerevisiae*, *cdc5Δ* cells arrest as large doublets (140). Despite being under yeast-growth conditions, the filaments resembled hyphae in that they maintained polarized growth, lacked constrictions along their length, moved the nucleus from the mother yeast cell into the tube, required cyclase activity for elongation, and expressed some HSGs, many of which are virulence factors (97). A constriction

was present at the bud neck, due to the fact that polarized growth originated at the yeast bud that emerged prior to the cell cycle block. However, the filaments also are distinct from hyphae with respect to having wider diameters during earlier growth stages, forming in the absence of hyphal regulators Efg1p and Ras1p, expressing HSGs only at later stages of elongation (94, 97), and requiring the spindle checkpoint factor Bub2p for maintenance of polarized growth (97, 141). This filamentous growth may be a general response to a mitotic arrest in *C. albicans*, since it also occurs when mitosis is blocked through depletion of Clb2p, Hsp90p, and Rad52p, for example, or treatment with microtubule disrupting drugs such as nocodazole (106, 117, 142, 143). However, a direct role for Cdc5p in influencing polar morphogenesis can not be ruled out, since the various treatments that affect mitotic progression could in turn influence Cdc5p activity, the Plk Plo1 in *S. pombe* has been linked to tip growth in a cell-cycle independent manner, and Cdc5p in *S. cerevisiae* can bind regulators of the actin cytoskeleton (67, 144). The nature of the filaments produced through Cdc5p depletion and mitotic arrest remain elusive (107, 145).

Blocking the *C. albicans* yeast cell cycle in other phases also results in polarized growth, but the filamentous cells are not identical. For example, yeast cells depleted of the G1 cyclin Cln3p arrest in G1 phase, enlarge, then form filaments that are true hyphae based on several characteristics, including a requirement for the hyphal signaling pathway factors Efg1p and Ras1p (94) and the formation of unconstricted septa. This suggests a relationship between the G1 phase of the yeast cell cycle and hyphal development in *C. albicans*, but the mechanisms remain unclear. Further, blocking yeast cells in S phase results in elongated cells (96, 146). While they superficially resemble mitotic-arrested cells, they are different with respect to having much shorter lengths, distinct transcription profiles (96), and not requiring factors such as Bub2p (96, 146).

The filamentous cells that are produced through Cdc5p depletion or a block in mitosis may be important for survival in the host. For example, maintenance of polarized growth in cells arrested in mitosis through depletion of Cdc5p or Hsp90p requires the spindle checkpoint factor Bub2p, unlike the situation in true hyphae or S-phase arrested yeast cells (97, 141). Another spindle checkpoint factor, Mad2p, is required for filaments that form in response to nocodazole but not in true hyphae (142). Intriguingly, *BUB2* and *MAD2* are not essential for yeast growth *in*

vitro, but *MAD2* and another checkpoint factor, *SWE1*, are important for growth *in vivo* and for virulence (142, 147). One model is that yeast cells experiencing a stress on the cell cycle in a host environment have the ability to grow in a polarized manner and express HSGs in order to escape that environment (96, 97, 145).

Collectively, the data support the idea that Cdc5p is an important regulator of mitosis in *C. albicans* and that mitotic checkpoint-associated polarized growth may be important for pathogenesis within the host. However, the precise roles of Cdc5p and the mechanisms controlling mitosis, associated polarized growth and expression of HSGs, which are normally under the control of environmental signaling pathways, remain unclear. Previous work on filaments produced through depletion of Hsp90p identified the requirement of a novel pathway that included the transcription factor Hms1p (148). However, the mechanisms underlying polarized growth and HSG expression in response to other treatments that specifically block mitosis, including Cdc5p depletion, are not clear. Further, the nature of these polarized cells and any connection with true hyphae remain unknown (149).

1.4 Objectives

Differentiation and cell proliferation are crucial for virulence in *C. albicans*, but our understanding of the mechanisms that regulate these processes in the pathogen is far from complete. To this end, we are interested in defining the functions of select mitotic regulators in order to construct a framework of the networks governing mitotic progression in *C. albicans*, and in exploring the mechanisms that underlie the unique relationship between mitotic progression, polarized growth and expression of virulence genes that exists in this organism.

Our hypothesis is that Cdc5p in *C. albicans* employs conserved but also novel mechanisms to regulate mitosis, and influences morphogenesis in a manner that links mitosis with the developmental process of hyphal growth as a virulence-enhancing strategy. My specific objectives include: a) Characterizing a putative downstream mitotic target of Cdc5p, the APC/C, and determining its contribution to mitotic regulation and possibly morphogenesis; b) Defining the nature of the filaments that form in response to Cdc5p-depletion and determining the novel

mechanisms by which mitosis is linked to polarized growth and virulence gene expression; and c) Determining the mechanisms of action of Cdc5p during mitosis and morphogenesis. Through this work, we will gain significant insights into the control of cell proliferation in the pathogen, identify variations in eukaryotic mitotic regulatory circuits, and uncover novel circuitry linking mitosis with important virulence-determining traits.

1.5 References

1. **Morgan DO.** 2007. The Cell Cycle: Principles of Control. Chapter 1: The Cell Cycle. Pages: 1-9.
2. **Suryadinata R, Sadowski M, Sarcevic B.** 2010. Control of cell cycle progression by phosphorylation of cyclin-dependent kinase (CDK) substrates. *Biosci Rep* **30**:243-255.
3. **Santamaria D, Ortega S.** 2006. Cyclins and CDKS in development and cancer: lessons from genetically modified mice. *Front Biosci* **11**:1164-1188.
4. **Coffman JA.** 2004. Cell cycle development. *Dev Cell* **6**:321-327.
5. **Garcia-Muse T, Steinberg G, Perez-Martin J.** 2003. Pheromone-induced G2 arrest in the phytopathogenic fungus *Ustilago maydis*. *Eukaryot Cell* **2**:494-500.
6. **Lew DJ, Reed SI.** 1995. Cell cycle control of morphogenesis in budding yeast. *Curr Opin Genet Dev* **5**:17-23.
7. **Vidwans SJ, Su TT.** 2001. Cycling through development in *Drosophila* and other metazoa. *Nat Cell Biol* **3**:E35-39.
8. **Cote P, Hogues H, Whiteway M.** 2009. Transcriptional analysis of the *Candida albicans* cell cycle. *Mol Biol Cell* **20**:3363-3373.
9. **Cross FR, Buchler NE, Skotheim JM.** 2011. Evolution of networks and sequences in eukaryotic cell cycle control. *Philos Trans R Soc Lond B Biol Sci* **366**:3532-3544.
10. **Arnone JT, Walters AD, Cohen-Fix O.** 2013. The dynamic nature of the nuclear envelope: lessons from closed mitosis. *Nucleus* **4**:261-266.
11. **Bachant J, Jessen SR, Kavanaugh SE, Fielding CS.** 2005. The yeast S phase checkpoint enables replicating chromosomes to bi-orient and restrain spindle extension during S phase distress. *J Cell Biol* **168**:999-1012.
12. **Zhang D, Oliferenko S.** 2013. Remodeling the nuclear membrane during closed mitosis. *Curr Opin Cell Biol* **25**:142-148.
13. **Darieva Z, Pic-Taylor A, Boros J, Spanos A, Geymonat M, Reece RJ, Sedgwick SG, Sharrocks AD, Morgan BA.** 2003. Cell cycle-regulated transcription through the FHA domain of Fkh2p and the coactivator Ndd1p. *Curr Biol* **13**:1740-1745.
14. **Rudner AD, Murray AW.** 2000. Phosphorylation by Cdc28 activates the Cdc20-dependent activity of the anaphase-promoting complex. *J Cell Biol* **149**:1377-1390.
15. **Rahal R, Amon A.** 2008. Mitotic CDKs control the metaphase-anaphase transition and trigger spindle elongation. *Genes Dev* **22**:1534-1548.
16. **Amon A.** 1997. Regulation of B-type cyclin proteolysis by Cdc28-associated kinases in budding yeast. *EMBO J* **16**:2693-2702.
17. **Archambault V, Glover DM.** 2009. Polo-like kinases: conservation and divergence in

- their functions and regulation. *Nat Rev Mol Cell Biol* **10**:265-275.
18. **Nigg EA.** 2001. Mitotic kinases as regulators of cell division and its checkpoints. *Nat Rev Mol Cell Biol* **2**:21-32.
 19. **Miele L.** 2004. The biology of cyclins and cyclin-dependent protein kinases: an introduction. *Methods Mol Biol* **285**:3-21.
 20. **Mujtaba T, Dou QP.** 2011. Advances in the understanding of mechanisms and therapeutic use of bortezomib. *Discov Med* **12**:471-480.
 21. **Murray AW.** 2004. Recycling the cell cycle: cyclins revisited. *Cell* **116**:221-234.
 22. **Manchado E, Eguren M, Malumbres M.** 2010. The anaphase-promoting complex/cyclosome (APC/C): cell-cycle-dependent and -independent functions. *Biochem Soc Trans* **38**:65-71.
 23. **Simpson-Lavy KJ, Oren YS, Feine O, Sajman J, Listovsky T, Brandeis M.** 2010. Fifteen years of APC/cyclosome: a short and impressive biography. *Biochem Soc Trans* **38**:78-82.
 24. **Castro A, Bernis C, Vigneron S, Labbe JC, Lorca T.** 2005. The anaphase-promoting complex: a key factor in the regulation of cell cycle. *Oncogene* **24**:314-325.
 25. **Song L, Rape M.** 2011. Substrate-specific regulation of ubiquitination by the anaphase-promoting complex. *Cell Cycle* **10**:52-56.
 26. **Cohen-Fix O, Peters JM, Kirschner MW, Koshland D.** 1996. Anaphase initiation in *Saccharomyces cerevisiae* is controlled by the APC-dependent degradation of the anaphase inhibitor Pds1p. *Genes Dev* **10**:3081-3093.
 27. **Visintin R, Craig K, Hwang ES, Prinz S, Tyers M, Amon A.** 1998. The phosphatase Cdc14 triggers mitotic exit by reversal of Cdk-dependent phosphorylation. *Mol Cell* **2**:709-718.
 28. **Schwab M, Neutzner M, Mocker D, Seufert W.** 2001. Yeast Hct1 recognizes the mitotic cyclin Clb2 and other substrates of the ubiquitin ligase APC. *EMBO J* **20**:5165-5175.
 29. **Barford D.** 2011. Structure, function and mechanism of the anaphase promoting complex (APC/C). *Q Rev Biophys* **44**:153-190.
 30. **Primorac I, Musacchio A.** 2013. Panta rhei: the APC/C at steady state. *J Cell Biol* **201**:177-189.
 31. **Wash R, Robbins JA, Cross FR.** 2010. The emerging role of APC/CCdh1 in controlling differentiation, genomic stability and tumor suppression. *Oncogene* **29**:1-10.
 32. **Kim AH, Bonni A.** 2007. Thinking within the D box: initial identification of Cdh1-APC substrates in the nervous system. *Mol Cell Neurosci* **34**:281-287.
 33. **Konishi Y, Stegmuller J, Matsuda T, Bonni S, Bonni A.** 2004. Cdh1-APC controls axonal growth and patterning in the mammalian brain. *Science* **303**:1026-1030.
 34. **Aulia S, Tang BL.** 2006. Cdh1-APC/C, cyclin B-Cdc2, and Alzheimer's disease pathology. *Biochem Biophys Res Commun* **339**:1-6.
 35. **Saunders WS.** 2002. The FEAR factor. *Mol Cell* **9**:207-209.
 36. **Queralt E, Lehane C, Novak B, Uhlmann F.** 2006. Downregulation of PP2A(Cdc55) phosphatase by separase initiates mitotic exit in budding yeast. *Cell* **125**:719-732.
 37. **Rahal R, Amon A.** 2008. The Polo-like kinase Cdc5 interacts with FEAR network components and Cdc14. *Cell Cycle* **7**:3262-3272.
 38. **Liang F, Jin F, Liu H, Wang Y.** 2009. The molecular function of the yeast polo-like kinase Cdc5 in Cdc14 release during early anaphase. *Mol Biol Cell* **20**:3671-3679.

39. **Bardin AJ, Visintin R, Amon A.** 2000. A mechanism for coupling exit from mitosis to partitioning of the nucleus. *Cell* **102**:21-31.
40. **Visintin R, Hwang ES, Amon A.** 1999. Cfi1 prevents premature exit from mitosis by anchoring Cdc14 phosphatase in the nucleolus. *Nature* **398**:818-823.
41. **Noton E, Diffley JF.** 2000. CDK inactivation is the only essential function of the APC/C and the mitotic exit network proteins for origin resetting during mitosis. *Mol Cell* **5**:85-95.
42. **Trinkle-Mulcahy L, Lamond AI.** 2006. Mitotic phosphatases: no longer silent partners. *Curr Opin Cell Biol* **18**:623-631.
43. **Cuif MH, Possmayer F, Zander H, Bordes N, Jollivet F, Couedel-Courteille A, Janoueix-Lerosey I, Langsley G, Bornens M, Goud B.** 1999. Characterization of GAPCenA, a GTPase activating protein for Rab6, part of which associates with the centrosome. *EMBO J* **18**:1772-1782.
44. **Moreno CS, Lane WS, Pallas DC.** 2001. A mammalian homolog of yeast *MOB1* is both a member and a putative substrate of striatin family-protein phosphatase 2A complexes. *J Biol Chem* **276**:24253-24260.
45. **Vitulo N, Vezzi A, Galla G, Citterio S, Marino G, Ruperti B, Zermiani M, Albertini E, Valle G, Barcaccia G.** 2007. Characterization and evolution of the cell cycle-associated mob domain-containing proteins in eukaryotes. *Evol Bioinform Online* **3**:121-158.
46. **Wurzenberger C, Gerlich DW.** 2011. Phosphatases: providing safe passage through mitotic exit. *Nat Rev Mol Cell Biol* **12**:469-482.
47. **Lowery DM, Mohammad DH, Elia AE, Yaffe MB.** 2004. The Polo-box domain: a molecular integrator of mitotic kinase cascades and Polo-like kinase function. *Cell Cycle* **3**:128-131.
48. **Elia AE, Cantley LC, Yaffe MB.** 2003. Proteomic screen finds pSer/pThr-binding domain localizing Plk1 to mitotic substrates. *Science* **299**:1228-1231.
49. **Elia AE, Rellos P, Haire LF, Chao JW, Ivins FJ, Hoepker K, Mohammad D, Cantley LC, Smerdon SJ, Yaffe MB.** 2003. The molecular basis for phosphodependent substrate targeting and regulation of Plks by the Polo-box domain. *Cell* **115**:83-95.
50. **Miller CT, Gabrielse C, Chen YC, Weinreich M.** 2009. Cdc7p-Dbf4p regulates mitotic exit by inhibiting Polo kinase. *PLoS Genet* **5**:e1000498.
51. **Archambault V, D'Avino PP, Deery MJ, Lilley KS, Glover DM.** 2008. Sequestration of Polo kinase to microtubules by phosphoprime-independent binding to Map205 is relieved by phosphorylation at a CDK site in mitosis. *Genes Dev* **22**:2707-2720.
52. **Garcia-Alvarez B, de Carcer G, Ibanez S, Bragado-Nilsson E, Montoya G.** 2007. Molecular and structural basis of polo-like kinase 1 substrate recognition: Implications in centrosomal localization. *Proc Natl Acad Sci U S A* **104**:3107-3112.
53. **Glover DM, Hagan IM, Tavares AA.** 1998. Polo-like kinases: a team that plays throughout mitosis. *Genes Dev* **12**:3777-3787.
54. **Nigg EA.** 1998. Polo-like kinases: positive regulators of cell division from start to finish. *Curr Opin Cell Biol* **10**:776-783.
55. **Sakchaisri K, Asano S, Yu LR, Shulewitz MJ, Park CJ, Park JE, Cho YW, Veenstra TD, Thorner J, Lee KS.** 2004. Coupling morphogenesis to mitotic entry. *Proc Natl Acad Sci U S A* **101**:4124-4129.
56. **Toyoshima-Morimoto F, Taniguchi E, Nishida E.** 2002. Plk1 promotes nuclear translocation of human Cdc25C during prophase. *EMBO Rep* **3**:341-348.

57. **Park CJ, Park JE, Karpova TS, Soung NK, Yu LR, Song S, Lee KH, Xia X, Kang E, Dabanoglu I, Oh DY, Zhang JY, Kang YH, Wincovitch S, Huffaker TC, Veenstra TD, McNally JG, Lee KS.** 2008. Requirement for the budding yeast polo kinase Cdc5 in proper microtubule growth and dynamics. *Eukaryot Cell* **7**:444-453.
58. **Lenart P, Petronczki M, Steegmaier M, Di Fiore B, Lipp JJ, Hoffmann M, Rettig WJ, Kraut N, Peters JM.** 2007. The small-molecule inhibitor BI 2536 reveals novel insights into mitotic roles of polo-like kinase 1. *Curr Biol* **17**:304-315.
59. **Elowe S, Hummer S, Uldschmid A, Li X, Nigg EA.** 2007. Tension-sensitive Plk1 phosphorylation on BubR1 regulates the stability of kinetochore microtubule interactions. *Genes Dev* **21**:2205-2219.
60. **do Carmo Avides M, Tavares A, Glover DM.** 2001. Polo kinase and Asp are needed to promote the mitotic organizing activity of centrosomes. *Nat Cell Biol* **3**:421-424.
61. **Alexandru G, Uhlmann F, Mechtler K, Poupart MA, Nasmyth K.** 2001. Phosphorylation of the cohesin subunit Scc1 by Polo/Cdc5 kinase regulates sister chromatid separation in yeast. *Cell* **105**:459-472.
62. **Sumara I, Vorlaufer E, Stukenberg PT, Kelm O, Redemann N, Nigg EA, Peters JM.** 2002. The dissociation of cohesin from chromosomes in prophase is regulated by Polo-like kinase. *Mol Cell* **9**:515-525.
63. **Lee KS, Park JE, Asano S, Park CJ.** 2005. Yeast polo-like kinases: functionally conserved multitask mitotic regulators. *Oncogene* **24**:217-229.
64. **Uhlmann F, Wernic D, Poupart MA, Koonin EV, Nasmyth K.** 2000. Cleavage of cohesin by the CD clan protease separin triggers anaphase in yeast. *Cell* **103**:375-386.
65. **Hansen DV, Loktev AV, Ban KH, Jackson PK.** 2004. Plk1 regulates activation of the anaphase promoting complex by phosphorylating and triggering SCFbetaTrCP-dependent destruction of the APC Inhibitor Emi1. *Mol Biol Cell* **15**:5623-5634.
66. **Moshe Y, Boulaire J, Pagano M, Hershko A.** 2004. Role of Polo-like kinase in the degradation of early mitotic inhibitor 1, a regulator of the anaphase promoting complex/cyclosome. *Proc Natl Acad Sci U S A* **101**:7937-7942.
67. **Yoshida S, Kono K, Lowery DM, Bartolini S, Yaffe MB, Ohya Y, Pellman D.** 2006. Polo-like kinase Cdc5 controls the local activation of Rho1 to promote cytokinesis. *Science* **313**:108-111.
68. **Atkins BD, Yoshida S, Saito K, Wu CF, Lew DJ, Pellman D.** 2013. Inhibition of Cdc42 during mitotic exit is required for cytokinesis. *J Cell Biol* **202**:231-240.
69. **Petronczki M, Lenart P, Peters JM.** 2008. Polo on the Rise—from Mitotic Entry to Cytokinesis with Plk1. *Dev Cell* **14**:646-659.
70. **Shirayama M, Zachariae W, Ciosk R, Nasmyth K.** 1998. The Polo-like kinase Cdc5p and the WD-repeat protein Cdc20p/fizzy are regulators and substrates of the anaphase promoting complex in *Saccharomyces cerevisiae*. *EMBO J* **17**:1336-1349.
71. **Zitouni S, Nabais C, Jana SC, Guerrero A, Bettencourt-Dias M.** 2014. Polo-like kinases: structural variations lead to multiple functions. *Nat Rev Mol Cell Biol* **15**:433-452.
72. **Fu Z, Malureanu L, Huang J, Wang W, Li H, van Deursen JM, Tindall DJ, Chen J.** 2008. Plk1-dependent phosphorylation of FoxM1 regulates a transcriptional programme required for mitotic progression. *Nat Cell Biol* **10**:1076-1082.
73. **Zhang J, Yuan C, Wu J, Elsayed Z, Fu Z.** 2015. Polo-like kinase 1-mediated phosphorylation of Forkhead box protein M1b antagonizes its SUMOylation and facilitates its mitotic function. *J Biol Chem* **290**:3708-3719.

74. **Seki A, Coppinger JA, Jang CY, Yates JR, Fang G.** 2008. Bora and the kinase Aurora a cooperatively activate the kinase Plk1 and control mitotic entry. *Science* **320**:1655-1658.
75. **Bruinsma W, Macurek L, Freire R, Lindqvist A, Medema RH.** 2014. Bora and Aurora-A continue to activate Plk1 in mitosis. *J Cell Sci* **127**:801-811.
76. **Archambault V, Carmena M.** 2012. Polo-like kinase-activating kinases: Aurora A, Aurora B and what else? *Cell Cycle* **11**:1490-1495.
77. **Halova L, Petersen J.** 2011. Aurora promotes cell division during recovery from TOR-mediated cell cycle arrest by driving spindle pole body recruitment of Polo. *J Cell Sci* **124**:3441-3449.
78. **Johnson TM, Antrobus R, Johnson LN.** 2008. Plk1 activation by Ste20-like kinase (Slk) phosphorylation and polo-box phosphopeptide binding assayed with the substrate translationally controlled tumor protein (TCTP). *Biochemistry* **47**:3688-3696.
79. **Tavernier N, Noatynska A, Panbianco C, Martino L, Van Hove L, Schwager F, Leger T, Gotta M, Pintard L.** 2015. Cdk1 phosphorylates SPAT-1/Bora to trigger PLK-1 activation and drive mitotic entry in *C. elegans* embryos. *J Cell Biol* **208**:661-669.
80. **Ferris DK, Maloid SC, Li CC.** 1998. Ubiquitination and proteasome mediated degradation of polo-like kinase. *Biochem Biophys Res Commun* **252**:340-344.
81. **Visintin C, Tomson BN, Rahal R, Paulson J, Cohen M, Taunton J, Amon A, Visintin R.** 2008. APC/C-Cdh1-mediated degradation of the Polo kinase Cdc5 promotes the return of Cdc14 into the nucleolus. *Genes Dev* **22**:79-90.
82. **Park JE, Soung NK, Johmura Y, Kang YH, Liao C, Lee KH, Park CH, Nicklaus MC, Lee KS.** 2010. Polo-box domain: a versatile mediator of polo-like kinase function. *Cell Mol Life Sci* **67**:1957-1970.
83. **Botchkarev VV, Jr., Rossio V, Yoshida S.** 2014. The budding yeast Polo-like kinase Cdc5 is released from the nucleus during anaphase for timely mitotic exit. *Cell Cycle* **13**:3260-3270.
84. **Dupont PF.** 1995. *Candida albicans*, the opportunist. A cellular and molecular perspective. *J Am Podiatr Med Assoc* **85**:104-115.
85. **Shepherd MG, Poulter RT, Sullivan PA.** 1985. *Candida albicans*: biology, genetics, and pathogenicity. *Annu Rev Microbiol* **39**:579-614.
86. **Corner BE, Magee PT.** 1997. *Candida* pathogenesis: unravelling the threads of infection. *Curr Biol* **7**:R691-694.
87. **Sobel JD.** 2002. Treatment of vaginal *Candida* infections. *Expert Opin Pharmacother* **3**:1059-1065.
88. **Beck-Sague C, Jarvis WR.** 1993. Secular trends in the epidemiology of nosocomial fungal infections in the United States, 1980-1990. National Nosocomial Infections Surveillance System. *J Infect Dis* **167**:1247-1251.
89. **Edmond MB, Wallace SE, McClish DK, Pfaller MA, Jones RN, Wenzel RP.** 1999. Nosocomial bloodstream infections in United States hospitals: a three-year analysis. *Clin Infect Dis* **29**:239-244.
90. **Miller LG, Hajjeh RA, Edwards JE, Jr.** 2001. Estimating the cost of nosocomial candidemia in the united states. *Clin Infect Dis* **32**:1110.
91. **Morschhauser J.** 2010. Regulation of multidrug resistance in pathogenic fungi. *Fungal Genet Biol* **47**:94-106.
92. **Orasch C, Marchetti O, Garbino J, Schrenzel J, Zimmerli S, Muhlethaler K, Pfyffer G, Ruef C, Fehr J, Zbinden R, Calandra T, Bille J.** 2014. *Candida* species

- distribution and antifungal susceptibility testing according to European Committee on Antimicrobial Susceptibility Testing and new vs. old Clinical and Laboratory Standards Institute clinical breakpoints: a 6-year prospective candidaemia survey from the fungal infection network of Switzerland. *Clin Microbiol Infect* **20**:698-705.
93. **Prasad R, Kapoor K.** 2005. Multidrug resistance in yeast *Candida*. *Int Rev Cytol* **242**:215-248.
 94. **Bachewich C, Whiteway M.** 2005. Cyclin Cln3p links G1 progression to hyphal and pseudohyphal development in *Candida albicans*. *Eukaryot Cell* **4**:95-102.
 95. **Gow NA.** 2013. A developmental program for *Candida* commensalism. *Nat Genet* **45**:967-968.
 96. **Bachewich C, Nantel A, Whiteway M.** 2005. Cell cycle arrest during S or M phase generates polarized growth via distinct signals in *Candida albicans*. *Mol Microbiol* **57**:942-959.
 97. **Bachewich C, Thomas DY, Whiteway M.** 2003. Depletion of a polo-like kinase in *Candida albicans* activates cyclase-dependent hyphal-like growth. *Mol Biol Cell* **14**:2163-2180.
 98. **Park HO, Bi E.** 2007. Central roles of small GTPases in the development of cell polarity in yeast and beyond. *Microbiol Mol Biol Rev* **71**:48-96.
 99. **Jones LA, Sudbery PE.** 2010. Spitzenkorper, exocyst, and polarisome components in *Candida albicans* hyphae show different patterns of localization and have distinct dynamic properties. *Eukaryot Cell* **9**:1455-1465.
 100. **Basilana M, Blyth J, Arkowitz RA.** 2003. Cdc24, the GDP-GTP exchange factor for Cdc42, is required for invasive hyphal growth of *Candida albicans*. *Eukaryot Cell* **2**:9-18.
 101. **Basilana M, Hopkins J, Arkowitz RA.** 2005. Regulation of the Cdc42/Cdc24 GTPase module during *Candida albicans* hyphal growth. *Eukaryot Cell* **4**:588-603.
 102. **Pande K, Chen C, Noble SM.** 2013. Passage through the mammalian gut triggers a phenotypic switch that promotes *Candida albicans* commensalism. *Nat Genet* **45**:1088-1091.
 103. **Miller MG, Johnson AD.** 2002. White-opaque switching in *Candida albicans* is controlled by mating-type locus homeodomain proteins and allows efficient mating. *Cell* **110**:293-302.
 104. **Whiteway M, Bachewich C.** 2007. Morphogenesis in *Candida albicans*. *Annu Rev Microbiol* **61**:529-553.
 105. **Baumer M, Braus GH, Irniger S.** 2000. Two different modes of cyclin clb2 proteolysis during mitosis in *Saccharomyces cerevisiae*. *FEBS Lett* **468**:142-148.
 106. **Bensen ES, Clemente-Blanco A, Finley KR, Correa-Bordes J, Berman J.** 2005. The mitotic cyclins Clb2p and Clb4p affect morphogenesis in *Candida albicans*. *Mol Biol Cell* **16**:3387-3400.
 107. **Berman J.** 2006. Morphogenesis and cell cycle progression in *Candida albicans*. *Curr Opin Microbiol* **9**:595-601.
 108. **Crampin H, Finley K, Gerami-Nejad M, Court H, Gale C, Berman J, Sudbery P.** 2005. *Candida albicans* hyphae have a Spitzenkorper that is distinct from the polarisome found in yeast and pseudohyphae. *J Cell Sci* **118**:2935-2947.
 109. **Bishop A, Lane R, Beniston R, Chapa-y-Lazo B, Smythe C, Sudbery P.** 2010. Hyphal growth in *Candida albicans* requires the phosphorylation of Sec2 by the Cdc28-Ccn1/Hgc1 kinase. *EMBO J* **29**:2930-2942.

110. **Anderson JM, Soll DR.** 1987. Unique phenotype of opaque cells in the white-opaque transition of *Candida albicans*. *J Bacteriol* **169**:5579-5588.
111. **Sudbery PE.** 2001. The germ tubes of *Candida albicans* hyphae and pseudohyphae show different patterns of septin ring localization. *Mol Microbiol* **41**:19-31.
112. **Vazquez-Torres A, Balish E.** 1997. Macrophages in resistance to candidiasis. *Microbiol Mol Biol Rev* **61**:170-192.
113. **Odds FC, Van Nuffel L, Dams G.** 1998. Prevalence of *Candida dubliniensis* isolates in a yeast stock collection. *J Clin Microbiol* **36**:2869-2873.
114. **Braun BR, Head WS, Wang MX, Johnson AD.** 2000. Identification and characterization of *TUP1*-regulated genes in *Candida albicans*. *Genetics* **156**:31-44.
115. **Braun BR, Johnson AD.** 1997. Control of filament formation in *Candida albicans* by the transcriptional repressor *TUP1*. *Science* **277**:105-109.
116. **Lo HJ, Kohler JR, DiDomenico B, Loebenberg D, Cacciapuoti A, Fink GR.** 1997. Nonfilamentous *C. albicans* mutants are avirulent. *Cell* **90**:939-949.
117. **Shapiro RS, Uppuluri P, Zaas AK, Collins C, Senn H, Perfect JR, Heitman J, Cowen LE.** 2009. Hsp90 orchestrates temperature-dependent *Candida albicans* morphogenesis via Ras1-PKA signaling. *Curr Biol* **19**:621-629.
118. **Brown DH, Jr., Giusani AD, Chen X, Kumamoto CA.** 1999. Filamentous growth of *Candida albicans* in response to physical environmental cues and its regulation by the unique *CZF1* gene. *Mol Microbiol* **34**:651-662.
119. **Stoldt VR, Sonneborn A, Leuker CE, Ernst JF.** 1997. Efg1p, an essential regulator of morphogenesis of the human pathogen *Candida albicans*, is a member of a conserved class of bHLH proteins regulating morphogenetic processes in fungi. *EMBO J* **16**:1982-1991.
120. **Biswas S, Van Dijck P, Datta A.** 2007. Environmental sensing and signal transduction pathways regulating morphopathogenic determinants of *Candida albicans*. *Microbiol Mol Biol Rev* **71**:348-376.
121. **Lu Y, Su C, Mao X, Raniga PP, Liu H, Chen J.** 2008. Efg1-mediated recruitment of NuA4 to promoters is required for hypha-specific Swi/Snf binding and activation in *Candida albicans*. *Mol Biol Cell* **19**:4260-4272.
122. **Calvet HM, Yeaman MR, Filler SG.** 1997. Reversible fluconazole resistance in *Candida albicans*: a potential in vitro model. *Antimicrob Agents Chemother* **41**:535-539.
123. **Zeidler U, Lettner T, Lassnig C, Muller M, Lajko R, Hintner H, Breitenbach M, Bito A.** 2009. *UME6* is a crucial downstream target of other transcriptional regulators of true hyphal development in *Candida albicans*. *FEMS Yeast Res* **9**:126-142.
124. **Wang A, Raniga PP, Lane S, Lu Y, Liu H.** 2009. Hyphal chain formation in *Candida albicans*: Cdc28-Hgc1 phosphorylation of Efg1 represses cell separation genes. *Mol Cell Biol* **29**:4406-4416.
125. **Zheng X, Wang Y, Wang Y.** 2004. Hgc1, a novel hypha-specific G1 cyclin-related protein regulates *Candida albicans* hyphal morphogenesis. *EMBO J* **23**:1845-1856.
126. **Liu H.** 2002. Co-regulation of pathogenesis with dimorphism and phenotypic switching in *Candida albicans*, a commensal and a pathogen. *Int J Med Microbiol* **292**:299-311.
127. **Braun BR, Kadosh D, Johnson AD.** 2001. *NRG1*, a repressor of filamentous growth in *C. albicans*, is down-regulated during filament induction. *EMBO J* **20**:4753-4761.
128. **Fukata M, Nakagawa M, Kaibuchi K.** 2003. Roles of Rho-family GTPases in cell polarisation and directional migration. *Curr Opin Cell Biol* **15**:590-597.

129. **Jaffe AB, Hall A.** 2005. Rho GTPases: biochemistry and biology. *Annu Rev Cell Dev Biol* **21**:247-269.
130. **Johnson DI.** 1999. Cdc42: An essential Rho-type GTPase controlling eukaryotic cell polarity. *Microbiol Mol Biol Rev* **63**:54-105.
131. **Greig JA, Sudbery IM, Richardson JP, Naglik JR, Wang Y, Sudbery PE.** 2015. Cell cycle-independent phospho-regulation of Fkh2 during hyphal growth regulates *Candida albicans* pathogenesis. *PLoS Pathog* **11**:e1004630.
132. **Ofir A, Kornitzer D.** 2010. *Candida albicans* cyclin Clb4 carries S-phase cyclin activity. *Eukaryot Cell* **9**:1311-1319.
133. **Clemente-Blanco A, Gonzalez-Novo A, Machin F, Caballero-Lima D, Aragon L, Sanchez M, de Aldana CR, Jimenez J, Correa-Bordes J.** 2006. The Cdc14p phosphatase affects late cell-cycle events and morphogenesis in *Candida albicans*. *J Cell Sci* **119**:1130-1143.
134. **Jaspersen SL, Charles JF, Tinker-Kulberg RL, Morgan DO.** 1998. A late mitotic regulatory network controlling cyclin destruction in *Saccharomyces cerevisiae*. *Mol Biol Cell* **9**:2803-2817.
135. **Gonzalez-Novo A, Labrador L, Pablo-Hernando ME, Correa-Bordes J, Sanchez M, Jimenez J, Vazquez de Aldana CR.** 2009. Dbf2 is essential for cytokinesis and correct mitotic spindle formation in *Candida albicans*. *Mol Microbiol* **72**:1364-1378.
136. **Jimenez J, Castelao BA, Gonzalez-Novo A, Sanchez-Perez M.** 2005. The role of MEN (mitosis exit network) proteins in the cytokinesis of *Saccharomyces cerevisiae*. *Int Microbiol* **8**:33-42.
137. **Milne SW, Cheetham J, Lloyd D, Shaw S, Moore K, Paszkiewicz KH, Aves SJ, Bates S.** 2014. Role of *Candida albicans* Tem1 in mitotic exit and cytokinesis. *Fungal Genet Biol* **69**:84-95.
138. **Shirayama M, Matsui Y, Toh EA.** 1994. The yeast *TEM1* gene, which encodes a GTP-binding protein, is involved in termination of M phase. *Mol Cell Biol* **14**:7476-7482.
139. **Song S, Lee KS.** 2001. A novel function of *Saccharomyces cerevisiae* *CDC5* in cytokinesis. *J Cell Biol* **152**:451-469.
140. **Kitada K, Johnson AL, Johnston LH, Sugino A.** 1993. A multicopy suppressor gene of the *Saccharomyces cerevisiae* G1 cell cycle mutant gene *dbf4* encodes a protein kinase and is identified as *CDC5*. *Mol Cell Biol* **13**:4445-4457.
141. **Senn H, Shapiro RS, Cowen LE.** 2012. Cdc28 provides a molecular link between Hsp90, morphogenesis, and cell cycle progression in *Candida albicans*. *Mol Biol Cell* **23**:268-283.
142. **Bai C, Ramanan N, Wang YM, Wang Y.** 2002. Spindle assembly checkpoint component CaMad2p is indispensable for *Candida albicans* survival and virulence in mice. *Mol Microbiol* **45**:31-44.
143. **Andaluz E, Ciudad T, Gomez-Raja J, Calderone R, Larriba G.** 2006. Rad52 depletion in *Candida albicans* triggers both the DNA-damage checkpoint and filamentation accompanied by but independent of expression of hypha-specific genes. *Mol Microbiol* **59**:1452-1472.
144. **Robertson AM, Hagan IM.** 2008. Stress-regulated kinase pathways in the recovery of tip growth and microtubule dynamics following osmotic stress in *S. pombe*. *J Cell Sci* **121**:4055-4068.
145. **Gale CA, Berman J.** 2012. Cell Cycle and Growth Control in *Candida* Species, *Candida*

- and Candidiasis, Second Edition doi:doi:10.1128/9781555817176.ch8. American Society of Microbiology.
146. **Soll DR, Stasi M, Bedell G.** 1978. The regulation of nuclear migration and division during pseudo-mycelium outgrowth in the dimorphic yeast *Candida albicans*. *Exp Cell Res* **116**:207-215.
 147. **Gale CA, Leonard MD, Finley KR, Christensen L, McClellan M, Abbey D, Kurischko C, Bensen E, Tzafrir I, Kauffman S, Becker J, Berman J.** 2009. *SLA2* mutations cause *SWE1*-mediated cell cycle phenotypes in *Candida albicans* and *Saccharomyces cerevisiae*. *Microbiology* **155**:3847-3859.
 148. **Shapiro RS, Sellam A, Tebbji F, Whiteway M, Nantel A, Cowen LE.** 2012. Pho85, Pcl1, and Hms1 signaling governs *Candida albicans* morphogenesis induced by high temperature or Hsp90 compromise. *Curr Biol* **22**:461-470.
 149. **Sudbery PE.** 2011. Growth of *Candida albicans* hyphae. *Nat Rev Microbiol* **9**:737-748.

CHAPTER 2

Ch. 2: Orthologues of the APC/C coactivators Cdc20p and Cdh1p are important for mitotic progression and morphogenesis in *Candida albicans*.

Chapter 2 demonstrates the first characterization of the Anaphase Promoting Complex/Cyclosome (APC/C) cofactors Cdc20p and Cdh1p during mitosis and morphogenesis in *C. albicans*. The Anaphase-Promoting Complex/Cyclosome (APC/C) is a conserved regulator of mitosis. In mid-mitosis, APC/C activity depends on Cdc20p, which targets proteins such as Securin associated with the metaphase-to-anaphase transition, and B-type cyclins related to mitotic exit, for degradation. The APC/C then falls under the control of Cdh1p, which targets Cdc20p, Cdc5p, Clb2p and various spindle factors for destruction, thus allowing exit from mitosis (1). Intriguingly, APC/C activity extends beyond mitotic cell cycle control (1) as Cdc20p and Cdh1p function is also important for the stability of factors involved in developmental processes (2, 3). Since the APC/C is crucial for mitotic progression in most systems, and is a target of Plks and the Spindle Assembly Checkpoint, we hypothesized that it may also be an important regulator of mitosis in *C. albicans*, and mediate in part the influence of Cdc5p. We utilized genetic and biochemical approaches to demonstrate that Cdc20p has conservation in function in that it is required for the metaphase to anaphase transition and mitotic exit, and contributes to the degradation of the mitotic cyclin Clb2p. Its absence also resulted in filaments identical to Cdc5p-depleted cells, suggesting that the factors lie in a pathway governing mitotic progression and associated polar growth. The APC/C co-activator Cdh1p also showed conservation in being required for mitotic exit, but was novel in that cells lacking the factor were enlarged, unlike the situation in *S. cerevisiae* where *cdh1*Δ cells are very small. This was the first report of APC/C function in mitosis and morphogenesis of *C. albicans*. The results suggest variations in the mitotic networks between *S. cerevisiae* and *C. albicans*, which has important implications for controlling growth.

ABSTRACT

The conserved anaphase-promoting complex/cyclosome (APC/C) mediates protein degradation during mitotic progression. Conserved coactivators Cdc20p and Cdh1p regulate the APC/C during early to late mitosis and G1 phase. *Candida albicans* is an important fungal pathogen of humans, and forms highly polarized cells when mitosis is blocked through depletion of the polo-like kinase (Plk) Cdc5p or other treatments. However, the mechanisms governing mitotic progression and associated polarized growth in the pathogen are poorly understood. In order to gain insights on these processes, we characterized *C. albicans* orthologues of Cdc20p and Cdh1p. Cdc20p-depleted cells were blocked in early or late mitosis with elevated levels of Cdc5p and the mitotic cyclin Clb2p, suggesting that Cdc20p is essential and has some conserved functions during mitosis. However, the yeast cells formed highly polarized buds rather than large doublets like *S. cerevisiae cdc20* mutants, implying a distinct role in morphogenesis. In comparison, *cdh1Δ/cdh1Δ* cells were viable, but showed enrichment of Clb2p and Cdc5p, suggesting that Cdh1p is important for mitotic exit. The *cdh1Δ/cdh1Δ* phenotype was pleiotropic, consisting of normal or enlarged yeast, pseudohyphae, and some elongated buds, whereas *S. cerevisiae cdh1Δ* yeast cells were reduced in size. Thus, *C. albicans* Cdh1p may have some distinct functions. Finally, absence of Cdh1p or Cdc20p had minor or no effect on hyphal development, respectively. Overall, the results suggest that Cdc20p and Cdh1p may be APC/C activators that are important for mitosis but also morphogenesis in *C. albicans*. Their novel features imply additional variations in function and underscore rewiring in the emerging mitotic regulatory networks of the pathogen.

2.1 INTRODUCTION

Ubiquitin-mediated protein degradation plays a key role in regulating many stages of cell cycle progression. E3 ubiquitin ligases cooperate with E1 ubiquitin activating and E2 ubiquitin conjugating enzymes to add ubiquitin residues to specific factors, thereby targeting them for degradation via the proteasome (4). The APC/C represents an E3 ubiquitin ligase system that is crucial for controlling mitotic progression and maintenance of G1 phase (4). The APC/C is required to reduce mitotic cyclin-dependent kinase (CDK) activity, separate sister chromatids, disassemble the mitotic spindle, and load DNA replication origins (5). APC/C substrate specificity is determined by conserved coactivators, including Cdc20p and Cdh1p (4, 5). Cdc20p targets the degradation of proteins associated with the metaphase to anaphase transition and mitotic exit. In *S. cerevisiae*, this includes the securin Pds1p (6), and B-type cyclins such as Clb2p and Clb5p, for example (7-9). In the absence of Cdc20p, *S. cerevisiae* cells arrest in metaphase (10) or in later stages of mitosis if Pds1p is also absent (11). Towards the end of mitosis and during G1 phase, APC/C activity is regulated by Cdh1p, which maintains degradation of Clb2p and targets other mitotic regulators for destruction, including Cdc20p, the Plk Cdc5p, and various spindle factors (12-16). *CDH1* in *S. cerevisiae* is not essential, due to activity of the Cdc28p/Clb2p inhibitor Sic1p; *cdh1Δ sic1Δ* cells are not viable (17). However, *cdh1Δ* cells grow slowly with mild delays in mitotic exit and abnormalities in spindle formation (17, 18). The cells are small and accelerate expression of the ribonucleotide reductase *RNR1*, demonstrating that Cdh1p has a negative influence on Start (19). Intriguingly, APC/C activity extends beyond mitotic cell cycle control (4, 20), as Cdc20p and Cdh1p function is also important for the stability of factors involved in developmental processes, including axon growth and dendrite morphogenesis, for example (2, 3).

Candida albicans is one of the most common fungal pathogens of humans, and exists in different forms, including white phase yeast, mating-competent opaque phase yeast, pseudohyphae, hyphae, or chlamydospores (21). Differentiation is an important virulence-determining trait, because mutants incapable of switching between cell types are significantly less pathogenic (22, 23). The regulation of developmental events, including the yeast-to-hyphal switch for example, has been extensively investigated, and involves a diversity of environmental

cues and signaling pathways (21, 24-27). However, the mechanisms governing basic cell proliferation, including mitotic progression, are much less understood. Transcriptional responses of *C. albicans* yeast cells passing through mitosis show some similarity to those of *S. cerevisiae* cells (28, 29), but functional studies on many of the associated genes are lacking. Of the few factors investigated, several show differences in function from their orthologues in *S. cerevisiae*, and influence morphogenesis. For example, absence of the CDK Cdc28p results in a pleiotropic, filamentous phenotype (30), unlike in *S. cerevisiae* (10). The two B-type cyclins in *C. albicans*, Clb2p and Clb4p, must be degraded for exit from mitosis (31), but unlike in *S. cerevisiae*, Clb2p is not required for mitotic entry; Clb2p-depleted cells arrest in telophase and form elongated buds. Expression of a non-degradable form of Clb2p also results in elongated buds in *C. albicans* (31). In contrast, Clb4p-depleted cells are delayed at earlier stages of mitosis, and form pseudohyphae. Clb4p was also shown to function as an S phase cyclin (32). Absence of Sol1p, a functional homologue of the Cdc28p/Clb2p inhibitor Sic1p, resulted in transient elongated bud growth (33), while depletion of Mcm1p, a proposed transcriptional regulator of G2/M-associated genes in *C. albicans* (29), lead to the production of pseudohyphae followed by hyphae (34). Mitotic effects, however, were not reported in either case. *C. albicans* has orthologues of Cdc14p phosphatase, which activates Cdh1p upon being released from the nucleolus by the Cdc14p Early Anaphase Release (FEAR) pathway and the Mitotic Exit Network (MEN) following degradation of Pds1p in *S. cerevisiae* (35-39), as well as the MEN kinase Dbf2p. Both factors were important for mitotic exit and cell separation, but had additional novel functions and were differentially required for cell viability compared to the situation in *S. cerevisiae* (40, 41). Cdc5p, a polo-like kinase associated with the MEN and FEAR pathways in *S. cerevisiae* (42), is required at earlier stages of mitosis in *C. albicans*, and its depletion resulted in elongated bud growth (43, 44), in contrast to the large doublet morphology of *cdc5* null mutants in *S. cerevisiae* (45). Mitotic spindle checkpoints are not well defined in *C. albicans*, but orthologues of Mad2p and Bub2p were found to be dispensable for yeast and hyphal growth (43, 46, 47), yet important for elongated bud growth associated with mitotic arrest (43, 46). Thus, some key factors controlling mitosis have been identified in *C. albicans*, but a comprehensive picture of the mitotic regulatory networks is lacking.

The roles of ubiquitin-mediated protein degradation in cell cycle progression of *C.*

albicans are also poorly understood. The Skp, Cullin, F-box (SCF) E3 ubiquitin ligase complex targets degradation of proteins during G1/S to G2/M phases of the cell cycle in most systems, and orthologues of some components have been characterized in *C. albicans*, including Cdc4p, Grr1p and Cdc53p (33, 48-50). Absence of these factors resulted in pseudohyphal and/or hyphal growth. Specific cell cycle defects in the absence of Cdc4p or Cdc53p were not reported, but Grr1p influenced G1 cyclin stability, suggesting that SCF activity may be important for G1/S phase of the cell cycle (49). APC/C activity, on the other hand, has not been investigated to date in *C. albicans*.

In order to gain more insights on the regulation of mitosis in *C. albicans*, and explore the link between mitotic progression and polarized morphogenesis, we characterized orthologues of APC/C activators Cdc20p and Cdh1p. While both factors show some conservation in mitotic function, their novel features imply additional distinct roles. Overall, our results suggest that the APC/C is important for mitosis and morphogenesis in *C. albicans*, and underscore variations in the mitotic regulatory networks of the pathogen.

2.2 MATERIALS AND METHODS

2.2.1 Strains, oligonucleotides, plasmids, culture conditions, RNA extraction

Strains, oligonucleotides and plasmids used in this study are listed in Tables 2.1, 2.2 and 2.3 respectively. Strains were grown at 30°C in synthetic minimal medium containing 0.67% yeast nitrogen base, 2% glucose and all amino acids. For conditional expression of the *MET3* promoter, minimal inducing medium (-MC) lacking methionine and cysteine or minimal repressing medium (+MC) containing 2.5 mM methionine and 0.5 mM cysteine was utilized (51). Alternatively strains were grown in rich medium (YEPD) containing 1% yeast extract, 2% peptone and 2% dextrose (52). To investigate cells under hyphal-inducing conditions, 10% fetal bovine serum (FBS) (Wisent Inc, St. Bruno, QC) was added to minimal or rich medium, and cells were incubated at 37°C. For phenotypic assays, strains were grown overnight, diluted into fresh medium to an O.D._{600nm} of 0.2, and collected after indicated times. Total RNA extraction and Northern blotting were carried out as previously described (43).

Table 2.1: *Candida albicans* strains used in this study

Strains	Genotype	Source
BWP17	<i>ura3Δ:imm434/ura3Δ:imm434, his1Δ::hisG/his1Δ::hisG arg4Δ::hisG/arg4Δ::hisG</i>	Wilson <i>et al.</i> 1999
HCCA1	<i>CDC20/cdc20Δ::URA3</i>	This study
HCCA5	<i>CDH1/cdh1Δ::URA3</i>	This study
HCCA7	<i>CDC5/cdc5Δ::hisG</i>	This study
HCCA26	<i>cdh1Δ::URA3/MET3::CDH1-HIS1</i>	This study
HCCA45	<i>cdh1Δ::URA3/cdh1Δ::HIS1</i>	This study
HHCA100	BWP17 pRM100 (<i>URA3, HIS1</i>)	This study
HHCA109	<i>cdc20Δ::URA3/MET3::CDC20-HIS1</i>	This study
HHCA118	<i>cdc5Δ::hisG/MET3::CDC5-ARG4</i>	This study
HHCA131	<i>cdc5Δ::hisG/MET3::CDC5-ARG4 CDH1/cdh1Δ::URA3</i>	This study
HHCA143	<i>cdc5Δ::hisG/MET3::CDC5-ARG4 cdh1Δ::HIS1/cdh1Δ::URA3</i>	This study
HHCA153	<i>cdh1Δ::URA3/cdh1Δ::ARG4</i>	This study
AG120	<i>CDC5/CDC5-TAP-URA3</i>	This study
AG139	<i>CLB2/CLB2-HA-HIS1</i>	This study
AG145	<i>CDC20/cdc20Δ::URA3, CLB2/CLB2-HA-HIS1</i>	This study
AG153	<i>cdc20Δ::URA3/MET3::CDC20-ARG4 CLB2/CLB2-HA-HIS1</i>	This study
AG191	<i>cdc20Δ::URA3/MET3::CDC20::HIS1 CDC5/CDC5-TAP-ARG4</i>	This study
AG262	<i>cdh1Δ::HIS1/cdh1Δ::URA3, CDC5/CDC5-TAP-ARG4</i>	This study
AG268	<i>cdh1Δ::URA3/cdh1Δ::HIS1 CLB2/CLB2-HA-ARG4</i>	This study

Table 2.2: Oligonucleotides used in this study

HCGS1	AGTCATTTCCATCCATCAGTCTAATCAACT
HCGS1R	GGATTGTAGTTGATCAATGATATGGATCTT
HC2F	GCTTATTTCCATTCAACTATAATACTTATTCAACCCCTAA CATTATGTCATTGGTATCTCCCAACAGTAAACCAACAAT TTATAGGGCGAATTGGA GCT C
HC2R	ATATGGTTTGCATTAAGTAAAATCGTTTGGTAGTGACCA CTCTTTGGTGGTTTTACAATGCCAAAATCGTTATTATAGA GGACGGTATCGATAAGCTTGA
HCGS21F	ATGTCATTGGTATCTCCCAACAGTAAACCA
HCGS4B	TATATGTATTTCTGGTGCCGCACTAGGTAA
HCGS22F	AAGATCCATATCATTGATCAACTACAATCCGGATCCTGGA GGATGAGGAG
HCGS22R	TGGTTTACTGTTGGGAGATACCAATGACATCATGTTTTCTG GGGAGGGTA
HC3F	CTGTTTGAGACTCCTAGGTCGCCATCACGATCAACCAGA AGTCTAAATCCTCCCAAGTTGAACGAAATGGGTGCTATA CATATAGGGCGAATTGGAGCTC
HC3R	CCCGTTTCAAAGAAGACATTTGGGTTTATTGTTGATTGAATT TCTGTATCAATTGGCTGCAGTTACTCCAGGACAACCTTAGACG GTATCGATAAGCTTGA
HC5F	CTGTTTGAGACTCCTAGGTCGCCATCACGATCAACCAGA AGTCTAAATCCTCCCAAGTTGAACGAAATGGGTGCTATA CAGGAT CCTGGAGGATGAGGAG
HC5R	GATTTGCTTCCTCTTCTTCTAATTTCTATTTTATTATCAG CGTTTCTAGTGTCTTCTCAAATCCGGTAGTATTTCTCAT GTTTTCTGGGGAGGGTA
HCGS7F	TCTATCAGCAGGTCATGAAGACTACAAACT
HCGS7R2	AGATGTTCAACTCTTGATTAGTATGGATTG
HCGS16F	TTCAAGTCGTTCAAGTGAAAGTGTCACATT
HCGS16R	ATGACCAGGCCAATGGCTATATAATTTCGAG
HCGS17F	AGACCTTCTAAGGACAATGCTATCCGTAATTATAGGGCGA ATTGGAGCTCTATAGGGCGAATTGGAGCTC
HCGS17R	AATGTGACACTTTCACCTTTCACCTTGAACGACTTGAAGACG GTATC GAT AAG CTTGA
HCGS13F	TCGAGCAGGACCAATTGCGATGTAATCAAA
HCGS13R	GGTTAAACCTCTTTAATAATCAATGCTGGT
HCGS14F	ACCAGCATTGATTATTAAGAGGTTTAACCGGATCCCCCT TTAG TAAGA
HCGS14R	CTGTAAAGGTTGTGAACGAAGCGCCGACATGTTTTCTGGG GAGGGTA

HCGS15F	ATG TCG GCG CTT CGT TCA CAA CCT TTA CAG
HCGS15R	TAA AGA ATC TAA CCT CTG GTT CAG ACA CTC
HCGS32F	CAGAAGAAGTGGTACCAAGC
HCGS32R	CTCTTCTGCTTCTGCTACCA
HCGS33F	TGGTAGCAGAAGCAGAAGAGCGGATCCCCGGGTAAATTA
HCGS33R	ACCTAGATCCAATAGTCATCGAATTCCGGAATATTTATG AGAAAC
HCGS34F	GATGACTATTGG ATCTAGGT
HCGS34R	TCTGAAACATGATTG AGTAG
AG1F	TTTGAAGCAAGGAAACTTTCAGCATGAAAATGTTCCGGAC TGTATGGAGAAGATAATGGTCATCAAAGAAGCTATCAAGAA AAAAGCATTAAAGAAGCTGGTCGACGGATCCCCGGGTT
AG1R	TATTATATCTCTTGTGTTTATAATGAATATGGGCTACAGTTCA ATTTGCAAGTGTCTACTAAATAAAAGGATGTTTATTAGCAA CGTGAAAGTGGCA
AG2F	TAT TCGATGAATTCGAGCTCGTT
AG2R	GCCAGGGCGTTTAACTCAA
AG4F	ATAGTTACGATTAGTGGTGG
AG4R	GGTCGACGGATCCCCGGGTTATACCCATACGATGTTCCCTGAC
AG5F	TCGATGAATTCGAGCTCGTT ATCAGGAAGAGATTTGTTTGATGAACGATTATCGACCCATAGGC TAACATTAGAAGATGATGACGAAGAAGAAGAAATAGTGGTAGCA
AG5R	CAGAAGGAAGAGGGTCGACGGATCCCCGGGTT ATTATAGGGTAATGCACATAACTCATGTTTCTTTTTCATTTT CTCATTTATGCATTGTAAAGATAAGAACCTAGATCCAATAGTCAT
AG6F	CAAACTTTATCGATGAATTCGAGCTCGTT
AG6R	GAAGTAGGGGAAAGAAGTCA
AGHCURA3F	AGTAGGACACCAATGGGTTG AAGATCCATATCATTGATCAACTACAATCCGGATCCGGATGG
AGHC22F	TATAAACG AAGATCCATATCATTGATCAACTACAATCCGGATCCCCCCTTT
AGHC-NAT-1F	AGTAAGA AAGATCCATATCATTGATCAACTACAATCCAATTAACCCTCACT
AGHC-NAT-1R	AAAGGG TGGTTTACTGTTGGGAGATACCAATGACATTAATACGACTC
AGHC22R	ACTATAGGG AAGATCCATATCATTGATCAACTACAATCCGGATCCCCCCTTTAG TAAGA

Table 2.3:	Plasmids used in this study	Source
pRM100	pUC19 <i>URA3,HIS1</i>	J. Pla
pBS- <i>CaURA3</i>	pBluescript <i>URA3</i>	A. J. P. Brown
<i>pBS-CaARG4</i>	PBluescript <i>ARG4</i>	C. Bachewich
pBS- <i>CaHIS1</i>	pBluescript <i>HIS1</i>	C. Bachewich
pFA- <i>HIS1</i> -Met3p	pFA <i>HIS1</i> -Met3p	Gola <i>et al.</i> 2003
pFA- <i>ARG4</i> -Met3p	pFA <i>ARG4</i> -Met3p	Gola <i>et al.</i> 2003
pFA- <i>HIS1</i> -Mal2p	pFA <i>HIS1</i> -Mal2p	Gola <i>et al.</i> 2003

2.2.2 Strain construction

A strain carrying a single copy of *CDC5* under control of the *MET3* promoter was created. The first copy of *CDC5* (orf19.6010) was deleted from strain BWP17 using the *URA3* blaster method as previously described (44, 53), followed by looping out of the *URA3* marker and selection on 5'-fluorootic acid (Sigma-Aldrich, Oakville, ON) (44), resulting in strain HCCA7. The second copy of *CDC5* was then placed under the regulation of the *MET3* promoter, using a PCR fusion construct (54, 55). Oligonucleotides HCGS13F and HCGS13R amplified 640 bp of 5' *CDC5* flanking sequence from genomic DNA (gDNA), while oligonucleotides HCGS15F and HCGS15R amplified the *CDC5* start site and 518 bp of downstream sequence. Oligonucleotides HCGS14F and HCGS14R amplified an *ARG4-MET3* fragment from plasmid pFA-ARG4-MET3 (56). The 3 resulting fragments were combined and amplified with oligonucleotides HCGS13F and HCGS15R, and the final promoter replacement construct was transformed into strain HCCA7, resulting in strain HCCA118. In order to construct a strain containing a single copy of *CDC20* under the control of the *MET3* promoter, oligonucleotides HC2F and HC2R containing 80 bp homology to the 5' and 3' *CDC20* flanks, respectively, amplified *URA3* from pBS-*CaURA3*. The product was transformed into strain BWP17, generating strain HCCA1. To place the remaining copy of *CDC20* under the control of a *MET3* promoter, oligonucleotides HCGS1 and HCGS1R amplified 515 bp of *CDC20* 5' flanking sequence and oligonucleotides HCGS21F and HCGS4B amplified a fragment containing the *CDC20* start site and 720 bp of downstream sequence. A *HIS1-MET3* fragment was amplified from plasmid pFA-HIS-MET3 (56) with oligonucleotides HCGS22F and HCGS22R. The products were combined in a fusion PCR reaction with oligonucleotides HCGS1 and HCGS4B, and the resulting construct was

transformed into strain HCCA1, resulting in strain HCCA109. An isogenic control strain was created by transforming pRM100 into strain BWP17, creating strain HCCA100.

In order to delete both copies of *CDH1*, oligonucleotides HC3F and HC3R containing 80 bp of *CDH1* 5' and 3' flanking sequences, respectively, were used to amplify *URA3* from plasmid pBS-CaURA3. The resulting deletion construct was transformed into strain BWP17, generating strain HCCA5. To replace the second copy of *CDH1* with *HIS1*, oligonucleotides HCGS7F and HCGS7R2 amplified a 620 bp fragment homologous to the 5' flank of *CDH1*, while oligonucleotides HCGS16F and HCGS16R amplified a 560 bp fragment homologous to the 3' flank. Oligonucleotides HCGS17F and HCGS17R amplified a *HIS1* fragment from plasmid pBS-CaHIS1. The products were combined in a PCR reaction with oligonucleotides HCGS7F and HCGS16R, and the final construct was transformed into strain HCCA5, resulting in strain HCCA45. A second deletion strain was constructed in a similar manner, except that the remaining *CDH1* allele of strain HCCA5 was replaced with an *ARG4* marker, resulting in strain HHCA153. The *ARG4*-containing fragment was amplified from pBS-CaARG4 with oligonucleotides HC3F and HC3R. In order to determine if Cdh1p was in the same functional pathway as Cdc5p, one copy of *CDH1* was replaced with *URA3*, as described above, in strain HCCA118, resulting in strain HHCA131. The second copy was replaced with *HIS1*, as described, resulting in strain HCCA143. In order to confirm the *CDH1* deletion phenotype, a strain carrying a single copy of *CDH1* under control of the *MET3* promoter was created. Oligonucleotides HC5F and HC5R containing 80 bp homology to sequences upstream and downstream of the *CDH1* start site, respectively, amplified a *HIS1-MET3* fragment from pFA-HIS1-MET3 (56). The product was transformed into strain HCCA5, resulting in strain HCCA26. All strains were confirmed by PCR and Southern blot analysis (data not shown).

In order to tag Clb2p with three copies of hemagglutinin (HA), *HA-HIS1* was amplified from plasmid pFA-HA-HIS1 (57) with oligonucleotides AG4F and AG4R. The product was used as a template in a PCR fusion reaction with oligonucleotides AG5F and AG5R, which contained 100 bp homology to regions lying upstream and downstream from the stop codon of *CLB2*, respectively. The fusion construct was transformed into strains BWP17 and HCCA1, generating strains AG139 and AG145, respectively. The remaining copy of *CDC20* in strain

AG145 was placed under the control of a *MET3* promoter as described, with the exception of using an *ARG4-MET3* fragment amplified from plasmid pFA-ARG4-MET3 (56) with oligonucleotides AGHC22F and HCGS22R. The final fusion product was transformed into strain AG145, resulting in strain AG153. Clb2p was similarly tagged with HA in strain HHCA45, with the exception of using pFA-HA-ARG4 (57) as a template with oligonucleotides AG4F and AG4R, resulting in strain AG268. In order to tag Cdc5p with TAP, PCR fragments containing either *URA3* or *ARG4* and 100 bp homology to sequences immediately up and downstream from the stop codon of *CDC5* were created with oligonucleotides AG1F, AG1R and plasmids pFA-TAP-URA3 or pFA-TAP-ARG4 (57). PCR constructs were transformed into strains BWP17, HCCA109 and HCCA45, resulting in strains AG120, AG191 and AG262, respectively. All tagged strains were confirmed by PCR and Western blotting.

PCR reactions utilized Expand Long Template Polymerase (Roche Diagnostics, Laval, QC). Cells were transformed using lithium acetate (56, 58) with modifications. Transformation mixtures were incubated overnight at 30°C and heat shocked at 43°C for 15-60 min prior to plating on selective medium. For increased transformation efficiency in the conditional *CDC5* strains, cells were grown overnight in minimal inducing medium lacking methionine and cysteine, then transferred into rich YEPD medium for at least 1.0 h prior to transformation.

2.2.3 Cell staining, imaging

To visualize nuclei, cells were fixed with 70% ethanol for a minimum of 1 h, stained with 1 µg/ml of 4', 6'-diamidino-2-phenylindole dihydrochloride (DAPI) (Sigma-Aldrich) for 20 min, and washed with sterile water. To visualize septa, fixed cells were subsequently stained with 2 µg/ml calcofluor white (Sigma-Aldrich) for 10 min. For immunolocalization of α -tubulin, overnight cultures of cells were diluted to an O.D._{600nm} of 0.2, and incubated for the indicated times in minimal or rich medium. An equal volume of 2X fixative, containing 8% paraformaldehyde, 80 mM PIPES pH 7.0, 10 mM MgSO₄, 50 mM EGTA, 8 mM AEBSF, 20 µg/ml leupeptin, and 2 µM aprotinin was added to cells. Following 20 min of fixation, cells were washed twice with chilled PE buffer (40 mM PIPES, 25 mM EGTA pH 7.0). Cell walls were digested with 10 µg/ml Zymolaze 100T in 1.2 M Sorbitol, 2% BSA, and protease inhibitors as

described for 30 min at 37°C. Cells were then rinsed twice with ice-cold PE buffer, permeabilized with ice-cold 0.1% Nonidet P-40 detergent for 5 min, and rinsed with PE buffer. Cells were incubated overnight at 4°C in anti- α -tubulin antibody (DM1A, Sigma-Aldrich) (1:100) in PE buffer containing 0.05% sodium azide, and 2% BSA. Cells were washed with PE buffer and incubated in sheep anti-mouse FITC secondary antibody (Sigma-Aldrich) (1:100) in the dark for 2 h at room temperature. Cells were then rinsed with PE buffer and stained with 1 μ g/ml DAPI for 20 min. Cells were examined on a Leica DM6000B microscope (Leica Microsystems Canada Inc. Richmond Hill, ON) equipped with a Hamamatsu-ORCA ER camera (Hamamatsu Photonics, Hamamatsu City, Japan) using 63X, or 100X objectives and DAPI (460nm) or FITC (520nm) filters. Images were captured with Openlab software (Improvision Inc, Perkin Elmer, Waltham, MS).

2.2.4 Protein extraction and Western blotting

Protein extracts were prepared according to Bensen *et al.*, 2005 with some modifications. For assays involving conditional expression of *CDC20*, exponential phase cells grown in minimal inducing (-MC) medium were diluted to an O.D._{600nm} of 0.1 in either minimal repressing (+MC) or inducing medium, and collected after 3 or 6 h of incubation at 30°C. In order to determine the levels of Clb2p-HA and Cdc5p-TAP in *cdh1 Δ /cdh1 Δ* cells, strains were incubated overnight in YEPD medium supplemented with 50 μ g/ml uridine. A proportion of the overnight culture was collected, while the remaining cells were diluted to an O.D. _{600nm} of 0.1 in fresh YEPD, incubated at 30°C, and collected at the indicated times. Proportions of budded cells were scored for each time point. Protein was extracted from cell pellets by adding 20 μ l of RIPA buffer (10 mM sodium phosphate, 1% Triton X 100, 0.1% SDS, 10 mM EDTA, 150 mM NaCl, pH 7.0, 1 mM AESBF, 5 μ g/ml of leupeptin and 5 μ g/ml of aprotinin) and 200 μ l of glass beads. Cells were disrupted for 3 x 45 sec in a bead beater (Biospec Products, Bartlesville, OK), with 2 min intervals on ice. An additional 200 μ l of RIPA buffer was added, and the extracts were centrifuged at 13,500 rpm for 5 min at 4°C. The supernatants were collected and stored at -80°C. Protein was quantified using the Bradford assay (Bio-Rad, Mississauga, ON), and 30 μ g were loaded onto SDS PAGE gels. Proteins were transferred to PVDF membrane (Bio-Rad), and blocked with TBST (50 mM Tris, pH 7.5, 137 mM NaCl, 0.1% Tween-20) containing 5% skim

milk for 1 h. Blots were washed 3 x 15 min in TBST, and incubated for 1.5 h in 0.4 µg/ml anti-HA antibody (12CA5, Roche) or 0.05 µg/ml anti-TAP (Thermo Scientific Open Biosystems, Huntsville, AL) diluted in TBST. Blots were rinsed 3 x 15 min in TBST and incubated for 1 h in a 1:10,000 dilution of horseradish peroxidase-conjugated secondary antibody. After washing, blots were developed using ECL (GE Healthcare, VWR, Ville Mont-Royal, QC). Blots were stripped and incubated with 0.2 µg/ml of anti-PSTAIRES (Santa Cruz Biotechnology, Santa Cruz, CA) as a loading control. Western blots were quantified using ImageJ (<http://rsb.info.nih.gov/ij/index.html>), according to <http://lukemiller.org/index.php/2010/11/analyze-gels-and-westernblots-with-image-j/>. Briefly, band density for Cdc5p-TAP, Clb2p-HA or PSTAIRES in each lane of a single blot was divided by that of the first lane for the given protein, in order to determine relative densities. The relative densities of Cdc5p-TAP or Clb2p-HA were then divided by the relative densities of PSTAIRES for the corresponding lane to obtain adjusted relative densities.

2.2.5 Cell size measurements

In order to determine the effect of deleting *CDH1* on cell size, strains HHCA45 and HHCA100 were incubated in YEPD medium at 30°C to an O.D._{600nm} of 0.8, sonicated, and fixed in 70% ethanol. Approximately 20,000 cells were analysed by forward light scattering, using a Becton-Dickinson LSRII Analytic Flow Cytometer. Alternatively, the lengths and widths were measured in approximately 100 cells in the yeast form, and multiplied to obtain values in µm². Measurements were taken from mother cells only, where the width corresponded to the widest part of the cell (59). Axial ratios were measured by dividing the length by the width of cells.

2.3 RESULTS

2.3.1 Depletion of Cdc20p results in highly polarized growth of yeast buds under yeast growth conditions

In order to further our understanding of how mitosis is regulated and linked to polarized morphogenesis in *C. albicans*, the potential involvement of APC/C activity was explored by characterizing orthologues of APC/C activators. We first investigated *CDC20* (*orf19.122*; <http://www.candidagenome.org/>), which shares 51% identity at the protein level with its

orthologue in *S. cerevisiae*. *CDC20* function was determined by constructing a strain carrying a single copy under control of the *MET3* promoter (51). Strains HCCA109 (*cdc20Δ::URA3/MET3::CDC20-HIS1*) and HCC100 (*CDC20/CDC20 URA3+ HIS1+*) were used for subsequent analyses. When incubated at 30°C for 2 days, both strains formed normal yeast colonies on solid inducing medium (-MC). However, on repressing medium (+MC), cells depleted of Cdc20p generated filaments, while control cells formed smooth colonies and grew in the yeast form (Fig. 2.1A). In liquid medium, the majority of cells depleted of Cdc20p for 3 h at 30°C were large-budded, many of which contained a short polarized extension. By 7 h, the cells contained highly elongated buds (Table 2.4, Figs. 2.1B, 2.2A), indicating maintenance of polarized growth. After 24 h, some cells contained constrictions and branches similar to pseudohyphae, and many were no longer viable, as shown with propidium iodide staining (Fig. S2.1), suggesting that *CDC20* may be an essential gene. In contrast, cells from the control strain (HCCA100) grew in the yeast form in either inducing or repressing medium (Table 2.2, Fig. 2.1B). The Cdc20p-depleted phenotype differs from that of *CDC20* null mutants in *S. cerevisiae*, which consist of large doublets (10). However, the phenotype resembles that of Cdc5p-depleted cells, suggesting that Cdc20p and Cdc5p may lie in the same pathway that governs mitotic progression and influences elongated bud growth.

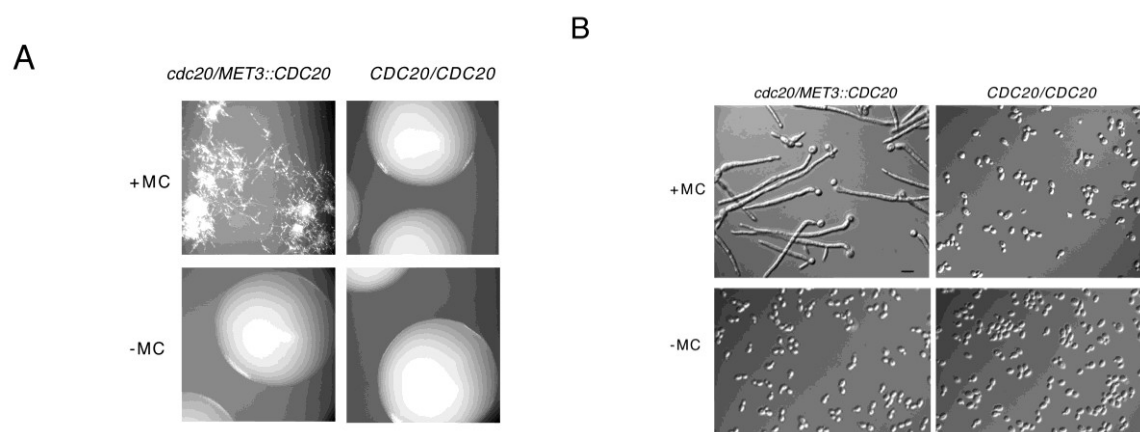


Figure 2.1: Depletion of Cdc20p results in filament formation under yeast growth conditions. (A) Strains HCCA109 (*cdc20Δ::URA3/MET3::CDC20-HIS1*) and HCCA100 (*CDC20/CDC20 URA3+ HIS1+*) were grown overnight in inducing medium (-MC), streaked onto either solid inducing or repressing (+MC) medium, and incubated at 30°C for 48 h. (B) Overnight cultures of the same strains were diluted in liquid repressing or inducing medium, and incubated for 7 h at 30°C. Bar: 10 μm.

Table 2.4: Number of nuclei¹ and cell morphology¹ in Cdc20p-depleted cells²

	<u>Number of nuclei</u>				<u>Cell morphology</u>		
	1	2	3	Frag ³	Unbudded/ small bud	Large bud	Elongated bud
<i>cdc20/</i>							
<i>MET3::CDC20</i>							
0 h (n=236)	81.8	18.2	0	0	91.1	8.9	0
3 h (n=173)	71.6	28.4	0	0	12.7	53.1	34.1
6 h (n=216)	22.2	54.2	2.8	20.8	3.0	2.0	95.0
<i>CDC20/CDC20</i>							
0 h (n=145)	95.0	4.8	0	0	93.1	6.9	0
3 h (n=120)	82.5	12.5	0	0	70.0	26.7	3.3
6 h (n=132)	84.0	16.0	0	0	74.2	23.5	2.3

¹ Values are expressed in %

² Cells from strains HCCA109 (*cdc20::URA3/MET3::CDC20-HIS1*) and HCCA100 (*CDC20/CDC20 URA3+ HIS1+*) were incubated in repressing medium (+MC) at 30°C and collected at indicated time points. Cells were fixed and stained with DAPI.

³ Fragmentation of chromosomes.

2.3.2 Cdc20p is required for early and late stages of nuclear division

Since Cdc20p is required for the metaphase to anaphase transition and mitotic exit in *S. cerevisiae* (6, 11), we next determined whether Cdc20p in *C. albicans* influenced mitosis. After 3 h of Cdc20p depletion, when most cells were either large doublets or slightly elongated, 28.4% contained two nuclei, while 71.6% contained a single nucleus (Table 2.4, Fig. 2.2A). In 72.6% of these cells, the nucleus was located in the mother cell with unsegregated chromosomes, suggesting a metaphase delay. The single nucleus was located in the bud neck in the remaining cells. At 6 h, when most cells were highly elongated, the majority contained two nuclei (Table 2.4). Nuclei were located exclusively in the filament of approximately 60% of these cells. In contrast, control cells showed normal proportions of budding cells and number of nuclei at 6 h (Table 2.4, Fig. 2.2A). To confirm the phase of mitosis in which Cdc20p is required, spindle patterns were analyzed by immunolocalizing α -tubulin. After 3 h in repressing medium, approximately 70% of *cdc20* Δ /*MET3::CDC20* cells were in mitosis, with 52.5% containing short rod-like metaphase spindles, and 18.5% containing long telophase spindles (Table 2.5, Fig. 2.2B). The remaining 29.0% of cells showed only spindle pole body staining, visualized as single or double spots, indicating cells were in interphase. At 6 h, 70.9% of cells contained long spindles, although the presence of cytoplasmic microtubules interfered with quantification in some cells. In contrast, fewer control cells contained mitotic spindles (Table 2.5). These results suggest that depletion of Cdc20p leads to an initial delay at metaphase, followed by a block in telophase, implying a role for Cdc20p at both stages of mitosis. In comparison, *CDC20* mutants in *S. cerevisiae* arrest in metaphase with a single nucleus positioned at the bud neck (10). In the absence of the securin Pds1p, however, the cells arrest in later stages of mitosis, consistent with an additional role during mitotic exit (9, 11, 60). Our results further suggest that polarized growth upon Cdc20p depletion is associated with an initial delay in metaphase.

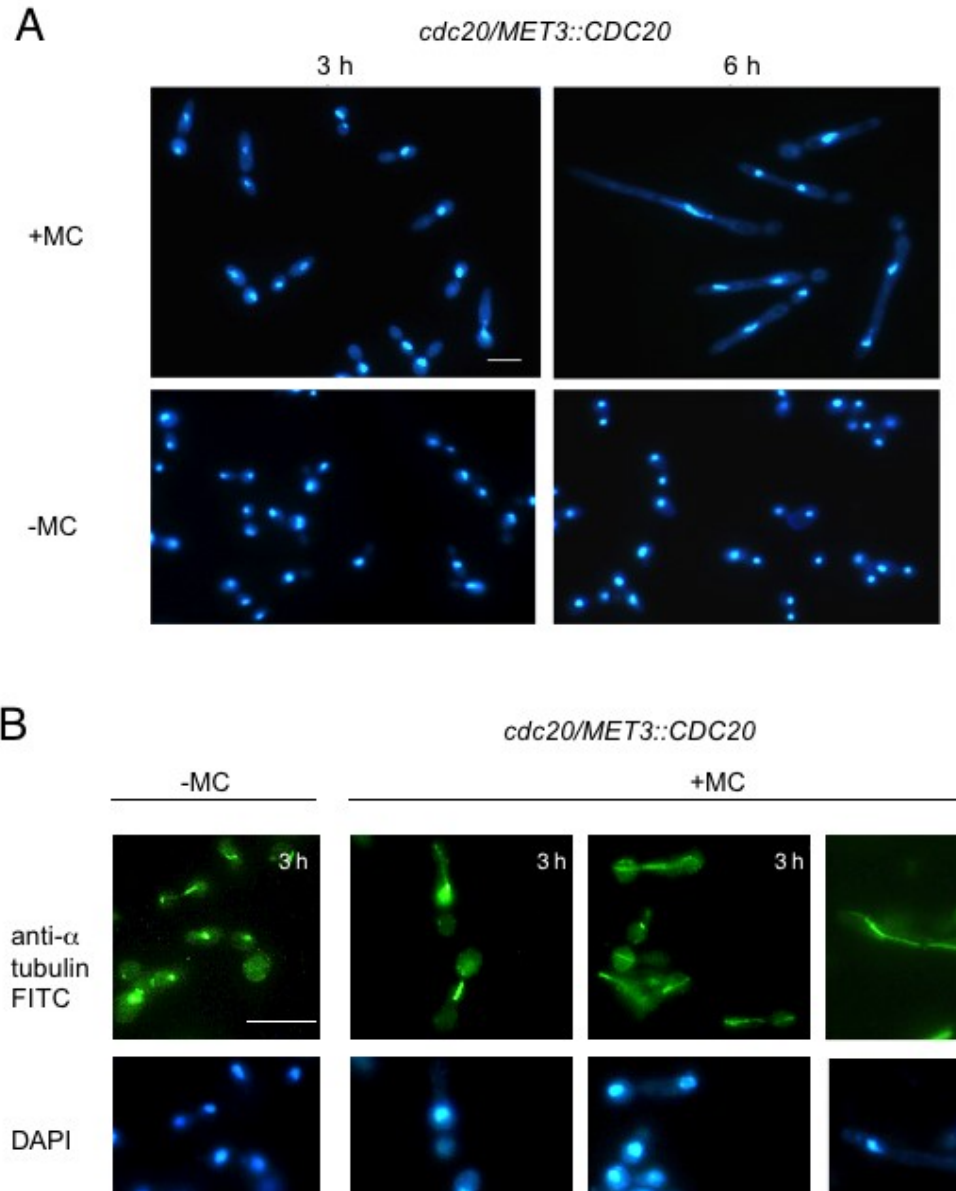


Figure 2.2: Cdc20p depletion results in a delay in metaphase and telophase. (A) Strains HCCA109 (*cdc20 Δ ::URA3/MET3::CDC20-HIS1*) and HCCA100(*CDC20/CDC20 URA3+ HIS1+*) were diluted into inducing (-MC) or repressing medium (+MC) for the indicated times, fixed, and stained with DAPI. (B) Strain HCCA109 was incubated in repressing or inducing medium for the indicated times, processed for immunolocalization of α tubulin, and stained with DAPI. Bar: 10 μ m.

Table 2.5: Spindle patterns¹ in Cdc20p-depleted cells²

<u>Strain</u>	<u>Interphase</u> ³	<u>Mitosis</u> ⁴	
		<u>early</u>	<u>late</u>
<i>cdc20/MET3::CDC20</i>			
3 h (n=200)	29.0	52.5	18.5
6 h (n= 320)	16.3	12.8	70.9
<i>CDC20/CDC20</i>			
3 h (n= 179)	83.2	3.9	12.8
6 h (n= 154)	77.2	13.0	9.7

¹ Values are expressed in %.

² Cells from strain HCCA109 (*cdc20::URA3/MET3::CDC20-HIS1*) and HCCA100 (*CDC20/CDC20 URA3+ HIS1+*) were incubated in repressing medium (+MC) for indicated times at 30°C and processed for immunofluorescence of α tubulin.

³ Cells containing single or double spots of tubulin representing spindle pole bodies without spindles indicated cells were in interphase.

⁴ Cells containing short rod-like spindles were in early mitosis, while those with longer spindles were in later stages of mitosis.

2.3.3 Cdc20p-depleted cells express *HWP1* at later stages of growth

We previously demonstrated that cells depleted of Cdc5p expressed some hyphal-associated genes, including *HWP1*, at later stages of growth (43, 44). In order to determine whether Cdc20p-depleted cells showed a similar response, *HWP1* expression was investigated by Northern blotting. When incubated in inducing medium (-MC), exponential phase *cdc20Δ/MET3::CDC20* yeast cells did not demonstrate expression of *HWP1* (Fig. 2.3). Incubation in repressing medium (+MC) for 6 h, which resulted in highly elongated buds, also did not induce *HWP1* expression. However, after 9 h in repressing medium, *HWP1* was strongly expressed in *cdc20Δ/MET3::CDC20* cells, in contrast to control cells (*CDC20/CDC20*) under identical conditions (Fig. 2.3). Thus, depletion of Cdc20p also results in delayed induction of a hyphal-associated gene.

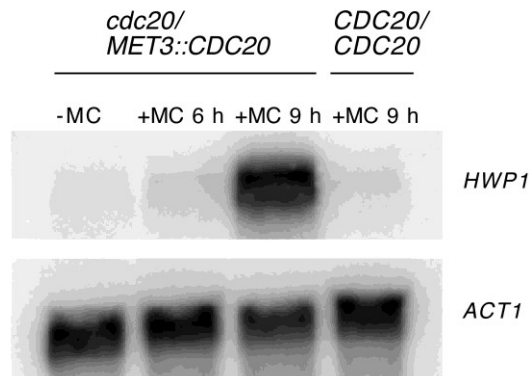


Figure 2.3: *HWP1* is expressed in Cdc20p-depleted cells at later stages of growth. Northern blot containing 20 μ g of total RNA extracted from exponential phase cells of strain HHCA109 (*cdc20Δ::URA3/MET3::CDC20-HIS1*) incubated in inducing medium (-MC) or when transferred to repressing medium (+MC) and incubated for the indicated times. Control strain BWP17 (*CDC20/CDC20*) was incubated in repressing medium for 9 h. *ACT1* was used as a loading control.

2.3.4 Cells lacking Cdh1p have a pleiotropic phenotype

Cdh1p regulates APC/C activity during late stages of mitosis and into G1 phase (9, 17, 18, 61). *Orf19.2084* of *C. albicans* is annotated as *CDHI* (<http://www.candidagenome.org/>), and shares 43.8% identity at the protein level with Cdh1p from *S. cerevisiae*. In order to investigate *CDHI* function, the alleles were sequentially replaced with *URA3* and *HIS1* markers, resulting in strain HCCA45. When incubated on solid YEPD medium at 30°C for two days, *cdh1Δ/cdh1Δ* colonies contained uneven edges, and were smaller in diameters and more elevated than control colonies (Fig. 2.4A). When grown in liquid YEPD medium for 7 h, approximately 70% of *cdh1Δ/cdh1Δ* cells were in a yeast form, while the remaining cells consisted of pseudohyphae and irregular-shaped elongated cells, as well as a small proportion of elongated buds (Fig. 2.4B, Table 2.6). A few cells (2.5%) showed narrow diameters, similar to true hyphae. In contrast, 97.5% of *CDHI/CDHI* cells grew in a normal yeast form (Fig. 2.4B, Table 2.6). To confirm that the phenotype was due to absence of Cdh1p, a strain containing a single copy of *CDHI* under control of the *MET3* promoter was created (HHCA26). When incubated in repressing medium (+MC) for 8 h, *cdh1Δ/MET3::CDHI* cells showed a pleiotropic phenotype, similar to *cdh1Δ/cdh1Δ* cells, whereas the control strain (HCCA100) formed normal yeast (Fig. S2.2). Some filamentation and abnormal cell morphologies were also observed in *cdh1Δ/MET3::CDHI* cells in inducing medium, but at lower frequencies compared to repressing conditions, which may reflect overexpression of *CDHI*. In *S. cerevisiae*, cells lacking Cdh1p were greatly reduced in size (19). However, the length-by-width measurements *C. albicans* cells only in the yeast form were greater in the absence of Cdh1p ($28.7 \pm 1.5 \mu\text{m}^2$, s.e.m., n=110, HHCA45 vs. $18.0 \pm 0.6 \mu\text{m}^2$, S.E.M, n=99, HHCA100) (Fig. S2.3). Forward light scattering confirmed that absence of Cdh1p did not result in a subpopulation of smaller cells; rather, cells were either similar or larger in size than control cells (Fig. 2.4C). Although the mean axial ratios did not greatly differ (1.31 ± 0.03 , n= 110, *cdh1Δ/cdh1Δ* vs 1.41 ± 0.03 , n=99, *CDHI/CDHI* cells), more *cdh1Δ/cdh1Δ* cells demonstrated identical length and width measurements (19.1%, n=110, *cdh1Δ/cdh1Δ* vs 7.0 %, n=99, *CDHI/CDHI* cells), indicating a subpopulation of cells were more round. Overall, the difference in phenotype from *S. cerevisiae* *cdh1Δ* cells (19) suggests that *C. albicans* Cdh1p may have some distinct functions.

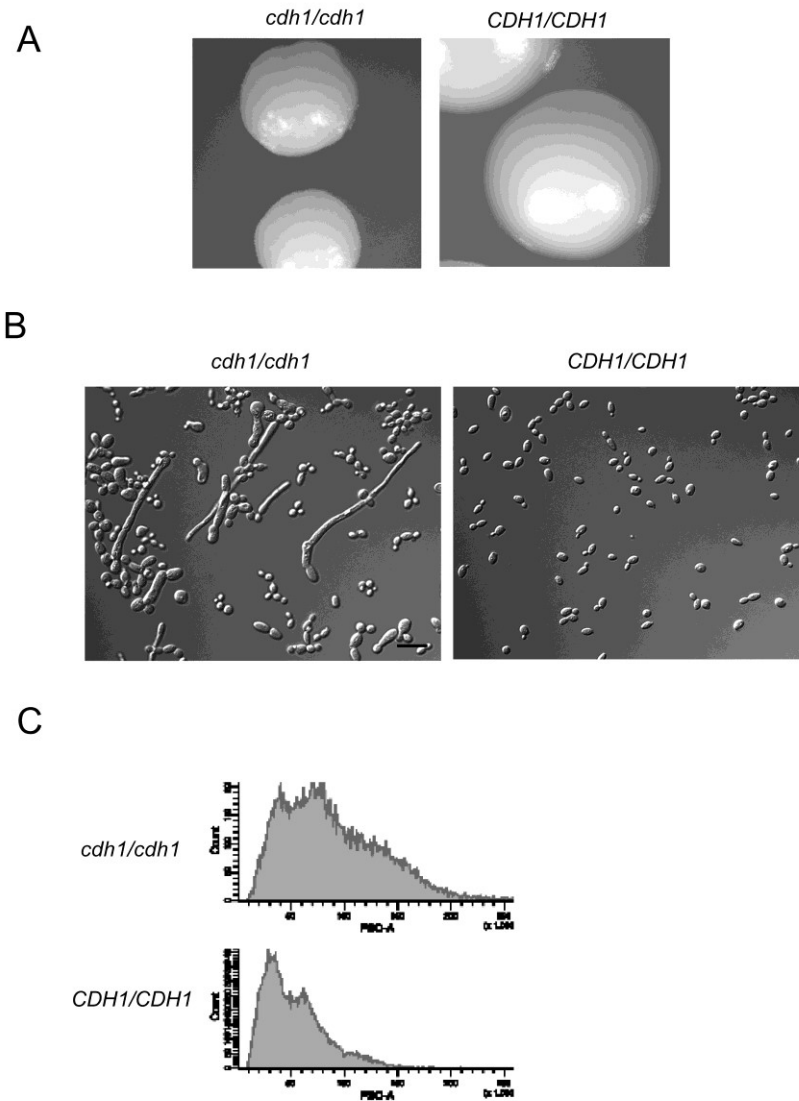
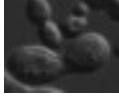


Figure 2.4: Cells lacking Cdh1p demonstrate a pleiotropic phenotype. (A) Strains HCCA45 (*cdh1Δ::URA3/cdh1Δ::HIS1*) and HCCA100 (*CDH1/CDH1 URA3+ HIS1+*) were incubated on YEPD plates for 48 h at 30 °C. (B) Strains incubated in liquid YEPD medium for 7 h and fixed. Bar: 10μm. (C) Strains incubated as in (B) were sonicated, fixed and subjected to forward (FSC-A) light scattering.

Table 2.6: Proportion of *CDH1*-deleted cells¹ exhibiting different morphologies

	Yeast	Pseudohyphal ²	Enlongated bud
			
<i>Δcdh1Δcdh1</i> (n=212)	68.9	19.4	11.7
<i>CDH1/CDH1</i> (n=202)	96.5	3.5	0

¹Values expressed in %. Overnight cultures of strains HCCA45 (*cdh1::URA3/cdh1::HIS1*) and HCCA100 (*CDH1/CDH1 URA3+ HIS1+*) were diluted into fresh YEPD medium, and incubated at 30°C for 7 h.

²Includes irregular-shaped, elongated cells and standard pseudohyphal cells (87).

2.3.5 Cdh1p is important, but not essential, for nuclear division and septation

Cdh1p in *S. cerevisiae* is important for mitotic exit; its absence results in a higher number of cells with separated nuclei and elongated spindles (17, 18), as well as abnormalities in chromosome segregation and spindle structure (62). To determine whether Cdh1p influenced mitosis in *C. albicans*, cells were incubated in YEPD for 7 h, fixed, processed for immunolocalization of α -tubulin, and/or stained with DAPI and calcofluor. In the absence of Cdh1p (HCCA45), slightly more cells contained long spindles compared to control cells (HCCA100) (30.8%, n=260 vs. 20.0%, n=240), suggesting a moderate delay in telophase. However, spindle microtubules appeared abnormal in some cells, and were often difficult to score due to abundant cytoplasmic microtubules (Fig. 2.5A). Nuclear division was also deregulated in 14.8% (n=216) of *cdh1 Δ /cdh1 Δ* cells. For example, two or more nuclei were present in unbudded yeast cells (5.1%), as well as in compartments of pseudohyphae and elongated buds (5.1%). Another proportion of pseudohyphal cells (4.6%) lacked nuclei in some compartments. In contrast, 100% of control cells (n=200) contained a normal number of nuclei. Notably, in 6.9% of *cdh1 Δ /cdh1 Δ* cells containing a single nucleus, the organelle was located across the bud neck (Fig. 2.5B), compared to 2.2% of control cells. Calcofluor staining demonstrated that *cdh1 Δ /cdh1 Δ* cells formed septa, but the presence of elongated and multi-budded cells (Fig. 2.5B) suggests some defects in cell separation. In comparison, elongated buds and defects in cytokinesis were observed in *S. cerevisiae* cells overexpressing *CDH1* or carrying a constitutively active form, but not when *CDH1* was absent (17, 63). Thus, most *C. albicans* cells lacking *CDH1* undergo nuclear division, septation, and cell separation, but a proportion of cells showing defects in these processes, coupled with the moderate increase in the number of telophase spindles, suggests that Cdh1p in *C. albicans* may influence the regulation of mitotic exit.

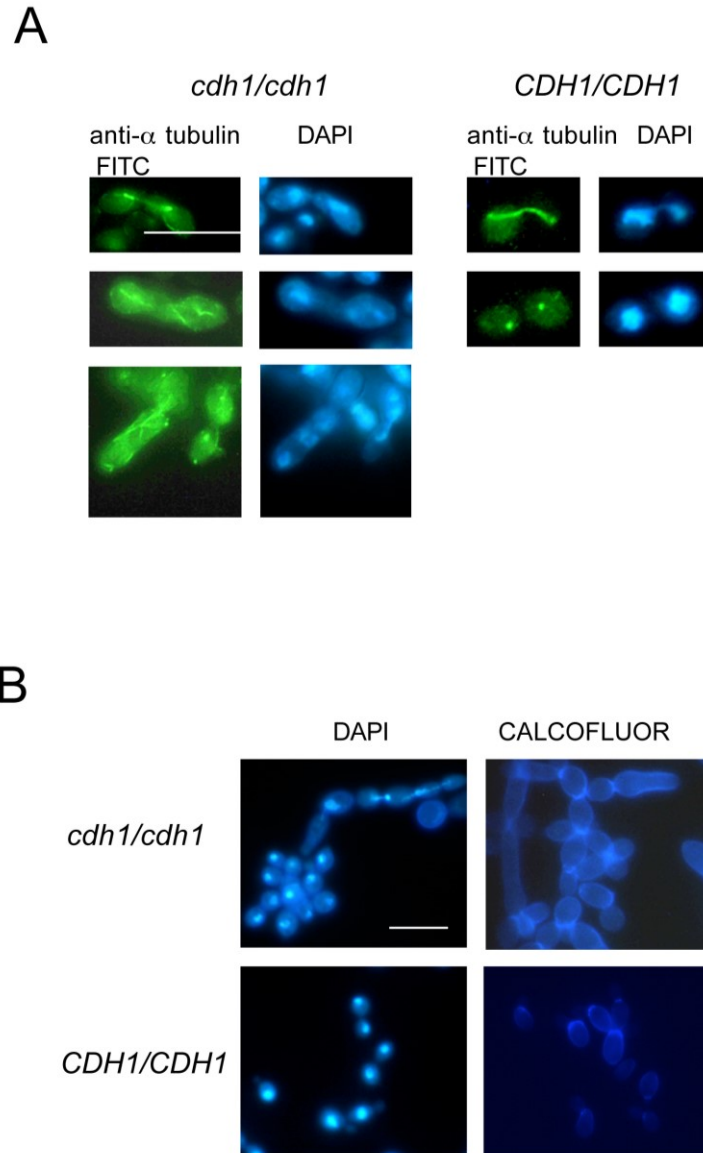


Figure 2.5: Absence of Cdh1p results in some defects in nuclear division and spindle formation. (A) Strains HCCA45 (*cdh1 Δ ::URA3/cdh1 Δ ::HIS1*) and HCCA100 (*CDH1/CDH1*) were incubated in YEPD medium for 7 h, fixed and stained with either DAPI or calcofluor. (B) Strains were incubated as in (A), processed for immunolocalization of α -tubulin and stained with DAPI. Bars: 10 μ m.

2.3.6 Clb2p and Cdc5p are elevated in Cdc20p and Cdh1p-depleted cells

Cdc20p directs APC/C-dependent degradation of the cohesin Pds1p in *S. cerevisiae*, and contributes to initial degradation of the mitotic cyclin Clb2p (7, 60). Cdh1p, on the other hand, activates APC/C-dependent degradation of Clb2p towards the end of mitosis and into G1 phase, and targets degradation of the Plk Cdc5p, as well as other factors including Cdc20p (7, 13-15, 17, 64). To determine whether Cdc20p and Cdh1p influence mitotic progression in *C. albicans* through similar means, we tagged Clb2p with HA and Cdc5p with TAP in strains lacking Cdc20p or Cdh1p. Following depletion of Cdc20p (+MC), Clb2p-HA was elevated relative to levels in the same strain (AG153) under *CDC20* inducing conditions (-MC), particularly at 3 h, as well as compared to control cells (AG139) grown in either inducing or repressing medium (Fig. 2.6A). In addition, Cdc5p-TAP was enriched in repressing vs inducing medium in *cdc20Δ/MET3::CDC20* cells (AG191), and compared to that in control cells (AG120) in either medium (Fig. 2.6A). Untagged control strain BWP17 did not show any signal for either protein. These results suggest that Cdc20p influences the stability of Clb2p, as well as Cdc5p, consistent with the notion that Cdc20p-depleted cells were blocked in mitosis. Since Cdh1p maintains degradation of Clb2p and Cdc5p into G1 phase in *S. cerevisiae*, we next investigated the levels of Clb2p-HA and Cdc5p-TAP in overnight cultures of *cdh1Δ/cdh1Δ* (AG268, AG262) and *CDH1/CDH1* (AG139, AG120) cells that were semi-synchronized in an unbudded state, and at subsequent time points after inoculation into fresh medium. In overnight cultures, when approximately 90% of the cells were unbudded, the control strains showed very little signal for Cdc5p-TAP or Clb2p-HA. However, as cells proceeded to bud, the levels of both proteins increased (Fig. 2.6B), consistent with both factors peaking later in the cell cycle (29, 65). In contrast, overnight cultures of strains lacking Cdh1p, which contained similar proportions of unbudded cells as the control strains, demonstrated strong enrichment of Cdc5p-TAP and Clb2p-HA (Fig. 2.6B). Cdc5p-TAP levels continued to accumulate as more cells proceeded through the cell cycle, as expected if Cdh1p were important in targeting its degradation. However, Clb2p-HA levels did not increase over time (Fig. 2.6B). In comparison, both factors were strongly elevated in *cdh1Δ* cells of *S. cerevisiae* (9, 14, 17, 18, 64). These results suggest that *C. albicans* Cdh1p influences degradation of similar mitotic targets as its orthologue in *S. cerevisiae*. However, the fact that Clb2p did not continue to accumulate with longer incubation periods suggests that additional factors may contribute to Clb2p degradation in the presence and/or absence of Cdh1p.

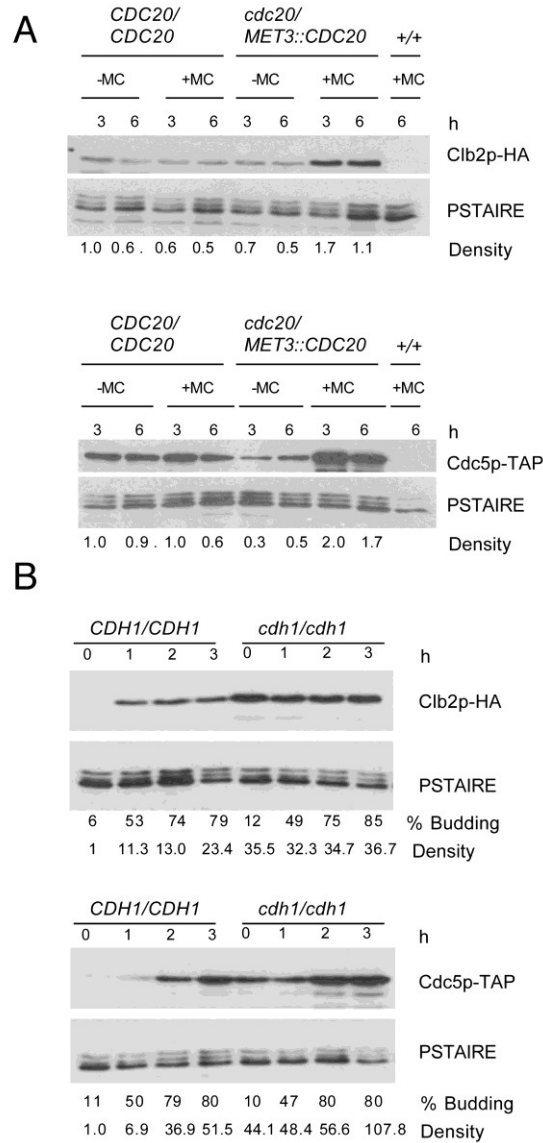


Figure 2.6: Clb2p and Cdc5p levels in cells lacking Cdc20p or Cdh1p. Western blots determining the levels of Clb2p-HA and Cdc5p-TAP. (A) Exponential phase cultures of strains AG191 (*cdc20Δ::URA3/MET3::CDC20::HIS1, CDC5/CDC5-TAP-ARG4*), AG153 (*cdc20Δ::URA3/MET3::CDC20-ARG4 CLB2/CLB2-HA-HIS1*), AG139 (*CLB2/CLB2-HA-HIS1*) and AG120 (*CDC5/CDC5-TAP-URA3*) grown in inducing medium (-MC) were diluted into fresh inducing or repressing medium (+MC) and collected at the indicated times. Strain BWP17 (+/+) was incubated in +MC medium for 6 h and included as an untagged control. (B) Strains AG139 (*CLB2/CLB2-HA-HIS1*), AG120 (*CDC5/CDC5-TAP-URA3*), AG268 (*cdh1Δ::URA3/cdh1Δ::HIS1 CLB2/CLB2-HA-ARG4*) and AG262 (*cdh1Δ::HIS1/cdh1Δ::URA3, CDC5/CDC5-TAP-ARG4*) were collected after overnight incubation in YEPD medium (time '0'), or after diluting into fresh YEPD medium and incubating for 1, 2 or 3 h. Anti-PSTAIRE was used as a loading control. Proportions of budded cells are indicated. Density values represent adjusted relative density (see Materials and Methods).

2.3.7 Absence of Cdh1p does not influence Cdc5p-depleted polarized growth

Cdh1p lies downstream of Cdc5p function in *S. cerevisiae*, as the latter is a component of the FEAR and MEN pathways that act to release Cdc14p from the nucleolus and ultimately activate Cdh1p (35-39). Cdh1p then acts back on Cdc5p by targeting it for degradation (14, 15). Since a small proportion of elongated buds were observed in *C. albicans* cells lacking *CDH1*, it is possible that Cdh1p contributes in part to the polarized growth response observed in Cdc5p-depleted cells. In order to address this question, both copies of *CDH1* were deleted from a strain carrying a single copy of *CDC5* under control of the *MET3* promoter (HCCA143). After incubation in repressing medium for 7 h, 80.2% of cells lacking *CDH1* and depleted of Cdc5p contained elongated buds, compared to 91% of cells depleted of Cdc5p only (HCCA126) (see Table 5 in Chou *et al.*, 2011). Elongated cells in the two strains appeared similar, even after 24 h of Cdc5p depletion (see Fig. 7 in Chou *et al.*, 2011). In contrast, only 11.7% of cells lacking *CDH1* (HHCA45) or 2.0 % of cells containing both *CDH1* and *CDC5* (HHCA100) demonstrated elongated buds (see Table 5 in Chou *et al.*, 2011). Thus, absence of Cdh1p did not result in synergistic effects with Cdc5p depletion, suggesting that the factors may lie in the same functional pathway in *C. albicans*.

2.3.8 Cdc20p does not influence serum-induced hyphal growth, while Cdh1p has a moderate effect

Since Cdc20p and Cdh1p influence morphogenesis, we next investigated whether the factors were important for serum-induced hyphal formation. The *cdc20/MET3::CDC20* and control strains were first incubated in repressing medium at 30°C for 2 h in order to deplete Cdc20p before addition of serum. Cells were then transferred to fresh repressing medium with 10% serum and incubated at 37°C for 3 h. Prior to the addition of serum, the majority of cells were either large doublets or slightly polarized (Table 2.4). Exposure to serum resulted in the emergence of hyphae from elongated daughter buds or from one bud of large doublets (Fig. 2.7). Hyphae resembled those of control cells, and were only moderately shorter in length ($41.2 \pm 1.2 \mu\text{m}$, s.e.m n=56, compared to $45.2 \pm 2.2 \mu\text{m}$, s.e.m; n=52), demonstrating that Cdc20p is not important for hyphal formation. Since germ tubes emerged from yeast cells that were blocked in mitosis, and preferentially from a pre-existing polarized site, the results also support the notion that hyphal induction can occur during mitosis (66). Cdc20p was important for nuclear division in hyphal cells, since 89.3% (n=56) of cells

depleted of Cdc20p contained one nucleus, while 92.3% (n=52) of control cells contained two to three nuclei as well as septa. In comparison, 70.5% (n=374) of $\Delta cdh1/\Delta cdh1$ cells were able to form hyphae when incubated in YEPD medium containing 10% serum for 3 h at 37°C, compared to 91% (n=110) of control cells (Fig. 2.7). The remaining cells were more pseudohyphal in appearance. Thus, Cdh1p may have a moderate effect on hyphal formation.

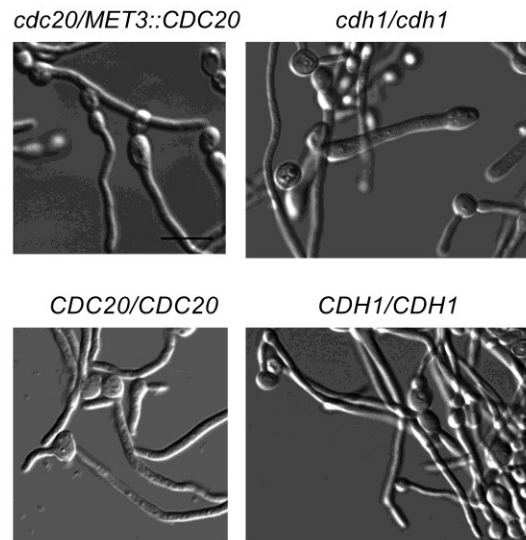


Figure 2.7: Hyphal formation in the absence of Cdc20p or Cdh1p. Strains HCCA109 (*cdc20::URA3/MET3::CDC20-HIS1*) and HCCA100 (*CDC20/CDC20 URA3+ HIS1+*) were incubated in repressing medium for 2 h at 30°C prior to transferring into fresh repressing medium containing 10% fetal bovine serum. Cells were grown for 3 h at 37°C. Strains HCCA45 (*cdh1::URA3/cdh1::HIS1*) and HCCA100 (*CDH1/CDH1*) were incubated in YEPD medium containing 10% fetal bovine serum for 3 h at 37°C. Bar: 10 μ m.

2.4 DISCUSSION

2.4.1 Cdc20p is important for the metaphase-to-anaphase transition and mitotic exit

Our characterization of *CDC20* and *CDH1* provides the first picture of potential APC/C function in *C. albicans*. Since Cdc20p-depleted cells were delayed in metaphase and telophase, and contained elevated levels of Clb2p, the results suggest that Cdc20p is required for the metaphase-to-anaphase transition and mitotic exit, consistent with the function of Cdc20p in *S. cerevisiae* (11, 15). However, *C. albicans* lacks a sequence homologue of *PDS1*, or any other

known securin, which is a major target of Cdc20p (67, 68). A unique Pds1p functional homologue may exist in *C. albicans*, as was found for the Sic1 homologue, Sol1p (33) and serve as a Cdc20p target. Alternatively, Cdc20p may function through different mechanisms. In other systems, blocking separase activity via Cdk/cyclin B-dependent phosphorylation can also inhibit anaphase progression, but this is thought to act in concert with securin and/or compensate for its loss (69-71). Thus, Cdc20p is important for key stages of mitotic progression in *C. albicans*, as in other systems, but the absence of a conserved Pds1p/securin homologue suggests that it may target a different factor(s), consistent with other modes of cell cycle re-wiring in the pathogen (29, 65). The similar defects in mitosis and morphogenesis resulting from depletion of Cdc20p and Cdc5p suggest that these factors may lie in the same mitotic pathway. In support of this, Cdc20p and Cdc5p directly or indirectly interact in *S. cerevisiae* (72) and higher organisms (73, 74), respectively. Plks can also act upstream of the SAC factor Mad2p in other systems (75, 76), which binds and inactivates Cdc20p (77). Our demonstration that Cdc5p-TAP increased during depletion of Cdc20p may be an indirect effect of mitotic arrest. However, the decrease in Cdc5p-TAP levels under *CDC20*-inducing conditions is intriguing, since there were no differences in growth rate (data not shown) or phenotype of *cdc20Δ/MET3::CDC20* vs *CDC20/CDC20* cells in inducing medium. The relationship between Cdc20p and Cdc5p and their precise roles in the mitotic regulatory networks of *C. albicans* are currently under investigation.

2.4.2 Cdh1p influences mitotic exit but does not behave as a repressor of Start

Our results demonstrate that Cdh1p influences Clb2p and Cdc5p degradation, and that a moderately higher proportion of *cdh1Δ/cdh1Δ* cells contained telophase spindles, similar to the situation in *S. cerevisiae*. Collectively this suggests that *C. albicans* Cdh1p is important for mitotic exit, and may target conserved factors during late stages of mitosis and G1 phase (7, 13-15, 17, 64). Since *CDH1* is not essential, additional factors must be required for mitotic exit. In *S. cerevisiae*, the Cdk inhibitor Sic1p contributes to this function; *Δcdh1 Δsic1* cells are not viable and arrest in a large-budded state (17). The *C. albicans* Sic1p homologue, Sol1p, is also not essential (33). However, its role in mitosis was not determined, and the deletion phenotype consisted of most cells containing elongated buds when in exponential phase, but reverting to a yeast growth mode at higher cell density, unlike *cdh1Δ/cdh1Δ* cells. Sic1p and Cdh1p are activated by Cdc14p phosphatase in *S. cerevisiae* (78), which in turn is regulated by the FEAR

and MEN pathways (35-39). Although Cdc14p is also important for Clb2p degradation and mitotic exit in *C. albicans* (40), its relationship with Cdh1p is not clear since *cdc14Δ/cdc14Δ* cells were defective in cell separation and did not form elongated buds. Similarly, the MEN kinase Dbf2p does not appear to be tightly coordinated with Cdc14p, unlike in *S. cerevisiae* (28).

Despite its conserved features, Cdh1p also demonstrated some variations in function. First, Clb2p was enriched in unbudded *cdh1Δ/cdh1Δ* cells, but did not accumulate with longer incubation periods, in contrast to that seen with Cdc5p-TAP, or Clb2p levels in *CDH1* mutants of *S. cerevisiae* (17). This suggests that Cdh1p contributes to Clb2p degradation in *C. albicans*, but that another factor(s) may be involved and/or become more important in the absence of Cdh1p. Second, deletion of *CDH1* did not reduce cell size, but resulted in yeast cell enlargement, in striking contrast to the situation in *S. cerevisiae* (19). This phenotype is not consistent with a role in negatively regulating Start, unlike that demonstrated with *S. cerevisiae* Cdh1p. The *C. albicans cdh1Δ/cdh1Δ* phenotype shared more similarity with *S. cerevisiae* cells overexpressing *CDH1* or carrying a constitutively active mutant (17, 63). Thus, the results suggest that *C. albicans* Cdh1p has conserved and possibly novel functions, and underscore the notion that the pathways governing mitotic progression in *C. albicans* involve distinct features (40, 41, 44). Future investigations of Cdh1p targets and regulation will provide further insights on its roles and the mitotic circuitry of the pathogen.

2.4.3 Cdc20p and Cdh1p influence yeast morphogenesis and polar growth patterns

Our results demonstrate that elongated bud growth is coupled to mitotic defects caused by depletion of Cdc20p. In contrast, absence of *CDC20* (10) or other conditions that arrest mitosis in *S. cerevisiae* result in a yeast doublet morphology. The polarized phenotype could arise from a defect in the ability of yeast buds to switch from apical to isometric growth (31), and Cdc20p may contribute to this process in *C. albicans*. Other conditions that arrest mitosis, S or G2/M phase, or depletion of Hsp90p, result in similar elongated cells (31, 43, 44, 46, 47, 65, 79). The common response is mediated by different cell cycle checkpoint factors, where investigated (65). For example, the DNA damage and replication checkpoint kinase Rad53p mediates filamentous growth in response to H₂O₂ and genotoxic stresses (80, 81), while the spindle checkpoint factors Bub2p and Mad2p are important for polarized growth in response to mitotic arrest (43, 46).

Intriguingly, Bub2p and Mad2p are dispensable for yeast and hyphal growth (43, 46), while Rad53p plays an additional role in hyphal development (62). It's not clear if the different checkpoints converge on a similar pathway or process to influence polarized bud growth (65), and the downstream targets remain elusive. Since Cdc20p is a target of the checkpoint factor Mad2p in other systems (77), it may influence the stability of factors important for the polarized response in *C. albicans*. It will be informative to determine whether inactivation of Cdc20p is a common feature of elongated bud growth induced by other conditions, or if it plays only an indirect role. In *S. cerevisiae*, apical bud growth is associated with Cdc28p/G1 cyclin activity, while a switch to isometric growth occurs when Cdc28p associates with B-type cyclins like Clb2p (82, 83). Down-regulation of Cdc28p/Clb2p activity, through activation of Swe1p-dependent inhibitory phosphorylation of Cdc28p or other means, results in cell elongation (82, 83). However, yeast cell elongation in *C. albicans* may involve some different mechanisms, since Clb2p stabilization or absence induces the response (31), Clb2p was elevated in Cdc20p-depleted cells, Swe1p is only partly required for elongated growth of Rad52p-depleted or hydroxyurea (HU)-treated cells (81, 84), and absence of Cdc20p and Cdh1p did not induce polarized growth in *S. cerevisiae*. If the response is due to defects in switching to isometric bud growth, it is not clear why hyphal-associated genes, such as *HWPI* (43, 84), become strongly induced. It is possible that cell fate changes occur during later stages of polar growth (44), or checkpoints may activate a separate pathway with hyphal-like characteristics (65). Indeed, specific *RAD53* mutations prevent cell elongation but not cell cycle arrest in response to HU, implying a direct role in polarized growth (80). Although the underlying mechanisms remain unclear, polarized bud growth may be important for pathogenesis (65), since the cells can express virulence factors (43, 84), and absence of *MAD2* (46), *SWE1* (85) or *TRX1* (81) reduces virulence.

Cdh1p may contribute in part to cell elongation through its influence on mitotic progression. However, our results suggest an additional role in hyphal morphogenesis. The small proportion of *cdh1Δ/cdh1Δ* cells unresponsive to serum could reflect cell-to-cell variations in the elevated levels of Clb2p, as overexpression of Clb2p or Clb4p compromises true hyphal growth (31). Consistently, other factors important for mitotic exit in *C. albicans* influenced hyphal growth, albeit in a stronger manner (40, 41). Although a pseudohyphal state can preclude

hyphal differentiation, as seen in cells lacking Gin4p, Hsl1p and Fkh2p (59, 86), staining *cdh1Δ/cdh1Δ* cell walls prior to incubation in serum revealed that unresponsive cells were not all pseudohyphae (data not shown). Thus, Cdh1p influences polarized morphogenesis in a complex manner. The phenotype of *cdh1Δ/cdh1Δ* cells could be a secondary response to defects in cell cycle progression, but it is intriguing that Cdh1p function is independently linked to developmental regulators in metazoans and in *S. cerevisiae* (4, 20).

Overall, we have identified key factors that contribute to the regulatory networks governing mitosis and associated polar morphogenesis in *C. albicans*. Our results highlight additional functional variations in important mitotic regulators compared to other systems, consistent with the emerging theme of cell cycle re-wiring in the pathogen (29, 65).

2.5. ACKNOWLEDGMENTS

The authors thank J. Wendland, M. Whiteway, P. Sudbery, J. Pla, and A. Brown for plasmids, reviewers for their insightful comments, and L. Bourget (Biotechnology Research Institute, National Research Council of Canada) for assistance with light scattering measurements. This work was supported by a National Research Council of Canada (NSERC) Discovery Grant number 312035-2005 to CB.

2.6 REFERENCES

1. **Li M, Zhang P.** 2009. The function of APC/CCdh1 in cell cycle and beyond. *Cell Div* **4**:2.
2. **Kim AH, Bonni A.** 2007. Thinking within the D box: initial identification of Cdh1-APC substrates in the nervous system. *Mol Cell Neurosci* **34**:281-287.
3. **Konishi Y, Stegmuller J, Matsuda T, Bonni S, Bonni A.** 2004. Cdh1-APC controls axonal growth and patterning in the mammalian brain. *Science* **303**:1026-1030.
4. **Manchado E, Eguren M, Malumbres M.** The anaphase-promoting complex/cyclosome (APC/C): cell-cycle-dependent and -independent functions. *Biochem Soc Trans* **38**:65-71.
5. **Simpson-Lavy KJ, Oren YS, Feine O, Sajman J, Listovsky T, Brandeis M.** Fifteen years of APC/cyclosome: a short and impressive biography. *Biochem Soc Trans* **38**:78-82.
6. **Cohen-Fix O, Peters JM, Kirschner MW, Koshland D.** 1996. Anaphase initiation in

- Saccharomyces cerevisiae* is controlled by the APC-dependent degradation of the anaphase inhibitor Pds1p. *Genes Dev* **10**:3081-3093.
7. **Baumer M, Braus GH, Irniger S.** 2000. Two different modes of cyclin clb2 proteolysis during mitosis in *Saccharomyces cerevisiae*. *FEBS Lett* **468**:142-148.
 8. **Shirayama M, Toth A, Galova M, Nasmyth K.** 1999. APC(Cdc20) promotes exit from mitosis by destroying the anaphase inhibitor Pds1 and cyclin Clb5. *Nature* **402**:203-207.
 9. **Wasch R, Cross FR.** 2002. APC-dependent proteolysis of the mitotic cyclin Clb2 is essential for mitotic exit. *Nature* **418**:556-562.
 10. **Hartwell LH, Mortimer RK, Culotti J, Culotti M.** 1973. Genetic Control of the Cell Division Cycle in Yeast: V. Genetic Analysis of cdc Mutants. *Genetics* **74**:267-286.
 11. **Lim HH, Goh PY, Surana U.** 1998. Cdc20 is essential for the cyclosome-mediated proteolysis of both Pds1 and Clb2 during M phase in budding yeast. *Curr Biol* **8**:231-234.
 12. **Juang YL, Huang J, Peters JM, McLaughlin ME, Tai CY, Pellman D.** 1997. APC-mediated proteolysis of Ase1 and the morphogenesis of the mitotic spindle. *Science* **275**:1311-1314.
 13. **Schwab M, Neutzner M, Mocker D, Seufert W.** 2001. Yeast Hct1 recognizes the mitotic cyclin Clb2 and other substrates of the ubiquitin ligase APC. *Embo J* **20**:5165-5175.
 14. **Charles JF, Jaspersen SL, Tinker-Kulberg RL, Hwang L, Szidon A, Morgan DO.** 1998. The Polo-related kinase Cdc5 activates and is destroyed by the mitotic cyclin destruction machinery in *S. cerevisiae*. *Curr Biol* **8**:497-507.
 15. **Shirayama M, Zachariae W, Ciosk R, Nasmyth K.** 1998. The Polo-like kinase Cdc5p and the WD-repeat protein Cdc20p/fizzy are regulators and substrates of the anaphase promoting complex in *Saccharomyces cerevisiae*. *Embo J* **17**:1336-1349.
 16. **Hildebrandt ER, Hoyt MA.** 2001. Cell cycle-dependent degradation of the *Saccharomyces cerevisiae* spindle motor Cin8p requires APC(Cdh1) and a bipartite destruction sequence. *Mol Biol Cell* **12**:3402-3416.
 17. **Schwab M, Lutum AS, Seufert W.** 1997. Yeast Hct1 is a regulator of Clb2 cyclin proteolysis. *Cell* **90**:683-693.
 18. **Visintin R, Prinz S, Amon A.** 1997. CDC20 and CDH1: a family of substrate-specific activators of APC-dependent proteolysis. *Science* **278**:460-463.
 19. **Jorgensen P, Nishikawa JL, Breitkreutz BJ, Tyers M.** 2002. Systematic identification of pathways that couple cell growth and division in yeast. *Science* **297**:395-400.
 20. **Wasch R, Robbins JA, Cross FR.** The emerging role of APC/CCdh1 in controlling differentiation, genomic stability and tumor suppression. *Oncogene* **29**:1-10.
 21. **Whiteway M, Bachewich C.** 2007. Morphogenesis in *Candida albicans*. *Annu Rev Microbiol* **61**:529-553.
 22. **Lo HJ, Kohler JR, DiDomenico B, Loebenberg D, Cacciapuoti A, Fink GR.** 1997. Nonfilamentous *C. albicans* mutants are avirulent. *Cell* **90**:939-949.
 23. **Saville SP, Lazzell AL, Monteagudo C, Lopez-Ribot JL.** 2003. Engineered control of cell morphology in vivo reveals distinct roles for yeast and filamentous forms of *Candida albicans* during infection. *Eukaryotic cell* **2**:1053-1060.
 24. **Bastidas RJ, Heitman J, Cardenas ME.** 2009. The protein kinase Tor1 regulates adhesin gene expression in *Candida albicans*. *PLoS Pathog* **5**:e1000294.
 25. **Shen J, Cowen LE, Griffin AM, Chan L, Kohler JR.** 2008. The *Candida albicans* pescadillo homolog is required for normal hypha-to-yeast morphogenesis and yeast proliferation. *Proc Natl Acad Sci U S A* **105**:20918-20923.

26. **Carlisle PL, Banerjee M, Lazzell A, Monteagudo C, Lopez-Ribot JL, Kadosh D.** 2009. Expression levels of a filament-specific transcriptional regulator are sufficient to determine *Candida albicans* morphology and virulence. *Proc Natl Acad Sci U S A* **106**:599-604.
27. **Biswas S, Van Dijck P, Datta A.** 2007. Environmental sensing and signal transduction pathways regulating morphopathogenic determinants of *Candida albicans*. *Microbiol Mol Biol Rev* **71**:348-376.
28. **Spellman PT, Sherlock G, Zhang MQ, Iyer VR, Anders K, Eisen MB, Brown PO, Botstein D, Futcher B.** 1998. Comprehensive identification of cell cycle-regulated genes of the yeast *Saccharomyces cerevisiae* by microarray hybridization. *Mol Biol Cell* **9**:3273-3297.
29. **Cote P, Hogues H, Whiteway M.** 2009. Transcriptional analysis of the *Candida albicans* cell cycle. *Molecular biology of the cell* **20**:3363-3373.
30. **Umeyama T, Kaneko A, Niimi M, Uehara Y.** 2006. Repression of *CDC28* reduces the expression of the morphology-related transcription factors, Efg1p, Nrg1p, Rbf1p, Rim101p, Fkh2p and Tec1p and induces cell elongation in *Candida albicans*. *Yeast* **23**:537-552.
31. **Bensen ES, Clemente-Blanco A, Finley KR, Correa-Bordes J, Berman J.** 2005. The mitotic cyclins Clb2p and Clb4p affect morphogenesis in *Candida albicans*. *Molecular biology of the cell* **16**:3387-3400.
32. **Ofir A, Kornitzer D.** *Candida albicans* cyclin Clb4 carries S-phase cyclin activity. *Eukaryot Cell* **9**:1311-1319.
33. **Atir-Lande A, Gildor T, Kornitzer D.** 2005. Role for the SCF*CDC4* ubiquitin ligase in *Candida albicans* morphogenesis. *Molecular biology of the cell* **16**:2772-2785.
34. **Rottmann M, Dieter S, Brunner H, Rupp S.** 2003. A screen in *Saccharomyces cerevisiae* identified *CaMCM1*, an essential gene in *Candida albicans* crucial for morphogenesis. *Mol Microbiol* **47**:943-959.
35. **Pereira G, Manson C, Grindlay J, Schiebel E.** 2002. Regulation of the Bfa1p-Bub2p complex at spindle pole bodies by the cell cycle phosphatase Cdc14p. *J Cell Biol* **157**:367-379.
36. **Shou W, Seol JH, Shevchenko A, Baskerville C, Moazed D, Chen ZW, Jang J, Charbonneau H, Deshaies RJ.** 1999. Exit from mitosis is triggered by Tem1-dependent release of the protein phosphatase Cdc14 from nucleolar RENT complex. *Cell* **97**:233-244.
37. **Stegmeier F, Visintin R, Amon A.** 2002. Separase, polo kinase, the kinetochore protein Slk19, and Spo12 function in a network that controls Cdc14 localization during early anaphase. *Cell* **108**:207-220.
38. **Sullivan M, Uhlmann F.** 2003. A non-proteolytic function of separase links the onset of anaphase to mitotic exit. *Nat Cell Biol* **5**:249-254.
39. **Visintin R, Hwang ES, Amon A.** 1999. Cfi1 prevents premature exit from mitosis by anchoring Cdc14 phosphatase in the nucleolus. *Nature* **398**:818-823.
40. **Clemente-Blanco A, Gonzalez-Novo A, Machin F, Caballero-Lima D, Aragon L, Sanchez M, de Aldana CR, Jimenez J, Correa-Bordes J.** 2006. The Cdc14p phosphatase affects late cell-cycle events and morphogenesis in *Candida albicans*. *Journal of cell science* **119**:1130-1143.
41. **Gonzalez-Novo A, Labrador L, Pablo-Hernando ME, Correa-Bordes J, Sanchez M,**

- Jimenez J, Vazquez de Aldana CR.** 2009. Dbf2 is essential for cytokinesis and correct mitotic spindle formation in *Candida albicans*. *Mol Microbiol* **72**:1364-1378.
42. **Archambault V, Glover DM.** 2009. Polo-like kinases: conservation and divergence in their functions and regulation. *Nature reviews. Molecular cell biology* **10**:265-275.
43. **Bachewich C, Nantel A, Whiteway M.** 2005. Cell cycle arrest during S or M phase generates polarized growth via distinct signals in *Candida albicans*. *Molecular microbiology* **57**:942-959.
44. **Bachewich C, Thomas DY, Whiteway M.** 2003. Depletion of a polo-like kinase in *Candida albicans* activates cyclase-dependent hyphal-like growth. *Molecular biology of the cell* **14**:2163-2180.
45. **Kitada K, Johnson AL, Johnston LH, Sugino A.** 1993. A multicopy suppressor gene of the *Saccharomyces cerevisiae* G1 cell cycle mutant gene *dbf4* encodes a protein kinase and is identified as *CDC5*. *Mol Cell Biol* **13**:4445-4457.
46. **Bai C, Ramanan N, Wang YM, Wang Y.** 2002. Spindle assembly checkpoint component CaMad2p is indispensable for *Candida albicans* survival and virulence in mice. *Molecular microbiology* **45**:31-44.
47. **Finley KR, Bouchonville KJ, Quick A, Berman J.** 2008. Dynein-dependent nuclear dynamics affect morphogenesis in *Candida albicans* by means of the Bub2p spindle checkpoint. *J Cell Sci* **121**:466-476.
48. **Butler DK, All O, Goffena J, Loveless T, Wilson T, Toenjes KA.** 2006. The GRR1 gene of *Candida albicans* is involved in the negative control of pseudohyphal morphogenesis. *Fungal Genet Biol* **43**:573-582.
49. **Li WJ, Wang YM, Zheng XD, Shi QM, Zhang TT, Bai C, Li D, Sang JL, Wang Y.** 2006. The F-box protein Grr1 regulates the stability of Ccn1, Cln3 and Hof1 and cell morphogenesis in *Candida albicans*. *Mol Microbiol* **62**:212-226.
50. **Trunk K, Gendron P, Nantel A, Lemieux S, Roemer T, Raymond M.** 2009. Depletion of the cullin Cdc53p induces morphogenetic changes in *Candida albicans*. *Eukaryot Cell* **8**:756-767.
51. **Care RS, Trevethick J, Binley KM, Sudbery PE.** 1999. The *MET3* promoter: a new tool for *Candida albicans* molecular genetics. *Molecular microbiology* **34**:792-798.
52. **Sherman F.** 1991. Getting started with yeast. *Methods Enzymol.* **194**:3-21.
53. **Fonzi WA, Irwin MY.** 1993. Isogenic strain construction and gene mapping in *Candida albicans*. *Genetics* **134**:717-728.
54. **Yang L, Ukil L, Osmani A, Nahm F, Davies J, De Souza CP, Dou X, Perez-Balaguer A, Osmani SA.** 2004. Rapid production of gene replacement constructs and generation of a green fluorescent protein-tagged centromeric marker in *Aspergillus nidulans*. *Eukaryot Cell* **3**:1359-1362.
55. **Noble SM, Johnson AD.** 2005. Strains and strategies for large-scale gene deletion studies of the diploid human fungal pathogen *Candida albicans*. *Eukaryot Cell* **4**:298-309.
56. **Gola S, Martin R, Walther A, Dunkler A, Wendland J.** 2003. New modules for PCR-based gene targeting in *Candida albicans*: rapid and efficient gene targeting using 100 bp of flanking homology region. *Yeast* **20**:1339-1347.
57. **Lavoie H, Sellam A, Askew C, Nantel A, Whiteway M.** 2008. A toolbox for epitope-tagging and genome-wide location analysis in *Candida albicans*. *BMC genomics* **9**:578.
58. **Chen DC, Yang BC, Kuo TT.** 1992. One-step transformation of yeast in stationary phase. *Current genetics* **21**:83-84.

59. **Wightman R, Bates S, Amornrattanapan P, Sudbery P.** 2004. In *Candida albicans*, the Nim1 kinases Gin4 and Hsl1 negatively regulate pseudohypha formation and Gin4 also controls septin organization. *J Cell Biol* **164**:581-591.
60. **Yeong FM, Lim HH, Padmashree CG, Surana U.** 2000. Exit from mitosis in budding yeast: biphasic inactivation of the Cdc28-Clb2 mitotic kinase and the role of Cdc20. *Mol Cell* **5**:501-511.
61. **Zachariae W, Shin TH, Galova M, Obermaier B, Nasmyth K.** 1996. Identification of subunits of the anaphase-promoting complex of *Saccharomyces cerevisiae*. *Science* **274**:1201-1204.
62. **Ross KE, Cohen-Fix O.** 2003. The role of Cdh1p in maintaining genomic stability in budding yeast. *Genetics* **165**:489-503.
63. **Robbins JA, Cross FR.** 2010. Requirements and reasons for effective inhibition of the anaphase promoting complex activator *CDH1*. *Mol Biol Cell* **21**:914-925.
64. **Visintin C, Tomson BN, Rahal R, Paulson J, Cohen M, Taunton J, Amon A, Visintin R.** 2008. APC/C-Cdh1-mediated degradation of the Polo kinase Cdc5 promotes the return of Cdc14 into the nucleolus. *Genes Dev* **22**:79-90.
65. **Berman J.** 2006. Morphogenesis and cell cycle progression in *Candida albicans*. *Current opinion in microbiology* **9**:595-601.
66. **Hazan I, Sepulveda-Becerra M, Liu H.** 2002. Hyphal elongation is regulated independently of cell cycle in *Candida albicans*. *Molecular biology of the cell* **13**:134-145.
67. **Ciosk R, Zachariae W, Michaelis C, Shevchenko A, Mann M, Nasmyth K.** 1998. An ESP1/PDS1 complex regulates loss of sister chromatid cohesion at the metaphase to anaphase transition in yeast. *Cell* **93**:1067-1076.
68. **Uhlmann F, Lottspeich F, Nasmyth K.** 1999. Sister-chromatid separation at anaphase onset is promoted by cleavage of the cohesin subunit Scc1. *Nature* **400**:37-42.
69. **Huang X, Hatcher R, York JP, Zhang P.** 2005. Securin and separase phosphorylation act redundantly to maintain sister chromatid cohesion in mammalian cells. *Mol Biol Cell* **16**:4725-4732.
70. **Stemmann O, Gorr IH, Boos D.** 2006. Anaphase topsy-turvy: Cdk1 a securin, separase a CKI. *Cell Cycle* **5**:11-13.
71. **Holland AJ, Taylor SS.** 2008. Many faces of separase regulation. *SEB Exp Biol Ser* **59**:99-112.
72. **Snead JL, Sullivan M, Lowery DM, Cohen MS, Zhang C, Randle DH, Taunton J, Yaffe MB, Morgan DO, Shokat KM.** 2007. A coupled chemical-genetic and bioinformatic approach to Polo-like kinase pathway exploration. *Chem Biol* **14**:1261-1272.
73. **Reimann JD, Freed E, Hsu JY, Kramer ER, Peters JM, Jackson PK.** 2001. Emi1 is a mitotic regulator that interacts with Cdc20 and inhibits the anaphase promoting complex. *Cell* **105**:645-655.
74. **Moshe Y, Boulaire J, Pagano M, Hershko A.** 2004. Role of Polo-like kinase in the degradation of early mitotic inhibitor 1, a regulator of the anaphase promoting complex/cyclosome. *Proc Natl Acad Sci U S A* **101**:7937-7942.
75. **Ahonen LJ, Kallio MJ, Daum JR, Bolton M, Manke IA, Yaffe MB, Stukenberg PT, Gorbsky GJ.** 2005. Polo-like kinase 1 creates the tension-sensing 3F3/2 phosphoepitope and modulates the association of spindle-checkpoint proteins at kinetochores. *Curr Biol* **15**:1078-1089.

76. **Park CJ, Park JE, Karpova TS, Soung NK, Yu LR, Song S, Lee KH, Xia X, Kang E, Dabanoglu I, Oh DY, Zhang JY, Kang YH, Wincovitch S, Huffaker TC, Veenstra TD, McNally JG, Lee KS.** 2008. Requirement for the budding yeast polo kinase Cdc5 in proper microtubule growth and dynamics. *Eukaryot Cell* **7**:444-453.
77. **Zich J, Hardwick KG.** 2010. Getting down to the phosphorylated 'nuts and bolts' of spindle checkpoint signalling. *Trends Biochem Sci* **35**:18-27.
78. **Stegmeier F, Amon A.** 2004. Closing mitosis: the functions of the Cdc14 phosphatase and its regulation. *Annu Rev Genet* **38**:203-232.
79. **Sherwood RK, Bennett RJ.** 2008. Microtubule motor protein Kar3 is required for normal mitotic division and morphogenesis in *Candida albicans*. *Eukaryot Cell* **7**:1460-1474.
80. **Shi QM, Wang YM, Zheng XD, Lee RT, Wang Y.** 2007. Critical role of DNA checkpoints in mediating genotoxic-stress-induced filamentous growth in *Candida albicans*. *Molecular biology of the cell* **18**:815-826.
81. **da Silva dantas A, Patterson, M.J., Smith, D., MacCallum, D.M., Erwig, L.P., Morgan, B.A., and Quinn, J.** 2010. Thioredoxin regulates multiple hydorgen peroxide-induced signaling pathways in *Candida albicans*. *Mol. Cell Biol.* **30**:4550-4563.
82. **Rua D, Tobe BT, Kron SJ.** 2001. Cell cycle control of yeast filamentous growth. *Curr Opin Microbiol* **4**:720-727.
83. **Pruyne D, Bretscher A.** 2000. Polarization of cell growth in yeast. I. Establishment and maintenance of polarity states. *Journal of cell science* **113 (Pt 3)**:365-375.
84. **Andaluz E, Ciudad T, Gomez-Raja J, Calderone R, Larriba G.** 2006. Rad52 depletion in *Candida albicans* triggers both the DNA-damage checkpoint and filamentation accompanied by but independent of expression of hypha-specific genes. *Molecular microbiology* **59**:1452-1472.
85. **Gale CA, Leonard MD, Finley KR, Christensen L, McClellan M, Abbey D, Kurischko C, Bensen E, Tzafrir I, Kauffman S, Becker J, Berman J.** 2009. SLA2 mutations cause *SWE1*-mediated cell cycle phenotypes in *Candida albicans* and *Saccharomyces cerevisiae*. *Microbiology* **155**:3847-3859.
86. **Bensen ES, Filler SG, Berman J.** 2002. A forkhead transcription factor is important for true hyphal as well as yeast morphogenesis in *Candida albicans*. *Eukaryotic cell* **1**:787-798.
87. **Sudbery P, Gow, N. and Berman, J.** 2004. The distinct morphological states of *Candida albicans*. *Trends Microbiol.* **12**:317-324.

2.7 SUPPLEMENTARY DATA

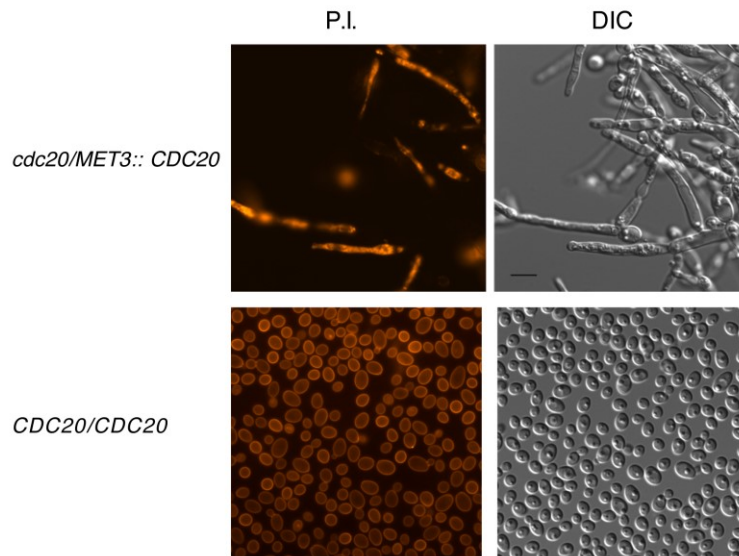


Figure S2.1: Cells depleted of Cdc20p lose viability by 24h. Strain HCCA109 (*cdc20/MET3::CDC20*) was incubated in repressing medium for 24 h. Cells were collected and stained with propidium iodide (P.I.) for 24 h. Strain HCCA100 (*CDC20/CDC20*) grown for 24 h is included as a control. Bar: 10 μ m.

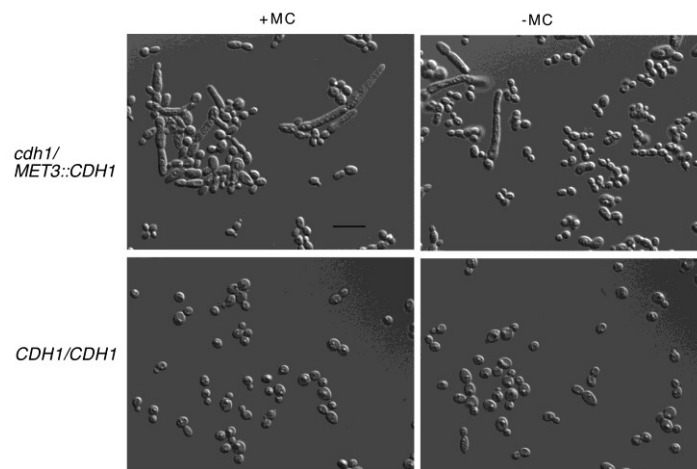


Figure S2.2: Repression of *CDH1* results in a pleiotropic phenotype including some filamentous growth, while overexpression results in more moderate effects. Strains HCCA26 (*cdh1/MET3::CDH1*) and HCCA100 (*CDH1/CDH1*) were incubated in inducing medium overnight, diluted in repressing (+MC) and inducing medium (-MC) and incubated for 8 h at 30°C. Bar: 15 μ m.

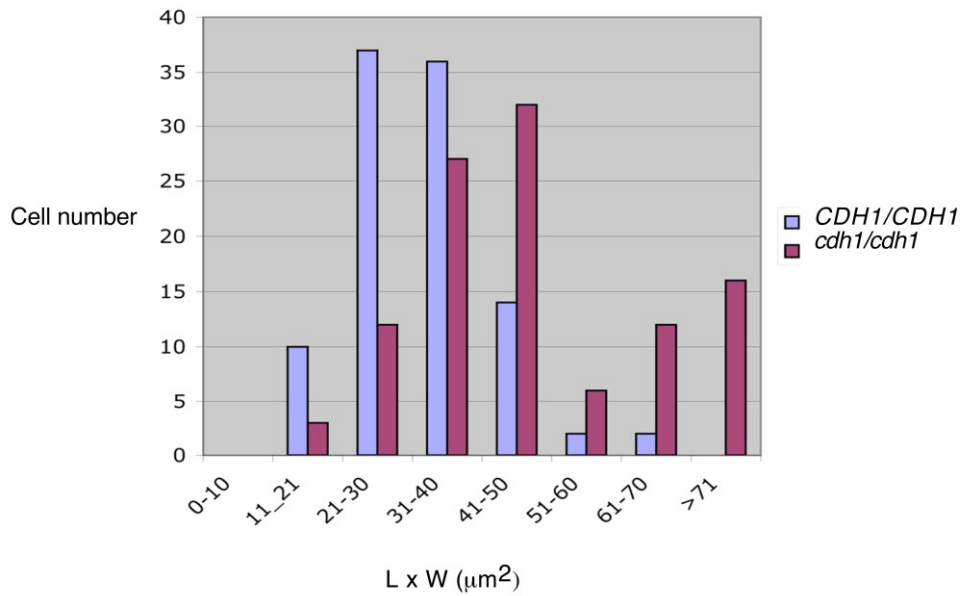


Figure S2.3: Length by width measurements of yeast form cells in the presence and absence of Cdh1p. Strains HCCA45 (*cdh1 Δ /cdh1 Δ*) and HCCA100 (*CDH1/CDH1*) were incubated in YEPD medium for 7 h, and fixed. The lengths and widths of cells only in the yeast form were measured from DIC images obtained with a 100x objective.

CHAPTER 3

Ch. 3: Depletion of the mitotic kinase Cdc5p in *C. albicans* results in the formation of elongated buds that switch to the hyphal fate over time in a Ume6p-dependent manner.

Chapter 3 addresses the nature of the filaments produced through depletion of Cdc5p, and the mechanisms by which blocking mitosis leads to a change in growth mode and expression of hyphal genes that are normally induced by environmental conditions. The formation of filaments in *C. albicans* upon depletion of Cdc5p, or blocking mitosis through other means, is novel but the identity of the cells remains controversial (1). Another study demonstrated that similar filaments arising from mitotic-blocked cells depleted of Hsp90p required a novel transcription factor, Hms1p (2). Based on previous data, we hypothesized that the Cdc5p-depleted cells represented different cell forms in time, such that they were initially elongated buds due to defects in the yeast bud switching from polar to isometric growth in early mitosis, but switched to the hyphal fate in response to maintenance of polarized growth at the yeast bud. In order to test this hypothesis, we conducted a time-course based analysis of aspects of the polar growth machinery in Cdc5p-depleted cells using cell imaging and biochemical approaches, and genetically tested for the requirement of hyphal signaling pathway regulators. Cdc5p-depleted cells show hyphal-diagnostic features at only later stages of polarized growth, and that these require induction of the core hyphal regulator *UME6*, but not *HMS1*. Induction of *UME6* in Cdc5p-depleted cells may occur in response to maintenance of polarized growth. The results expand on the multiple strategies with which *C. albicans* can modulate growth mode and expression of virulence determinants. This versatility may aid escape from stressful environments and promote survival in the host.

ABSTRACT

The fungal pathogen *Candida albicans* differentiates between yeast, hyphae and pseudohyphae in order to enhance survival in the human host. Environmental cues induce hyphal development and expression of hyphal-specific genes. Filaments also result from yeast cell cycle arrest, but the nature of these cells and their mechanisms of formation are less clear. We previously demonstrated that depletion of the mitotic polo-like kinase Cdc5p resulted in the production of filaments under yeast growth conditions that were distinct from hyphae with respect to several criteria, yet expressed hyphal-specific genes at later stages. In order to clarify the nature of these growth forms and their relationship to true hyphae, we conducted time course-based investigations of aspects of the polar growth machinery, which can distinguish cell types. During later stages of Cdc5p depletion, the myosin light chain Mlc1p demonstrated a Spitzenkörper-like localization in the tips of some filaments, and the Cdc42p GAP Rga2p became hyper-phosphorylated, as in true hyphae. Hyphal-specific genes *HWPI*, *UME6* and *HGC1* were strongly expressed at approximately the same time. *HWPI* expression was dependent on Ume6p, and absence of Ume6p or Hgc1p influenced late-stage filament integrity. Finally, polarized growth and *UME6* expression in Cdc5p-depleted cells were independent of the transcription factor Hms1p. Thus, depleting Cdc5p generates elongated buds that switch to the hyphal fate over time through a mechanism that involves *UME6* induction, possibly in response to maintenance of polarized growth. The results expand on the multiple strategies with which *C. albicans* can modulate growth mode and expression of virulence determinants.

3.1 INTRODUCTION

Candida albicans is one of the most common opportunistic fungal pathogens of humans. It exists as a commensal in the gastrointestinal or genitourinary tracts in healthy individuals, but can cause a range of infections under immune-compromised conditions (3-5), with mortality rates associated with systemic infections reaching as high as 60% (6-8).

An important aspect of *C. albicans* biology in terms of virulence is its ability to differentiate into multiple cell types, including yeast, pseudohyphae, and hyphae. The cells can be distinguished with respect to numerous features. Yeast cells grow via budding that initiates at the G1/S transition of the cell cycle, and a ring of septins marks the future bud emergence site. Initial bud outgrowth is polar, and associated with a high concentration of actin patches, but switches to an isometric mode near mitosis, when the actin patches disperse evenly around the bud (9, 10). Tips of yeast buds also contain a polarisome, which regulates actin filament formation at growth sites (11-13). Polarisome components transiently localize to growing bud tips, then re-locate to the bud neck later in the cell cycle. Nuclear division takes place across the mother-bud neck, and cytokinesis follows the break down of the septin ring (1, 14). Pseudohyphae are chains of elongated yeast cells with an extended G2 phase that do not separate after cytokinesis, and show constrictions at septation sites (14, 15). They also contain septin rings at the initial bud site, and a high concentration of actin patches and a polarisome in the bud tip during polarized growth. These relocate to future septation sites near the onset of mitosis, and the nucleus divides across the bud neck (14). Filamentous hyphae are distinct in that they maintain polarized growth and a high concentration of actin patches at the tip. A transient septin band appears at the mother-germ tube neck, followed by formation of septin rings within the germ tube, where the first nuclear division takes place (1, 14, 16). Hyphae can contain a polarisome, but also possess a proposed vesicle supply center, similar to the Spitzenkörper found in tips of filamentous fungal hyphae (17, 18). The Spitzenkörper is visualized as a 3D spot at hyphal tips with FM4-64 staining, or through localization of Mlc1p (12), Sec4p (13), Sec2p (11) or Bni1p (12). These factors are maintained at the growing tip and simultaneously localize to subapical septation sites. Hyphal tips are also distinct from yeast or pseudohyphal buds in that they exclude localization of Rga2p, a GTPase activating protein (GAP) for Cdc42p, the master regulator of actin polarization and polarity (19). Rga2p is hyperphosphorylated in hyphae, which

results in down-regulation and exclusion from the tip, and consequently the continued maintenance of Cdc42p activity (19). In contrast, Rga2p locates at the tips of small and medium yeast and pseudohyphal buds (19, 20). Hyphae lack constrictions at septation sites, and do not have extended cell cycle phases like pseudohyphae, indicating that hyphal growth runs independently of the cell cycle (10, 21).

The ability to switch between cell types in different environments of the host is crucial for pathogenesis (22, 23). An understanding of the mechanisms that underlie cell differentiation may thus reveal new targets for treating infection. The regulation of the yeast-to-hyphal switch has been extensively investigated, and requires elevated temperature in combination with other environmental cues (21, 24). High temperature is sensed by the heat shock protein Hsp90p (25), whereas other cues are mediated by a diversity of signaling pathways, including MAPK and cAMP-based signaling, for example (24, 26). An important downstream target required for hyphal formation under most inducing conditions is the transcription factor Efg1p, which in turn regulates expression of several hyphal-specific genes (HSGs), including the cell wall protein Hwp1p, and other hyphal regulators such as Ume6p (22, 27). Yeast cells lacking Ume6p initiate but do not maintain hyphal growth, and *UME6* overexpression can drive hyphal formation under yeast growth conditions (28). Ume6p in turn maintains expression of *HGC1*, a cyclin-related factor that is specifically expressed in hyphal cells and required for maintaining hyphal growth (21, 29-31).

C. albicans yeast cells can convert into additional filamentous growth forms in response to cell cycle arrest, in the absence of any hyphal-inducing environmental cues. For example, if yeast cells are depleted of the G1 cyclin Cln3p and arrest in G1 phase, the cells first enlarge then form filaments that in many cases present clear characteristics of hyphae, such as polarized growth, nuclear division within the filament, unconstricted septa, and a requirement for the hyphal signaling pathway factors Efg1p and Ras1p (32, 33). This suggests that a relationship exists between the G1 phase of the cell cycle and hyphal development in *C. albicans*, but the mechanisms remain unclear (21, 34).

Blocking yeast cells in other cell cycle stages, including S, G2/M or M phase, also results in highly polarized growth (25, 35-42). However, the nature of these cells is less clear. For example, cells arrested in mitosis through depletion of the polo-like kinase Cdc5p resemble hyphae in that they maintain polarized growth, lack constrictions along their lengths, move the nucleus from the mother yeast cell into the tube, require cyclase activity, and express some HSGs (36, 37). A constriction is present at the bud neck, due to the fact that polarized growth originates at the yeast bud that emerges prior to the cell cycle block. However, the filaments are also distinct from hyphae in their initial widths, ability to form in the absence of Efg1p, and expression of HSGs exclusively at later stages of elongation (36, 37). Further, maintenance of polarized growth requires the spindle checkpoint factor Bub2p, unlike the situation in true hyphae or S-phase arrested cells (37, 43). Intriguingly, Bub2p and another spindle checkpoint factor, Mad2p, are required for polarized growth under other conditions that block mitosis, including depletion of the heat shock factor Hsp90p (43) or exposure to nocodazole (44), respectively. Further, checkpoint factors like Mad2p and Swe1p are required for virulence (44, 45). Thus, not all polar growth forms in *C. albicans* are created in the same manner, and checkpoint-associated polarized growth may be important for pathogenesis in the host. Previous work on filaments produced through depletion of Hsp90p identified the involvement of a novel pathway that included the transcription factor Hms1p (2). However, the mechanisms underlying polarized growth and HSG expression in response to other treatments that specifically block mitosis, G2/M or S phase, are not clear. Further, the nature of these polarized cells and any connection with true hyphae remain unknown (21).

Here, we characterized polarized cells that form in response to a mitotic block induced by depletion of Cdc5p kinase. Through investigating aspects of the polar growth machinery and exploring other hyphal-diagnostic features, we provide evidence that Cdc5p-depleted cells may initially represent elongated buds, but switch to the hyphal fate over time through a mechanism that involves Ume6p but is independent of Hms1p. Our results extend the array of strategies in *C. albicans* for modulating growth form and HSG gene expression, which are important for virulence.

3.2 MATERIALS AND METHODS

3.2.1 Strains, oligonucleotides, plasmids and culture conditions

Strains, oligonucleotides and plasmids used in this study are listed in Tables 3.1, 3.2 and 3.3, respectively. Strains were incubated in synthetic medium (0.7% yeast nitrogen base, 2.0 g adenine, 2.5 g uridine, 2.0 g tryptophan, 1.0 g histidine, 1.0 g arginine, 1.0 g methionine, 1.5 g tyrosine, 1.5 g isoleucine, 7.5 g valine, 1.5 g lysine, 2.5 g phenylalanine, 5.0 g glutamic acid, 10.0 g threonine and 3.0 g leucine per 50 L) containing either 2.0% glucose (SD) or 2.0% sodium succinate (SS) to repress or induce expression from the *PCK1* promoter, respectively (46). Alternatively, SD medium lacking (-MC) or containing (+MC) 2.5 mM methionine and 0.5 mM cysteine was utilized to induce or repress expression from the *MET3* promoter, respectively (47). Other strains were grown in rich medium (YEPD) containing 1.0% yeast extract, 2.0% peptone and 2.0% dextrose. Media were supplemented with 50.0 µg/ml of uridine, except when *URA3* prototrophs were selected (48). For hyphal induction, medium was supplemented with 10.0% fetal bovine serum (FBS) (Wisent Inc.) and cells were incubated at 37°C. Pseudohyphae were induced by incubating cells in YEPD or SS medium at 36°C. For most conditions, strains were grown overnight, diluted into fresh medium to an O.D._{600nm} of 0.1 to 0.2, and collected after indicated times. For growth assays, the O.D._{600nm} was recorded at the indicated time intervals. Samples for RNA or protein analysis were collected at the indicated time points and stored at -80°C until extraction.

Table 3.1: Strains used in this study

Strain	Genotype	Source
RM1000	<i>ura3Δ::imm434/ura3Δ::1 imm434 his1Δ::hisG/his1Δ::hisG</i>	Negredo <i>et al.</i> 1997
BWP17	<i>ura3Δ::imm434/ura3Δ::imm434 his1Δ::hisG/his1Δ::hisG</i> <i>arg4Δ::hisG/arg4Δ::hisG</i>	Wilson <i>et al.</i> , 1999
SC5314	<i>URA3/URA3, HIS1/HIS1</i>	Fonzi and Irwin, 1993
CB104	<i>cdc5Δ::hisG/cdc5Δ::HIS1 PCK1::CDC5-URA3</i>	Bachewich <i>et al.</i> , 2003
CB105	<i>cdc5Δ::hisG/cdc5Δ::HIS1 PCK1::CDC5-hisG</i>	Bachewich <i>et al.</i> , 2003
CB400	RM1000 (pRM100 <i>URA3+</i> , <i>HIS1+</i>)	Bachewich <i>et al.</i> , 2003
CDC5-25	<i>CDC5/cdc5Δ::hisG</i>	This study
AG240	<i>cdc5Δ::hisG/cdc5Δ::HIS1 PCK1::CDC5-hisG</i> <i>MLC1/MLC1-GFP-URA3</i>	This study
AG332	<i>MLC1/MLC1-GFP-URA3</i>	This study
AG374	<i>RGA2/RGA2-HA-URA3</i>	This study
AG379	<i>cdc5Δ::hisG/cdc5Δ::HIS1 PCK1::CDC5-hisG</i> <i>RGA2/RGA2-HA-URA3</i>	This study
AG500	<i>cdc5Δ::hisG/MET3::CDC5-ARG4</i>	This study
AG509	<i>cdc5Δ::hisG/MET3::CDC5-ARG4</i>	This study
AG518	<i>cdc5Δ::hisG/MET3::CDC5-ARG4, UME6/ume6Δ::URA3</i>	This study
AG530, 531	<i>cdc5Δ::hisG/MET3::CDC5-ARG4,</i> <i>ume6Δ::URA3/ume6Δ::HIS1</i>	This study
AG536, 540	<i>cdc5Δ::hisG/MET3::CDC5-ARG4, HGC1/hgc1Δ::URA3</i>	This study
AG547	AG509 pRM100 (<i>URA3+HIS1+</i>)	This study
AG553	AG500 pRM100 (<i>URA3+HIS1+</i>)	This study
AG574, 577	<i>cdc5Δ::hisG/MET3::CDC5-ARG4,</i> <i>hgc1Δ::URA3/hgc1Δ::HIS1</i>	This study
AG570, 572	<i>cdc5Δ::hisG/MET3::CDC5-ARG4, HMS1/hms1Δ::URA3</i>	This study
AG579-581	<i>cdc5Δ::hisG/MET3::CDC5-ARG4,</i> <i>hms1Δ::URA3/hms1Δ::HIS1</i>	This study

Table 3.2: Oligonucleotides used in this study

Name	Sequence	Source
AG2R	ATAGTTACGATTAGTGGTGG	This study
AG4F	GGTCGACGGATCCCCGGGTATACCCATACGATGTTCCCTGAC	Lavoie <i>et al.</i> , 2008
AG4R	TCGATGAATTCGAGCTCGTT	Lavoie <i>et al.</i> , 2008
AG15F	AGAATTTCCCGGGAGTTGCTTATTATTGAT	This study
AG15R	TGGAAGTAAATTGAGGATATTGATGTTTGG	This study
AG16F	CCAAACATCAATATCCTCAATTTACTTCCATATAGGGCGAAT TGGAGCTC	This study
AG16R	CCGTCAACCGTCAACCTGTTAATTCTTAATGACGGTATCGAT AAGCTTGA	This study
AG17F	ATTAAGAATTAACAGGTTGACGGTTGACGG	This study
AG17R	TAAGGTTTAGACTTTTCCGTATGATGAAAC	This study
AG19F	ATTAGAAACCAACAGAGGAA	This study
AG19R	TTGTCGTAGTTGTTGAACTA	This study
AG20F	ATGAGTTATTA AAAAGGGGTCAATGTA ACTTCTGATGGAAAT GTGGATTATGTTGAA TTTGTCAAATCAATTTTAGACCAAGGTGCTGGCGCAGGTGCT TC	This study
AG20R	TTGGCATATATTACTCTCAAAGTAACTTATCAAGTACTACA TAAAACTTCAAATAA ACGGTATCCAATTCGAACAAGACCCGCATAGGCCACTAGTG GA	This study
AG21F	CAAGAAATCATCAACAGACC	This study
AG21R	TCCGTCATCATAATTGGTGC	This study
AG52F	AACTTTAGCGAAGGATGAATCCGGTGTA AAAAGAAATGACCG ATATGGGATTTAGAAATGA TACAACAGAGTTACTATTGACAGAATCACATAGAATCTTTGG TCGACGGATCCCCGGGT	This study
AG52R	TACCCAAAAACAATTTAATACCATTGAATACTTGATCCGTA ATGGACATAGAAA ACTAGAA ATGTATCTGAATCCACA ACTAAAAGATATTCATTAACATCGA TGAATTCGAGCTCGTT	This study
AG53R	CTCTGCCAGGATACTACTTG	This study
AG66R	GTACGTGTGATGATGATGAT	This study
AG75F	AATTCTGTCCTCCTCCCCTCAAAGTTTCTA	This study
AG75R	AAGTGTTGGGTATTGGTTTGATGCTTTGAT	This study
AG76F	GAGAATGGAGAATGGAGAAAGATGTTGTTA	This study
AG76R	GGACGAATAAAGGATACTTTCCAGTAGTGT	This study

AG77F	ATCAAAGCATCAAACCAATACCCAACACTTTATAGGGCGAA TTGGAGCTC	This study
AG77R	TAACAACATCTTTCTCCATTCTCCATTCTCGACGGTATCGAT AAGCTTGA	This study
AG78F	CCTATCCACATACATACACA	This study
AG78R	CGGACTTTGTAGTAATCAAG	This study
AG88F	ACCATCCACTTCAACTTACTTTTACTTTC	This study
AG88R	ACCATCCACTTCAACTTACTTTTACTTTC	This study
AG89F	GAGGAAAATGAAAGGGACCAATCTGTCTAT	This study
AG89R	TTCCCGGCTAGTTTTTATATCCAGTGGATT	This study
AG90F	ATCACTATCCCCTCCCTAAAAGAATAGTAGTATAGGGCGAA TTGGAGCTC	This study
AG90R	ATAGACAGATTGGTCCCTTTCATTTTCCTCGACGGTATCGAT AAGCTTGA	This study
AG91F	TGCTTCAAGACGTGACTTGG	This study
AG91R	CACTTACTCCAGAAAATAGC	This study
AG92F	ACACCAACAATGGTAATGGT	This study
AG92R	CTAGTCTTAGTTGGAGCAGA	This study
AG93F	AGCCAAACAGATACAGATAC	This study
AG93R	TTTAGGGAGGGGATAGTGAT	This study
AG99F	GACACACAAACAAACACCCC	This study
AG99R	AGGTTGGTTTGGTTTGCTCT	This study
AG115F	GGGTAAAGAG ATACCAAGAG	This study
AG115R	AGTGTAATGGGTTTAGTTGC	This study
AG101F	GTTGGGACTAGGATTGGTAAAGC	Carlisle and Kadosh, 2010
AG101R	GATGTGGAGTAGACTTGGATAATGG	Carlisle and Kadosh, 2010
HHHWP1F	CTAAACCAGCTGCTCCAAAAT	This study
HHHWP1R	GTTGTTACCAGCACCTTCAA	This study
ACT1-129F	CATGGTTGGTATGGGTCAAAA	This study
ACT1-104R	TCAATTCTAATAACGAGGTGGTCTTTC	This study
HH08F	TTCTGGCTCCAAATCATTG	This study
HH08R	TATAAGGCTGCATAACTAAG	This study
HC10F	CGAGCAGGACCAATTGCGATGTAATCAAATTGTAAACATG AGTCTGTGTCTATTTCGCT ACTACTAACCTTAGAGTGTTGGATCCCCCTTTAGTAAGA	This study
HC10R	GACAGGAGTAATGTTATTAGCTCTAGCATTGAGCTGGCCACT ATTCAATGGCTGTAAAGG TTGTGAACGAAGCGCCGACATGTTTTCTGGGGAGGGTA	This study
HC11F	ACTATGAATAGAGAAAGCAG	This study

HCGS13F	TCGAGCAGGACCAA TTGCGA TGT AA TCAA	Chou <i>et al.</i> , 2011
HCGS13R	GGTT AACCTCTTT AA T AA TCAA TGCTGGT	Chou <i>et al.</i> , 2011
HCGS14F	ACCAGCATTGATTATTAAGAGGTTTAACCGGATCCCCCCTT TAGTAAGA	Chou <i>et al.</i> , 2011
HCGS14R	CTGTAAAGGTTGTGAACGAAGCGCCGACATGTTTTCTGGGG AGGGTA	Chou <i>et al.</i> , 2011
HCGS15F	ATGTCGGCGCTTCGTTCAACAACCTTTACAG	Chou <i>et al.</i> , 2011
HCGS15R	TAAAGAATCTAACCTCTGGTTCAGACTC	Chou <i>et al.</i> , 2011
HH43F	ATGGTTACACCCGATTCAAC	This study
HH08F	TTCTGGCTCCAAATCATTG	This study
HH08R	TATAAGGCTGCATAACTAAG	This study
CaURA3F	GGTAATACCGTAAAGAAACA	This study
CaMET3R	TGGGGAGGGTATTTACTTTTAAAT	This study
CaARG4F	ACTATGGATATGTTGGCTAC	This study
CaHIS1R	ACTGGGATATCAGCTGCAGG	This study

Table 3.3: Plasmids used in this study

Name	Source
pRM1000	J. Pla
pBS-CaURA3	A.P.J. Brown
pBS-CaHIS1	C. Bachewich
pFA-ARG4-Met3p	Gola <i>et al.</i> , 2003
pFA-HA-URA3	Lavoie <i>et al.</i> , 2008
pFA-GFP-URA3	Gola <i>et al.</i> , 2003

3.2.2 Strain Construction

In order to tag the C-terminus of *RGA2* with three copies of the hemagglutinin epitope (HA), an *HA-URA3* cassette from plasmid pFA-HA-URA3 (49) was amplified with oligonucleotides AG4F and AG4R. The product was used as a template in a fusion PCR with oligonucleotides AG52F and AG52R, which contained 100 bp complementary to regions lying immediately upstream or downstream of the stop codon of *RGA2*, respectively. The fusion construct was transformed into strains RM1000 and CB105, resulting in strains AG374 and AG379, respectively. In order to tag the C-terminus of *MLC1* with Green Florescent Protein (GFP), the *GFP-URA3* cassette from pFA-GFP-URA3 (50) was amplified using oligonucleotides AG20F and AG20R, which contained 80 bp complementary to regions lying upstream or downstream of the stop codon of *MLC1*, respectively, and 20 bp corresponding to regions flanking *GFP-URA3*. The PCR product was transformed into strains RM1000 and CB105, resulting in strains AG332 and AG240, respectively. In order to create a strain containing a single copy of *CDC5* under the control of the *MET3* promoter in the BWP17 background, one copy of *CDC5* was deleted using the *URA3* blaster method (37, 51), followed by looping out of the *URA3* marker and selection on 5'-fluoroorotic acid (Sigma-Aldrich), resulting in strain CDC5-25. To place the second copy of *CDC5* under control of the *MET3* promoter, oligonucleotides HCGS13F and HCGS13R were used to amplify a 636 bp fragment lying upstream of the *CDC5* start codon, while oligonucleotides HCGS15F and HCGS15R amplified a 514 bp fragment immediately downstream of the start site. Oligonucleotides HCGS14F and HCGS14R amplified an *ARG4-MET3* fragment from plasmid pFA-ARG4-MET3 (50). The three fragments were combined and the fusion product was amplified with oligonucleotides HCGS13F and HCGS15R. The final construct was transformed into strain CDC5-25, resulting in strain AG509. Alternatively, oligonucleotides HC10F and HC10R, which contain 80 bp of sequence upstream and downstream of the START codon of *CDC5*, respectively, were used to amplify an *ARG4-MET3* cassette from pFA-ARG4-MET3 (50). The product was transformed into strain CDC5-25, resulting in strain AG500. In order to delete *UME6*, oligonucleotides AG15F and AG15R were used to amplify a 620 bp fragment lying upstream of the *UME6* start codon, while oligonucleotides AG17F and AG17R amplified a 490 bp fragment lying downstream of the stop codon. Oligonucleotides AG16F and AG16R amplified a *URA3* fragment from plasmid pBS-CaURA3 (A.J.P. Brown). The products were combined in a PCR reaction with oligonucleotides

AG15F and AG17R, and the final product was transformed into strain AG500, resulting in strain AG518. The second copy of *UME6* was replaced with a *HIS1*-containing fusion product produced in a similar manner with the exception of utilizing pBS-CaHIS1 (C. Bachewich) with oligonucleotides AG16F and AG16R resulting in strains AG530 and AG531. In order to delete *HGCI*, oligonucleotides AG75F and AG75R were used to amplify a 580 bp fragment lying upstream of the *HGCI* start codon, while oligonucleotides AG76F and AG76R amplified a 670 bp fragment lying downstream of the stop codon. Oligonucleotides AG77F and AG77R amplified a *URA3* fragment from plasmid pBS-CaURA3. The products were combined and the fusion product was produced with oligonucleotides AG75F and AG76R. The final product was transformed into strains AG500 and AG509, resulting in strains AG536 and AG540, respectively. The second copy of *HGCI* was replaced with a *HIS1*-containing fusion product produced in a similar manner with the exception of utilizing pBS-CaHIS1 with oligonucleotides AG77F and AG77R. The resulting strains included AG574 and AG577. In order to delete *HMS1*, oligonucleotides AG88F and AG88R amplified a 680 bp fragment lying upstream of the *HMS1* Start codon, oligonucleotides AG89F and AG89R amplified a 490 bp fragment lying downstream of the Stop codon, and AG90F and AG90R amplified a *URA3* fragment from plasmid pBS-CaURA3. The products were combined and the fusion product was produced with oligonucleotides AG88F and AG89R. The final product was transformed into strains AG500 and 509, resulting in strains AG570 and AG572, respectively. The second copy of *HMS1* was replaced with a *HIS1*-containing fusion product produced in a similar manner with the exception of utilizing pBS-CaHIS1 with oligonucleotides AG90F and AG90R. The resulting strains included AG579-AG581 and AG584-AG585, respectively. In order to produce control strains that were isogenic to deletion strains with respect to markers, pRM100 (pUC19 *URA3*⁺, *HIS*⁺; J. Pla) was transformed into strains AG500 and AG509, resulting in strains AG553 and AG547, respectively. Strains were confirmed for correct integration using PCR with oligonucleotide pairs AG21F and AG21R, (*RGA2*), CaURA3F and AG53R (*MLC1*), CaARG4F and AG2R, HC11F and CaMET3R (*CDC5*), AG19F and AG19R, AG19F and CaHIS1R, HH43F and AG66R (*UME6*), CaURA3F and AG78R, AG78F and CaHIS1R, HH08F and HH08R (*HGCI*), or CaURA3F and AG91R, AG91F and CaHIS1R, AG92F and AG92R (*HMS1*). Deletion strains were also confirmed with Southern blotting, utilizing the DIG Hybridization System (Roche Diagnostics, Mannheim, Germany). Genomic DNA was extracted according to Rose *et al.*, 1990

(52). DIG-labeled probes were prepared using oligonucleotides AG93F and AG93R, AG99F and AG99R, AG115F and AG115R to confirm *hms1*Δ/Δ, *hgc1* Δ/Δ and *ume6* Δ/Δ strains respectively.

3.2.3 Northern blotting

RNA was extracted with TRI-Reagent (Bioshop). Briefly, pellets of cultures were lyophilized (53) in a freeze drier (ThermoSavant, ModulyoD) at -50°C. The dried material was ground using a mortar and pestle (53). Powder was transferred to occupy approximately 70.0-80.0 μl in an Eppendorf tube, and combined with 1.0 ml of TRI-Reagent. RNA was subsequently extracted as previously described (54). The final RNA pellet was re-precipitated with one-tenth volume of 3.0 M sodium acetate (pH 5.3) and three volumes of 95.0% ethanol. A total of 20.0 μg RNA was separated on a 1.0% gel, transferred to Zetaprobe membrane (BioRad), and incubated with ³²P-labeled probes (T7 Quick Prime Kit, Amersham Pharmacia Biotech), as previously described (37, 54). Probes consisted of approximately 700-800 bp fragments complementary to the open readings frames of *HMS1*, *UME6*, *HHWP1*, *HGC1* and *ACT1*, and were amplified with oligonucleotides AG92F and AG92R, AG101F and AG101R, HHHWP1F and HHHWP1R, HH08F and HH08R and ACT1-129F and ACT1-104R, respectively. Northern blots were visualized with a phosphoimager (Typhoon Variable Mode Imager, GE Healthcare). Blots were quantified as described previously (39).

3.2.4 Protein extraction and Western blotting

Protein extracts were prepared according to Liu *et al.*, 2010 (53). Extracted protein was quantified using the Bradford assay (Bio-Rad, Mississauga). For protein samples treated with calf intestinal alkaline phosphatase (CIP) (New England Biolabs), EDTA and sodium vanadate were excluded from the HK extraction buffer. Dephosphorylation of proteins was done using 10U of CIP per 10.0 ug of protein at 37°C for 90 min. Western blotting was done as described previously (39). Briefly, 20.0 μg of protein was loaded onto an SDS-PAGE gel and after electrophoresis proteins were transferred to a polyvinylidene difluoride (PVDF) membrane (BioRad). Membranes were blocked with Tris-buffered saline–Tween (TBST; 50 mM Tris [pH 7.5], 137.0 mM NaCl, 0.1% Tween 20) containing 5.0% skim milk for 1.0 h. Blots were washed three times for 15 min in TBST and incubated for 1.5 h in 0.4 μg/ml anti-HA antibody (12CA5; Roche) diluted in TBST. Blots were rinsed three times for 15 min in TBST and incubated for 1.0

h in a 1:10,000 dilution of horseradish peroxidase-conjugated anti-mouse secondary antibody (KPL). After washing, blots were developed using the Amersham ECL Western blotting analysis system (GE Healthcare). Blots were stripped and incubated with 0.2 µg/ml of anti-PSTAIRES (Santa Cruz Biotechnology) as a loading control. Western blots were quantified using ImageJ as described previously (39).

3.2.5 Cell staining and imaging

Cells were stained with filipin (Sigma) according to Martin and Konopka 2004 (55). Briefly, freshly dissolved filipin was added to 1.0 ml of cell culture to a final concentration of 0.01 mg/ml. Cultures were incubated for a further 10 min at room temperature in the dark, centrifuged for 1.0 min at 10 000 rpm, and washed with sterile water. Cells were then mounted on slides and immediately examined on a Leica DM6000B microscope (Leica Microsystems Canada Inc., Richmond Hill, ON, Canada) equipped with a Hamamatsu-ORCA ER camera (Hamamatsu Photonics, Hamamatsu City, Japan) using either HCX PL APO 63x NA 1.40-0 oil or HCX PLFLUO TAR 100x NA 1.30-0.6 oil objectives and the DAPI (460nm) filter. Images were captured with either Openlab software (Improvision Inc., Perkin-Elmer, Waltham, MA) or Volocity (Improvision Inc., Perkin-Elmer, Waltham, MA). Propidium iodide staining was carried out as previously described (35). In order to visualize Mlc1p-GFP, liquid cultures of strain AG240 were first incubated in SS medium at 30°C overnight, washed with sterile water, diluted to a final O.D._{600nm} of 0.2 in fresh SS medium and incubated for 6.0 h at 30°C to produce yeast cells, 6.0 h at 36°C to form pseudohyphae, or 2.0 h at 37°C with the inclusion of 10.0% calf serum to induce hyphae. In order to repress *CDC5*, overnight cultures were diluted into SD medium to a final O.D._{600nm} of 0.2 and incubated at 30°C for various times. Cultures were centrifuged at 3 000 rpm for 1 min and media were removed until approximately 100.0 µl remained. Cells were resuspended, mounted on microscope slides and immediately visualized on the Leica DM6000B microscope, utilizing a GFP filter (chroma HQ41020 Narrow-band EGFP) and HCX PL APO 63x NA 1.40-0 oil or HCX PLFLUO TAR 100x NA 1.30-0.6 oil objectives. Alternatively, resuspended cells were mounted on a premade 2.0% ultrapure low melting point agarose (Invitrogen) pad on a microscope slide, onto which a coverslip was applied and sealed with VALAP (1:1:1 Vaseline: Laonolin: Paraffin). Slides were immediately visualized with a Zeiss Confocal LSM 510 META/LSM 5 LIVE microscope, fitted with a Plan Apochromat 63/1.4

oil DIC objective (pixel size of 0.109 μm). Mlc1p-GFP was observed using the 488 nm diode laser and a LP505 emission filter. Mlc1p-GFP localization was similarly observed when overnight cultures of cells were alternatively washed, diluted to a final O.D._{600nm} of 0.1 in selected media, applied to a premade agar pad on a microscope slide, which was then placed in moist chambers in incubators at the required temperatures. At set times, a slide was removed, fitted with a cover slip as described, and immediately observed on the Zeiss Confocal microscope. For time-lapse imaging of Mlc1p-GFP, overnight cultures of cells were diluted into SD medium, applied to the agar pad and sealed as described, then mounted on the Zeiss Confocal microscope. Images were recorded every 30 min, and Z-stacks with a 0.1 μm step were acquired. In order to localize Mlc1p-GFP and FM4-64 (Invitrogen) simultaneously, dye was added to cultures to a final concentration of 40.0 μM (12) and cells were immediately mounted on microscope slides containing agar pads. Mlc1p-GFP and FM4-64 labelling were visualized on the Zeiss Confocal LSM 510 microscope using the 488 nm diode laser (100 mW) with a BP 500-525 emission filter and the 532 nm diode laser with a LP 650 emission filter. In order to obtain 3D images and carry out surface rendering of Mlc1p organization in the tips of cells, Z-stacks with a 0.1 μm step acquired with the Zeiss Confocal LSM 510 META/LSM 5 LIVE microscope and the surface rendering module of IMARIS 7.3 software (Bitplane, Switzerland, www.bitplane.com) were utilized. The 3D volume rendering was applied equally for all pictures. The thresholding was based on local contrast; for the Spitzenkörper, a diameter of the largest sphere was equivalent to 0.9 μm without smoothing (surface grain of 0.217 μm), whereas for the filament tube, a smoothing was applied (surface area detail level of 0.5 μm).

3.3 RESULTS

3.3.1 Enriched filipin staining is present in tips of Cdc5p-depleted filaments but also in incipient buds of yeast and pseudohyphae

In order to define the nature of Cdc5p-depleted cells, we characterized aspects of the associated polar growth machinery. Previous work demonstrated that tips of hyphae, but not yeast or pseudohyphae, contain enriched lipid rafts visualized with filipin stain (55). If filaments produced through Cdc5p depletion were originally elongated yeast buds that switched to a hyphal fate over time, filipin may be present at the tips but at a later time point. To address this

hypothesis, overnight cultures of *CDC5* conditional (*AG240; cdc5::hisG/cdc5::HIS1 PCK1::CDC5-hisG*) and control (*AG332; CDC5/CDC5*) strains were diluted into repressing medium (SD) and incubated at 30°C for 0, 2, 4 or 6 h. The control strain was also incubated in SD medium containing 10% serum at 37°C to induce hyphae, or in SD medium at 36°C to trigger formation of pseudohyphae. Cells were then stained with filipin and visualized. In serum-induced cells, filipin was observed as an enriched signal in the tips of the majority of hyphae (Table 3.4, Fig. 3.1), as previously reported (55). In comparison, cells depleted of Cdc5p for 2 h showed homogeneous staining on the cell periphery but enriched signal at tips of yeast buds (Fig. 3.1). By 4-6 h of Cdc5p depletion, when the majority of cells were elongated, an enriched filipin signal was observed at the tips (Table 3.4). At similar time points, 100% of control cells were in the yeast form at various stages of budding. However, the majority of small to medium-sized yeast buds at later time points also showed enriched filipin signal. A localized spot of the filipin signal was observed in some yeast cells lacking buds, possibly corresponding to the incipient bud site, and control cells grown under pseudohyphal conditions also showed enriched filipin signal at the tips of small and medium-sized buds (Fig. 3.1). Thus, polar sites of growth show enriched filipin staining, irrespective of cell type. It is not clear why our findings differ from those previously reported (55). The enriched signal at yeast buds was not dependent on the type of medium used, since incubating control cells in YEPD gave similar results (data not shown). However, a consistently enriched signal was observed at tips only when the filipin solution was freshly prepared from powder as opposed to being thawed from a dissolved master stock. Thus, our results suggest that enriched filipin signal can be found at polar growth sites in diverse cell types of *C. albicans* and is not specific to true hyphae. Similar to our findings, enriched filipin signal is associated with yeast bud tips of *Cryptococcus neoformans* as well as in mating projections (56).

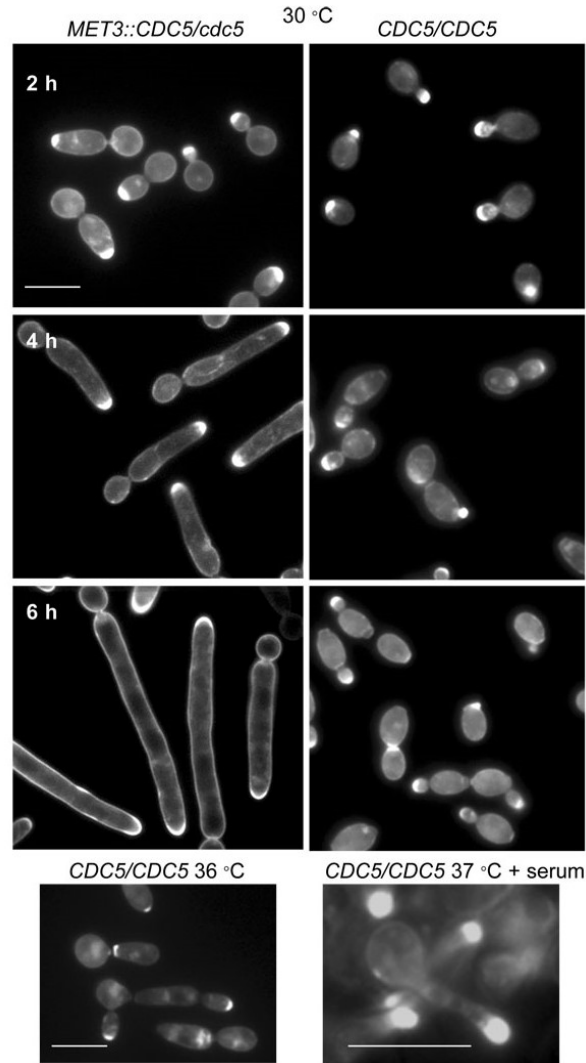


Figure 3.1: Tips of Cdc5p-depleted cells and young buds of yeast and pseudohyphae show enriched filipin staining, similar to hyphal tips. Overnight cultures of strains AG240 (*cdc5::hisG/cdc5::HIS1 PCK1::CDC5-hisG, MLC1/MLC1-GFP-URA3*) and AG332 (*CDC5/CDC5, MLC1/MLC1-GFP-URA3*) grown at 30°C in inducing medium (SS) were diluted into repressing medium (SD) and incubated at 30°C for the indicated times. Strain AG332 was also incubated in SD medium at 36°C for 6 h to promote pseudohyphal growth or SD medium supplemented with 10% FBS at 37°C for 90 min. to induce hyphae. Live cells were stained with filipin for 10 min, washed with sterile water and immediately examined by fluorescence microscopy. Bars: 10 μm.

Table 3.4: Proportion (%) of different cell morphologies and corresponding frequency of tip-enriched filipin signal in different cell types¹.

	<u>Unbudded</u>	<u>Small Bud²</u>	<u>Medium Bud²</u>	<u>Large Bud²</u>	<u>Elongated Bud²</u>	<u>Hyphae</u>
30°C						
<u>cdc5/PCK1::CDC5</u>						
0 h (n=120)	59/0	1/1	33/0	5/0	2/0	0/0
2 h (n=120)	19/0	15/15	34/28	13.5/12	18.5/17	0/0
4 h (n=106)	0/0	0/0	0/0	0/0	100/96	0/0
6 h (n=101)	0/0	0/0	0/0	0/0	100/84	0/0
<u>CDC5/CDC5</u>						
0 h (n=106)	91/0	0/0	2/0	7/0	0/0	0/0
2 h (n=123)	34/11 ³	17/17	24/24	25/25	0/0	0/0
4 h (n=117)	10/7 ³	9.5/9.5	49.5/44.5	31/4	0/0	0/0
6 h (n=117)	22/6 ³	13/13	35/31	30/0	0/0	0/0
36°C						
<u>CDC5/CDC5</u>						
(n=110)	3/0	17/17	41/35.5	39/4.5	0/0	0/0
37°C + serum						
<u>CDC5/CDC5</u>						
(n=35)	0/0	0/0	0/0	0/0	0/0	100/98

¹Strains AG240 (*cacdc5::hisG/cacdc5::HIS1 PCK1::CaCDC5-hisG, MLC1/MLC1-GFP-URA3*) and AG332 (*MLC1/MLC1-GFP-URA3*) were grown overnight at 30°C in inducing medium (SS), washed, diluted into repressing medium (SD) and incubated at 30°C for set times. Cells of strain AG332 were grown at 36°C for 4 h to promote pseudohyphal growth. Cells of strain AG332 were grown at 37°C with media supplemented with 10% FBS for 1.5 h to induce hyphal growth. Cells were stained with filipin for 10 min and analyzed by microscopy. Values represent percentage of cell morphology/percentage of those cells containing enriched filipin signal at a bud or filament tip.

²Buds scored as small were up to 0.25x in length that of the mother yeast cell, medium buds ranged from 0.25 to 0.5x the mother cell length, large buds were 0.5-1.0x the length of the mother yeast cell, and elongated buds contained lengths that were longer than that of the mother yeast cell.

³Non-budded cells with a polar spot of filipin signal on the surface.

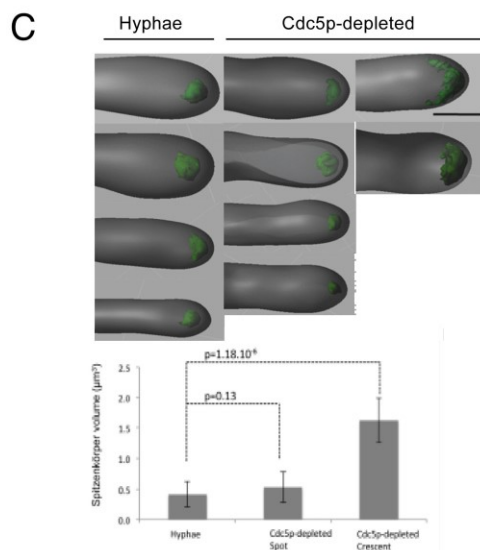
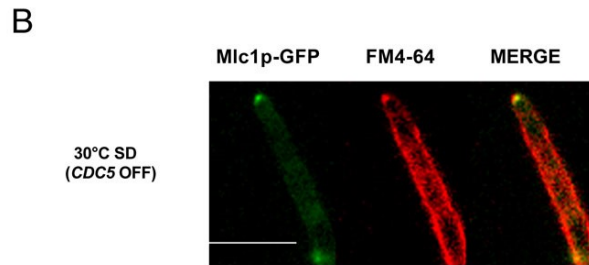
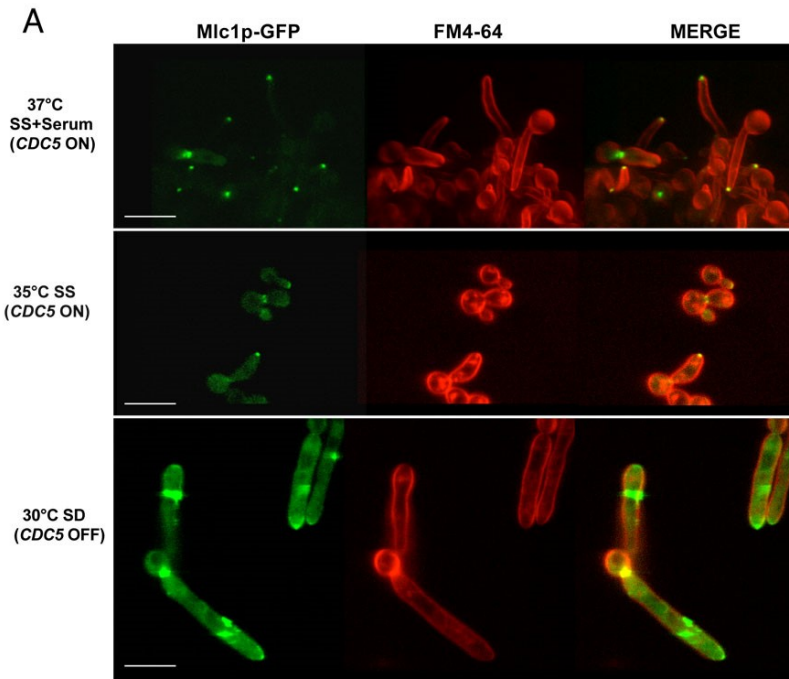
3.1.2 The myosin light chain Mlc1p is localized in a hyphal-specific manner in a proportion of Cdc5p-depleted cells

Previous work demonstrated that tips of *C. albicans* hyphae were distinct from those of yeast or pseudohyphal buds in that they contained a vesicle supply center or Spitzenkörper, similar to that found in tips of hyphae in filamentous fungi (12, 21, 57, 58). The Spitzenkörper in *C. albicans* hyphae was visualized as an FM4-64-staining, 3D spot just distal to or at the tip (12). The myosin light chain Mlc1p, the Rab GTPase Sec4p and its guanine nucleotide exchange factor (GEF), Sec2p, co-localize to this spot and are simultaneously found at subapical sites of septation (11-13). In contrast, these factors initially localize as a crescent at the tips of growing yeast and pseudohyphal buds, then re-localize to the bud neck prior to septation (12, 13). In order to clarify the nature of Cdc5p-depleted cells and elucidate mechanisms associated with their polarized growth, we explored the localization and organization of Mlc1p. *MLC1* was tagged at the C-terminus with GFP in cells containing a single copy of *CDC5* under control of the *PCK1* promoter (*cdc5Δ::hisG/PCK1::CDC5::HIS1, MLC1/MLC1-GFP-URA3*; AG240) (Fig. S3.1). We first investigated whether Mlc1p-GFP localized in the predicted manner under hyphal, yeast, and pseudohyphal conditions. Cells were incubated in *CDC5*-inducing medium (SS) overnight, washed and diluted into fresh SS medium containing 10% serum and incubated at 37° C to induce hyphae, or in SS medium without serum at either 30°C or 36°C to produce yeast or pseudohyphae, respectively. Under hyphal-inducing conditions, Mlc1p-GFP localized as a spot in the tips of germ tubes. FM4-64 staining of hyphal tips proved difficult, but in some hyphae a spot at the tip colocalized with that of Mlc1p-GFP (Fig. 3.2A). In yeast or pseudohyphal cells, Mlc1p-GFP localized either as a crescent in the tips of small buds, or at the bud neck (Fig. 3.2A). In addition, a spot of Mlc1p-GFP was observed in the tips of some incipient buds of yeast and pseudohyphae, where FM4-64 was also observed, suggesting that a Spitzenkörper-like structure was also present in these cells but only during very early stages of polarization, as previously reported (12, 13). Thus, Mlc1p-GFP localized in a predictable manner in the different cell types.

We next explored the localization of Mlc1p-GFP in cells depleted of Cdc5p. After incubating the same strain (AG240) in repressing medium (SD) at 30°C for 4 h, most cells were elongated with a mean length of 16.8 μm ± 0.6 (s.e.m., n=100) and contained a constriction at the bud neck, due to polarization during mitosis from a preformed bud (37). However, in two

separate trials, approximately 30% of cells contained a spot-like pattern of Mlc1p-GFP at the tips (Fig. 3.2A, Table 3.5). Intriguingly, most of these cells demonstrated simultaneous Mlc1p-GFP localization in subapical regions, either at the bud neck or along the long axis of the filament, the latter of which could indicate deregulated attempts at septation (Fig. 3.2A). The remaining cells showed Mlc1p-GFP at the tip in the form of a crescent and/or at the bud neck, or did not contain a signal (Table 3.5). In order to determine whether the frequency of cells containing spots of Mlc1p-GFP in the tip increased over time, we next analyzed Mlc1p-GFP in cells depleted of Cdc5p for 12 h. The total number of cells showing any signal was reduced, but approximately 20% contained a spot pattern of Mlc1p-GFP at the tips (Table 3.5). The spot was dynamic and would rapidly disappear with longer exposure time, comparable to that reported for Mlc1p-YFP in hyphal cells (11-13). A similar localization of Mlc1p-GFP with FM4-64 was not frequent, but observed in some tips (Fig. 3.2B). In order to confirm that the tip-localized spot of Mlc1p-GFP in Cdc5p-depleted cells was in a 3D organization (12), a 3D surface rendering of confocal image stacks was utilized. The results demonstrate that the spots were present in all focal planes and corresponded to a 3D structure at the tip, similar to that found in serum-induced hyphae (Fig. 3.2C) (12). The mean volume of Mlc1p-GFP spots in Cdc5p-depleted cell tips was similar to that in hyphae (Fig. 3.2C). The 3D rendering also confirmed the crescent organization of Mlc1p-GFP in other tips of Cdc5p-depleted cells (Fig. 3.2C). Thus, a proportion of Cdc5p-depleted cells shows hyphal-specificity in Mlc1p-GFP localization. However, the frequency of occurrence was not enhanced at 12 h depletion. In order to obtain more refined information on the temporal dynamics of localization, Mlc1p-GFP was visualized in live cells over a time course of *CDC5* repression. By 2 h, when cells were still in the yeast form and contained buds, Mlc1p-GFP was only detected at some bud necks (Fig. 3.2D). At 3 h, some cells were polarized and displayed Mlc1p-GFP signal at the tips that was maintained for the duration of the time course (Fig. 3.2D). Analysis of the tips at higher magnification confirmed that Mlc1p-GFP was in the form of a spot in some filaments (Fig. 3.2D). At 4 h, Mlc1p-GFP simultaneously appeared in subapical regions as short bands that often localized parallel to the long axis of the Cdc5p-depleted filaments. Mlc1p-GFP then localized as a perpendicular band, resembling that of a septum (Fig. 3.2D). In other tips, Mlc1p-GFP was observed in a crescent organization (Fig. 3.2D) or no signal was present. Collectively, these results demonstrate that at least a sub-population of Cdc5p-depleted cells show hyphal-specificity in Mlc1p-GFP organization, and this feature does not appear to be

associated with initial stages of polarized growth.



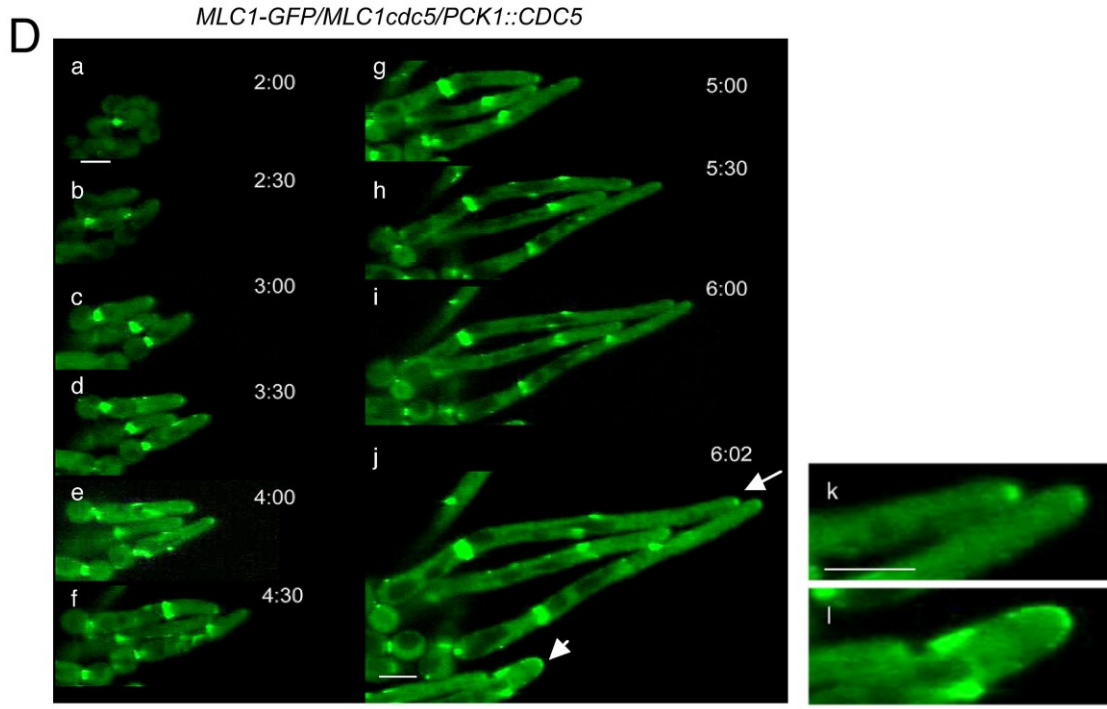


Figure 3.2: Mlc1p-GFP localization in Cdc5p-depleted cells. (A) Overnight cultures of strain AG240 (*cdc5::hisG/cdc5::HIS1 PCK1::CDC5-hisG, MLC1/MLC1-GFP-URA3*) grown at 30°C in inducing medium (SS) were diluted into fresh SS medium supplemented with 10% FBS at 37°C for 2 h to induce hyphae, SS medium at 36°C for 5 h to promote pseudohyphal growth, or SD repressing medium at 30°C for 4 h to deplete Cdc5p. Prior to mounting on slides and imaging, FM4-64 was introduced to cell cultures. (B) Cells depleted of Cdc5p as in (A) but for 6 h. Bars: 10 μ m. (C) 3D imaging and volume measurements of Mlc1p-GFP signals in tips of serum-induced hyphae and Cdc5p-depleted cells prepared as described in (A). The surface rendering module of the IMARIS 7.3 software was based on 0.1 μ m step Z-stacks. Student's T-tests were performed relative to the mean volume of Mlc1p-GFP spots in hyphae. (D) Time course of Mlc1p-GFP localization in Cdc5p-depleted cells. Strain AG240 was incubated in SS inducing medium as described in (A), transferred to a pre-made agarose pad consisting of SD repressing medium on a microscope slide, sealed with VALAP and visualized with LSM 510 confocal microscope fitted with a x 63 objective. Images were recorded every 30 min, and Z stack series consisting of 0.1 μ m steps were acquired.

Table 3.5: Mlc1p-GFP localization patterns in cells depleted of Cdc5p¹.

	Tip			Sub-apical			Tip + sub-apical ²	
	Spot	Crescent	No signal	Bud-neck	Filament	No signal	Spot + bud-neck	Crescent + bud-neck
Cdc5p depletion (h)								
4 (n=107)	32.0	21.0	47.0	91.0	0	9.0	94.0	95.0
(n=112)	37.0	34.0	29.0	89.0	0	11.0	97.6	92.0
12 (n=58)	22.5	3.5	74.0	N.D.	17.5	82.5	15.4	0
(n=54)	27.0	4.0	69.0	N.D.	35.0	65.0	33.3	50.0

¹Strain AG240 (*cdc5::hisG/cdc5::HIS1 PCK1::CDC5-hisG, MLC1/MLC1-GFP-URA3*) was grown overnight at 30°C in inducing medium (SS), washed, diluted into repressing medium (SD) and incubated at 30°C for 4 or 12 h. Values are expressed as percentage of total cells.

²Of cells that contained signal in the tip, percentage that simultaneously showed signal in subapical regions.

3.1.3 The Cdc42p GAP Rga2p shows an increase in phosphorylation and decrease in abundance during later stages of Cdc5p depletion

Previous work demonstrated that Cdc28p/Hgc1p-dependent phosphorylation and down-regulation of the Cdc42p GAP, Rga2p, were required for hyphal growth (19, 20). This phosphorylation correlates with exclusion of Rga2p-GFP from the tips (19). In contrast, Rga2p-GFP is present in the tips of yeast and pseudohyphal buds (19). An increase in Rga2p phosphorylation also occurs during initial yeast bud outgrowth, but this is transient and independent of Hgc1p (19). In order to further address the nature of Cdc5p-depleted cells, we tagged *RGA2* at the C-terminus with three copies of hemagglutinin (HA), resulting in strains AG374 (*RGA2/RGA2-HA-URA3*) and AG379 (*cdc5::hisG/cdc5::HIS1 PCK1::CDC5-hisG, RGA2/RGA2-HA-URA3*) (Fig. S3.2). Overnight cultures of cells grown in SS inducing medium were diluted into fresh SS or SD repressing medium and incubated for various time periods at 30°C. In SD medium, Rga2p-HA demonstrated a shift to a higher molecular weight by 6-7.5 h of Cdc5p depletion (Fig. 3.3A). In contrast, Rga2p-HA in control cells did not show similar modifications (Fig. 3.3A). In order to determine whether the band shift was due to an increase in phosphorylation, the experiment was repeated in the presence or absence of calf intestinal phosphatase (CIP). When cells were incubated in repressing medium for 9 h, the Rga2p-HA band shift in Cdc5p-depleted cells was suppressed in the presence of CIP (Fig. 3.3B). Rga2p-HA in control cells showed some CIP-dependent size reduction, suggesting a basal level of phosphorylation, but this was minor compared to that observed in Cdc5p-depleted cells. However, cells lacking Cdc5p also showed a decrease in the abundance of Rga2p-HA over time. In order to distinguish whether this was due to a decrease in protein expression/stability vs differences in gel loading, samples were separated on a higher concentration gel that allowed for detection of the lower molecular weight loading control protein Cdc28p. In repressing medium, a decrease in Rga2p-HA intensity was observed at later time points, in contrast to that observed in control cells, and Cdc28p signal indicated that this was not due to differences in loading (Fig. S3.3). Moreover, the intensity of Rga2p-HA signal was consistent between time points when cells were incubated in *CDC5*-inducing medium (Fig. S3.3), indicating that the effect was specific to depletion of Cdc5p. Thus, in the absence of Cdc5p, Rga2p is modified at the level of phosphorylation and stability and/or expression, suggesting down-regulation of activity, as seen in true hyphae. However, this occurs during later stages of *CDC5* repression, consistent with the

hypothesis that the filaments may be elongated buds that switch to a hyphal fate over time.

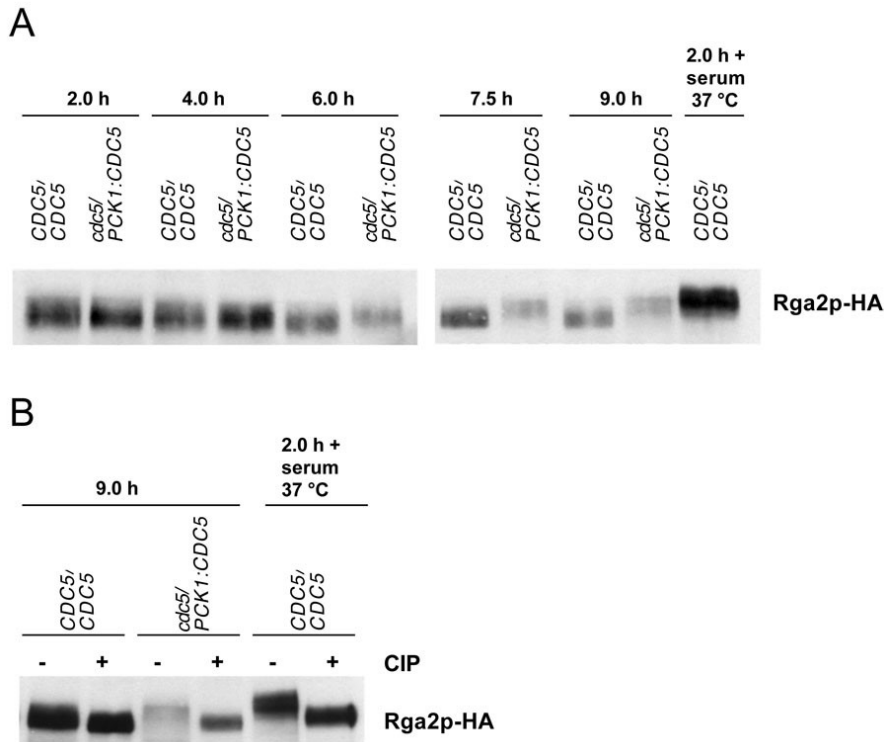


Figure 3.3: Rga2p undergoes a phosphorylation-dependent shift in Cdc5p-depleted cells. (A) Western blot of overnight cultures of strains AG374 (*CDC5/CDC5, RGA2/RGA2-HA-URA3*) and AG379 (*cacdc5::hisG/cacdc5::HIS1 PCK1::CaCDC5-hisG, RGA2/RGA2-HA-URA3*) that were grown in SS medium, diluted into SD repressing medium at 30°C and collected at the indicated time points. Strain AG374 was also incubated in SD medium supplemented with 10% Fetal Bovine Serum (FBS) for 2 h at 37°C to induce hyphae. **(B)** Western blot of select protein samples from (A) either in the presence (+) or absence (-) of calf intestinal alkaline phosphatase (CIP).

3.1.4 A core regulator of hyphal growth, *UME6*, and other HSGs including *HGC1* and *HWPI* are induced in Cdc5p-depleted cells at or near hyphal-specific levels

Ume6p is a core regulator of hyphal growth, as it controls many hyphal-specific genes (HSGs) and high levels of expression are sufficient to drive hyphal growth from yeast cells (28, 59). Our previous work involving time course-based transcription profiles of Cdc5p-depleted cells demonstrated that *UME6* and other HSGs such as *HGC1* and *HWPI* are induced but only at later stages (36). However, HSGs also can be expressed in pseudohyphae, albeit at levels lower

than those in hyphae (15, 60, 61). In order to clarify whether expression levels of *UME6*, *HWP1* and *HGC1* in *Cdc5p*-depleted cells were similar to those in hyphae, Northern blots were utilized to quantify expression during a time course of *CDC5* repression. Overnight cultures (CB104, CB400) were diluted into SD repressing medium and incubated at 30°C for various periods of time. Wild-type cells of strain SC5314 were also incubated in SD medium at 30°C or 37°C with the addition of 10% serum to obtain yeast and hyphal samples, respectively, for comparison. Expression was detectable by 7 h, where *UME6* levels were higher than those of *HGC1* or *HWP1* (Fig. 3.4). Expression levels of all three genes continued to increase such that by 9-11 h of *CDC5* repression, they were at or near those in serum-induced hyphae (Fig. 3.4). Intriguingly, the period of induction correlated with that of *Rga2p* modifications, suggesting that major changes took place in the cells at this time, and that these are consistent with features of true hyphae.

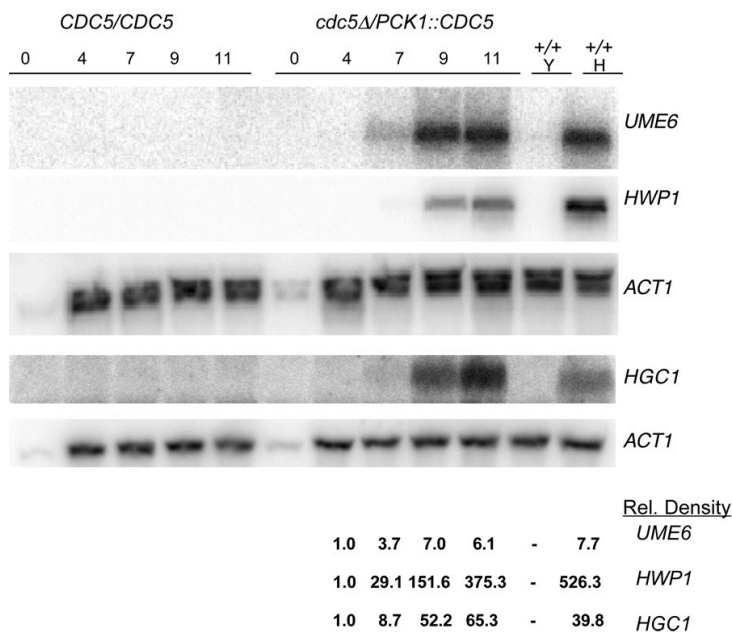


Figure 3.4: *UME6*, *HWP1* and *HGC1* expression is induced at later time points of *Cdc5p* depletion. Overnight cultures of strains CB400 (*URA3+HIS1+*) and CB104 (*cacdc5Δ::hisG/cacdc5Δ::HIS1/PCK1::CaCDC5-URA3*) were transferred from SS to SD repressing medium and incubated at 30°C for the indicated time points. Strain SC5314 (*+/+*) was also grown in either SD medium at 30°C for 8 h to promote yeast growth (Y) or SD medium supplemented with 10% FBS at 37°C for 2 h to induce hyphae (H). *ACT1* was used as loading control. Density values represent adjusted relative densities and were calculated using ImageJ as described in Chou *et al.*, 2011 (39).

3.1.5 Ume6p influences expression of *HWPI* and morphology of Cdc5p-depleted filaments at later stages of growth

If Cdc5p-depleted cells were elongated buds that adapted a hyphal fate over time, we predict that a regulator(s) of hyphal development should influence late stage Cdc5p-depleted growth and HSG expression. Since Cdc5p-depleted filaments do not require the hyphal signaling pathway component Efg1p (37), but strongly induce *UME6*, we asked if this expression was functional and required for hyphal-specific features observed in the cells. In order to address this question, both copies of *UME6* were deleted from a *CDC5*-conditional strain, resulting in strains AG530 and AG531 (*cdc5::hisG/MET3::CDC5-ARG4, ume6::URA3/ume6::HIS1*) (Fig. S3.4). Overnight cultures of strains AG530 and the control strain AG553 (*cdc5::hisG/MET3::CDC5-ARG4, UME6/UME6, URA3+ HIS1+*) were diluted into +MC repressing medium and incubated for various periods for morphology determination and RNA extraction. In the absence of *UME6*, Cdc5p-depleted cells were able to grow in a polarized manner and the filaments resembled those of control cells at 6 h (Fig. 3.5) and later time points of 9 and 11 h (data not shown). However, a clear difference in morphology was observed with longer incubation (14-24 h) in that the filaments appeared more wide, vacuolated, and surrounded by more cell debris compared to control cells (Fig. 3.5). More cells also stained with propidium iodide, suggesting that loss of *UME6* affects cell integrity (Fig. S3.6). We next asked if Ume6p was required for expression of *HWPI* in Cdc5p-depleted cells. Northern blots of RNA obtained from strains AG530 and AG531 incubated in repressing medium for 11 h demonstrated that *HWPI* expression was severely reduced in the absence of *UME6* (Fig. 3.6). *HGCI* expression was also reduced, but to a lesser extent (Fig. 3.6). Thus, Ume6p influences the morphology of late-stage Cdc5p-depleted cells, and influences *HWPI* and *HGCI* expression. Since *HGCI* was also induced in Cdc5p-depleted cells, we asked if it influenced the Cdc5p-depleted cell phenotype. Both copies of *HGCI* were deleted from a *CDC5* conditional strain, resulting in strains AG574 and AG577 (*cdc5::hisG/MET3::CDC5-ARG4, hgc1::URA3/hgc1::HIS1*) (Fig S3.5). In the absence of *HGCI*, Cdc5p-depleted cells could polarize and morphology was similar to control cells at early stages of growth (Fig. 3.5). However, similar to cells lacking Ume6p, morphology was affected at later growth stages as cells appeared more vacuolated and stained more readily with propidium iodide (Fig. S3.6). Absence of Hgc1p did not influence *HWPI* or *UME6* expression (Fig. 3.6), similar to that reported in true hyphae (30).

Thus, Ume6p and Hgc1p are important for morphology and integrity of later-stage Cdc5p-depleted filaments, and Ume6p is required for expression of *HWPI* and in part, *HGC1*. Since similar features are found in true hyphae, the results support the model that Cdc5p-depleted cells may switch to the hyphal fate over time in a manner dependent on the hyphal regulators Ume6p and Hgc1p.

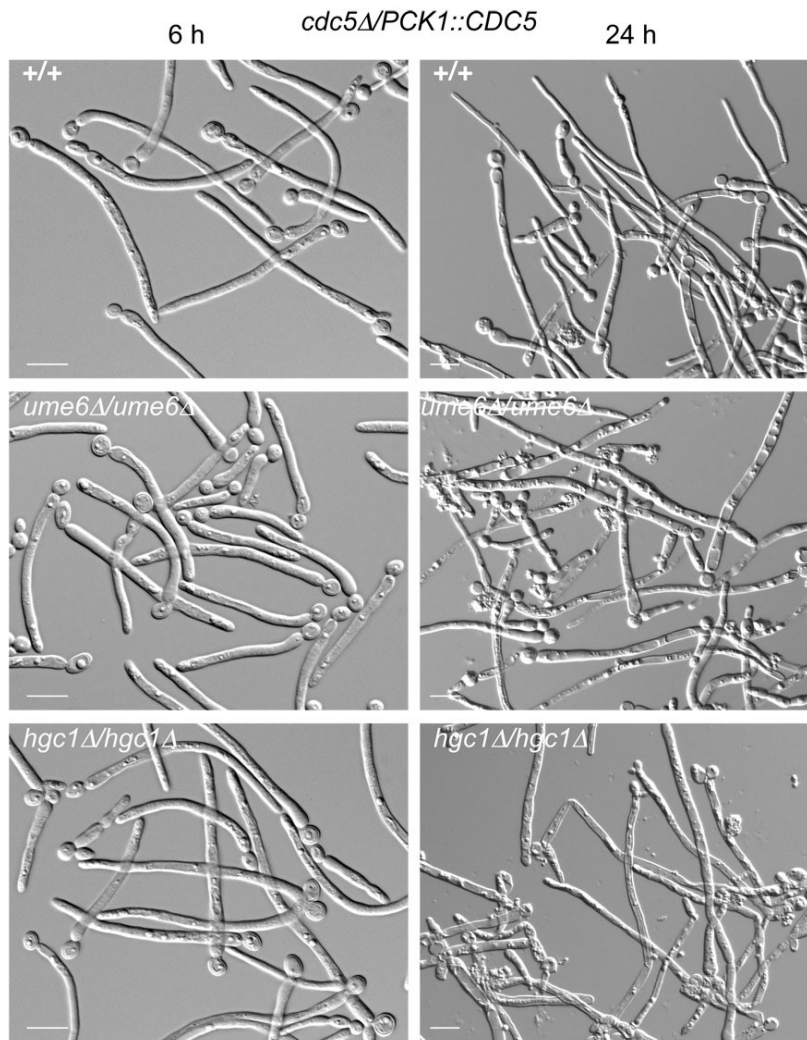


Figure 3.5: Absence of *UME6* or *HGC1* influences the shape and integrity of Cdc5p-depleted filaments at only later stages of growth. Overnight cultures of strains AG553 (*cdc5Δ::hisG/MET3::CDC5-ARG4, URA3+ HIS1+*, *UME6/UME6, HGC1/HGC1*), AG530 (*cdc5Δ::hisG/MET3::CDC5-ARG4, ume6Δ::URA3/ume6Δ::HIS1, HGC1/HGC1*) and AG574 (*cdc5Δ::hisG/MET3::CDC5::ARG4, hgc1Δ::URA3/hgc1Δ::HIS, UME6/UME6*) in -MC inducing medium were diluted into +MC repressing medium and incubated at 30°C for 6 or 24 h. Samples at 6 h were fixed in 70% ethanol prior to viewing while 24 h samples were live when mounted on microscope slides. Bars: 10 μm.

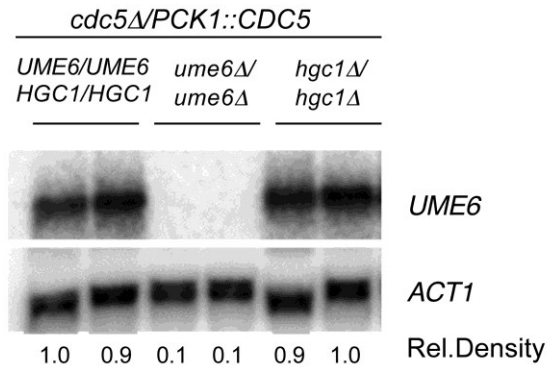
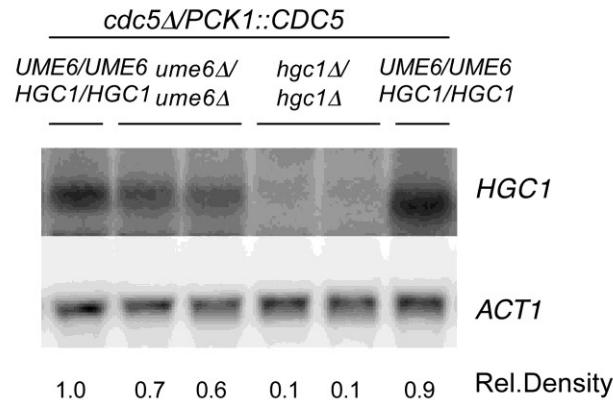
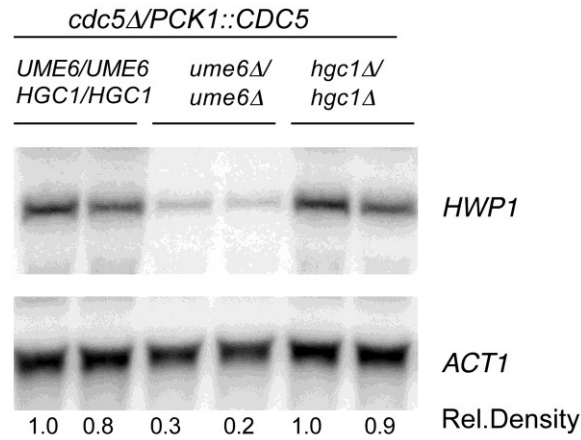


Figure 3.6: Expression levels of *HWP1* and *HGC1* are reduced in *Cdc5p*-depleted cells lacking *UME6*. Overnight cultures of strains AG553, AG547 (*cdc5::hisG/MET3::CDC5-ARG4 URA3+HIS1+*), AG530, AG531(*cdc5::hisG/MET3::CDC5-ARG4 ume6::URA3/ume6::HIS1*) and AG574, AG577 (*cdc5::hisG/MET3::CDC5-ARG4 hgc1::URA3/hgc1::HIS1*) were diluted into +MC repressing medium and incubated at 30°C for 11 h. *ACT1* was used as loading control. Density values represent adjusted relative densities and were calculated using ImageJ as described in Chou *et al.*, 2011 (39).

3.1.6 Cdc5p-depleted cells do not require Hms1p for polarized growth or expression of *UME6* and *HWPI*

The regulation of *UME6* is complex and not fully understood (62). Under hyphal-inducing conditions, its expression is controlled by transcription factors, such as Efg1p, that are under control of various environment-responsive signaling pathways (21, 24). Since Cdc5p-depleted cells adapt a hyphal fate at later stages of growth in the absence of hyphal-inducing environmental cues, the mechanisms underlying *UME6* induction in these cells remain unclear. One possibility is a signaling pathway involving the transcription factor Hms1p, which links the heat shock protein Hsp90p to polar morphogenesis and expression of HSGs (2). Hsp90p influences many cellular processes, including mitotic progression, and its absence results in highly polarized filaments that express several HSGs in a cAMP-dependent manner (2, 63), similar to that shown for cells resulting from depletion of Cdc5p (36, 37) or other factors that cause S or M phase arrest in *C. albicans* yeast cells (32, 38, 39, 42, 44, 64). Hms1p binds promoters of five HSGs, including *UME6*, and its absence prevents polarized growth and strongly reduces *HWPI* and *UME6* expression in Hsp90p-compromised cells (2). In order to determine whether the Cdc5p-depleted cell phenotype also requires Hms1p, both copies of *HMS1* were deleted from a *CDC5* conditional strain, resulting in strains AG579, AG580 and AG581 (*cdc5::hisG/MET3::CDC5-ARG4*, *hms1::URA3/hms1::HIS1* cells) (Fig. S3.7). In the absence of *HMS1*, Cdc5p-depleted cells were able to grow in a polar manner. Filament morphology was similar to that of control cells, even at later time points, although some blunt tips were noted (Fig. 3.7A). The filaments did not display the loss of integrity as seen in the absence of Ume6p or Hgc1p (Fig. 3.7A; Fig. S3.6). Further, *UME6* and *HWPI* expression was not reduced in the absence of *HMS1* (Fig. 3.7B). Thus, Cdc5p-depleted cells grow in a polarized fashion and induce *UME6* and *HWPI* expression via alternate mechanisms.

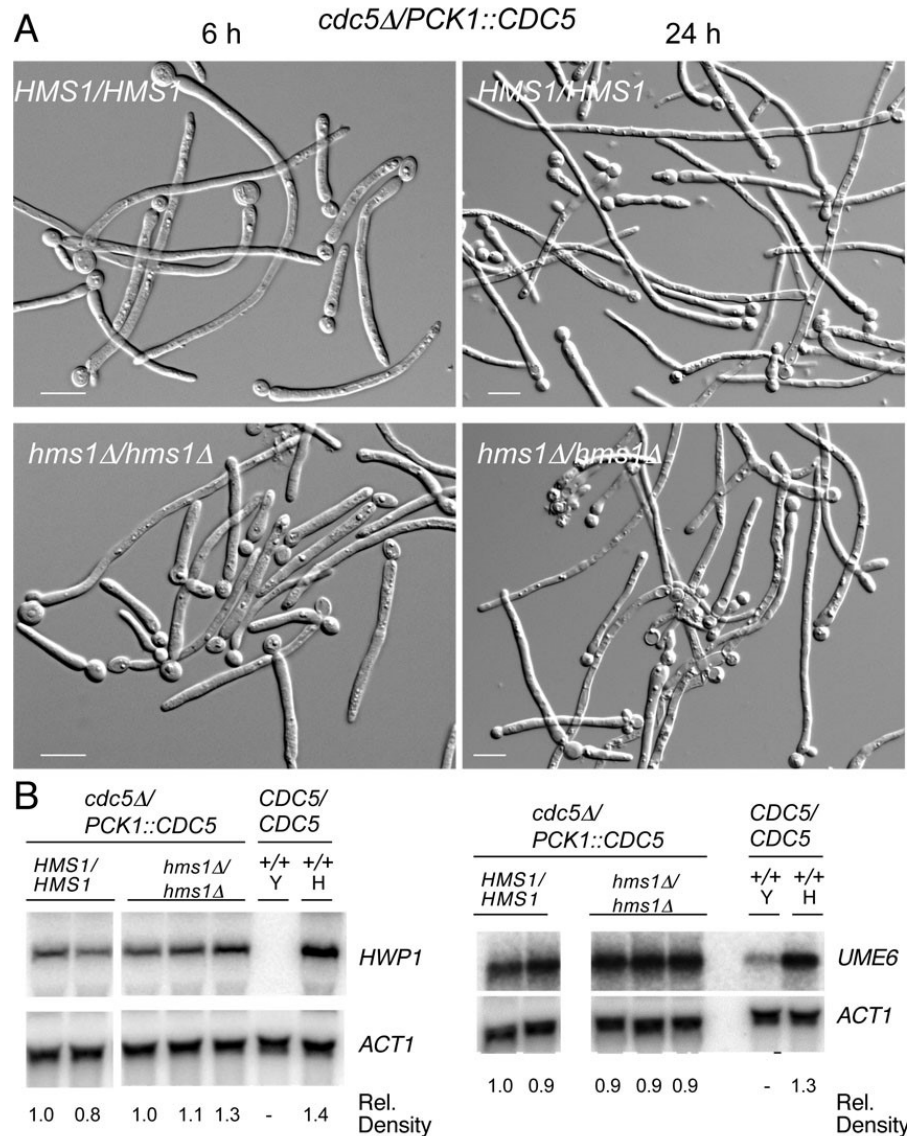


Figure 3.7: Absence of *HMS1* does not prevent polarized growth or expression of *UME6* and *HWP1* in *Cdc5p*-depleted cells.

(A) Overnight cultures of strains AG553 (*cdc5Δ::hisG/MET3::CDC5-ARG4*, *URA3+ HIS1+*, *HMS1/HMS1*), and AG580 (*cdc5Δ::hisG/MET3::CDC5-ARG4*, *hms1Δ::URA3/hms1Δ::HIS1*) were diluted into +MC repressing medium and incubated at 30°C for 6 or 24 h. Samples at 6 h were fixed in 70% ethanol while 24 h samples were observed live under the microscope. Bars: 10 μm.

(B) Overnight cultures of strains AG553, AG547 (*cdc5::hisG/MET3::CDC5-ARG*, *URA3+ HIS1+*, *HMS1/HMS1*) and AG579, AG580 AG581 (*cdc5::hisG/MET3::CDC5-ARG4 hms1::URA3/hms1::HIS1*) were diluted into +MC repressing medium and incubated at 30°C for 11 h. Strain *SC5314* (+/+) was also grown in +MC medium at either 30°C for 8 h to promote yeast growth (Y) or supplemented with 10% FBS at 37°C for 2 h to induce hyphae (H). *ACT1* was used as loading control. Density values represent adjusted relative (Rel.) densities and were calculated using ImageJ as described in Chou *et al.*, 2011 (39).

3.4 DISCUSSION

Arresting yeast cells of *C. albicans* in mitosis results in the formation of filaments that maintain polarized growth and express HSGs, much like true hyphae. However, the nature of these growth forms and the mechanisms underlying their generation has been elusive. Here, we show that filaments produced through depletion of the mitotic polo-like kinase Cdc5p have characteristics of elongated buds during early stages of elongation, but demonstrate several features diagnostic of true hyphae at later growth stages, including Spitzenkörper-like localization of Mlc1p, phosphorylation of the Cdc42p GAP Rga2p, and strong expression of hyphal-associated genes such as *UME6*, *HGC1*, and *HWP1*. *HWP1* expression was strongly dependent on Ume6p, and absence of Ume6p or Hgc1p influenced the maintenance, but not initiation, of filament morphology and integrity. Finally, polar growth and *UME6* expression in Cdc5p-depleted cells were independent of Hms1p, unlike filaments produced through depletion of Hsp90p (2). Thus, polar cells that form in response to Cdc5p depletion may initially represent elongated buds, but switch to the hyphal fate over time through a mechanism that involves a novel mode of *UME6* induction.

3.4.1 Cdc5p-depleted cells are elongated buds during initial stages of polarized growth

We previously suggested that filaments produced through Cdc5p depletion were not hyphae during early growth stages based on their transcription profiles, a requirement for the spindle checkpoint factor Bub2p, and independence of the hyphal regulator Efg1p (36). Our time course-based investigations of aspects of the polar growth machinery support this notion, and suggest that the cells may be elongated buds (36). Unlike hyphal germ tubes, emerging tips of Cdc5p-depleted cells did not demonstrate a 3D spot-like localization of Mlc1p-GFP, and Rga2p was not hyperphosphorylated. Further, Cdc5p-depleted filaments grew in a polar manner for an extended time in the absence of Ume6p or Hgc1p, unlike serum-induced germ tubes (28, 30, 59). Elongated bud formation could be due to defects in the ability of the bud to switch from polar to isometric growth. In *S. cerevisiae*, yeast buds grow in a polar manner from G1/S to late G2 phase of the cell cycle, and then switch to isometric growth (65). The switch is regulated in part by the CDK Cdc28p falling under control of the B-type cyclin Clb2p, which in turn causes disassembly of the Cdc24p-Bem1p-Cla4p complex, a decrease in Cdc42p-GTP, and depolarization of actin patches (65, 66). In *C. albicans*, yeast buds show similar growth patterns

but the precise timing and mechanisms underlying the depolarizing switch are not yet known (1, 10, 12, 67). Since *C. albicans* Cdc5p is required in early mitosis (36, 37), it is conceivable that its absence may influence the depolarization machinery. In *S. cerevisiae*, absence of Cdc5p results in a large budded cell (68, 69), but overexpression (70) or Cdc5p mutations that deregulate septin organization or Swe1p function produce elongated buds, albeit not as long as those observed in *C. albicans* (71-73). Cdc5p also activates Rho1p at the division site, negatively regulates Cdc42p activity in late mitosis to permit cytokinesis, and physically interacts with the Cdc42p GAP Bem3p, demonstrating links between polo-like kinases and cytoskeletal and polarity-regulating factors (74, 75). Further, the polo kinase Plo1p in *S. pombe* influences new and stress-induced polarized growth (76, 77). Although the functions and targets of Cdc5p in *C. albicans* are not yet known, it is possible that Cdc5p depletion deregulates the bud growth pattern, resulting in elongated buds.

3.4.2 Cdc5p-depleted cells may switch to the hyphal fate in a Ume6p-dependent manner

Since Cdc5p-depleted cells expressed several HSGs at later stages of growth, we previously proposed that they became hyphal-like (36, 39). However, pseudohyphae also express HSGs, albeit at reduced levels, questioning this hypothesis (15, 60, 61). We now provide data that support the model that Cdc5p-depleted cells might switch to the hyphal fate over time. First, Cdc5p-depleted cells express HSGs at later stages of development, including *HWPI*, *UME6* and *HGCI*, at levels approximating those in serum-induced hyphae. Second, the Cdc42p GAP Rga2p showed enhanced phosphorylation at approximately the same time as *UME6* induction. Rga2p hyperphosphorylation is also observed in serum-induced hyphae, which results in down-regulation and a corresponding maintenance of Cdc42p at the hyphal tip (19, 20). Although Rga2p is hyperphosphorylated in yeast, this is only observed during initial yeast bud outgrowth (19). Since Rga2p was not detectably phosphorylated during early stages of Cdc5p depletion, when the cells were clearly polarizing, the phosphorylation observed at later time points can not be due to maintenance of phosphorylation associated with incipient bud growth. Cdc5p-depleted cells also showed reduced levels of Rga2p, unlike the situation in serum-induced hyphae. Although novel, this reinforces the net effect of Rga2p down-regulation. This protein depletion was not a global effect, since Cdc28p did not show detectable decreases in abundance during Cdc5p shut-off. Third, absence of Ume6p and a known downstream target, Hgc1p, influenced

the morphology and integrity of Cdc5p-depleted cells at later stages of growth, and *HWP1* expression was dependent in large part on Ume6p. Similarly, Ume6p and Hgc1p are required for maintenance, but not initiation, of serum-induced hyphal growth (30, 59). Finally, a proportion of Cdc5p-depleted cells showed hyphal-specific features (12) in Mlc1p-GFP localization, including a 3D spot organization in the tip that could be maintained over time, and simultaneous localization at the tip and the bud neck or along the subapical region. Many other cells contained a crescent organization of Mlc1p-GFP in the tip, like pseudohyphae, and by 12 h of Cdc5p depletion, fewer cells contained any signal. These observations may be due to the dynamic nature of Mlc1p-GFP signal (12), possible differences in growth rate, and heterogeneity in the timing and extent to which a change in fate might take place. Although the simultaneous localization of Mlc1p-GFP at the tip and in subapical regions could simply reflect a block in the cell cycle, a 3D spot organization in the tip implies that the cells were not all simply pseudohyphae. Collectively, the data suggest that Cdc5p-depleted cells can adapt a hyphal fate, under low temperature and low pH conditions.

The mechanisms underlying the emergence of hyphal-specific features in Cdc5p-depleted cells may involve the gradual induction of *UME6*. Ume6p can regulate the transition from yeast to pseudohyphae to hyphae in a dose-dependent manner (61). Maintenance, but not initiation, of hyphal growth requires induction of *UME6*, which in turn maintains expression of HSGs, including *HGCI*. Hgc1p/Cdc28p activity in turn is required for Rga2p phosphorylation in true hyphae (19, 20). At later stages of Cdc5p-depletion, *UME6* was expressed while Rga2p was phosphorylated. *UME6* was required for *HWP1* expression, and influenced filament morphogenesis, supporting the idea that gradual induction of *UME6* may underlie the cell fate change. In one model, expression of *UME6* may induce HSGs, and Hgc1p in turn may interact with Cdc28p to help drive the switch to a hyphal fate. Although it is not known if phosphorylation of Rga2p in Cdc5p-depleted cells requires Hgc1p, it is noteworthy that the timing of *UME6* and *HGCI* induction correlated with that of Rga2p phosphorylation. We can not rule out the possibility that Rga2p down-regulation is the initiating cue, but this by itself can not generate polarized growth under yeast growth conditions; *C. albicans* cells lacking Rga2p or another Cdc42p GAP, Bem3p, grow as yeast and strains lacking both GAPs show hyperpolarized growth and some other hyphal features under pseudohyphal, but not yeast growth conditions (19,

20). It is also possible that several initiating mechanisms are involved, as *HGC1* expression was only partly dependent on Ume6p, as seen in true hyphae (20).

3.4.3 Induction of *UME6* in the absence of environmental cues or Hms1p suggests additional modes of regulation

A critical question is how depletion of Cdc5p leads to induction of *UME6*. To date, *UME6* expression has been shown to be dependent on several environment-induced hyphal signaling pathway components, such as Efg1p, Tec1p, Cph1p and Eed1p, for example, and is repressed by Nrg1p and Tup1p (21, 28). Alternatively, *UME6* is induced by the transcription factor Hms1p in response to heat treatment or depletion of Hsp90p (63). Intriguingly, Ume6p is stabilized under several hyphal-inducing conditions and can influence its own expression in a positive feedback loop (62, 78). Since Cdc5p-depleted filaments form in the absence of hyphal-inducing cues and Efg1p (37) and did not require Hms1p for polarized growth or *UME6* expression, induction of *UME6* under these conditions involves alternative mechanisms. Given the delayed emergence of hyphal features and expression patterns in these cells, one possibility involves maintenance of polarized growth and corresponding changes in actin. Previous work demonstrated that stabilized actin contributes to upregulation of *HWPI* expression in *C. albicans*, G-actin interacts with Cyr1p of the cAMP pathway, and tip localization of Cdc42p is associated with expression of the hyphal transcription program (79-82). Maintaining polarized growth of a bud could result in modification of the actin cytoskeleton and associated regulators at the tip that in turn influence aspects of the hyphal signaling pathways. Thus, similar to a block in G1 phase, arresting *C. albicans* yeast cells in mitosis may ultimately result in hyphal growth and expression of important virulence factors, albeit utilizing alternative initiating mechanisms. Linking filamentous growth and associated gene expression patterns to perturbations in yeast cell cycle phase progression may provide an advantage for *C. albicans* in the presence of stresses that impinge on the cell cycle within the host environments (14, 35, 36, 43,44). In summary, our results shed light on the nature of mitotic-arrested, Cdc5p-depleted cells, and expand on the multiple strategies with which *C. albicans* can modulate growth mode and expression of developmental factors, including *UME6*, which are important for pathogenesis.

3.5 ACKNOWLEDGEMENTS

The authors thank M. Whiteway for comments on the manuscript. This work was supported by NSERC Discovery Grant N00944 to CB and NSERC PGSD Graduate Student Scholarship to AG. We would like to thank Centre for Microscopy and Cell Imaging (CMCI) at Concordia University for their help in microscopic pictures.

3.6 REFERENCES

1. **Sudbery P, Gow N, Berman J.** 2004. The distinct morphogenic states of *Candida albicans*. Trends in Microbiology **12**:317-324.
2. **Shapiro RS, Sellam A, Tebbji F, Whiteway M, Nantel A, Cowen LE.** 2012. Pho85, Pcl1, and Hms1 signaling governs *Candida albicans* morphogenesis induced by high temperature or Hsp90 compromise. Current Biology : CB **22**:461-470.
3. **Dupont PF.** 1995. *Candida albicans*, the opportunist. A cellular and molecular perspective. Journal of the American Podiatric Medical Association **85**:104-115.
4. **Odds FC.** 1985. Morphogenesis in *Candida albicans*. Critical Reviews in Microbiology **12**:45-93.
5. **Corner BE, Magee PT.** 1997. *Candida* pathogenesis: unravelling the threads of infection. Current Biology : CB **7**:R691-694.
6. **Boonyasiri A, Jearanaisilavong J, Assanasen S.** 2013. Candidemia in Siriraj Hospital: epidemiology and factors associated with mortality. Journal of the Medical Association of Thailand = Chotmaihet thangphaet **96 Suppl 2**:S91-97.
7. **Hsueh PR, Graybill JR, Playford EG, Watcharananan SP, Oh MD, Ja'alam K, Huang S, Nangia V, Kurup A, Padiglione AA.** 2009. Consensus statement on the management of invasive candidiasis in Intensive Care Units in the Asia-Pacific Region. International Journal of Antimicrobial Agents **34**:205-209.
8. **Leroy O, Gangneux JP, Montravers P, Mira JP, Gouin F, Sollet JP, Carlet J, Reynes J, Rosenheim M, Regnier B, Lortholary O, AmarCand Study G.** 2009. Epidemiology, management, and risk factors for death of invasive *Candida* infections in critical care: a multicenter, prospective, observational study in France (2005-2006). Critical Care Medicine **37**:1612-1618.
9. **Staebell M, Soll DR.** 1985. Temporal and spatial differences in cell wall expansion during bud and mycelium formation in *Candida albicans*. Journal of General Microbiology **131**:1467-1480.
10. **Hazan I, Sepulveda-Becerra M, Liu H.** 2002. Hyphal elongation is regulated independently of cell cycle in *Candida albicans*. Molecular Biology of the Cell **13**:134-145.
11. **Bishop A, Lane R, Beniston R, Chapa-y-Lazo B, Smythe C, Sudbery P.** 2010. Hyphal growth in *Candida albicans* requires the phosphorylation of Sec2 by the Cdc28-Ccn1/Hgc1 kinase. The EMBO Journal **29**:2930-2942.
12. **Crampin H, Finley K, Gerami-Nejad M, Court H, Gale C, Berman J, Sudbery P.** 2005. *Candida albicans* hyphae have a Spitzenkorper that is distinct from the polarisome found in yeast and pseudohyphae. Journal of Cell Science **118**:2935-2947.

13. **Jones LA, Sudbery PE.** 2010. Spitzenkorper, exocyst, and polarisome components in *Candida albicans* hyphae show different patterns of localization and have distinct dynamic properties. *Eukaryotic Cell* **9**:1455-1465.
14. **Sudbery PE.** 2001. The germ tubes of *Candida albicans* hyphae and pseudohyphae show different patterns of septin ring localization. *Molecular Microbiology* **41**:19-31.
15. **Berman J.** 2006. Morphogenesis and cell cycle progression in *Candida albicans*. *Current Opinion in Microbiology* **9**:595-601.
16. **Warena AJ, Konopka JB.** 2002. Septin function in *Candida albicans* morphogenesis. *Molecular Biology of the Cell* **13**:2732-2746.
17. **Gierz G, Bartnicki-Garcia S.** 2001. A three-dimensional model of fungal morphogenesis based on the vesicle supply center concept. *Journal of Theoretical Biology* **208**:151-164.
18. **Virag A, Harris SD.** 2006. The Spitzenkorper: a molecular perspective. *Mycological Research* **110**:4-13.
19. **Zheng XD, Lee RTH, Wang YM, Lin QS, Wang Y.** 2007. Phosphorylation of Rga2, a Cdc42 GAP, by CDK/Hgc1 is crucial for *Candida albicans* hyphal growth. *Embo Journal* **26**:3760-3769.
20. **Court H, Sudbery P.** 2007. Regulation of Cdc42 GTPase activity in the formation of hyphae in *Candida albicans*. *Molecular Biology of the Cell* **18**:265-281.
21. **Sudbery PE.** 2011. Growth of *Candida albicans* hyphae. *Nature reviews. Microbiology* **9**:737-748.
22. **Lo HJ, Kohler JR, DiDomenico B, Loebenberg D, Cacciapuoti A, Fink GR.** 1997. Nonfilamentous *C. albicans* mutants are avirulent. *Cell* **90**:939-949.
23. **Saville SP, Lazzell AL, Monteagudo C, Lopez-Ribot JL.** 2003. Engineered control of cell morphology in vivo reveals distinct roles for yeast and filamentous forms of *Candida albicans* during infection. *Eukaryotic Cell* **2**:1053-1060.
24. **Biswas S, Van Dijck P, Datta A.** 2007. Environmental sensing and signal transduction pathways regulating morphopathogenic determinants of *Candida albicans*. *Microbiology and Molecular Biology Reviews* : MMBR **71**:348-376.
25. **Shapiro RS, Uppuluri P, Zaas AK, Collins C, Senn H, Perfect JR, Heitman J, Cowen LE.** 2009. Hsp90 orchestrates temperature-dependent *Candida albicans* morphogenesis via Ras1-PKA signaling. *Current Biology* : CB **19**:621-629.
26. **Whiteway M, Bachewich C.** 2007. Morphogenesis in *Candida albicans*. *Annual Review of Microbiology* **61**:529-553.
27. **Stoldt VR, Sonneborn A, Leuker CE, Ernst JF.** 1997. Efg1p, an essential regulator of morphogenesis of the human pathogen *Candida albicans*, is a member of a conserved class of bHLH proteins regulating morphogenetic processes in fungi. *The EMBO Journal* **16**:1982-1991.
28. **Zeidler U, Lettner T, Lassnig C, Muller M, Lajko R, Hintner H, Breitenbach M, Bito A.** 2009. *UME6* is a crucial downstream target of other transcriptional regulators of true hyphal development in *Candida albicans*. *FEMS Yeast Research* **9**:126-142.
29. **Carlisle PL, Kadosh D.** 2010. *Candida albicans* Ume6, a filament-specific transcriptional regulator, directs hyphal growth via a pathway involving Hgc1 cyclin-related protein. *Eukaryotic Cell* **9**:1320-1328.
30. **Zheng X, Wang Y, Wang Y.** 2004. Hgc1, a novel hypha-specific G1 cyclin-related protein regulates *Candida albicans* hyphal morphogenesis. *The EMBO Journal* **23**:1845-1856.

31. **Wang Y.** 2009. CDKs and the yeast-hyphal decision. *Current Opinion in Microbiology* **12**:644-649.
32. **Bachewich C, Whiteway M.** 2005. Cyclin Cln3p links G1 progression to hyphal and pseudohyphal development in *Candida albicans*. *Eukaryotic Cell* **4**:95-102.
33. **Chapa y Lazo B, Bates S, Sudbery P.** 2005. The G1 cyclin Cln3 regulates morphogenesis in *Candida albicans*. *Eukaryotic Cell* **4**:90-94.
34. **Ofir A, Hofmann K, Weindling E, Gildor T, Barker KS, Rogers PD, Kornitzer D.** 2012. Role of a *Candida albicans* Nrm1/Whi5 homologue in cell cycle gene expression and DNA replication stress response. *Molecular Microbiology* **84**:778-794.
35. **Atir-Lande A, Gildor T, Kornitzer D.** 2005. Role for the SCF*CDC4* ubiquitin ligase in *Candida albicans* morphogenesis. *Molecular Biology of the Cell* **16**:2772-2785.
36. **Bachewich C, Nantel A, Whiteway M.** 2005. Cell cycle arrest during S or M phase generates polarized growth via distinct signals in *Candida albicans*. *Molecular Microbiology* **57**:942-959.
37. **Bachewich C, Thomas DY, Whiteway M.** 2003. Depletion of a polo-like kinase in *Candida albicans* activates cyclase-dependent hyphal-like growth. *Molecular Biology of the Cell* **14**:2163-2180.
38. **Bensen ES, Clemente-Blanco A, Finley KR, Correa-Bordes J, Berman J.** 2005. The mitotic cyclins Clb2p and Clb4p affect morphogenesis in *Candida albicans*. *Molecular Biology of the Cell* **16**:3387-3400.
39. **Chou H, Glory A, Bachewich C.** 2011. Orthologues of the anaphase-promoting complex/cyclosome coactivators Cdc20p and Cdh1p are important for mitotic progression and morphogenesis in *Candida albicans*. *Eukaryotic Cell* **10**:696-709.
40. **Andaluz E, Ciudad T, Gomez-Raja J, Calderone R, Larriba G.** 2006. Rad52 depletion in *Candida albicans* triggers both the DNA-damage checkpoint and filamentation accompanied by but independent of expression of hypha-specific genes. *Molecular Microbiology* **59**:1452-1472.
41. **Devasahayam G, Chaturvedi V, Hanes SD.** 2002. The Ess1 prolyl isomerase is required for growth and morphogenetic switching in *Candida albicans*. *Genetics* **160**:37-48.
42. **Shi QM, Wang YM, Zheng XD, Lee RT, Wang Y.** 2007. Critical role of DNA checkpoints in mediating genotoxic-stress-induced filamentous growth in *Candida albicans*. *Molecular Biology of the Cell* **18**:815-826.
43. **Senn H, Shapiro RS, Cowen LE.** 2012. Cdc28 provides a molecular link between Hsp90, morphogenesis, and cell cycle progression in *Candida albicans*. *Molecular Biology of the Cell* **23**:268-283.
44. **Bai C, Ramanan N, Wang YM, Wang Y.** 2002. Spindle assembly checkpoint component CaMad2p is indispensable for *Candida albicans* survival and virulence in mice. *Molecular Microbiology* **45**:31-44.
45. **Gale CA, Leonard MD, Finley KR, Christensen L, McClellan M, Abbey D, Kurischko C, Bensen E, Tzafrir I, Kauffman S, Becker J, Berman J.** 2009. *SLA2* mutations cause *SWE1*-mediated cell cycle phenotypes in *Candida albicans* and *Saccharomyces cerevisiae*. *Microbiology* **155**:3847-3859.
46. **Leuker CE, Sonneborn A, Delbruck S, Ernst JF.** 1997. Sequence and promoter regulation of the *PCK1* gene encoding phosphoenolpyruvate carboxykinase of the fungal pathogen *Candida albicans*. *Gene* **192**:235-240.
47. **Care RS, Trevethick J, Binley KM, Sudbery PE.** 1999. The MET3 promoter: a new tool for *Candida albicans* molecular genetics. *Molecular Microbiology* **34**:792-798.

48. **Bensen ES, Filler SG, Berman J.** 2002. A forkhead transcription factor is important for true hyphal as well as yeast morphogenesis in *Candida albicans*. *Eukaryotic Cell* **1**:787-798.
49. **Lavoie H, Sellam A, Askew C, Nantel A, Whiteway M.** 2008. A toolbox for epitope-tagging and genome-wide location analysis in *Candida albicans*. *BMC Genomics* **9**:578.
50. **Gola S, Martin R, Walther A, Dunkler A, Wendland J.** 2003. New modules for PCR-based gene targeting in *Candida albicans*: rapid and efficient gene targeting using 100 bp of flanking homology region. *Yeast* **20**:1339-1347.
51. **Fonzi WA, Irwin MY.** 1993. Isogenic strain construction and gene mapping in *Candida albicans*. *Genetics* **134**:717-728.
52. **Rose MD, Winston FM, Hieter P, Sherman F, Cold Spring Harbor Laboratory.** Press. 1990. *Methods in yeast genetics : a laboratory course manual*. Cold Spring Harbor Laboratory Press, Cold Spring Harbor, N.Y.
53. **Liu HL, Osmani AH, Ukil L, Son S, Markossian S, Shen KF, Govindaraghavan M, Varadaraj A, Hashmi SB, De Souza CP, Osmani SA.** 2010. Single-step affinity purification for fungal proteomics. *Eukaryotic Cell* **9**:831-833.
54. **Mogilevsky K, Glory A, Bachewich C.** 2012. The Polo-like kinase *PLKA* in *Aspergillus nidulans* is not essential but plays important roles during vegetative growth and development. *Eukaryotic Cell* **11**:194-205.
55. **Martin SW, Konopka JB.** 2004. Lipid raft polarization contributes to hyphal growth in *Candida albicans*. *Eukaryotic Cell* **3**:675-684.
56. **Nichols CB, Fraser JA, Heitman J.** 2004. PAK kinases Ste20 and Pak1 govern cell polarity at different stages of mating in *Cryptococcus neoformans*. *Molecular Biology of the Cell* **15**:4476-4489.
57. **Harold FM.** 1999. In pursuit of the whole hypha. *Fungal Genetics and Biology : FG & B* **27**:128-133.
58. **Harris SD.** 2009. The Spitzenkorper: a signalling hub for the control of fungal development? *Molecular Microbiology* **73**:733-736.
59. **Banerjee M, Thompson DS, Lazzell A, Carlisle PL, Pierce C, Monteagudo C, Lopez-Ribot JL, Kadosh D.** 2008. *UME6*, a novel filament-specific regulator of *Candida albicans* hyphal extension and virulence. *Molecular Biology of the Cell* **19**:1354-1365.
60. **Carlisle PL, Kadosh D.** 2013. A genome-wide transcriptional analysis of morphology determination in *Candida albicans*. *Molecular Biology of the Cell* **24**:246-260.
61. **Carlisle PL, Banerjee M, Lazzell A, Monteagudo C, Lopez-Ribot JL, Kadosh D.** 2009. Expression levels of a filament-specific transcriptional regulator are sufficient to determine *Candida albicans* morphology and virulence. *Proceedings of the National Academy of Sciences of the United States of America* **106**:599-604.
62. **Childers DS, Mundodi V, Banerjee M, Kadosh D.** 2014. A 5' UTR-mediated translational efficiency mechanism inhibits the *Candida albicans* morphological transition. *Molecular Microbiology* **92**:570-585.
63. **Shapiro RS, Zaas AK, Betancourt-Quiroz M, Perfect JR, Cowen LE.** 2012. The Hsp90 co-chaperone Sgt1 governs *Candida albicans* morphogenesis and drug resistance. *PloS One* **7**:e44734.
64. **Ciudad T, Andaluz E, Steinberg-Neifach O, Lue NF, Gow NA, Calderone RA, Larriba G.** 2004. Homologous recombination in *Candida albicans*: role of CaRad52p in DNA repair, integration of linear DNA fragments and telomere length. *Molecular Microbiology* **53**:1177-1194.

65. **Pruyne D, Bretscher A.** 2000. Polarization of cell growth in yeast. I. Establishment and maintenance of polarity states. *Journal of Cell Science* **113 (Pt 3):**365-375.
66. **Howell AS, Lew DJ.** 2012. Morphogenesis and the cell cycle. *Genetics* **190:**51-77.
67. **Soll DR, Herman MA, Staebell MA.** 1985. The involvement of cell wall expansion in the two modes of mycelium formation of *Candida albicans*. *Journal of General Microbiology* **131:**2367-2375.
68. **Jacobs CW, Adams AE, Szanislo PJ, Pringle JR.** 1988. Functions of microtubules in the *Saccharomyces cerevisiae* cell cycle. *The Journal of Cell Biology* **107:**1409-1426.
69. **Slater ML.** 1973. Effect of reversible inhibition of deoxyribonucleic acid synthesis on the yeast cell cycle. *Journal of Bacteriology* **113:**263-270.
70. **Song S, Grenfell TZ, Garfield S, Erikson RL, Lee KS.** 2000. Essential function of the polo box of Cdc5 in subcellular localization and induction of cytokinetic structures. *Molecular and Cellular Biology* **20:**286-298.
71. **Park CJ, Song S, Lee PR, Shou W, Deshaies RJ, Lee KS.** 2003. Loss of *CDC5* function in *Saccharomyces cerevisiae* leads to defects in Swe1p regulation and Bfa1p/Bub2p-independent cytokinesis. *Genetics* **163:**21-33.
72. **Sakchaisri K, Asano S, Yu LR, Shulewitz MJ, Park CJ, Park JE, Cho YW, Veenstra TD, Thorner J, Lee KS.** 2004. Coupling morphogenesis to mitotic entry. *Proceedings of the National Academy of Sciences of the United States of America* **101:**4124-4129.
73. **Song S, Lee KS.** 2001. A novel function of *Saccharomyces cerevisiae CDC5* in cytokinesis. *The Journal of Cell Biology* **152:**451-469.
74. **Atkins BD, Yoshida S, Saito K, Wu CF, Lew DJ, Pellman D.** 2013. Inhibition of Cdc42 during mitotic exit is required for cytokinesis. *The Journal of Cell Biology* **202:**231-240.
75. **Yoshida S, Kono K, Lowery DM, Bartolini S, Yaffe MB, Ohya Y, Pellman D.** 2006. Polo-like kinase Cdc5 controls the local activation of Rho1 to promote cytokinesis. *Science* **313:**108-111.
76. **Grallert A, Patel A, Tallada VA, Chan KY, Bagley S, Krapp A, Simanis V, Hagan IM.** 2013. Centrosomal MPF triggers the mitotic and morphogenetic switches of fission yeast. *Nature Cell Biology* **15:**88-95.
77. **Petersen J, Hagan IM.** 2005. Polo kinase links the stress pathway to cell cycle control and tip growth in fission yeast. *Nature* **435:**507-512.
78. **Lu Y, Su C, Solis NV, Filler SG, Liu H.** 2013. Synergistic regulation of hyphal elongation by hypoxia, CO₂, and nutrient conditions controls the virulence of *Candida albicans*. *Cell Host & Microbe* **14:**499-509.
79. **Bassilana M, Hopkins J, Arkowitz RA.** 2005. Regulation of the Cdc42/Cdc24 GTPase module during *Candida albicans* hyphal growth. *Eukaryotic Cell* **4:**588-603.
80. **Pulver R, Heisel T, Gonia S, Robins R, Norton J, Haynes P, Gale CA.** 2013. Rsr1 focuses Cdc42 activity at hyphal tips and promotes maintenance of hyphal development in *Candida albicans*. *Eukaryotic Cell* **12:**482-495.
81. **Wolyniak MJ, Sundstrom P.** 2007. Role of actin cytoskeletal dynamics in activation of the cyclic AMP pathway and *HWPI* gene expression in *Candida albicans*. *Eukaryotic Cell* **6:**1824-1840.
82. **Zou H, Fang HM, Zhu Y, Wang Y.** 2010. *Candida albicans* Cyr1, Cap1 and G-actin form a sensor/effector apparatus for activating cAMP synthesis in hyphal growth. *Molecular Microbiology* **75:**579-591.

3.7 SUPPLEMENTARY FIGURES

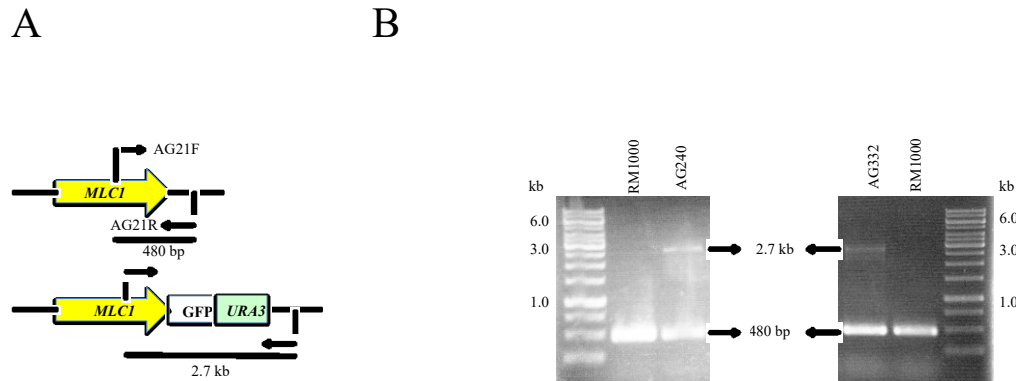


Figure S3.1: PCR confirmation of *MLC1/MLC1-GFP-URA3* strains. (A) Map and (B) ethidium-bromide stained gels showing products amplified with oligonucleotides AG21F and AG21R from strains RM1000 (*MLC1/MLC1*), AG240 (*cacdc5::hisG/cacdc5::HIS1 PCK1::CaCDC5-hisG, MLC1/MLC1-GFP-URA3*) and AG332 (*MLC1/MLC1-GFP-URA3*).

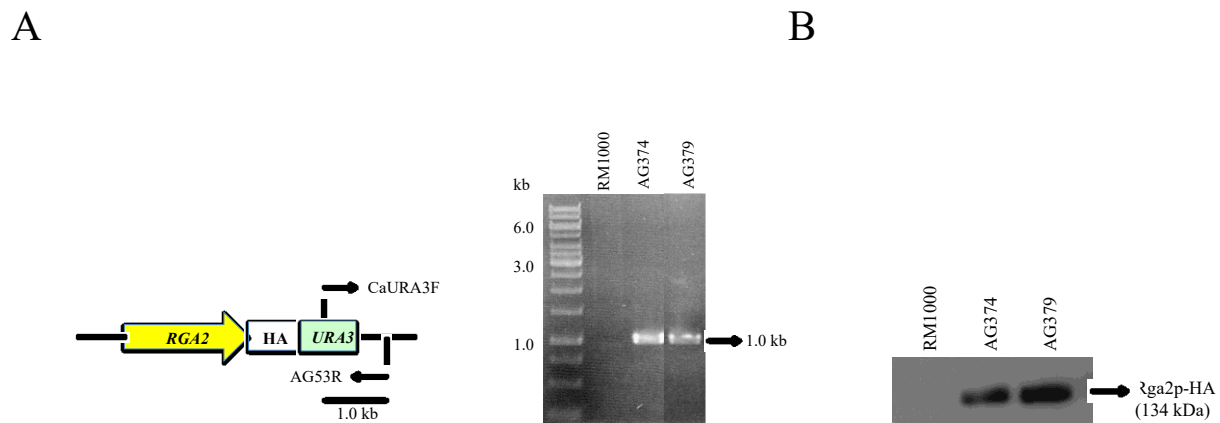
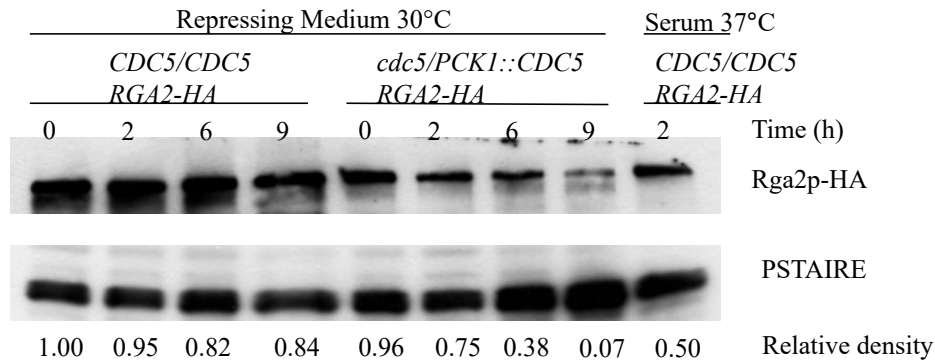


Figure S3.2: Confirmation of *RGA2/RGA2-HA-URA3* strains. (A) Map and ethidium-bromide stained gels showing products amplified with oligonucleotides CaURA3F and AG53R from strains AG374 (*RGA2/RGA2-HA-URA3*) and AG379 (*cacdc5::hisG/cacdc5::HIS1 PCK1::CaCDC5-hisG, RGA2/RGA2-HA-URA3*). (B) Western blot confirmation of strains AG374 and AG379.

A



B

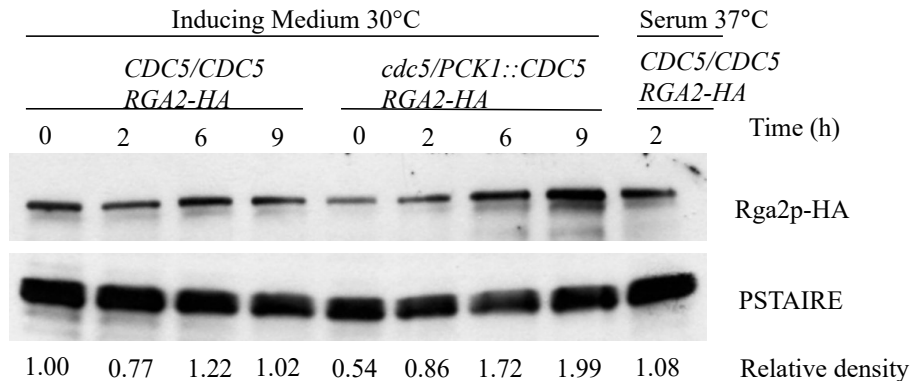
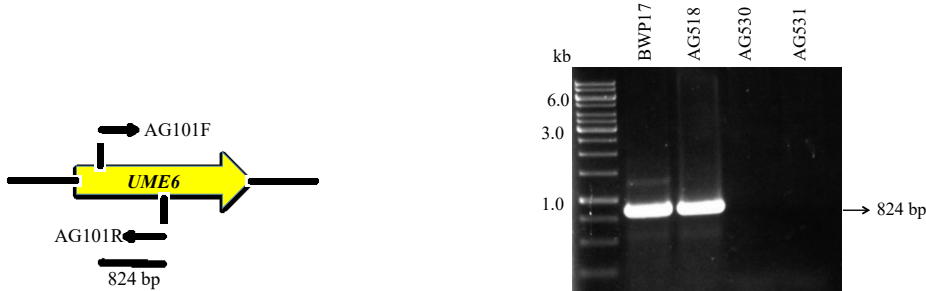


Figure S3.3: Rga2p-HA abundance in cells lacking vs. containing Cdc5p. (A) Western blot of overnight cultures of strains AG374 (*CDC5/CDC5*, *RGA2/RGA2-HA-URA3*) and AG379 (*cacdc5::hisG/cacdc5::HIS1 PCK1::CaCDC5-hisG*, *RGA2/RGA2-HA-URA3*) that were grown in SS medium, diluted into SD repressing medium at 30°C and collected at the indicated time points. Strain AG374 was also incubated in SD medium supplemented with 10% Fetal Bovine Serum (FBS) for 2 h at 37°C to induce hyphae. Samples were electrophoresed on a 10% SDS PAGE gel to allow for detection of Cdc28p (anti-PSTAIRE) as a loading control. Density values represent adjusted relative densities and were calculated using ImageJ as described in Chou *et al.*, 2011. (B) Western blot of the same strains prepared as in (A) with the exception of dilution into fresh SS inducing medium.

A



B

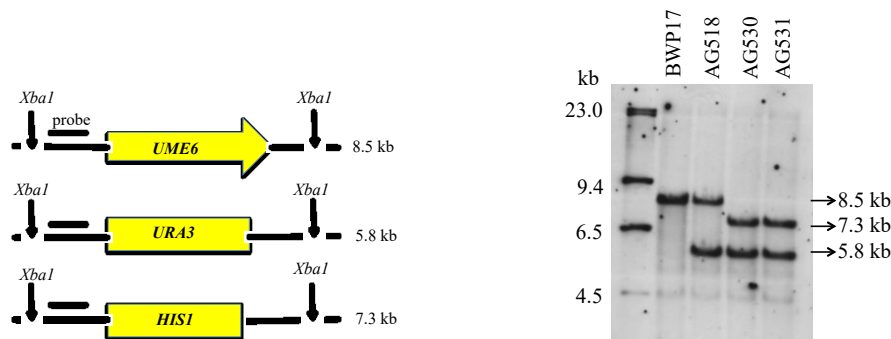
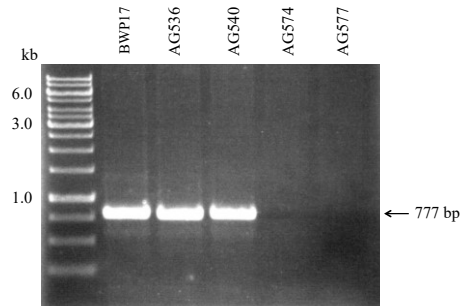
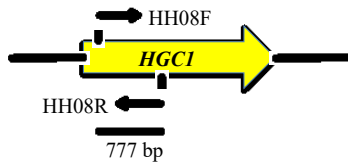


Figure S3.4: Confirmation of strains lacking *UME6*. (A) Map and ethidium-bromide-stained DNA gel showing bands amplified with oligonucleotides AG101F and AG101R from strains BWP17 (*UME6/UME6*), AG518 (*cdc5::hisG/MET3::CDC5::ARG4, UME6/ume6::URA3*) and AG530 and AG531 (*cdc5::hisG/MET3::CDC5::ARG4, ume6::URA3/ume6::HIS1*). (B) Southern blot. Digestion of gDNA with *Xba*I produced a wild-type band of 8.5 kb, a *ume6Δ::URA3* deletion band at 5.8 kb, and a *ume6Δ::HIS1* deletion band 7.3 kb. Absence of the *UME6* transcript in strains AG530 and AG531 was also confirmed by Northern blot (refer to Fig 5B).

A



B

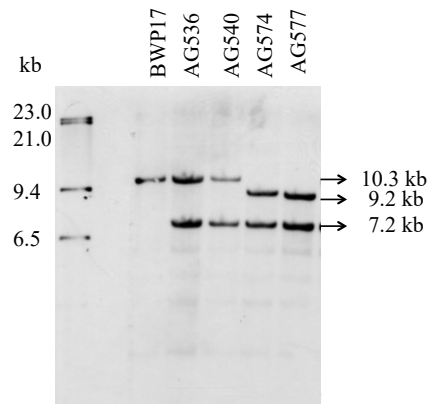
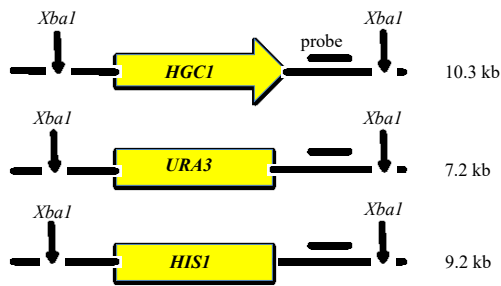


Figure S3.5: Confirmation of strains lacking *HGCI*. (A) Map and ethidium-bromide-stained DNA gel showing bands amplified with oligonucleotides HH08F and HH08R from strains BWP17, AG536 and AG540 (*cdc5::hisG/MET3::CDC5::ARG4, HGCI/hgc1::URA3*) and AG574 and AG577 (*cdc5::hisG/MET3::CDC5::ARG4, hgc1::URA3/hgc1::HIS1*). (B) Southern blot. Digestion of gDNA with *XbaI* produced a wild type band of 10.3 kb, an *hgc1Δ::URA3* deletion band at 7.2 kb, and an *hgc1Δ::HIS1* deletion band 9.2 kb.

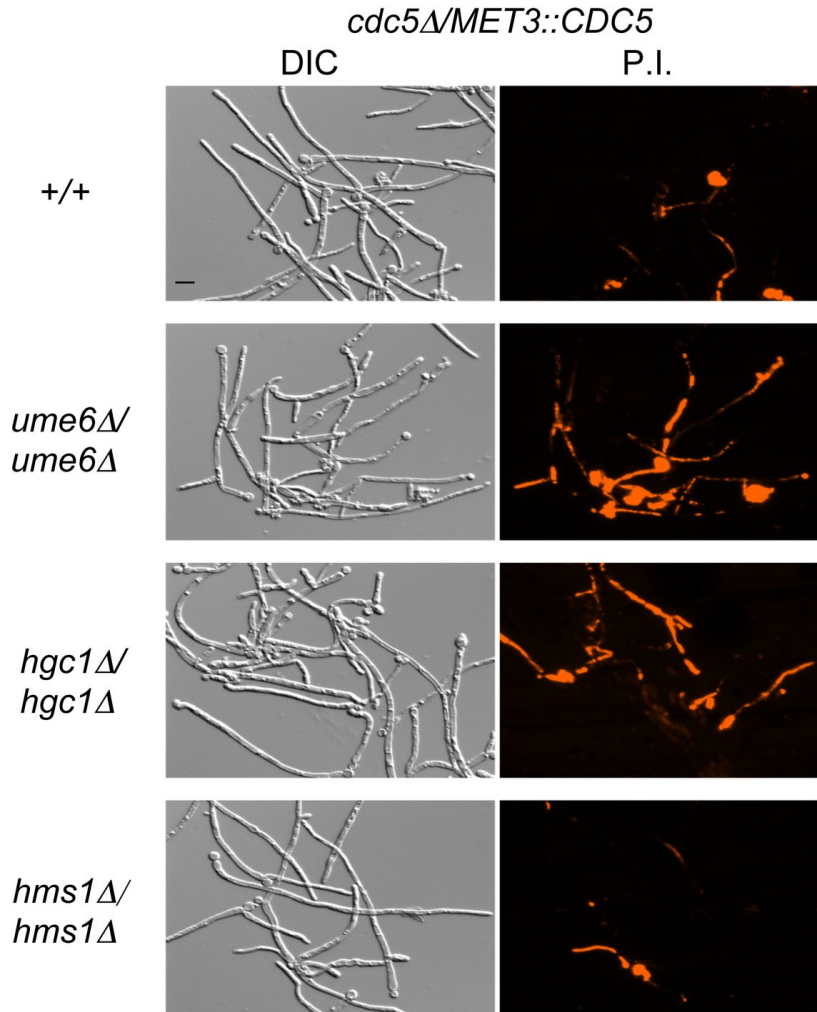
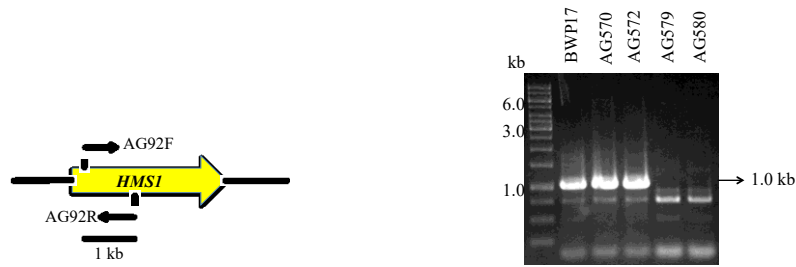
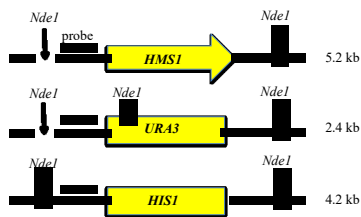


Figure S3.6: Propidium-iodide staining of cells lacking Cdc5p in different mutant backgrounds. Overnight cultures of strains AG553 (*cdc5Δ::hisG/MET3::CDC5-ARG4, URA3+HIS1*), AG530 (*cdc5Δ::hisG/MET3::CDC5-ARG4, ume6Δ::URA3/ume6Δ::HIS1*), AG574 (*cdc5Δ::hisG/MET3::CDC5-ARG4, hgc1Δ::URA3/hgc1Δ::HIS1*) and AG580 (*cdc5Δ::hisG/MET3::CDC5-ARG4, hms1Δ::URA3/hms1Δ::HIS1*) grown in inducing medium (-MC) were diluted into repressing medium (+MC) and incubated at 30°C for 14 h. Live cells were stained with propidium iodide (PI), washed with sterile water, and immediately examined by fluorescence microscopy. Bar: 10 μm.

A



B



C

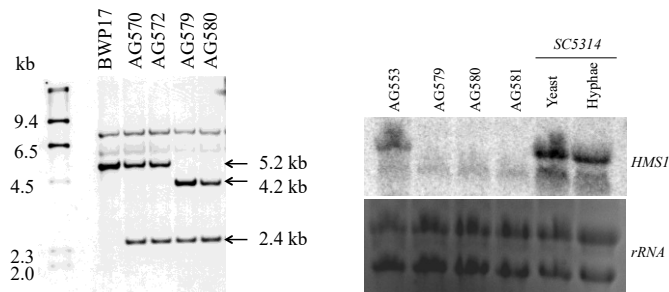


Figure S3.7: Confirmation of strains lacking *HMS1*. (A) Map and ethidium-bromide-stained DNA gel showing bands amplified with oligonucleotides AG92F and AG92R from strains BWP17 (*HMS1/HMS1*), AG570 and AG572 (*cdc5::hisG/MET3::CDC5::ARG4, HMS1/hms1::URA3*) and AG579 and AG580 (*cdc5::hisG/MET3::CDC5::ARG4, hms1::URA3/hms1::HIS1*). (B) Southern blot. Digestion of gDNA with *NdeI* produced a wild type band of 5.2 kb, an *hms1Δ::URA3* deletion band at 2.4 kb, and an *hms1Δ::HIS1* deletion band 4.2 kb. (C) Northern blot showing *HMS1* transcript in strains AG553 (*cdc5::hisG/MET3::CDC5::ARG4, URA3+ HIS1+*) and SC5314 grown in yeast (8 h at 37°C) or hyphal (2 h at 37°C with 10% FBS) conditions, and absence of transcript in strains AG579, AG580 and AG581 (*cdc5::hisG/MET3::CDC5::ARG4, hms1::URA3/hms1::HIS1*). *rRNA* stained with ethidium bromide is included as a loading control.

Movie S1: Time course analysis of Mlc1p-GFP in cells depleted of Cdc5p. Strain AG240 was incubated in SS inducing medium as described in (A), transferred to a pre-made agarose pad consisting of SD repressing medium on a microscope slide, sealed with VALAP and visualized with LSM 510 confocal microscope fitted with a x 63 objective. Images were recorded every 30 min, and Z stack series consisting of 0.1 μm steps were acquired.

CHAPTER 4

Ch. 4: Identification of a novel Polo-like kinase binding protein found specifically in the *Candida* genus of fungi that interacts with the spliceosome machinery.

Chapter 4 addresses the mechanisms of Cdc5p function during mitosis and possibly morphogenesis in *C. albicans*, through identifying its interacting factors with affinity purification followed by mass spectrometry. This work revealed a novel, previously uncharacterized protein, Orf19.3714p. Orf19.3714p does not have any homologues in organisms other than *Candida* species, indicating that it is *Candida*-specific. While not essential for yeast or hyphal growth, Cdc5p-depleted cells lacking Orf19.3714p were compromised in their ability to form long filaments, much like absence of the spindle factor checkpoint Bub2p, suggesting a possible influence on the spindle checkpoint. Intriguingly, Orf19.3714p binds numerous proteins of the spliceosome complex, in a manner that may be dependent on Cdc5p or a block in mitosis. We further completed a bioinformatic analysis of the spliceosome complex in *C. albicans*, which has not been investigated to date, and show that it is highly conserved in composition as compared to *S. cerevisiae*, with a few variations. We thus identified a putative novel polo-like kinase interacting factor that is specific to *Candida* species. We also provide the first evidence that polo-like kinase function may extend to regulation of RNA splicing. We propose that Cdc5p may influence splicing in *C. albicans* via Orf19.3714p, which in turn influences factors required for mitotic arrest.

ABSTRACT

Polo-like kinases are critical, multi-functional regulators of mitosis found in organisms ranging from yeast to man and are subject to intensive investigation, yet we lack a complete understanding of their mechanisms of action, substrates, and forms of regulation. We previously demonstrated that depletion of the polo-like kinase Cdc5p in *C. albicans* yeast cells impairs spindle elongation, resulting in a block in mitosis followed by initiation and maintenance of polarized growth from the yeast bud and induction of hyphal-specific genes. In order to determine the mechanisms of action of Cdc5p in *C. albicans*, we identified its interacting proteins using affinity purification followed by mass spectrometry. We show that Cdc5p binds a previously uncharacterized protein, Orf19.3714p, which is specific to *Candida* species. Orf19.3714p is not essential for yeast or hyphal growth *in vitro*, but is modified at the level of phosphorylation and abundance during a mitotic block, and is required in part for maintaining the polarized growth phenotype that occurs upon depletion of Cdc5p. Cdc5p-depleted cells lacking Orf19.3714p also showed a higher abundance of rebudding from the mother yeast cell, suggesting a potential influence on mitotic checkpoint function. Affinity purification of Orf19.3714p and mass spectrometry further demonstrated that Orf19.3714p interacts with a large number of proteins associated with the spliceosome in a manner that may be dependent on Cdc5p. Collectively, the data reveal a new interacting protein of the polo-like kinase family that is *Candida*-specific, and provide the first evidence for a possible link between polo-like kinase function and spliceosome activity.

4.1 INTRODUCTION

The Polo-like kinases (Plks) comprise a conserved subfamily of serine/threonine kinases that play critical roles in cell cycle regulation as well as in development. *Polo* from *Drosophila melanogaster* represents the founding member of the family, and homologues were subsequently found in *Caenorhabditis elegans* (PLK1-3) (1, 2) *Xenopus laevis* (Plx1-3) (3, 4), and mammals (PLK1-5) (5, 6). Fungi contain single homologues, such as Cdc5p in *Saccharomyces cerevisiae* (7), Plo1p in *Schizosaccharomyces pombe* (8), Cdc5p in *Candida albicans* (9), and PLKA in *Aspergillus nidulans* (PLKA) (10). Plks are also found in *Trypanosoma brucei* (TbPlk) (11), but are absent in plants (6, 12).

Plks are defined by a kinase domain in the amino-terminus and a polo box domain (PBD) in the carboxyl terminus (13). In most Plks, the PBD contains two conserved polo boxes (14) that function as a phosphopeptide binding domain and target Plks to subcellular locations by binding to proteins that previously have been phosphorylated by cyclin dependent kinases (CDKs) or by a Plk (15, 16). A consensus PBD binding motif for PLK1 consists of Ser-pSer/pThr-Pro/X (15), while an optimal phosphorylation consensus site consists of D/E-X-pS/pT- ϕ (17), where X is any amino acid and ϕ is hydrophobic amino acid. Plks can also interact with proteins in a phosphorylation-independent manner (18). The kinase and PBD are separated by a linker domain that shows little sequence conservation but is important for localization in some cases (19, 20).

Plks have emerged as critical regulators of multiple aspects of mitosis, including mitotic entry, spindle formation, chromosome segregation, mitotic exit, cytokinesis or septation, as well as in nuclear shape (21-23). For example, during the G2/M transition, PLK1 phosphorylates and activates CDC25C phosphatase, leading to mitotic entry (12, 24), while Cdc5p in *S. cerevisiae* targets Swe1p for degradation via phosphorylation, contributing to active Cdc28p/Clb2p and the G2/M transition (25). PLK1 regulates microtubule-stabilizing proteins that are important for aster and spindle formation (26), and is required for centrosome maturation and microtubule-kinetochore attachments (27, 28). Cdc5p influences microtubule growth and dynamics (29) and is important for spindle orientation but not elongation (30). During the metaphase-to-anaphase transition, PLK1 and Cdc5p phosphorylate the cohesin Scc1p to permit chromosome segregation

(31-34), as well as APC/C subunits, resulting in activation of the APC/C (35-38). Cdc5p is also a component of the Cdc Fourteen Early Anaphase Release (FEAR) and Mitotic Exit Network (MEN) pathways, which function to control release of the phosphatase Cdc14p from its inhibitor, Net1p, in the nucleolus, thereby allowing dephosphorylation of mitotic CDK targets, inactivation of CDK itself, and mitotic exit (33). In the FEAR pathway, Cdc5p interacts with Cdc14p and the Separase Esp1p (39). Within the MEN pathway, Cdc5p negatively regulates the GTPase-activating protein (GAP) complex Bub2p-Bfa1p (40). During cytokinesis, PLK1 recruits the Guanine Nucleotide Exchange Factor (GEF) Ect2p to the central spindle during anaphase, which permits accumulation of the GTPase RhoA and assembly of the contractile ring (28, 41). Similarly, Cdc5p phosphorylates Rho1p GEF proteins that in turn activate Rho1p at the bud neck for contractile ring formation (42). The PBD of Cdc5p also binds GAPs for Cdc42p and other factors that are involved in actin cytoskeleton organization (43). In some cases, Plks exert their function through regulating transcription. Plo1p, PLK1 and Cdc5p, for example, phosphorylate and activate transcription factors required for the M/G1 or G2/M transitions (44-47). PLK1 can also regulate expression of genes coding for tRNA and 5S rRNA through phosphorylating Brf1p, a component of RNA Pol III (48).

In addition to mitosis and cytokinesis, Plks can function in other cell cycle stages and in development (49-51). For example, PLK3 from humans is involved in the regulation of the G1/S transition and entry into S phase (52). Plks in mice, *D. melanogaster* and *C. elegans* are important in neuron differentiation, oocyte determination and meiosis, respectively (53-55) and PLKA from *A. nidulans* influences sexual development (10). Further, Plo1p in *S. pombe* was linked to a role in polarized growth, as phosphorylation of Plo1p is required for resumption of cell tip growth after recovery from cell cycle arrest induced by certain stresses (20, 56, 57).

Despite progress made in identifying numerous Plk functions and targets (13, 58, 59), a complete picture of their mechanisms of action and regulation is still lacking. Moreover, some distinctions in function and sequence, as seen with Plks from filamentous fungi and Trypanosomes, for example, (10, 60), highlight organism-specific features, which could provide important insights on the evolution of the Plk family (6, 12, 61).

C. albicans is an opportunistic fungal pathogen of humans that can cause infections ranging from mucosal to systemic, the latter of which are associated with high mortality rates (62). Current drug treatments can have several side effects (63-65), underlying the need to identify new factors that can be targeted for treating *C. albicans* infections. One aspect of the biology of *C. albicans* that is important for virulence is its ability to differentiate into multiple cell types, including white phase yeast, mating-competent opaque-phase yeast, pseudohyphae, hyphae, chlamyospores, or gastrointestinally induced transition (GUT) cells (66). *C. albicans* yeast cells are proposed to be ideal for dissemination in the blood stream, while the pseudohyphal and hyphal forms may be more advantageous for invading host tissue and escaping immune cells (67). *C. albicans* mutants locked in one cell form have reduced virulence (68-70), underlying the importance of differentiation during pathogenesis and the need to understand its regulation. The circuitry governing the yeast-to-hyphal switch has been extensively investigated, and involves a diversity of signaling pathways that mediate the environmental cues (71, 72).

Another aspect of *C. albicans* biology that is important for survival in the host and virulence is cell proliferation. However, we lack a comprehensive understanding of the cell cycle in *C. albicans*. Functional analyses of homologues of conserved mitotic regulators, including the CDK Cdc28p (73, 74), B-type cyclins Clb2p and Clb4p (89), APC/C cofactors Cdc20p and Cdh1p (75), Hsp90p (76, 77), MEN homologues Dbf2p, Tem1p and Cdc14p (78-81) and spindle checkpoint factors Mad2p and Bub2p (76, 82, 83), for example, have provided some insight. However, several of these factors show variations in function in *C. albicans* compared to orthologues in *S. cerevisiae* (84-86), suggesting re-wiring in the mitotic circuitry. Moreover, transcription profiles of *C. albicans* cells passing through mitosis showed some similarity to those in *S. cerevisiae* and *S. pombe*, but noted differences, including modulation of genes of unknown function (84), further raise the possibility of novel aspects of mitotic control in *C. albicans*.

C. albicans contains a homologue of another conserved mitotic regulator, the polo-like kinase, Cdc5p. Its depletion in yeast cells resulted in an early mitotic arrest with short spindles that were often mis-oriented (9). While *S. cerevisiae* cells lacking Cdc5p arrested as large

doublets, *C. albicans* yeast cells lacking Cdc5p were novel in switching to a polarized mode of growth and forming filaments (9, 87). These cells resemble hyphae in that they maintain polarized growth, lack constrictions along their length, move the nucleus from the mother yeast cell into the tube, require cyclase activity, and express some hyphal-specific genes (HSGs) that are virulence factors (9, 83). However, the filaments are also distinct from hyphae with respect to having a wider diameter during early growth stages, forming in the absence of some key hyphal regulators, expressing HSGs at only later stages of elongation and in the absence of any environmental input, and requiring the spindle checkpoint factor Bub2p for maintenance of polarized growth (9, 88). This growth response is not specific to Cdc5p depletion, as blocking mitosis through depletion of other essential genes (75, 77, 78, 89) or treatment with microtubule-destabilizing drugs such as nocodazole (82) also results in polarized growth that, where tested, requires spindle checkpoint factors Bub2p or Mad2p (76, 82). Arresting *C. albicans* yeast in S or G1 phase also results in polarized growth, but G1-phase arrested cells resemble true hyphae from their inception (88, 90), and S phase-arrested cells are not as highly elongated, do not require Bub2p and show different transcription profiles (9, 76). Since checkpoint factors like Mad2p and Swe1p are required for virulence in *C. albicans* (82, 91), checkpoint-associated polarized growth may be physiologically relevant for survival in the host and for pathogenesis (9, 82, 83). We recently provided evidence that suggests Cdc5p-depleted cells are initially elongated yeast buds but switch to a hyphal fate over time and initiate expression of HSGs in a novel, environment-independent manner (Glory, 2015, in revision). However, the mechanisms of action of Cdc5p in regulating mitosis and influencing polar bud growth in *C. albicans* remain unclear.

In order to address this question, we attempted to identify potential Cdc5p-interacting factors using 2-step affinity purification followed by mass spectrometry. Our work uncovered a previously uncharacterized protein, Orf19.3714p, which only has homologues in *Candida* species. Orf19.3714p is not essential for yeast or hyphal growth but is post-translationally modified in mitosis, required for Cdc5p-depleted polarized growth, and interacts with many RNA splicing machinery factors, including Prp19p and Brr1p. Our results have thus identified a novel, *Candida*-specific Plk-interacting factor, and for the first time link a Plk to a possible function in RNA splicing.

4.2 MATERIALS AND METHODS

4.2.1 Strains, oligonucleotides, plasmids and culture conditions

Strains, oligonucleotides and plasmids used in this study are listed in Tables 4.1, 4.2, and 4.3 respectively. Strains were incubated in synthetic medium (0.7% yeast nitrogen base, 2.0 g adenine, 2.5 g uridine, 2.0 g tryptophan, 1.0 g histidine, 1.0 g arginine, 1.0 g methionine, 1.5 g tyrosine, 1.5 g isoleucine, 7.5 g valine, 1.5 g lysine, 2.5 g phenylalanine, 5.0 g glutamic acid, 10.0 g threonine and 3.0 g leucine per 50.0 L) containing either 2.0% glucose (92) or 2.0% sodium succinate (SS) to repress or induce expression from the *PCK1* promoter, respectively (93). Alternatively, SD medium lacking (-MC) or containing (+MC) 2.5 mM methionine and 0.5 mM cysteine was utilized to induce or repress expression from the *MET3* promoter, respectively (94). Other strains were grown in rich medium (YEPD) containing 1.0% yeast extract, 2.0% peptone and 2.0% dextrose. For hyphal induction, medium was supplemented with 10.0% fetal bovine serum (FBS) (Wisent Inc, St. Bruno, QC) and cells were incubated at 37°C. For most conditions, strains were grown overnight, diluted into fresh medium to an O.D._{600nm} of 0.1 to 0.2, and collected after indicated times. For growth assays, the O.D._{600nm} was recorded at the indicated time intervals. Samples for RNA or protein analysis were collected at the indicated time points and stored at -80°C until extraction.

For plate growth assays, Spider solid medium (95) consisted of 10.0 g of nutrient broth (EMD), 10.0 g mannitol (BDH, VWR), 2.0 g of K₂HPO₄ (Fisher Scientific) and 13.5 g agar (Bioshop) for 0.5 L medium. The pH was adjusted to 7.5 and the medium was autoclaved. SLAD (Synthetic Low Ammonium Dextrose) plates (96) consisted of 0.8 g yeast nitrogen base without ammonia, supplemented with 50.0 μM ammonium sulphate, 10.0 g dextrose, and 10.0 g of five times prewashed agarose with sterile water per 500.0 ml medium. For serum plates, autoclaved YEPD agar medium prewarmed to 37°C was supplemented with FBS to a final concentration of 10.0%.

Table 4.1: Strains used in this study

Strain	Genotype	Source
RM1000	<i>ura3Δ::imm434/ura3Δ::1 imm434</i> <i>his1Δ::hisG/his1Δ::hisG</i>	Negredo et al.1997
BWP17	<i>ura3Δ::imm434/ura3Δ::imm434 his1Δ::hisG/his1Δ::hisG</i> <i>arg4Δ::hisG/arg4Δ::hisG</i>	Wilson et al., 1999
CAI4	<i>ura3Δ::imm434/ura3Δ::1 imm434</i>	Fonzi and Irwin, 1993
SC5314	<i>URA3/URA3, HIS1/HIS1</i>	Fonzi and Irwin, 1993
CB105	<i>cdc5Δ::hisG/PCK1::CDC5-HIS1</i>	Bachewich et al., 2003
CB108	<i>cdc5Δ::hisG/MET3::CDC5-URA3</i>	Bachewich et al., 2003
CB504	CAI4 (<i>MET3::URA3+</i>)	Bachewich et al., 2003
HCCa7	<i>CDC5/cdc5Δ::hisG</i>	Chou et al., 2011
HCCa23	<i>cdc20Δ::URA3/MET3::CDC20::HIS1</i>	Chou et al., 2011
AG180	<i>cdc5Δ::hisG/CDC5-TAP-URA3</i>	This study
AG191	<i>cdc20Δ::URA3/MET3::CDC20::HIS1,</i> <i>CDC5/CDC5-TAP-ARG4</i>	Chou et al., 2011
AG500	<i>cdc5Δ::hisG/MET3::CDC5-ARG4</i>	Ch. 3 thesis
AG517	<i>ORF19.3714/ORF19.3714-HA-URA3</i>	This study
AG523	<i>cacdc5Δ::hisG/PCK1::CDC5-HIS1,</i> <i>ORF19.3714/ORF19.3714-HA-URA3</i>	This study
AG614	<i>CDC5/CDC5-MYC-HIS1</i>	This study
AG622	<i>CDC5/CDC5-MYC-HIS1,</i> <i>ORF19.3714/ORF19.3714-HA-URA3</i>	This study
AG676	<i>ORF19.3714/orf19.3714Δ::URA3</i>	This study
AG680	<i>cdc5Δ::hisG/MET3::CDC5-ARG4,</i> <i>ORF19.3714/orf19.3714Δ::URA3</i>	This study
AG704	<i>cdc20Δ::URA3/MET3::CDC20::HIS1,</i> <i>ORF19.3714/ ORF19.3714-TAP-ARG4</i>	This study
AG707	<i>orf19.3714Δ::URA3/ORF19.3714-TAP-ARG4</i>	This study
AG717	<i>cdc5Δ::hisG/MET3::CDC5-ARG4,</i> <i>ORF19.3714/ ORF19.3714-TAP-URA3</i>	This study
AG692, 694	<i>orf19.3714Δ::URA3/orf19.3714Δ::HIS1</i>	This study
AG698, 700	<i>cdc5Δ::hisG/MET3::CDC5-ARG4,</i> <i>orf19.3714Δ::URA3/orf19.3714Δ::HIS1</i>	This study
AG721, 722	<i>orf19.3714Δ::URA3/orf19.3714Δ::HIS1,</i> <i>pBS-ARG4-ORF19.3714</i>	This study
AG727, 728	<i>orf19.3714Δ::URA3/orf19.3714Δ::HIS1 + pBS-ARG4</i>	This study

Table 4.2: Oligonucleotides used in this study

Name	Sequence	Source
AG1F	TTTGAAGCAAGGAAACTTTCAGCATGAAAATG TTCCGGACTGTATGGAGAAGATAATGGTCATCA AAGAAGCTATCAAGAAAAAAGCATTAAAGAAGCT GGTCGACGGATCCCCGGGT	This study
AG1R	TATTATATCTCTTGTTTTATAATGAATATGGGCTACA GTTCAATTTGCAGTAGTACTACTAAATAAAAGGA TGTTTATTAGCAACGTGAAAGTGGCATAT TCGATGAATTCGAGCTCGTT	This study
AG2F	GCCAGGGCGTTTAACTCAA	This study
AG2R	ATAGTTACGATTAGTGGTGG	This study
AG4F	GGTCGACGGATCCCCGGGTATACCCATAC GATGTTCTGAC	Lavoie <i>et al.</i> , 2008
AG4R	TCGATGAATTCGAGCTCGTT	Lavoie <i>et al.</i> , 2008
AG80F	GAATCAAAAAAATGAAATGATTATGGATGTTGATTA TGAACTTACTATTAATAATGGTAGATAGTATTAGTCA AACGATAAATTCAATAATTGAATCATTAGGTCGACG GATCCCCGGGT	This study
AG80R	AGATAGATATAGCTAGTGAAAGTGAAGTAGAGG AAGGTGGTGTAGAGGAAGAAGCAAAAGTAAATA CTCCAAAAGACTAGCTAAACATAACTCTATA TAGTCGATGAATTCGAGCTCGTT	This study
AG81R	GCTGATGAATATCCTCCTGA	This study
AG82F	CCATGCCATTCAGGAAAATGGCCACTATAT	This study
AG82R	GATCAGTTGATTCTGATTCAATAGGAGCAC	This study
AG83R	GATAGTATATTAGTTGGACCTGTCCCCGTA	This study
AG84F	GTGCTCCTATTGAATCAGAATCAACTGAT CTATAGGGCGAATTGGAGCTC	This study
AG85F	GACTAGCTTGTTGCTTGCT	This study
AG100F	TGTTCCGGACTGTATGGAGAAGATAATGGTCA TCAAAGAAGCTATCAAGAAAAAAGCATTAAAG AAGCTGGTGGTGGTCGGATCCCCGGGTAAATTA	This study
AG100R	TAATGAATATGGGCTACAGTTCAATTTGCAGT AGTACTACTAAATAAAAGGATGTTTATTAGC AACGTGAGAATTCCGGAATTTTATGAGAAAC	This study
AG111F	CTGAACAAGGTGAGAGTAAC	This study
AG111R	CTGTCACTGGCAATTCGTTC	This study
AG114F	GTACAAAATGAAAAAGACTACTATATAGAG	This study
AG114R	CTCTATATAGTAGTCTTTTTCATTTTGTACGACGG TATCGATAAGCTTGA	This study

AG116F	CTAGTG TACTAGGGCGTAGA	This study
AG116R	AAAGATACGCAGTTGGTAGC	This study
AG118R	GGTGGTCTCGAGAATGGTGATGCAGTGGTGGA	This study
AG119F	GGTGGTCCC GGGCTAGTGTACTAGGGCGTAGA	This study
AG120F	GGGCTGTTCTTGTCGTTGTT	This study
ACT1-129F	CATGGTTGGTATGGGTCAAAAA	Glory et al., 2014
ACT1-104R	TCAATTCTAATAACGAGGTGGTCTTTC	Glory et al., 2014
CaHIS1F	CCTGCAGCTGATATCCCAGT	This study
CaHIS1R	ACTGGGATATCAGCTGCAGG	This study
CaURA3F	GGTAATACCGTAAAGAAACA	Glory et al., 2014
CaURA3R	TTCAAATAAGCATTCCAACC	This study
CaARG4F	ACTATGGATATGTTGGCTAC	Glory et al., 2014

Table 4.3: Plasmids used in this study

Name	Source
pFA-TAP- <i>UAR3</i>	Lavoie <i>et al.</i> , 2008
pFA-TAP- <i>ARG4</i>	Lavoie <i>et al.</i> , 2008
pFA-HA- <i>URA3</i>	Lavoie <i>et al.</i> , 2008
pMG2093 (MYC- <i>HIS1</i>)	Bensen <i>et al.</i> , 2005
pBS-Ca <i>URA3</i>	A.J.P. Brown
pBS-Ca <i>HIS1</i>	C. Bachewich
pBS-Ca <i>ARG4</i>	C. Bachewich

4.2.2 Composition of PCR reaction mixes for DNA constructs

The PCR reaction mixes for DNA construct amplification were composed of 0.6 μ M oligonucleotides, 0.4 mM dNTPs, 50.0-100.0 ng of template, 3.75U of Expand Long Template Polymerase (Roche), and 1X Buffer 3.

4.2.3 Composition of PCR screening reaction mixes

PCR screening reaction mixes were composed of 0.6 μ M of oligonucleotides, 0.4 mM of dNTPs, 50.0-60.0 ng of gDNA as template, 3.0 mM of MgCl₂, 1X Taq Buffer with (NH₄)₂SO₄ and 1.0 U Taq DNA Polymerase (Fermentas).

4.2.4 Strain Construction

a. CDC5-TAP

In order to tag the C-terminus of *CDC5* with a tandem affinity purification (TAP) tag epitope (Protein A and Calmodulin-binding domain epitopes separated by a tobacco etch virus (TEV) protease cleavage site), the 2.3 kb TAP-URA3 cassette was amplified from 100.0 ng of plasmid pFA-TAP-URA3 (97) with oligonucleotides AG1F and AG1R, which contained 100 bp complementary to regions upstream and downstream from the stop codon of *CDC5* respectively and 20 bp complementary to the plasmid. The reaction conditions were as follows: 94°C for 4 min, followed by 25 cycles of 94°C for 1 min, 40°C for 1 min, 68°C for 2 min, followed by a 7 min extension at 68°C and storage at 4°C. The construct was purified using PCR purification kit (OMEGA) and 4.0 μ g was transformed into strain HCCa7 (*CDC5/cdc5 Δ ::hisG*) resulting into strain AG180 (*cdc5 Δ ::hisG/CDC5-TAP-URA3*). Similarly, a 2.9 kb TAP-ARG4 cassette was amplified from pFA-TAP-ARG4 and transformed into HCCa23 (*cdc20 Δ ::URA3/MET3::CDC20::HIS1*) resulting into strain AG191 (*cdc20 Δ ::URA3/MET3::CDC20::HIS1, CDC5/CDC5-TAP-ARG4*).

b. CDC5-MYC

In order to tag the C-terminus of *CDC5* with 13 copies of the myc epitope, the 3.8 kb *MYC-HIS1* cassette was amplified from 100.0 ng of plasmid pMG2093 (89) with oligonucleotides AG100F and AG100R, which contained 70 bp complementary to regions lying upstream and downstream from the stop codon of *CDC5* respectively and 20 bp complementary to the plasmid. The reaction conditions were as follows: 94°C for 4 min, followed by 25 cycles

of 94°C for 1 min, 41°C for 1 min, 68°C for 3 min and 50 sec, followed by a 7 min extension at 68°C and storage at 4°C. The construct was purified and 4.0 µg was transformed into strains RM1000 resulting in strain AG614 (*CDC5/CDC5-MYC-HIS1*).

c. *ORF19.3714-HA*

In order to tag the C-terminus of *ORF19.3714* with three copies of the hemagglutinin epitope (HA), the 1.7 kb *HA-URA3* cassette was amplified from 50.0 ng of plasmid pFA-HA-URA3 (97) with oligonucleotides AG4F and AG4R. The reaction conditions were as follows: 94°C for 3 min, followed by 25 cycles of 94°C for 30 sec, 40°C for 30 sec, 68°C for 1 min and 40 sec, followed by a 7 min extension at 68°C and storage at 4°C. The 100.0 ng of the product was used as a template in a fusion PCR to amplify a final 1.9 kb fragment with oligonucleotides AG80F and AG80R, which contained 100 bp homology to regions lying upstream and downstream from the stop codon of *ORF19.3714*, respectively, and 20 bp homology to the template. The reaction conditions were as follows: 94°C for 4 min, followed by 25 cycles of 94°C for 1 min, 40°C for 1 min, 68°C for 1 min 55 sec, followed by a 7 min extension at 68°C and storage at 4°C. The fusion construct was purified and 4.2 µg was transformed into strains RM1000 and CB105 (*cacdc5Δ::hisG/PCK1::CDC5-HIS1*) and AG614 (*CDC5/CDC5-MYC-HIS1*), resulting in strains AG517 (*ORF19.3714/ORF19.3714-HA-URA3*) and AG523 (*cacdc5Δ::hisG/PCK1::CDC5-HIS1, ORF19.3714/ORF19.3714-HA-URA3*) and AG622 (*CDC5/CDC5-MYC-HIS1, ORF19.3714/ORF19.3714-HA-URA3*) respectively.

d. *ORF19.3714-TAP*

In order to TAP tag the C-terminal of *ORF19.3714*, 2.9 kb fragment was amplified from 100.0 ng of pFA-TAP-ARG4 (97) using oligonucleotides AG80F and AG80R, which contained 100 bp homology to regions lying upstream and downstream from the stop codon of *ORF19.3714* respectively. The reaction conditions were as follows: 94°C for 4 min, followed by 25 cycles of 94°C for 1 min, 40°C for 1 min, 68°C for 2 min and 55 sec, followed by a 7 min extension at 68°C and storage at 4°C. The purified product (5.0 µg) was transformed into strains AG676 (*orf19.3714Δ::URA3*) and HCCa23 (*cdc20Δ::URA3/MET3::CDC20::HIS1*) resulting in strains AG707 (*orf19.3714Δ::URA3/ ORF19.3714-TAP-ARG4*) and AG704 (*cdc20Δ::URA3/MET3::CDC20::HIS1, ORF19.3714/ ORF19.3714-TAP-ARG4*) respectively. In order to TAP tag *ORF19.3714* using pFA-TAP-URA3, oligonucleotides AG80F and AG80R were used with above conditions except for extension time of 2 min 20 sec at 68°C to obtain a 2.3

kb fragment. Purified product (5.0 µg) was transformed into strain AG500 (*cdc5Δ::hisG/MET3::CDC5-ARG4*) resulting in strain AG717 (*cdc5Δ::hisG/MET3::CDC5-ARG4, ORF19.3714/ ORF19.3714-TAP-URA3*).

e. orf19.3714A/A

In order to delete *ORF19.3714*, oligonucleotides AG82F and AG82R amplified a 480 bp fragment lying upstream of the *ORF19.3714* start codon (5' flank), while oligonucleotides AG114F and AG83R amplified a 612 bp fragment lying downstream of the stop codon (3' flank) using 100.0 ng of BWP17 gDNA. The reaction conditions were as follows: 94°C for 3 min, followed by 25 cycles of 94°C for 30 sec, 49°C for 30 sec, 68°C for 30 sec, followed by a 7 min extension at 68°C and storage at 4°C for 5' flank. For 3' flank, the reaction conditions as follows: 94°C for 3 min, followed by 25 cycles of 94°C for 30 sec, 45°C for 30 sec, 68°C for 40 sec, followed by a 7 min extension at 68°C and storage at 4°C. Oligonucleotides AG84F and AG114R amplified a 1541 bp *URA3* fragment (middle cassette) from plasmid pBS-CaURA3 (A.J.P. Brown). The reaction conditions were as follows: 94°C for 3 min, followed by 25 cycles of 94°C for 30 sec, 40°C for 30 sec, 68°C for 1 min and 35 sec, followed by a 7 min extension at 68°C and storage at 4°C. All the products (5' flank: middle cassette: 3' flank) were combined in a 1:3:1 ratio as template in a fusion PCR with oligonucleotides AG82F and AG83R. The reaction conditions were as follows: 94°C for 3 min, followed by 10 cycles of 94°C for 30 sec, 50°C for 30 sec, 68°C for 2 min and 35 sec, followed by 15 cycles of 94°C for 10 sec, 50°C for 30 sec, 68°C for 2 min 35 sec with + 20 sec extension for each cycle, 69°C for 7 min and storage at 4°C. The final 2.5 kb product was purified and 3.5 µg was transformed into strains BWP17 and AG500, resulting in strain AG676 (*ORF19.3714/orf19.3714A::URA3*) and AG680 (*cdc5Δ::hisG/MET3::CDC5-ARG4, ORF19.3714/orf19.3714A::URA3*), respectively.

The second copy of *ORF19.3714* was replaced with a *HIS1*-containing fusion product produced in a similar manner with the exception of utilizing 100.0 ng of pBS-CaHIS1 (C. Bachewich) with oligonucleotides AG84F and AG114R, resulting in a 1.4 kb band. The reaction conditions were as follows: 94°C for 3 min, followed by 25 cycles of 94°C for 30 sec, 40°C for 30 sec, 68°C for 1 min and 35 sec, followed by a 7 min extension at 68°C and storage at 4°C. All the products (5' flank: middle cassette: 3' flank) were combined in a 1:3:1 ratio as template in a fusion PCR with oligonucleotides AG82F and AG83R. The reaction conditions were as follows:

94°C for 3 min, followed by 10 cycles of 94°C for 30 sec, 50°C for 30 sec, 68°C for 2 min and 25 sec, followed by 15 cycles of 94°C for 10 sec, 50°C for 30 sec, 68°C for 2 min 25 sec with + 20 sec extension for each cycle, 69°C for 7 min and storage at 4°C. The final 2.4 kb product was purified and 3.2 µg was transformed into AG676 and AG680 resulting in strains AG692, AG694 (*orf19.3714Δ::URA3/orf19.3714Δ::HIS1*) and AG698, AG700 (*cdc5Δ::hisG/MET3::CDC5-ARG4, orf19.3714Δ::URA3/orf19.3714Δ::HIS1*) respectively.

f. Strains where ORF19.3714 was reintroduced

In order to create strains where *ORF19.3714* was reintroduced, oligonucleotides AG119F and AG118R were used to amplify a 3949 bp fragment from 100 ng of gDNA that spanned 1840 bp of sequence upstream of the start codon, the open reading frame, and 262 bp downstream of the stop codon of *ORF19.3714*. The PCR conditions were as follows: 94°C for 3 min, followed by 30 cycles of 94°C for 30 sec, 47°C for 30 sec, 68°C for 3 min and 55 sec, followed by a 7 min extension at 68°C and storage at 4°C. The 2.0 µg of purified PCR product was digested with *XhoI* and *XmaI*, utilizing 1X BSA, 1X Buffer 4, 40 U *XhoI* (NEB), and 20 U *XmaI* (NEB). The reaction was incubated at 37°C overnight. In addition, 1.0 µg of plasmid pBS-ARG4 was similarly digested with *XhoI*, purified and then digested with *XmaI*. The digestion products were purified, and used for ligations. The ligation reaction mix was composed of a final concentration of 1X Ligase buffer, 200 U T4 DNA Ligase enzyme (New England BioLabs), 2.5 ng digested pBS-ARG4 and varied amounts of digested PCR product (0, 2.5, 5.0, 10.0, 20.0 ng) in a total volume of 10.0 µl. The reactions were incubated at 16°C overnight. The ligations were transformed into *E. coli* and random colonies were inoculated into 3.0 ml LB medium containing 100.0 µg/ml ampicillin. The samples were incubated at 37°C overnight, and plasmid DNA was extracted using the Plasmid Mini Kit I (OMEGA). Purified plasmid was then digested with *KpnI*, which sits in pBS-ARG4. The reactions were composed of 1X BSA, 1X Buffer 1, 20 U *KpnI* (NEB), 100.0 ng of purified plasmid, and incubated at 37°C. Positive integrations were confirmed by visualization of a 9008 bp vs a 5059 bp band on a DNA gel. The positive circular plasmid with insert (*E. coli* strain AG21) was cut with *PmlI* before transforming into *C. albicans* strain AG692, resulting in strains AG721 and AG722 (*orf19.3714Δ::URA3/orf19.3714Δ::HIS1, pBS-ARG4-ORF19.3714*). An isogenic strain was made by transforming uncut pBS-ARG4 into strain AG692 resulting in strains AG727 and AG728 (*orf19.3714Δ::URA3/orf19.3714Δ::HIS1 + pBS-ARG4*).

4.2.5 PCR screening

In order to confirm, strains AG180 (*cdc5Δ::hisG/CDC5-TAP-URA3*) and AG191 (*cdc20Δ::URA3/MET3::CDC20-HIS1, CDC5/CDC5-TAP-ARG4*), oligonucleotides AG2F and AG2R, which sit upstream and downstream of the region of integration, respectively, were used to amplify a 417 bp *CDC5*, 2491 bp *CDC5-TAP-URA3* or 3100 bp *CDC5-TAP-ARG4* band. The PCR conditions were as follows: 94°C for 3 min, followed by 30 cycles of 94°C for 30 sec, 38°C for 30 sec, 68°C for 2 min and 15 sec, followed by a 7 min extension at 72°C and storage at 4°C. In order to confirm strain AG614 (*CDC5/CDC5-MYC-HIS1*), oligonucleotides CaHIS1F, which sits in *HIS1*, and AG2R, which sits 420 bp downstream of the *CDC5* Stop codon and the region of integration were used to amplify a 921 bp fragment. The PCR conditions were as follows: 95°C for 3 min, followed by 30 cycles of 95°C for 30 sec, 43°C for 30 sec, 72°C for 55 sec, followed by a 7 min extension at 72°C and storage at 4°C. In order to confirm strains AG517 (*ORF19.3714/ORF19.3714-HA-URA3*) and AG523 (*cacdc5Δ::hisG/PCK1::CDC5-HIS1, ORF19.3714/ORF19.3714-HA-URA3*) and AG622 (*CDC5/CDC5-MYC-HIS1, ORF19.3714/ORF19.3714-HA-URA3*) oligonucleotides CaURA3F, which sits in *URA3* and AG81R, which sits 190 bp below the region of integration in the downstream sequence of *ORF19.3714* were used to amplify a 958 bp fragment. The PCR conditions were as follows: 95°C for 3 min, followed by 30 cycles of 95°C for 30 sec, 41°C for 30 sec, 72°C for 1 min and 40 sec, followed by a 7 min extension at 72°C and storage at 4°C. In order to confirm strains AG707 (*orf19.3714Δ::URA3/ORF19.3714-TAP-ARG4*) and AG704 (*cdc20Δ::URA3/MET3::CDC20-HIS1, ORF19.3714/ORF19.3714-TAP-ARG4*) for *ORF19.3714-TAP-ARG4* integration, oligonucleotides CaARG4F, which sits in *ARG4* and AG81R, which sits downstream in *ORF19.3714*, 190 bp below the region of integration, were used to amplify a 696 bp fragment. The PCR conditions were as follows: 95°C for 3 min, followed by 30 cycles of 95°C for 30 sec, 43°C for 30 sec, 72°C for 40 sec, followed by a 7 min extension at 72°C and storage at 4°C. In order to confirm the strain AG717 (*cdc5Δ::hisG/MET3::CDC5-ARG4, ORF19.3714/ORF19.3714-TAP-URA3*), oligonucleotides CaURA3F and AG81R amplified a 1153 bp fragment. The PCR conditions were as follows: 95°C for 3 min, followed by 30 cycles of 95°C for 30 sec, 43°C for 30 sec, 72°C for 1 min and 10 sec, followed by a 7 min extension at 72°C and storage at 4°C. In order to confirm strains AG676 (*ORF19.3714/orf19.3714Δ::URA3*) and AG680 (*cdc5Δ::hisG/MET3::CDC5-ARG4, ORF19.3714/orf19.3714Δ::URA3*),

oligonucleotide AG85F, which sits 233 bp upstream of the Start of *ORF19.3714*, before the region of integration, and CaURA3R, which sits in *URA3*, were used to amplify a 1991 bp fragment. The PCR reaction mix was composed of 0.5 μ M forward and reverse oligonucleotides, 0.2 mM dNTPs, 50.0 ng of template, 1.0 U of Q5 High Fidelity DNA Polymerase (New England Biolabs), and 1X Q5 reaction buffer. The PCR conditions were as follows: 98°C for 30 sec, followed by 30 cycles of 98°C for 10 sec, 59°C for 30 sec, 72°C for 1 min, followed by a 2 min extension at 72°C and storage at 4°C. In order to confirm strains AG692, AG694, AG698, and AG700 oligonucleotides AG85F, which sits upstream of the Start codon of *ORF19.3714*, 233 bp upstream of the region of integration cassette, and CaHIS1R, which sits in *HIS1*, were used to amplify a 1280 bp fragment. The PCR conditions were as follows: 95°C for 3 min, followed by 30 cycles of 95°C for 30 sec, 45°C for 30 sec, 72°C for 1 min and 15 sec, followed by a 7 min extension at 72°C and storage at 4°C. The absence of a wild type *ORF19.3714* band in strains AG692, AG694, AG698, and AG700 was tested with oligonucleotides AG111F and AG111R that amplify a 840 bp fragment within the *ORF*. The PCR conditions were as follows: 95°C for 3 min, followed by 30 cycles of 95°C for 30 sec, 45°C for 30 sec, 72°C for 50 sec, followed by a 7 min extension at 72°C and storage at 4°C. In order to confirm strains AG721 and AG722 (*orf19.3714 Δ ::URA3/orf19.3714 Δ ::HIS1*, pBS-*ARG4-ORF19.3714*), oligonucleotides AG120F, which sits in *ORF19.3714* 130 bp upstream of the region of integration and AG111R, which sits in *ORF19.3714*, were used to amplify a 3360 bp fragment. The PCR conditions were as follows: 94°C for 3 min, followed by 30 cycles of 94°C for 30 sec, 47°C for 30 sec, 68°C for 3 min and 20 sec, followed by a 7 min extension at 68°C and storage at 4°C.

4.2.6 Southern blotting

The *orf19.3714 Δ / Δ* strains were confirmed using Southern blotting with the DIG Hybridization System (Roche Diagnostics, Mannheim, Germany). For this, gDNA was extracted according to Rose *et al.*, 1990 (98), and digested with *Spe1*. A DIG-labeled probe was prepared using oligonucleotides AG116F and AG116R to confirm strains AG676, AG690, AG692, AG694, AG698 and AG700.

4.2.7 Northern blotting

RNA was extracted and Northern blotting was performed as previously described (9, 10).

Probes consisted of approximately 700-800 bp fragments complementary to the open reading frames of *ORF19.3714* and *ACT1* and were amplified with oligonucleotides AG111F and AG111R, and ACT1-129F and ACT1-104R, respectively. Northern blots were visualized with a phosphoimager (Typhoon Variable Mode Imager, GE Healthcare). Blots were quantified as described previously (75) using ImageJ.

4.2.8 Protein extraction and Western blotting:

Protein extracts were prepared according to Liu *et al.*, 2010 (99). Extracted protein was quantified using the Bradford assay (Bio-Rad). For protein samples treated with calf intestinal alkaline phosphatase (CIP) (New England Biolabs), EDTA and sodium vanadate were excluded from the HK extraction buffer. Dephosphorylation of proteins was performed using 10 U of CIP per 10.0 µg of protein at 37°C for 90 min. Western blotting was done as described previously (75). Briefly, 30.0 µg of protein was loaded onto SDS-PAGE gels and proteins were transferred to a polyvinylidene difluoride (PVDF) membrane (BioRad). Membranes were blocked with Tris-buffered saline–Tween (TBST; 50 mM Tris (98), 137.0 mM NaCl, 0.1% Tween 20) containing 5.0 % skim milk for 1.0 h. Blots were washed three times for 15 min in TBST and incubated for 1.5 h in 0.4 µg/ml anti-HA antibody (12CA5; Roche) or 1.5 h in 0.2 µg/ml anti-TAP antibody (Thermo Scientific) or overnight at 4°C in 2.5 µg/ml anti-c-MYC (Roche) diluted in TBST or overnight at 4°C in 1.0 µg/ml of anti-myc (Santa Cruz) diluted in TBST supplemented with 2.0% milk. Blots were rinsed three times for 15 min in TBST and incubated for 1.0 h in a 0.04 µg/ml of horseradish peroxidase-conjugated secondary antibody anti-mouse (KPL) or anti-rabbit (Santa Cruz). After washing, blots were developed using ECL (GE Healthcare; Amersham ECL Western blotting analysis system). Blots were stripped and incubated with 0.2 µg/ml of anti-PSTAIRE (Santa Cruz Biotechnology) as a loading control. Western blots were quantified using ImageJ as described previously (75).

4.2.9 Co-Immunoprecipitation

Overnight cultures of strains were diluted into 1.0 L of YEPD medium and incubated in 30°C until the O.D._{600nm} reached 0.8-1.0. The cultures were centrifuged for 4 min at 2095 g (Allegra X-12R Centrifuge Beckman Coulter; CAN 605169-AA), and the pellet was immersed in liquid nitrogen or dry ice and stored at -80°C. Protein was extracted as described above (99).

For co-immunoprecipitation, Mono HA 11 Affinity beads (Covance) or c-MYC beads (9E10) AC (Santa Cruz) were used. The beads were pre-washed using HK buffer (99) three times by centrifuging at 1500 X g (Thermo Electron Microlite RF) for 2 min at 4°C. Approximately 40.0 µl of prewashed beads (bead volume) were combined with 40.0 mg of protein, and incubated overnight at 4°C. The beads were washed 3 times in 1.0 ml HK buffer, and protein was eluted twice from the beads, first by boiling in 50.0 µl of 1X SDS sample buffer (50.0 mM Tris pH 6.8, 2.0% SDS, 0.01% Bromophenol blue, 10.0% Glycerol, 100.0 mM DTT) for 10 min, followed by boiling in 40.0 µl of 1 X SDS loading buffer. Eluted samples were centrifuged for 2 min at 15700 g (Eppendorf; Centrifuge 5415 D) at room temperature and combined. On SDS PAGE gels for Western blotting, 30.0 µl of eluate and 30.0 µg of whole cell extract were loaded. Western blotting was performed as described above.

4.2.10 One-step affinity purification for identification of phosphorylation sites

For *MET3* and *PCK1* regulated strains, overnight cultures grown in -MC or SS medium were washed and diluted to an O.D._{600 nm} of 0.3 in +MC or SD medium respectively and grown at 30°C for 4.0 h. Pellets were collected, protein was extracted (99), and approximately 100.0 mg was incubated with prewashed of IgG Sepharose 6 Fast Flow (GE Healthcare) or Mono HA 11 Affinity beads (Covance) (1:1 slurry in HK buffer; 50 µl of bead volume) overnight at 4°C. Beads were washed 3 times by centrifuging at 1500 g for 2 min at 4°C and protein was eluted by boiling in 60.0 followed by 50.0 µl 1X SDS PAGE buffer for the first and second elution, respectively. Eluates were separated on 1.5 mm SDS PAGE gels, and stained with Coomassie blue. Gel pieces corresponding to 100.0 kDa were excised and sent for processing and analysis via Orbitrap LC/MS (IRIC, University of Montreal). On a separate SDS PAGE gel, 5.0 µl of the eluate was separated and Western blotting was performed to confirm that Orf19.3714p appeared as multiple bands starting at approximately 100 kDa before sending the samples for mass spectrometry.

4.2.11 Two Step Affinity Purification

Affinity purification was carried out according to Rigaut *et al.* 1999 (100) and Liu *et al.* 2010 (99), with some modifications. Overnight cultures of TAP-tagged and isogenic control strains were inoculated in YEPD medium at 30°C, diluted to an O.D._{600nm} of 0.15 into 2.0 L of

YEPD medium, and collected at an O.D._{600nm} of 0.8-1.0 by centrifugation for 4 min at 2095 g. For *MET3*-regulated strains, overnight cultures grown in -MC medium were washed and diluted to an O.D._{600nm} of 0.3 in +MC medium. Pellets were collected after 4.0 h and frozen in liquid nitrogen or dry ice and stored at -80°C. Protein was extracted as described previously (99). For the first step of the affinity purification, approximately 200.0-250.0 mg of protein from cultures grown in YEPD medium or 100.0 mg from cultures grown in +MC medium were pre-cleared by adding pre-washed, 500.0 µl bead volume of Sepharose 6B (Sigma) beads (1:1 slurry in HK buffer) and rocking at 4°C for 30 min. The beads were removed by centrifuging at 600.0 g for 2 min at 4°C. The protein extract was then incubated with prewashed IgG Sepharose 6 Fast Flow (GE Healthcare) (1:1 slurry in HK buffer; 250.0 µl bead volume) for 4.0 h or overnight at 4°C. The bead-extract mix was poured into a Poly-Prep Chromatography Column (Bio-Rad) and beads were washed twice with 10.0 ml ice cold IPP300 buffer (25.0 mM Tris-HCl pH 8.0, 300.0 mM NaCl, 0.1% NP-40), once with 10.0 ml IPP150 buffer (25.0 mM Tris-HCl pH 8.0, 150.0 mM NaCl, 0.1% NP-40) and once with 10.0 ml TEV CB (25.0 mM Tris-HCl pH 8.0, 150.0 mM NaCl, 0.1% NP-40, 0.5 mM EDTA and 1.0 mM DTT). Beads were incubated with 1.0 ml TEV CB buffer containing 50.0 U of Ac-TEV protease (Invitrogen) in the column overnight at 4°C with rotation. The eluate (1.0 ml) was collected in a new column and beads were washed with another 1.0 ml TEV CB buffer. To the final 2.0 ml eluate, add 6.0 ml of CBB (25.0 mM Tris-HCl pH 8.0, 150.0 mM NaCl, 1.0 mM Mg acetate, 1.0 mM Imidazole, 2.0 mM CaCl₂), 24.0 µl of 1.0 M CaCl₂ and prewashed 150.0 µl bead volume of Calmodulin Sepharose 4B (GE Healthcare) (1:1 slurry in CBB buffer; 150.0 µl bead volume) and rocked for 1.0 h at 4°C. The beads were washed twice with 1.0 ml CBB (0.1% NP-40), and once with 1.0 ml CBB (0.02% NP-40). Protein was eluted from the beads by two separate additions of 1.0 ml CEB (25.0 mM Tris-HCl pH 8.0, 150.0 mM NaCl, 0.02% NP-40, 1.0 mM Mg acetate, 1.0 mM Imidazole, 20.0 mM EGTA, 10.0 mM β-mercaptoethanol). The elutions were combined and protein was precipitated by adding 1/4 volume of 50% room temperature trichloroacetic acid (TCA) (Sigma). The samples were incubated on ice for 30 min, centrifuged at 16,000 g for 10 min at 4°C. The protein pellet was washed with 1.0 ml of pre-chilled 80.0% acetone. Acetone was removed after centrifugation at 16000 g for 10 min at 4°C, and the samples were air-dried on ice for approximately 1.0 h until all acetone evaporated. The pellet was re-suspended in 30.0 µl 1 X SDS sample buffer and boiled for 10 min. The sample was loaded on an SDS-PAGE gel for silver staining (Bio-Rad) or run on

an SDS PAGE gel until the sample just entered the resolving gel (99). The latter gel was stained with Coomassie blue (Bio-Rad). The gel pieces corresponding to tagged and untagged strains were cut and sent for processing and analysis via Orbitrap LC/MS (IRIC, University of Montreal).

4.2.12 Plate growth assays

Overnight cultures of strains BH420 (*URA3+ HIS1+ ARG4+*), AG721, AG722 (*orf19.3714Δ::URA3/orf19.3714Δ::HIS1 + pBS-ORF19.3714-ARG4*), AG727 and AG728 (*orf19.3714Δ::URA3/orf19.3714Δ::HIS1 + pBS-ARG4*) in YEPD were diluted to O.D._{600nm} of 0.08 in sterile water and 5.0 µl of serial dilutions of 5X, 25X, 125X, 625X and 3125X were plated on YEPD and incubated at 30°C, 37°C or 42°C for 3 days. Serial dilutions on YEPD plates supplemented with 20.0 µM Calcoflour, 0.04% SDS or 1.5 M Sorbitol were incubated at 30°C for 3 days. Serial dilutions on YEPD plates supplemented with 25.0 mM hydroxyurea (HU), 0.01% MMS, 6.0 mM hydrogen peroxide (H₂O₂), 15.0 mM caffeine, or 10.0 nM rapamycin were incubated at 30°C for 48.0 h. For YEPD plates supplemented with 10.0% foetal bovine serum, Spider or SLAD plates, overnight cultures of strains BH420, AG721, AG727 in YEPD were diluted to an O.D._{600nm} of 0.005 in sterile water, 1.5 µl was added to 3.5 µl of water, and the total 5.0 µl volume was plated. Plates were incubated at 37°C for 5-7 days.

4.2.13 Cell staining and imaging

For Differential Interference Contrast (DIC) microscopy, cells were fixed in 70.0% ethanol for at least 1.0 h, washed twice with sterile water, and mounted on slides. To visualize nuclei, cells fixed in 70.0% ethanol were stained with 1.0 µg/ml of 4',6'-diamidino-2-phenylindole dihydrochloride (DAPI; Sigma-Aldrich) for 20 min, and washed with sterile water (75). Cells were then mounted on slides and examined on a Leica DM6000B microscope (Leica Microsystems Canada Inc., Richmond Hill, ON, Canada) equipped with a Hamamatsu-ORCA ER camera (Hamamatsu Photonics, Hamamatsu City, Japan) using either HCX PL APO 63x NA 1.40-0 oil or HCX PLFLUO TAR 100x NA 1.30-0.6 oil objectives and the DAPI (460-nm) filter. Images were captured with Volocity software (Improvision Inc., Perkin-Elmer, Waltham, MA).

4.3 RESULTS

4.3.1 Identification of Cdc5p-interacting factors reveals a previously uncharacterized protein, Orf19.3714p

The Plk Cdc5p in *C. albicans* is required for early stages of mitotic progression and influences yeast bud morphogenesis, but its mechanisms of action remain unknown. In order to address this question, we identified Cdc5p-interacting proteins using affinity purification and mass spectrometry. Strains carrying a copy of *CDC5* tagged at the C-terminus with a TAP tag were created (AG180: *cdc5::hisG/CDC5-TAP-URA3*) (Fig. 4.1A-B). Western blotting demonstrated that Cdc5p-TAP was expressed (Fig. 4.1C), and growth rates and yeast cell morphology of strain AG180 were normal (Fig. 4.1D, E). Thus, Cdc5p-TAP was considered functional and strains AG180 and BWP17 (*CDC5/CDC5*) were used for subsequent investigations. Following protein extraction and two-step affinity purification, a silver-stained gel demonstrated protein enrichment in the tagged vs. untagged strain (data not shown). The affinity purification was then repeated and samples were run just into the resolving portion of an SDS PAGE gel to allow for band compaction (99). After staining with Coomassie blue (Fig. 4.2), gel pieces were sent for analysis via Orbitrap LC/MS (IRIC, University of Montreal). The most abundant number of peptides corresponded to Cdc5p, followed by Cdc7p (Table 4.4), the catalytic component of the Dbf4p-Cdc7p kinase complex that is important for initiation of DNA replication (101, 102) and a known Cdc5p-interacting protein in *S. cerevisiae* (103). Remaining factors were represented by two peptides each, including members of the Hsp70p family of chaperones and a putative karyopherin β (Orf19. 2489p), homologues of which bind Cdc5p in *S. cerevisiae* (104-106). Proteins not previously known to bind Plks included ribosomal proteins (Rps5p, Rps17bp), as well as the uncharacterized proteins Orf19.3714p and Orf19.5287p (Table 4.5).

In order to enhance the detection of Cdc5p-interacting factors, we repeated the affinity purification from synchronized cells blocked in mitosis, through depletion of Cdc20p. We previously demonstrated that Cdc5p was enriched under these conditions (75). For this, overnight cultures of strains AG191 (*cdc20::URA3/MET3::CDC20::HIS1, CDC5/CDC5-TAP-ARG4*) (75) and an isogenic control strain BH420 (*URA3+*, *HIS1+*, *ARG4+*) were diluted into

repressing medium (+MC) for 4 h to deplete Cdc20p. Affinity purification of Cdc5p followed by mass spectrometry analysis revealed a higher abundance of peptides corresponding to Cdc5p compared to the previous trial (Table 4.5). Cdc7p and Dbf4p, which bind Cdc5p in *S. cerevisiae* (18, 107) were also highly enriched. The heat shock protein Hsp70p, as well as ribosomal and translational factors also co-purified (Table 4.5). Intriguingly, the uncharacterized protein Orf19.3714p was enriched relative to that in exponential-phase cells, and represented by the same number of peptides as Dbf4p (Table 4.5), suggesting a strong interaction. Thus, Cdc5p in *C. albicans* may interact with the Cdc7p-Dbf4p complex, similar to the situation in *S. cerevisiae*, but also uncharacterized factors, suggesting novel functions.

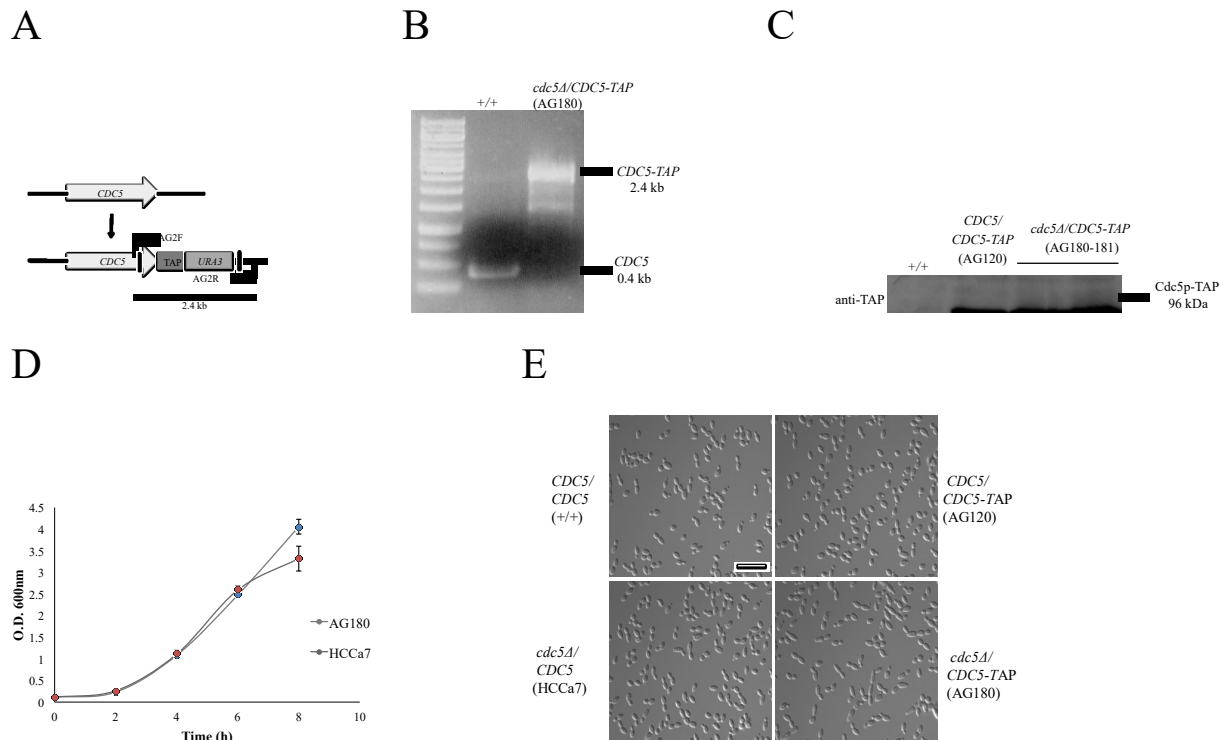


Figure 4.1: Confirmation of Cdc5p-TAP strains. (A) Map showing a PCR screening strategy to confirm correct integration of the TAP-containing construct. Vertical black lines designate the area of the transforming DNA construct. Oligonucleotides AG2F and AG2R generated a 0.4 kb *CDC5* wild-type or a 2.4 kb *CDC5-TAP-URA3* band. (B) Ethidium bromide-stained DNA gel showing positive strains AG180 (*cdc5Δ::hisG/CDC5-TAP-URA3*) and the negative control strain BWP17 (*CDC5/CDC5*). (C) Western blot containing 30 μ g of whole cell protein extracts from strains AG180 and BWP17 (+/+) incubated with anti-TAP antibody. (D) Growth curve of strains AG180 and HCCa7 (*CDC5/cdc5Δ::hisG*) incubated in YEPD medium at 30°C, represented by O.D._{600nm} over time. (E) Phenotype of strains BWP17, AG180, HCCa7 and AG120 (*CDC5/CDC5-TAP-URA3*) incubated in YEPD medium at 30°C for 8 h. Bar: 10 μ m.

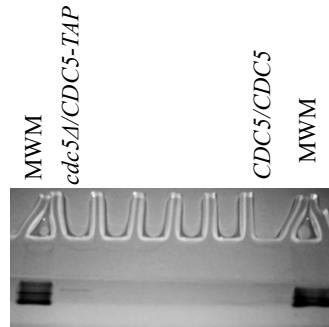


Figure 4.2: Coomassie-stained gel of tandem affinity-purified Cdc5p and control samples. Protein extracted from 2 L cultures of exponential-growing strains AG180 (*cdc5Δ::hisG/CDC5-TAP-URA3*) and BWP17 (*CDC5/CDC5*) were subjected to tandem affinity purification (99). Elutions were TCA precipitated, separated on an SDS PAGE gel into the resolving gel for band compaction, and stained with Coomassie blue. MWM: molecular weight marker.

Table 4.4: Orbitrap LC/MS analysis of putative Cdc5p-interacting proteins in exponential growing cells¹

Protein ID	Gene name ⁴	Present in control ²	Number of peptides ³	Protein description ⁴
CAL0005042	<i>CDC5/</i> <i>ORF19.6010</i>	No	16	Polo-like kinase; member of conserved Mcm1p regulon; depletion causes defects in spindle elongation and Cdc35p-dependent filamentation
CAL0005945	<i>CDC7/</i> <i>ORF19.3561</i>	No	5	Possibly an essential gene, putative kinase; cell-cycle regulated periodic mRNA expression
CAL0001101	<i>ORF19.3714</i>	No	2	Uncharacterized <i>ORF</i>
CAL0001639	<i>ORF19.2489</i>	No	2	Uncharacterized <i>ORF</i> ; Putative karyopherin beta; repressed by nitric oxide
CAL0000989	<i>RPS5/</i> <i>ORF19.4336</i>	No	2	Ribosomal protein S5; macrophage/ pseudohyphal-induced after 16 h; genes encoding cytoplasmic ribosomal subunits, translation factors
CAL0004332	<i>KAR2/</i> <i>ORF19.2013</i>	No	2	Similar to Hsp70 family chaperones; role in translocation of proteins into the endoplasmic reticulum
CAL0001208	<i>SSA2/</i> <i>ORF19.1065</i>	No	2	<i>HSP70</i> family chaperone; cell wall fractions; antigenic
CAF0006947	<i>RPS17B/</i> <i>ORF19.2329.1</i>	No	2	Ribosomal protein 17B; downregulated upon phagocytosis by murine macrophages
CAL0000006	<i>HSP70/</i> <i>ORF19.4980</i>	No	2	Putative hsp70 chaperone; role in entry into host cells; heat-shock
CAL0005101	<i>TUB2/</i> <i>ORF19.6034</i>	No	2	Beta-tubulin; functional homolog of <i>S. cerevisiae</i> Tub2
CAL0001367	<i>SSB1/</i> <i>ORF19.6367</i>	No	2	<i>HSP70</i> family heat shock protein; mRNA in yeast and germ tubes

¹Approximately 172 mg protein extracts from 2 L cultures of strains AG180 (*cdc5/CDC5-TAP*) and BWP17 (*CDC5/CDC5*) were subjected to tandem affinity purification (Rigaut *et al.* 1999, Lui *et al.*, 2010). Elutions were TCA-precipitated, run until just entering the resolving portion of an SDS PAGE gel (Lui *et al.*, 2010) stained with Coomassie blue, cut from the gel, and analysed using an LTQ-OrbitrapElite with nano-ESI.

²Peptides identified in both the tagged and the untagged control strains were excluded from the results.

³Peptides at a frequency of 1 were excluded from the results.

⁴Gene names and descriptions were obtained from the Candida Genome Database (<http://www.candidagenome.org/>).

Table 4.5: Orbitrap LC/MS analysis of putative Cdc5p-interacting proteins in cells blocked in mitosis¹

Protein ID	Gene name ⁴	Present in control ²	Number of peptides ³	Protein description ⁴
CAL0005042	<i>CDC5/ORF9.6010</i>	No	33	Polo-like kinase; member of conserved Mcm1 regulon; depletion causes defects in spindle elongation and Cdc35 dependent filamentation
CAL0005945	<i>CDC7/ORF19.3561</i>	No	12	Possibly an essential gene, Putative kinase; cell- cycle regulated periodic mRNA expression
CAL0002629	<i>DBF4/ORF19.5166</i>	No	10	Uncharacterized, putative Cdc7p-Dbf4p kinase, complex regulatory subunit cell-cycle regulated periodic mRNA expression
CAL0001101	<i>ORF19.3714</i>	No	10	Uncharacterized
CAL0006304	<i>RPL3/ORF19.1601</i>	No	4	Ribosomal protein, large subunit
CAL0005746	<i>CEF3 /ORF19.4152</i>	No	3	Translation elongation factor 3, predicted C-term nucleotide-binding active site
CAL0000006	<i>HSP70/ORF19.4980</i>	No	3	Putative hsp70 chaperone; role into in entry host cells
CAL0004511	<i>TUB1/ORF19.7308</i>	No	2	Alpha-tubulin, complements cold-sensitivity of <i>S. cerevisiae</i> tub1 mutant
CAL0000989	<i>RPS5/ORF19.4336</i>	No	2	Ribosomal protein S5; macrophage/ pseudohyphal -induced after 16 h
CAL0003652	<i>ORF19.5287</i>	No	2	Uncharacterized

¹Approximately 102 mg protein extracts from 2 L cultures of AG191 (*cdc20/MET3::CDC20, CDC5/CDC5-TAP*) and BH420 (*CDC5/CDC5*) strains were subjected to tandem affinity purification (Rigaut *et al.* 1999, Lui *et al.*, 2010). Elutions were TCA-precipitated and run just into the resolving portion of an SDS PAGE gel (Lui *et al.*, 2010). The compressed bands were stained with Coomassie blue, cut from the gel, and analysed using an LTQ-OrbitrapElite with nano-ESI.

²Peptides identified in both the tagged and the untagged control strains were excluded from the results.

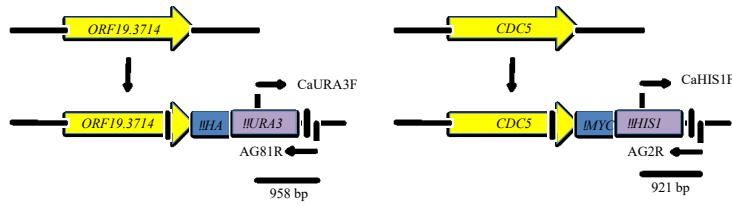
³Peptides at a frequency of 1 were excluded from the results.

⁴Gene names and descriptions were obtained from the *Candida* Genome Database (<http://www.candidagenome.org/>).

Since Orf19.3417p represents a potential novel Plk interacting factor, we focused subsequent investigations on this protein. In order to confirm that Orf19.3714p physically interacts with Cdc5p, we performed a co-immunoprecipitation. For this, *CDC5* and *ORF19.3714* were tagged with 13 copies of MYC or 3 copies of HA at the C-terminus, resulting in strains AG614 (*CDC5/CDC5-MYC-HIS1*) or AG517 (*ORF19.3714/ORF19.3714-HA-URA3*) respectively (Fig. 4.3). Next, *ORF19.3714* was tagged with HA in strain AG614, resulting in strain AG622 (*CDC5/CDC5-MYC-HIS1, ORF19.3714/ORF19.3714-HA-URA3*). Although PCR screening indicated correct integration of the constructs (Fig. 4.3), only Cdc5p-MYC was detected in Western blots of whole cell extracts (Fig. 4.4A). In order to determine whether this was due to low expression, we attempted to enrich Orf19.3714p-HA through affinity-purification. Under these conditions, Western blotting revealed an intense band of higher molecular weight than expected (100 kDa vs. 70 kDa). When this band was removed from the gel and analyzed with mass spectrometry, the presence of Orf19.3714p was confirmed (data not shown), suggesting post-translational modifications. When Orf19.3714p-HA was precipitated with anti-HA beads from strain AG622, Cdc5p-MYC co-purified (Fig. 4.4A). Moreover, Cdc5p-MYC was not detected from precipitations carried out in the control strain AG614. In reverse co-immunoprecipitation using anti-MYC beads, a faint band representing Orf19.3714p-HA was visible in the double-tagged strain, unlike in the control (Fig. 4.4B). Although whole cell extracts demonstrated faint bands when incubated with anti-HA antibody, these were of a different pattern than observed in the immuno-precipitate, and are likely non-specific. Thus, the data support a physical interaction between Cdc5p and Orf19.3714p.

Many Plk targets contain a polo box domain (PBD) binding motif, which consists of Ser-pSer/pThr-Pro/X (15), and/or an optimal Plk1 phosphorylation consensus site, consisting of D/E-X-pS/T-φ-X- D/E (17) or D/E/N-X-pS/T-φ (108), where X is any amino acid and φ is a hydrophobic amino acid. If Orf19.3714p were a substrate of Cdc5p, we predict that it may contain similar motifs. Sequence analysis revealed that Orf19.3714p contains nine PBD binding motifs and eleven Plk1 phosphorylation consensus sites. In comparison, Cdc7p and Dbf4p contain two or four, or zero or three, respectively (Fig. 4.5). Collectively, the data suggest that Orf19.3714p may be a target of Cdc5p.

A



B

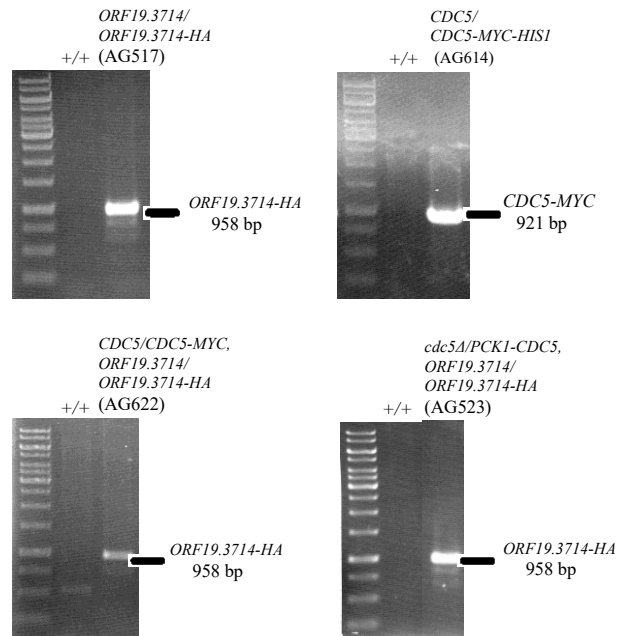
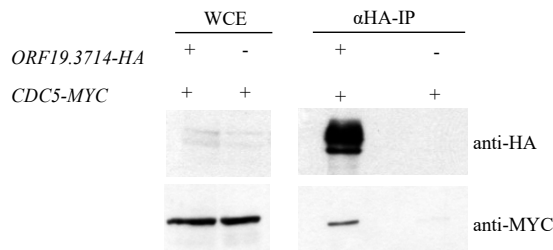


Figure 4.3: Confirmation of *ORF19.3714-HA* and *CDC5-MYC* strains. (A) Map showing a PCR screening strategy to confirm correct integration of the HA and MYC-containing constructs, respectively. Vertical black lines designate the area of the transforming DNA construct. Oligonucleotides CaURA3F and AG81R or CaHIS1F and AG2R generate a 958 bp *ORF19.3714-HA-URA3* band or a 921 bp *CDC5-MYC-HIS1* band, respectively (B) Ethidium bromide-stained DNA gel showing positive strains AG517 (*ORF19.3714/ORF19.3714-HA-URA3*), AG614 (*CDC5/CDC5-MYC-HIS1*), AG622 (*CDC5/CDC5-MYC-HIS1, ORF19.3714/ORF19.3714-HA-URA3*), AG523 (*cacdc5Δ::hisG, ORF19.3714/ORF19.3714-HA-URA3*), and the control strain BWP17 (*CDC5/CDC5, ORF19.3714/ORF19.3714*; +/+).

A



B

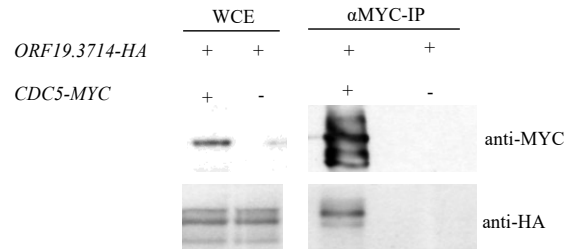


Figure 4.4: Co-immunoprecipitation confirming an interaction between Cdc5p and Orf19.3714p. Western blots of whole cell extracts (WCE) and immune-precipitates using αHA-IP (A) or αMYC-IP (B) beads. A total of 45 mg of protein from strains AG517 (*ORF19.3714/ORF19.3714-HA-URA3*), AG614 (*CDC5/CDC5-MYC-HIS1*) and AG622 (*CDC5/CDC5-MYC-HIS1, ORF19.3714/ORF19.3714-HA-URA3*) were incubated overnight with 45 μl of beads. Samples were processed for Western blotting.

Orf19.3714p

MALS EES P KLYPS STPLSNGNDRNPTVIQAT STPPPPPPALPDIST STPIETPWYYK
 RSTGSEEEEEEDTNNGNDDYDDYYQDDGETIQKTPSPNKS KGYRFNNQLDFA STPLNP
 SCTL SF SPMNKL NQLHLESQ LDMDFEEHLEIQGEEEEEDDDDD EYSLGNK TITTHE
 SESESEQGESNEINIKHFEPKYISSRRKRLHSESPDMMVLT PNVNYKNNVNDKNDVNDIT
 YGN DMS CNTTSTTT NTA T NTS AFKFSFNIS DST CPRQPKRRLKFKHESTRNILDN
 YAKKSILSQSSPFLYNDGGEGELPNEKYCYDNDENNSGISSGTD NKS NSKL ESTP
 SQT P ASSRA SSP PPLQQQQQK PRAQ PQQPQQ TSSSSSSKSGQ EYGETINGYKFVKPK
 NSMNNKLPQFK YETPINNRYHQ LCGYNSN NYQIMNELPV TAAAGLMPHGDEDDDDI
 HIGDRRIGDPYLNLSRDDDNHCDQETHDDGNQLREIYFKENRLLP LTPYFYQLKSLSDV
 QILALINYENLLKFYETILNG DETLYELLKQERIRWHPDKWIGKLNQKNEMIMDV DYE
 TIKMVD S ISQTINSIESL*

Cdc7p

MQEVLFYHQRS DQPPPPSQQSHLHA STPTPLSNMRRKQSS EDDPFKDRSCKSRKD
 ASTANLRLQQSL NSTH IRNSNLSKSYKHNETTEVANNLH DTTSQTTETEEFVTPNQ
 LDEQLEVA GRGGRGVVVEEQREEEEEEE EVTL EVL ENMQKLETNFPILATDYRLIDKIG
 SGT STVYKAESLTGKIRLGS DIWKSPPLKRNKRNILNFQQRKKNPIVALKQIYVT SSP
 NRIFNELHLLYMLSGNSRVA PLDLVLRFDQ QIVAILPYNH CDFREFYRDL PVKGIKKYL
 WELFQALDYIHGKGV IHRDLKPTNFL YDPRFGKGLVDFGLAERENISKNTK PETSTSS
 SGTATTTTTATTTTTTTTTINSSTASSAISTACPLN KDQKLINRHTKRLNVKGAY
 PKNDNRPPRRANRAGTRGFRAPEVLFKCTNQSTKIDIWSAGIIGFSILLRKFIFNSPTD
 TDAIL ELAWIFGYDKMAKCAELHGCGL EISMPEIHKSNGLIKIMYDFLMQEHINGCFPS
 DSVVYDTLELINESGEK FVKPVY TIREGISDIEKMKINEDFTKRHDDYKDHKYL MELLYG
 CFKM D P SKRLSAREILQLPFFHEILQISEDDTQDEFMQQNQTQTQEEEEEEDEVILS*

Dbf4p

MSKVEEHESVNNLKRKFP SLAKPRQPLKETNSNIPSPHKRAKIESPSKQOSTQPPQQPQ
 PQQPQQQEQKATHPKKSSHQSKNNDKLAGDEMHEWQQSWRRIMKSSIVYFEGDQQS
 LEYRKAHKLRLVGCKVTPFYDN NVT HSKRYPYDSK TYSPh IFSNVSKASIKVWNYD
 KVFRFLKHLGINIQTGVD ELAVNTHLTPSLTNNNEKPDLYNLLKEEKIYGSTRDPNA
 KRDDLHYLKGNYLYVYDLTQT V RPIAIREWSDHYVVMQLSLDGC PFIEDPTDQNSERK
 RLKRLRKF EANA HREALRLATYKMINGISMSVHGFTATSTSTDKVD EEE DSTV KE PSE
 DPRFRQPLNRN SSCMQSKAFEAMASGYNGASNAVQPSMDSNLNSAAAMAGGNGLGP
 LSQVPSKQLNLRRLMKKKTNTTEKKDKEHASGYCENCRVKYTNFDEHIMTNRHR
 NFACDRNFQDIDELIASLREKSLGNVISNGDYV*

Figure 4.5: Plk phosphorylation and Polo box domain-binding sites in Orf19.3714p, Cdc7p and Dbf4p from *C. albicans*. Conserved phosphorylation sites from Plk1 (highlighted in red or green) are D/E/N-X-pS/T-φ (108) (highlighted in red) or D/E-X-pS/T-φ-X- D/E (17) (highlighted in green) where X = any amino acid; φ = hydrophobic amino acid. Conserved Polo box binding site (highlighted in yellow) is S-pS/T-P (15). Common amino acids between Plk phosphorylation and PBD binding sites are highlighted in blue.

4.3.2 Orf19.3714p is a fungal-specific protein found primarily in *Candida* species

In order to determine the significance of the interaction between Cdc5p and Orf19.3714p, a bioinformatic analysis of Orf19.3714p was conducted. A BlastP search using NCBI (http://blast.ncbi.nlm.nih.gov/blast/Blast.cgi?PROGRAM=blastp&PAGE_TYPE=BlastSearch&LINK_LOC=blasthome) did not identify any sequence orthologues outside of fungi (data not shown). When using the Fungal Blast option in the *Saccharomyces* Genome Database (SGD) (<http://www.yeastgenome.org/>) against protein databases of all sequenced fungi, thirty-four hits were revealed, the top five of which corresponded to *Candida* species (Table 4.6). An additional hit in *Scheffersomyces stipites* corresponded to a BRIGHT/ARID domain-containing protein. This domain is found in a family of DNA binding proteins that play roles in embryonic development, cell lineage gene regulation and cell cycle control (109-111). However, this motif was not present in Orf19.3714p. Intriguingly, *S. cerevisiae* lacks a homologue, with the closest hit being YKR041W (SGD ID: S000001749; E value=0.031) (Table 4.6), which is uncharacterized but localizes to the mitotic spindle (112). A phylogenetic tree was then constructed using ClustalW2-Phylogeny (http://www.ebi.ac.uk/Tools/services/web/toolform.ebi?tool=clustalw2_phylogeny&sequence=clustalo-I20140826-180245-0622-20601651-pg) (113) for all 15 sequences obtained from an NCBI Blastp search against fungi that were aligned with the Clustal Omega multiple alignment tool (<http://www.ebi.ac.uk/Tools/msa/clustalo/>). Orf19.3714p grouped most closely with orthologues from *C. dubleniensis*, *C. tropicalis* and *C. maltosa* (Fig 4.6), which inhabit guts of humans, beetles, or both (114-116). Notably, *C. glabarata* did not contain a homologue, and it does not group within the clade containing *C. albicans*. Thus, Orf19.3714p is a fungal-specific protein with closest homologues found predominantly in *Candida* species.

Table 4.6: Fungal Protein Blast (Blastp) search in Saccharomyces Genome Database (SGD) using Orf19.3714p¹.

Sequences producing significant alignments	Score (bits)	E-value
ref XP_711053.1 hypothetical protein CaO19.3714 [<i>Candida albicans</i> SC5314]	785.1	9.30E-229
emb CAX40295.1 conserved hypothetical protein [<i>Candida dubliniensis</i> CD36...]	294.4	4.80E-164
gb EER32719.1 predicted protein [<i>Candida tropicalis</i> MYA-3404]	182.8	9.60E-91
gb EMG50075.1 hypothetical protein G210_4910, partial [<i>Candida maltosa</i> ...]	148	1.80E-79
emb CCG23050.1 hypothetical protein CORT_0D02020 [<i>Candida orthopsilosis</i>]	123.7	1.70E-63
gb EDK45146.1 hypothetical protein LELG_03325 [<i>Lodderomyces elongisporu...</i>]	110	2.80E-49
gb ABN67876.2 DNA-binding proteins Bright/BRCAA1/RBP1 and related proteins containing BRIGHT domain [<i>Scheffersomyces stipitis</i>]	107.8	4.60E-43
emb CAG84736.2 DEHA2A10164p [<i>Debaryomyces hansenii</i> CBS767]	101.5	1.60E-29
gb EEQ40644.1 hypothetical protein CLUG_04772 [<i>Clavispora lusitaniae</i> AT...]	79.3	8.60E-24
gb EDK37891.2 hypothetical protein PGUG_01989 [<i>Meyerozyma guilliermondi</i> ...]	55.7	7.60E-22
ref XP_004202544.1 Piso0_001385 [<i>Millerozyma farinosa</i> CBS 7064]	69.1	1.40E-19
gb EGW34027.1 hypothetical protein SPAPADRAFT_59439, partial [<i>Spathaspo...</i>]	41.3	9.00E-14
ref XP_006686021.1 hypothetical protein CANTEDRAFT_134293 [<i>Candida tenuis</i> AT...]	56.5	6.20E-11
gb EDO15314.1 hypothetical protein Kpol_448p1 [<i>Vanderwaltozyma polyspor...</i>]	46.9	4.30E-05
emb CCH46051.1 hypothetical protein BN7_5639 [<i>Wickerhamomyces ciferrii</i>]	38.5	0.0051
emb CCF55770.1 hypothetical protein KA FR_0A03350 [<i>Kazachstania africana</i> ...]	37.1	0.012
gb EHN01393.1 YKR041W-like protein [<i>Saccharomyces cerevisiae</i> x <i>Saccharo...</i>]	34.6	0.031
emb CAR27662.1 ZYRO0D03718p [<i>Zygosaccharomyces rouxii</i>]	33.6	0.042
emb CCE61780.1 hypothetical protein TPHA_0B01080 [<i>Tetrapisispora phaffii</i> ...]	37.8	0.078
gb EJT44913.1 YKR041W-like protein [<i>Saccharomyces kudriavzevii</i> IFO 1802...]	35.7	0.096
emb CCD23556.1 hypothetical protein NDAI_0B05230 [<i>Naumovozyma dairenensi</i> ...]	36.4	0.1
gb EDO04898.1 predicted protein [<i>Sclerotinia sclerotiorum</i> 1980 UF-70]	39.6	0.19
gb ESW98551.1 hypothetical protein HPODL_04175 [<i>Ogataea parapolyomorpha</i> ...]	30.1	0.3

emb CCA41099.1 hypothetical protein PP7435_Chr4-0949 [<i>Komagataella pasto...</i>]	32.5	0.34
gb EQB61141.1 hypothetical protein NAPIS_ORF01278 [<i>Nosema apis</i> BRL 01]	31.8	0.43
gb ESZ96896.1 hypothetical protein SBOR_2690 [<i>Sclerotinia borealis</i> F-41...]	37.4	0.74
gb EMD63823.1 hypothetical protein COCSADRAFT_37572 [<i>Bipolaris</i> <i>sorokini...</i>]	38.1	0.76
gb EGA78039.1 YKR041W-like protein [<i>Saccharomyces cerevisiae</i> Vin13]	33.6	0.77
emb CCE93985.1 hypothetical protein TDEL_0H01260 [<i>Torulasporea</i> <i>delbruecki...</i>]	31.1	0.8
emb CCE65312.1 hypothetical protein TPHA_0K01790 [<i>Tetrapisispora</i> <i>phaffii...</i>]	38.9	0.89
gb EIW62567.1 hypothetical protein TRAVEDRAFT_99513, partial [<i>Trametes ...</i>]	29.3	0.96
emb CDH15510.1 uncharacterized protein ZBAI_07297 [<i>Zygosaccharomyces bai...</i>]	31.5	0.98
gb EME44852.1 hypothetical protein DOTSEDRAFT_70792 [<i>Dothistroma septos...</i>]	35.3	0.98
gb ETS82393.1 hypothetical protein PFICI_04269 [<i>Pestalotiopsis fici</i> W10...]	28.6	0.99

¹Orf19.3714p sequence from CGD (<http://www.candidagenome.org/>) was subjected to Fungal Blast search against all the available protein sequences of fungi in SGD (<http://www.yeastgenome.org/>) using default parameters.

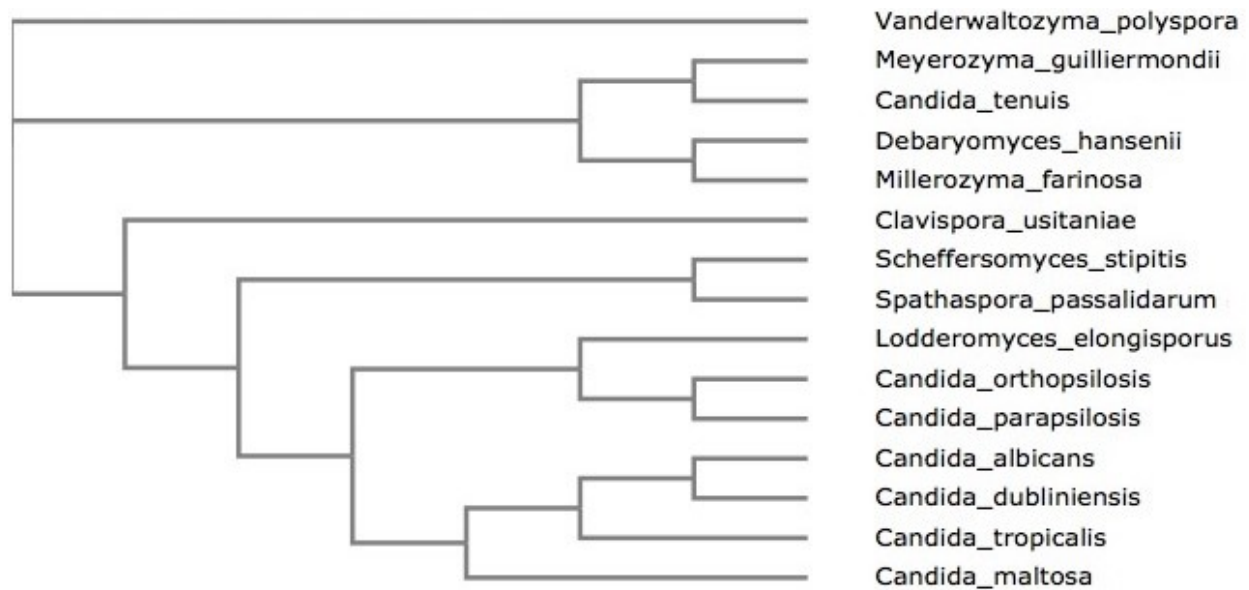


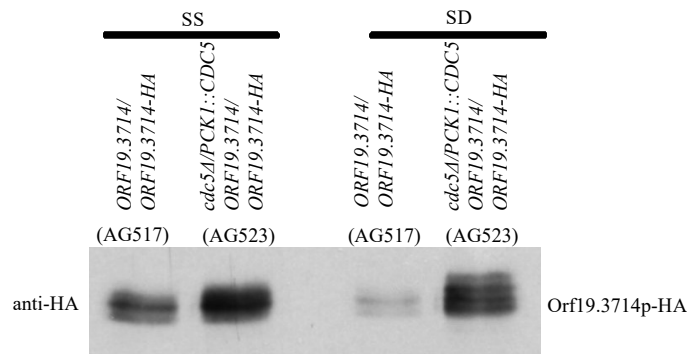
Figure 4.6: Neighbour-joining tree for Orf19.3714p using Clustal Omega. The Orf19.3714p sequence from the *Candida* Genome Database was entered into NCBI Blastp and compared against fungi. The sequences of all the 15 hits obtained were retrieved from NCBI GenBank and aligned in a Clustal multiple sequence alignment. Clustal Omega was used to obtain the phylogenetic tree.

4.3.3 Orf19.3714p is hyperphosphorylated in mitotic-arrested cells, and enriched in response to Cdc5p depletion, but reduced upon depletion of Cdc20p

If Orf19.3714p is a target of Cdc5p, we predict that it may be post-translationally modified in the presence vs. absence of Cdc5p. To test this possibility, *ORF19.3714* was tagged at the C-terminus with three copies of HA in the *CDC5* conditional strain CB105 (*cacdc5::hisG/cacdc5::HIS1 PCK1::CaCDC5-hisG*) (9), resulting in strain AG523 (*cacdc5::hisG/cacdc5::HIS1 PCK1::CaCDC5-hisG, ORF19.3714/ ORF19.3714-HA-URA3*) (Fig. 4.3). Overnight cultures of strains AG523 and AG517 (*ORF19.3714/ ORF19.3714-HA-URA3*) were diluted into fresh inducing (SS) or repressing (SD) (92) medium and incubated at 30°C for 4 h (SD) (92) or until the O.D._{600nm} reached 0.8. (SS). Western blots of affinity-purified samples demonstrated that Orf19.3714p migrated in a similar manner in SS and SD medium in strain AG517 (Fig. 4.7A). However, strain AG523 demonstrated that Orf19.3714p migrated as multiple bands of higher molecular weight in SD repressing medium that lacked Cdc5p vs. in SS inducing medium (Fig. 4.7A). In order to determine whether the band shift was due to

phosphorylation, the experiment was repeated in the presence or absence of CIP. CIP treatment reduced the appearance of multiple bands for Orf19.3714p-HA in SD medium (Fig. 4.7B). Some CIP-dependent size reduction was also observed in strain AG517 (Fig. 4.7B), suggesting a basal level of phosphorylation, but this was minor compared to that observed in *Cdc5p*-depleted cells. Thus, Orf19.3714p undergoes hyperphosphorylation under *Cdc5p*-depleted conditions.

A



B

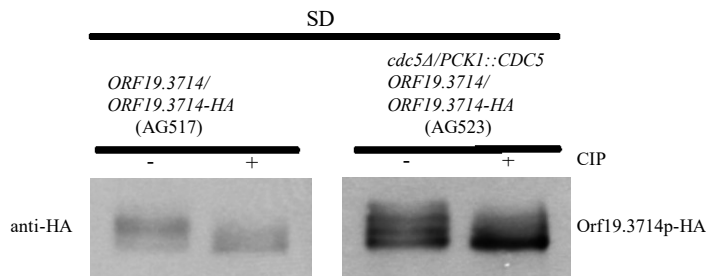


Figure 4.7: Orf19.3714p undergoes a phosphorylation-dependent shift in *Cdc5p*-depleted cells. (A) Overnight cultures of strains AG517 (*ORF19.3714/ORF19.3714-HA-URA3*) and AG523 (*cacdc5Δ::hisG, ORF19.3714/ORF19.3714-HA-URA3*) were diluted into either inducing SS or repressing SD medium, and collected after 4 h in SD or in exponential phase in SS. Whole cell extracts were incubated with anti-HA beads at 4°C overnight. (B) Anti-HA beads from (A) were treated with (+) or without (-) calf intestinal phosphatase (CIP).

In order to determine whether phosphorylation was specific to Cdc5p depletion vs. being a general response to a mitotic block, Orf19.3714p mobility was investigated in cells depleted of the Anaphase Promoting Complex/Cyclosome (APC/C) co-factor Cdc20p (75). For this, *ORF19.3714* was TAP-tagged at the C-terminus in a *CDC20* conditional strain (75), resulting in strain AG704 (*cdc20Δ::URA3/MET3::CDC20-HIS1, ORF19.3714/ ORF19.3714-TAP-ARG4*) (Fig. 4.8A, B). For comparison, *ORF19.3714* was also TAP-tagged in a *CDC5* conditional and an *ORF19.3714* heterozygous strain, resulting in strains AG717 (*cdc5Δ::hisG/MET3::CDC5-ARG4, ORF19.3714/ ORF19.3714-TAP-URA3*) and AG707 (*orf19.3714Δ::URA3/ORF19.3714-TAP-ARG4*) respectively, (Fig. 4.8A, B). The growth rate of strain AG707 containing a single allele of *ORF19.3714* tagged with TAP was similar to a control strain BH415 (*URA3+ ARG4+*), suggesting that the protein was functional (Fig. 4.8C). Intriguingly, Western blotting demonstrated that Orf19.3714p-TAP was detectable in whole cell extracts (Fig. 4.8D), unlike the HA-tagged protein. The ability to detect Orf19.3714p in whole cell extracts could be due to higher sensitivity of the anti-TAP vs. anti-HA antibody, and precluded the need to affinity-purify the protein for visualization. Thus, overnight cultures of strains were diluted into fresh inducing (-MC) or repressing (+MC) medium and incubated at 30°C for 4 h, collected, and processed for Western blotting. In Cdc20p-depleted cells, Orf19.3714p-TAP migrated as several higher molecular weight bands, although the effect was not as strong and the signal was less intense as that observed in Cdc5p-depleted cells (Fig. 4.9A). In contrast, Orf19.3714p-TAP migrated as a single lower molecular weight band in inducing medium and in control cells in either inducing or repressing medium (Fig. 4.9A-C). CIP-treatment of samples confirmed that the band shifts were due to phosphorylation (Fig. 4.9B, C). Further, when samples were separated on a higher concentration gel that allowed for detection of the lower molecular weight loading control protein Cdc28p, normalization of intensity levels confirmed that Orf19.3714p-TAP was reduced in Cdc20p-depleted cells, but enriched in Cdc5p-depleted cells (Fig. 4.9D).

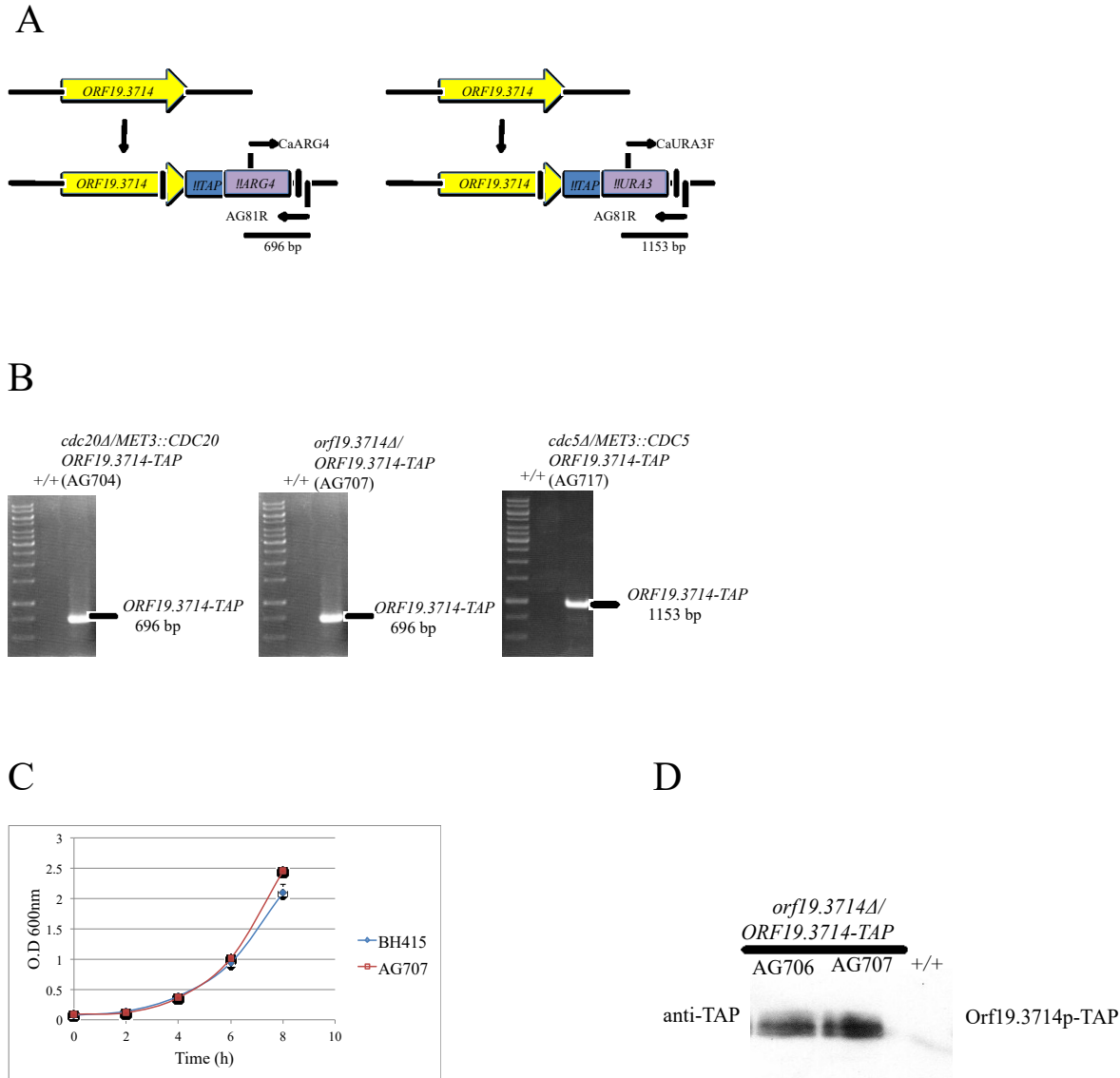


Figure 4.8: Confirmation of Orf19.3714p-TAP strains. (A) Map showing a PCR screening strategy to confirm correct integration of the TAP-containing construct. Vertical black lines designate the area of the transforming DNA construct. Oligonucleotides CaARG4 and AG81R generated a 696 bp *ORF19.3714-TAP-ARG4* band while oligonucleotides CaURA3F and AG81R generated a 1153 bp *ORF19.3714-TAP-URA3* band. (B) Ethidium bromide-stained DNA gels showing positive strains AG704 (*cdc20Δ::URA3/MET3::CDC20-HIS1, ORF19.3714/ORF19.3714-TAP-ARG4*), AG717 (*cdc5Δ::hisG/MET3::CDC5-ARG4, ORF19.3714/ORF19.3714-TAP-URA3*), AG707 (*orf19.3714Δ::URA3/ORF19.3714-TAP-ARG4*) and BWP17 (*ORF19.3714/ORF19.3714*). (C) Growth curves showing the mean O.D._{600nm} ± S.E.M from 3 different trials of strains BH415 (*URA3+ ARG4+*) and AG707 incubated in YPD medium at 30°C over time. (D) Western blot containing 30 μg of whole cell protein extracts from strains AG707, AG706 and BWP17 incubated with anti-TAP antibody.

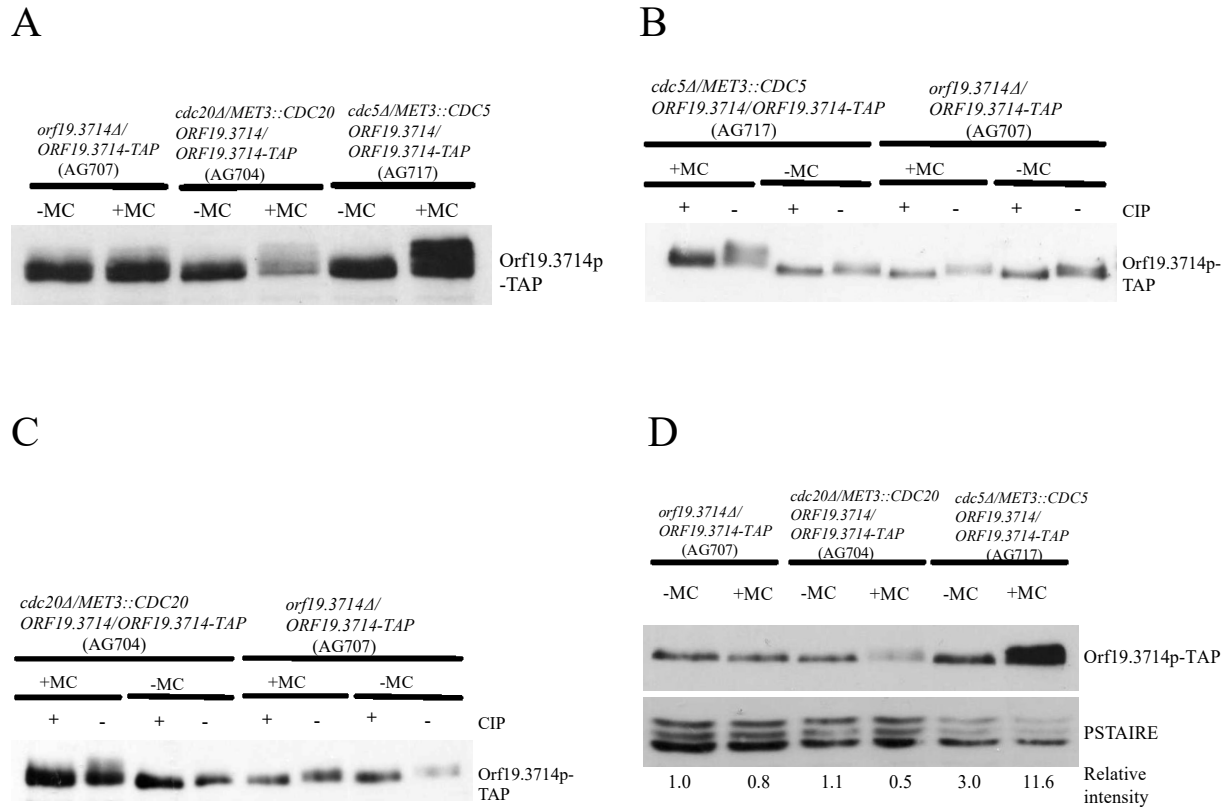


Figure 4.9: Orf19.3714p-TAP is phosphorylated in Cdc20p and Cdc5p-depleted cells, and shows a decrease or increase in abundance, respectively. (A) Overnight cultures of strains AG707 (*orf19.3714Δ::URA3/ORF19.3714-TAP-ARG4*), AG704 (*cdc20Δ::URA3/MET3::CDC20-HIS1, ORF19.3714/ ORF19.3714-TAP-ARG4*), and AG717 (*cdc5Δ::hisG/MET3::CDC5-ARG4, ORF19.3714/ ORF19.3714-TAP-URA3*) were washed and diluted into repressing (+MC) or inducing (-MC) medium and collected after 4 h at 30°C. Protein was extracted and samples were processed for Western blot. (B, C) Protein samples from (A) were treated with (+) or without (-) alkaline calf intestinal phosphatase (CIP). (D) Overnight cultures of strains AG707, AG704 and AG717 were diluted into +MC medium and collected after 4h at 30°C. Protein samples were separated on a 10% SDS-PAGE gel and probed with anti-TAP or loading control anti-PSTAIRE antibodies. Quantification was performed with ImageJ (75).

In order to determine whether the levels of *ORF19.3714* were modified at the transcript level under Cdc5p-depleted conditions, Northern blotting was performed. Overnight cultures of *CDC5* conditional (CB108; *cdc5Δ::hisG/MET3::CDC5-URA3*) and control (CB504; *CDC5/CDC5*, pMET3-*URA3*) (9) strains were diluted into repressing (+MC) medium and collected at given time points. Wild type cells of strain SC5314 (+/+) were also incubated in +MC medium at 30°C, or 37°C with the addition of 10% serum, to obtain yeast and hyphal samples, respectively, for comparison. *ORF19.3714* expression was not significantly increased at 4 h of repression, despite the increase in protein abundance observed at this time. Moderate increases were noted at 7 and 9 h of Cdc5p depletion, but not at 11 h. *ORF19.3714* was also moderately reduced in hyphae vs. yeast cells (Fig. 4.10). Thus, expression of *ORF19.3714* at the mRNA level does not correlate with the changes in the level of protein that take place upon a block in mitosis. Collectively the data thus suggest that Orf19.3714p undergoes post-translational modifications under conditions that block mitosis, including hyper-phosphorylation, and changes in abundance, where it is enriched in the absence of Cdc5p, but reduced under Cdc20p-depleted conditions.

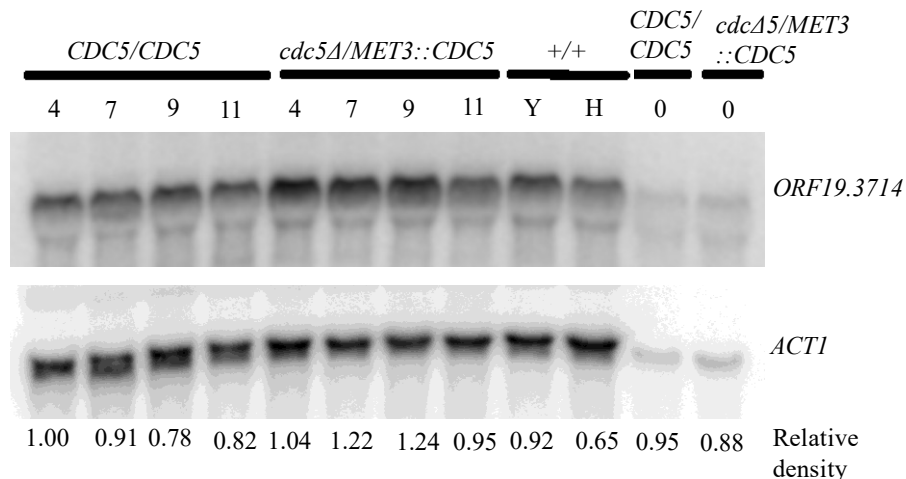


Figure 4.10: *ORF19.3714* does not show significant changes in expression during Cdc5p depletion, but is moderately reduced in serum-induced hyphae. Overnight cultures of strains CB504 (*CDC5/CDC5* + pMET3-*URA3*) and CB108 (*cdc5Δ::hisG/MET3::CDC5-URA3*) were diluted into repressing medium (+MC) and collected at indicated time points. Control strain SC5314 (+/+) was grown in +MC for 2h at 30°C to promote yeast growth (Y) and pre-warmed +MC supplemented with 10% FBS for 2h at 37°C to promote hyphal growth (H). *ACT1* was used as loading control. Quantification was performed with ImageJ (75).

In order to identify the sites on Orf19.3714p that may be phosphorylated in response to a mitotic block, Orf19.3714p was purified from strains AG523 (*cacdc5::hisG/cacdc5::HIS1 PCK1::CaCDC5-hisG, ORF19.3714/ ORF19.3714-HA-URA3*) and AG517 (*ORF19.3714/ ORF19.3714-HA-URA3*) that were incubated in repressing (SD) (92) medium for 4 h at 30°C. Gel pieces containing Orf19.3714p were cut and processed for mass spectrometry and phosphopeptide identification. Orf19.3714p from control cells was not phosphorylated. However, in Cdc5p-depleted cells, eight phosphorylated peptides were identified, five of which were the same sequence (LESTPISQSTPASSR) but phosphorylated on different residues (Table 4.7). Two phosphorylated amino acids were within Plk consensus polo box binding sites, and one was found within a Plk consensus phosphorylation site (Fig. 4.11). Two others were within minimal CDK consensus phosphorylation sites, Ser/Thr-Pro (S/T-P) (117). Of the other three peptides (AQPQPQPQTSSSSSSK; ASSPPPLQQQQQKPR; TITTHESESESEQGESNEINIK) (Table 4.7), one was phosphorylated within a Plk consensus PBD site that overlapped with a minimal CDK consensus phosphorylation site (data not shown). However, the fact that Orf19.3714p was significantly enriched in mitotic-blocked (sixty-one peptides) vs. exponential phase (seventeen peptides) cells, precludes an accurate comparison of detectable phospho-peptides between samples. Thus, we repeated the experiment with the exception of doubling the amount of input protein for the control strain and using TAP-tagged strains (AG707; (*orf19.3714::URA3/ ORF19.3714-TAP-ARG4* and AG717; *cdc5 Δ::hisG/MET3::CDC5-ARG4, ORF19.3714/ ORF19.3714-TAP-URA3*). However, only two phospho-peptides were identified in Cdc5p-depleted cells, and one of the two peptides was also present in the control strain (Table 4.7). Thus, the nature of the hyperphosphorylation of Orf19.3714p upon a mitotic block remains unclear, although it is notable that Orf19.3714p contains a total of sixteen consensus CDK phosphorylation sites (data not shown).

Table 4.7: Orbitrap LC/MS identification of phosphorylation sites in Orf19.3714p in the presence vs. absence of Cdc5p¹

Genotype (strain)	Protein ID	Gene name ²	Number of peptides ³	Phosphorylated peptide sequence ⁴
<i>ORF19.3714/</i> <i>ORF19.3714-HA</i> (AG517)	CAL0001101	<i>ORF19.3714</i>	17	None
<i>cdc5Δ/PCK1::CDC5</i> <i>ORF19.3714/</i> <i>ORF19.3714-HA</i> (AG523)	CAL0001101	<i>ORF19.3714</i>	61	LESTPISQSTPASSR +Phospho (ST)-S9; LESTPISQSTPASSR +Phospho (ST)-T10; LESTPISQSTPASSR +Phospho (ST)-S14; LESTPISQSTPASSR +Phospho (ST)-S13; LESTPISQSTPASSR +Phospho (ST)-S3; AQPQPQPQQTSSSSSSK +Phospho (ST)-S11; ASSPPPLQQQQQKPR + Phospho (ST)-S3; TITTHESESESEQGESNE INIK+ Phospho (ST)-T4 ASSPPPLQQQQQKPR +Phospho (ST)-S2; ASSPPPLQQQQQKPR + Phospho (ST)-S3; ASSPPPLQQQQQKPR + Phospho (ST)-S3;
<i>orf19.3714Δ/</i> <i>ORF19.3714-TAP</i> (AG707)	CAL0001101	<i>ORF19.3714</i>	15	ASSPPPLQQQQQKPR +Phospho (ST)-S2; ASSPPPLQQQQQKPR + Phospho (ST)-S3; ASSPPPLQQQQQKPR + Phospho (ST)-S3;
<i>cdc5Δ/MET3::CDC5</i> <i>ORF19.3714/</i> <i>ORF19.3714-TAP</i> (AG717)	CAL0001101	<i>ORF19.3714</i>	10	ASSPPPLQQQQQKPR + Phospho (ST)-S3;

¹Strains AG517 (*ORF19.3714/ORF19.3714-HA-URA3*) and AG523 (*cdc5Δ::hisG/PCK1::CDC5-HIS1, ORF19.3714/ORF19.3714-HA-URA3*) grown in SD medium for 4h while AG707 (*orf19.3714 Δ::URA3/ORF19.3714-TAP-ARG4*) and AG717 (*cdc5Δ::hisG/MET3::CDC5-ARG4, ORF19.3714/ORF19.3714-TAP-URA3*) grown in +MC medium for 4h were subjected to tandem affinity purification (99, 100). Approximately 90 mg protein extracts from AG517 and AG523 while 115 mg X 2 of protein extracts from AG707 and 115 mg of protein extract from AG717 were incubated with 40 μl of anti-HA and 50 μl anti-TAP beads respectively. Proteins were eluted from beads by boiling in sample buffer and run on SDS PAGE gel and stained with Coomassie blue, gel bands were cut from approximately 65-110 and 90-125 kDa for strains AG517, AG523 and AG707, AG717 respectively.

²Gene names were obtained from the Candida Genome Database (<http://www.candidagenome.org/>).

³Peptides corresponding to other genes/ORFs except Orf19.3714p were excluded from the table.

⁴Phosphorylated peptides were analysed using an LTQ-OrbitrapElite with nano-ESI.

MALSEESIPKLYPSSSTPLSNGNDRNPTVIQATSTPPPPPPPPALPDISTSTPIETPWYYK
 RSTGSESEEEEEEDTNGNDYDDYYQDDGETIQKTPSPNKSJKGYRFNNQLDFASTPLNPS
 CTLFSFSPMNKLNQLHLESQLDMDGFEEHLEIEQGEEEEEDDDDDDEYSLGNK**TITTHES**
ESESEQGESNEINIKHFEPKYISSRRKRLHSESPDMMVLTPNVNYKNNVNDKNDVNDITY
 GNDMSICNTTSTTTNTTATNTSAFKFSFSNISDSTPCPRQPQRKRLKFKHESTRNILDNLN
 YAKKSILSQSSFPPLYNDGGEGELPNEKYCYDNDDENNSGISSGSTDNKSINSK**LESTPI**
SQSTPASSRASSPPPLQQQQQKPRAPQPOPOQTSSSSSSKSGQEYGETINGYKFKVFKPK
 NSMNNTKLPQFKYETPINNNRYHQLCQGYNSNNYQIMNELPVTAAGLMPHGDEDDDDIHI
 GDRRIGDPYLNLSRDDDNDHCDQETHDDGNQLREIYFKENRLPLPTPYFYQLKSLSVDQIL
 ALINYENLLKFYETILNGDETLYELLKQERIRWHPDKWIGKLNQKNEMIMDVDYELTIKM
 VDSISQTINSIIESL*

Yellow: Peptides identified by mass spectrometry
Green: Phosphorylated residues

Figure 4.11: Identification of phosphorylated amino acids in Orf19.3714p in the absence of Cdc5p. Peptides (in yellow) and amino acids residues (in green) identified in Orf19.3714p purified from strain AG523 (*cacdc5Δ::hisG, ORF19.3714/ ORF19.3714-HA-URA3*) grown in repressing SD medium at 30°C for 4 h. About 87 mg of protein extract was incubated with 40 μl of anti-HA beads overnight at 4°C. Samples were eluted by boiling, separated on an SDS-PAGE gel and stained with Coomassie. Gel bands corresponding to approximately 100 kDa were cut for mass spectrometry.

4.3.4 ORF19.3714 is not essential for yeast vegetative growth or required for yeast cellular responses to a variety of stress conditions

In order to explore the function of Orf19.3714p, we utilized a genetic approach and deleted both copies of the gene from strain BWP17, resulting in strains AG692 and AG694 (*orf19.3714::URA3/orf19.3714::HIS1*) (Fig. 4.12A,B). Since the cells were viable, a control strain was constructed by re-introducing a copy of *ORF19.3714* into strain AG692, resulting in strains AG721 and AG722 (*orf19.3714::URA3/orf19.3714::HIS1 pBS-ORF19.3714-ARG4*) (Fig. 4.12C). A deletion strain isogenic for markers was also constructed by transforming strain AG692 with circular pBS-CaARG4, resulting in strains AG727 and AG728 (*orf19.3714::URA3/orf19.3714::HIS1 + pBS-ARG4*). In the absence of Orf19.3714p, yeast cell proliferation and phenotype were similar to those of control strains (Fig. 4.13). On solid medium, colony growth and morphology also did not show any significant differences (Fig. 4.14). We next asked if the absence of Orf19.3714p influenced yeast cellular responses to a diversity of stress and environmental conditions. Serial dilutions of strains were spotted on solid YEPD medium and incubated at 30, 37 or 42°C to test for temperature sensitivity, YEPD containing 20 μM Calcoflour, 0.04% SDS, or 1.0 M sorbitol to test for responses to cell wall stress and changes in

osmolarity, 30 mM hydroxyurea (HU) or 0.03% methanomethylsulphate (MMS) to investigate sensitivity to DNA replication and damage stress, respectively, 15 mM caffeine or 10 nM rapamycin to determine sensitivity to defective TOR pathway function, 6 mM hydrogen peroxide to determine sensitivity to oxidative stress (95), or 125 µg/ml benomyl to test for sensitivity to microtubule destabilization. However, absence of Orf19.3714p did not have an effect on growth or morphology under any conditions tested (Fig. 4.14).

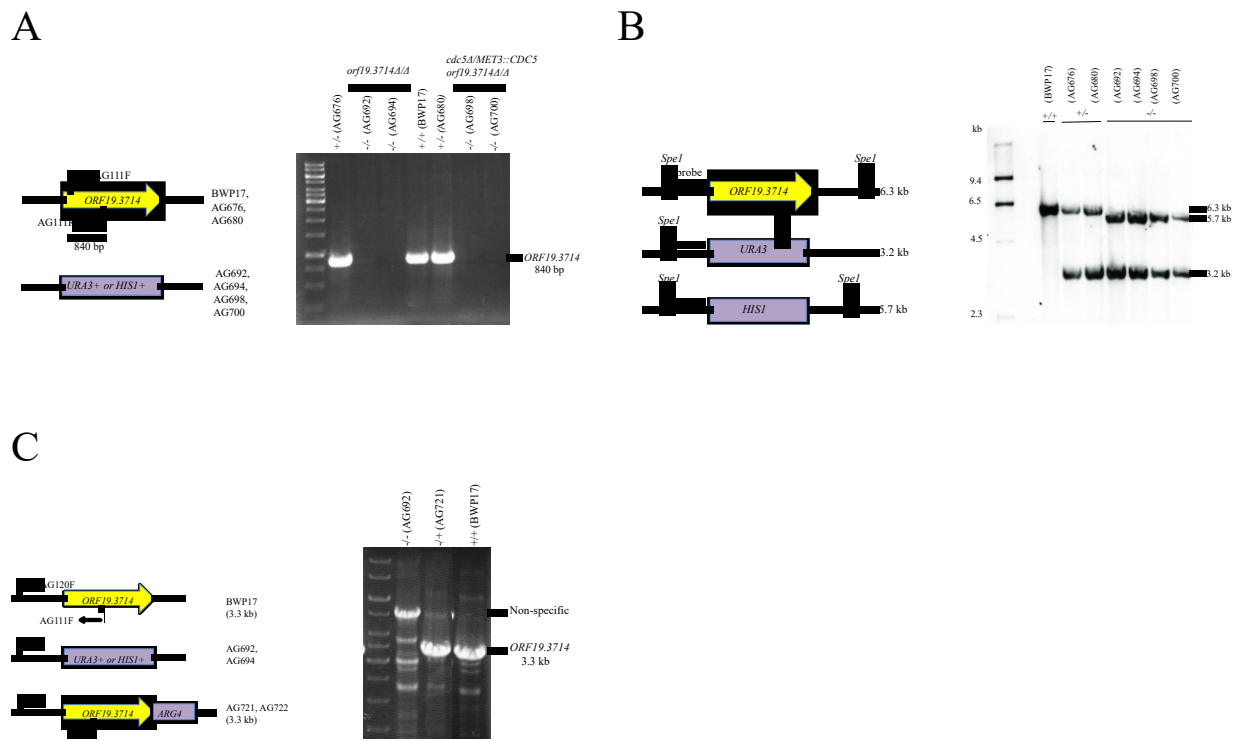
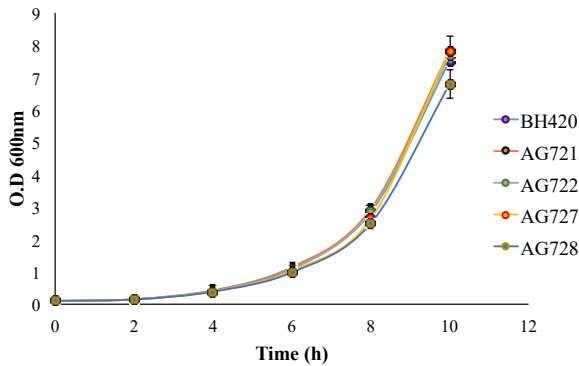
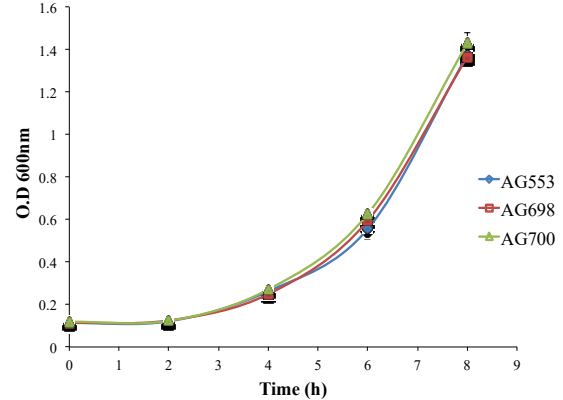


Figure 4.12: Confirmation of an *orf19.3714Δ/Δ* and *ORF19.3714* complement strains. (A) Map and ethidium- bromide-stained DNA gel showing an 840 bp band for wild type *ORF19.3714* in strain BWP17 (+/+), AG676 (*ORF19.3714/orf19.3714Δ::URA3*) and AG680 (*cdc5Δ::hisG/MET3::CDC5-ARG4, ORF19.3714/orf19.3714Δ::URA3*) and absence of bands in strains AG692, AG694 (*orf19.3714Δ::URA3/ orf19.3714Δ::HIS1*) and AG698, AG700 (*cdc5Δ::hisG/MET3::CDC5-ARG4, orf19.3714ΔΔ::URA3/ orf19.3714Δ::HIS1*) using oligonucleotides AG111F and AG111R. (B) Map and Southern blot confirming construction of strains. Digestion of gDNA with *SpeI* produced a wild type band of 6.3 kb, an *orf19.3714Δ::URA3* deletion band at 3.2 kb, and an *orf19.3714Δ::HIS1* deletion band 5.7 kb. (C) PCR map and ethidium- bromide-stained DNA gel showing a 3.3 kb band for wild type *ORF19.3714* in strains BWP17, AG721 (*orf19.3714::URA3/orf19.3714::HIS1* pBS-*ORF19.3714-ARG4*), and absence of a band for strain AG692 using oligonucleotides AG120F and AG111R.

A



B



C

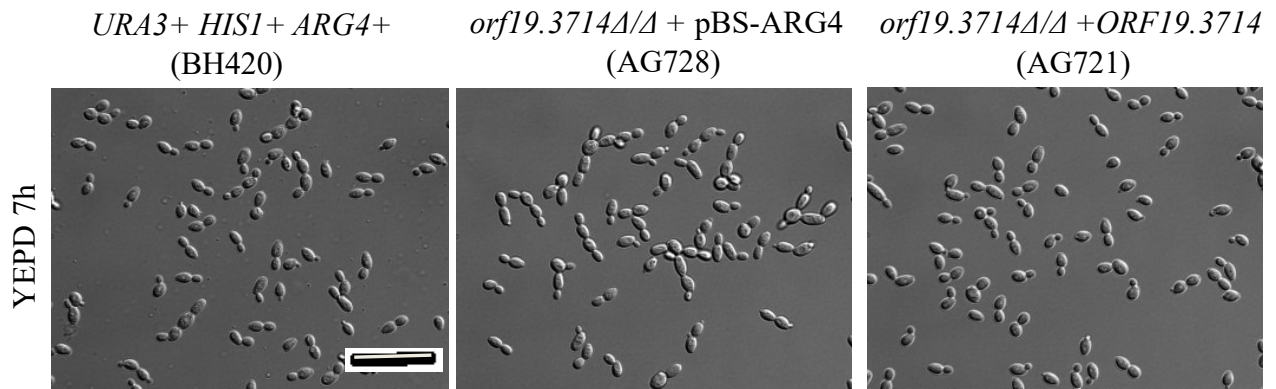


Figure 4.13: Absence of Orf19.3714p does not influence yeast growth or morphology. (A) Overnight cultures of strains BH420 (*ORF19.3714/ORF19.3714*, *URA3+ HIS1+ ARG4+*), AG721, 722 (*orf19.3714Δ::URA3/orf19.3714Δ::HIS1 + pBS-ORF19.3714-ARG4*), and AG727, 728 (*orf19.3714Δ::URA3/orf19.3714Δ::HIS1 + pBS-ARG4*) were diluted into fresh YEPD medium at 30°C and OD_{600nm} was recorded at indicated times. (B) Overnight cultures of strains AG553 (*cdc5Δ::hisG/MET3::CDC5-ARG4*, *URA3+ HIS1+*) and AG698, 700 (*cdc5Δ::hisG/MET3::CDC5-ARG4*, *orf19.3714Δ::URA3/orf19.3714Δ::HIS1*) were diluted into –MC inducing medium at 30°C and OD_{600nm} was recorded at indicated times. (C) Strains in (A) at 7 h were fixed in 70% EtOH prior to imaging. Bar: 10 μm.

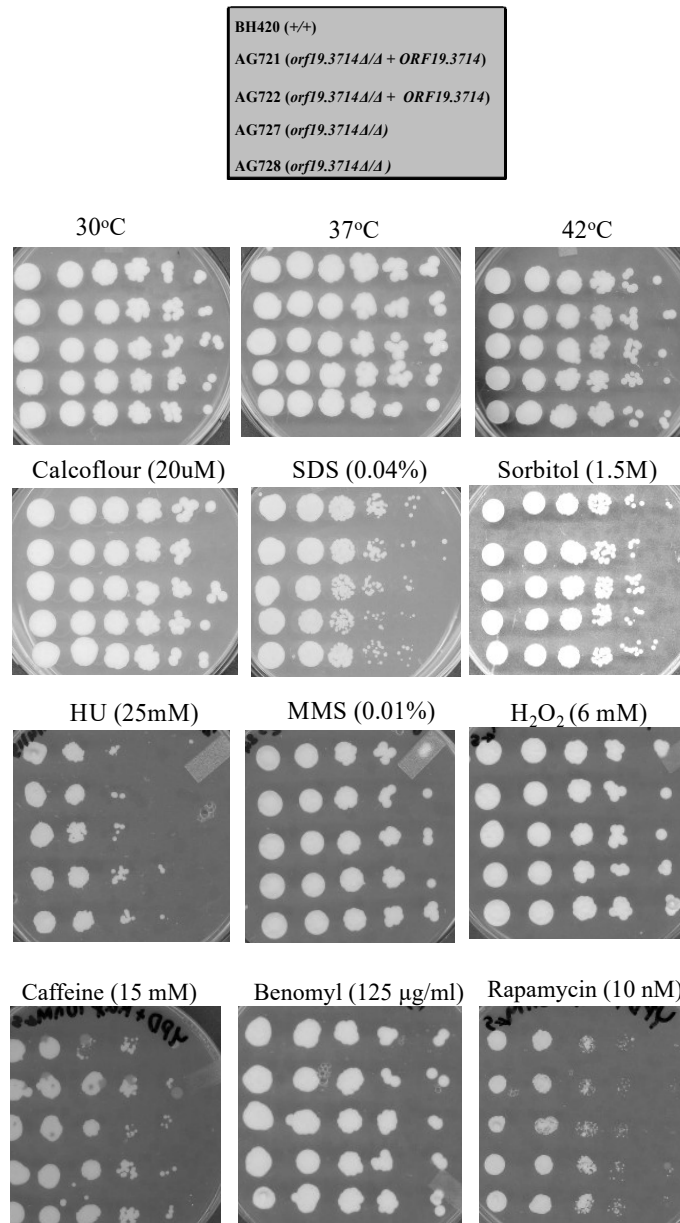


Figure 4.14: Orf19. 3714p is not required for yeast growth responses to a variety of environmental and chemical conditions. Overnight cultures of strains BH420 (*ORF19.3714/ORF19.3714*, *URA3* + *HIS1* + *ARG4* +), AG721, AG722 (*orf19.3714Δ::URA3/orf19.3714Δ::HIS1* + pBS-*ORF19.3714-ARG4*), and AG727 and AG728 (*orf19.3714Δ::URA3/orf19.3714Δ::HIS1* + pBS-*ARG4*) in YEPD medium were diluted to an O.D_{600nm} of 0.08 and serial dilutions were plated on solid YEPD medium and incubated at 30, 37, or 42°C for 48 h, on YEPD medium supplemented with 20 μM Calcoflour, 0.04% SDS or 1.5 M sorbitol and incubated at 30°C for 48 h, 25 mM HU, 0.01% MMS, 6 mM hydrogen peroxide (H₂O₂), 15 mM caffeine, 125 μg/ml benomyl or 10 nM rapamycin and incubated at 30°C for 48 h. Top panel shows the order of strains plated.

4.3.5 Orf19.3714p is not required for hyphal development, but influences filamentous growth in response to Cdc5p depletion

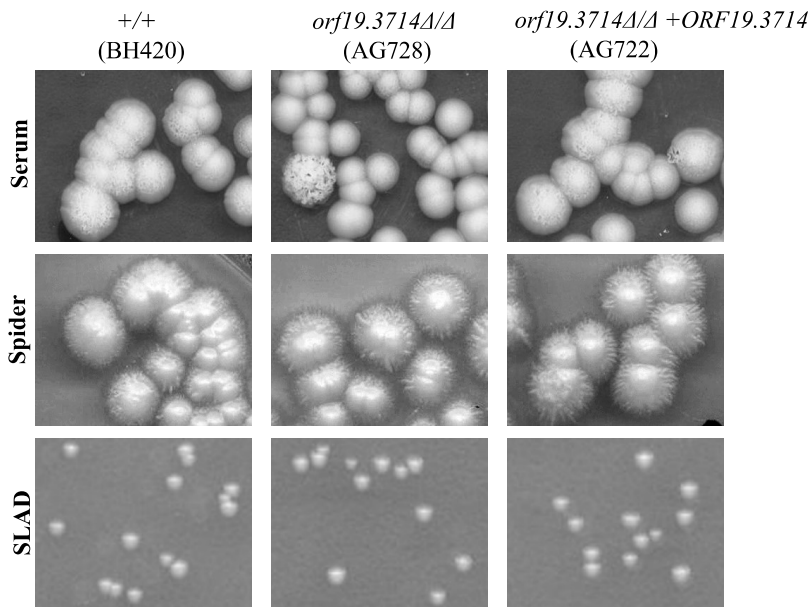
In order to determine whether Orf19.3714p was required for polarized growth, strains were tested for their ability to form hyphae in response to a diversity of hyphal-inducing conditions. Overnight cultures of strains BH420 (*URA3+ HIS1+ ARG4+*), AG722 (*orf19.3714::URA3/orf19.3714::HIS1* pBS-*ORF19.3714-ARG4*) and AG728 (*orf19.3714::URA3/orf19.3714::HIS1* + pBS-*ARG4*) grown in YEPD medium at 30°C were diluted and spotted onto nitrogen-limiting solid SLAD, Spider, or YEPD medium supplemented with 10% serum, and incubated at 37°C for three to five days (118) (96) (95). Orf19.3714p was not required for hyphae produced under any of these conditions (Fig. 4.15A). In order to determine whether absence of Orf19.3714p influenced hyphal growth under liquid-inducing conditions, strains were diluted into liquid YEPD containing 10% serum and incubated at 37°C. However, hyphae were able to form and were indistinguishable from those that formed in control cells (Fig. 4.15B). Hyphae were also able to form when incubated in liquid Spider medium at 37°C (data not shown).

Since Orf19.3714p may be a substrate for Cdc5p, we next asked if its absence would affect polarized growth that occurs in cells depleted of Cdc5p (9). For this, strains AG553 (*cdc5Δ::hisG/MET3::CDC5-ARG4 +URA3+ HIS1+*) and AG700 (*cdc5Δ::hisG/MET3::CDC5-ARG4, orf19.3714Δ::URA3/orf19.3714Δ::HIS1*) (Fig. 4.12) were diluted into repressing medium (+MC) and fixed at set times. In the absence of Orf19.3714p, polarized growth could still take place, but the filaments were often short and irregular in shape and/or showing multiple buds (Fig. 4.16A and 4.16C). This effect was not due to any growth defects as the cells lacking Orf19.3714p showed normal yeast growth rates under Cdc5p-inducing conditions (Fig. 4.13B). Intriguingly, after 4 h of Cdc5p depletion, 17.8% (n=157) of cells lacking Orf19.3714p showed re-budding from the mother yeast cell that previously formed an elongated bud, compared to 3.1% (n=191) of cells with Orf19.3714p. After 7 h of Cdc5p depletion, 81.3% (n=139) of cells lacking Orf19.3714p were rebudding from the mother yeast cell, compared to 11.5% (n=130) of cells containing Orf19.3714p. Rebudding from the mother yeast cell can reflect escape from a mitotic block (83, 119, 120), although cells stained with DAPI did not reveal obvious differences in the number of nuclei per cell (Fig. 4.16B). Similar results were obtained when the spindle

checkpoint factor Bub2p was depleted from Cdc5p (83), suggesting that Orf19.3714p might influence a mitotic checkpoint function.

In order to determine whether this effect was specific to Cdc5p depletion and/or mitotic arrest, strains were diluted into YEPD supplemented with 200 mM HU and incubated at 30°C for 7 h, conditions which block the cell cycle in S phase and also induce filament formation in *C. albicans* (83). Filaments appeared similar in all strains (Fig. 4.16D), indicating that Orf19.3714p is not required for polarized growth in response to an S phase arrest. Intriguingly, absence of Bub2p also did not influence HU-induced polarized growth (83). Thus, Orf19.3714p is important for maintaining polarized growth in response to Cdc5p depletion, and this may be related to a role in influencing the mitotic checkpoint.

A



B

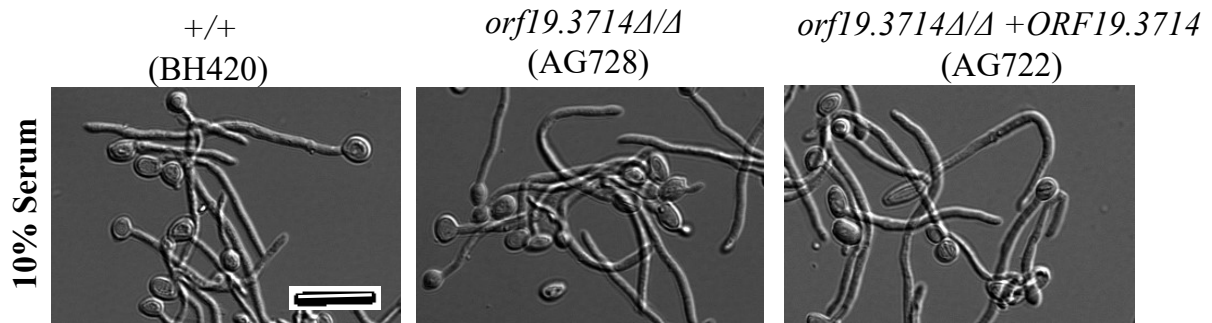
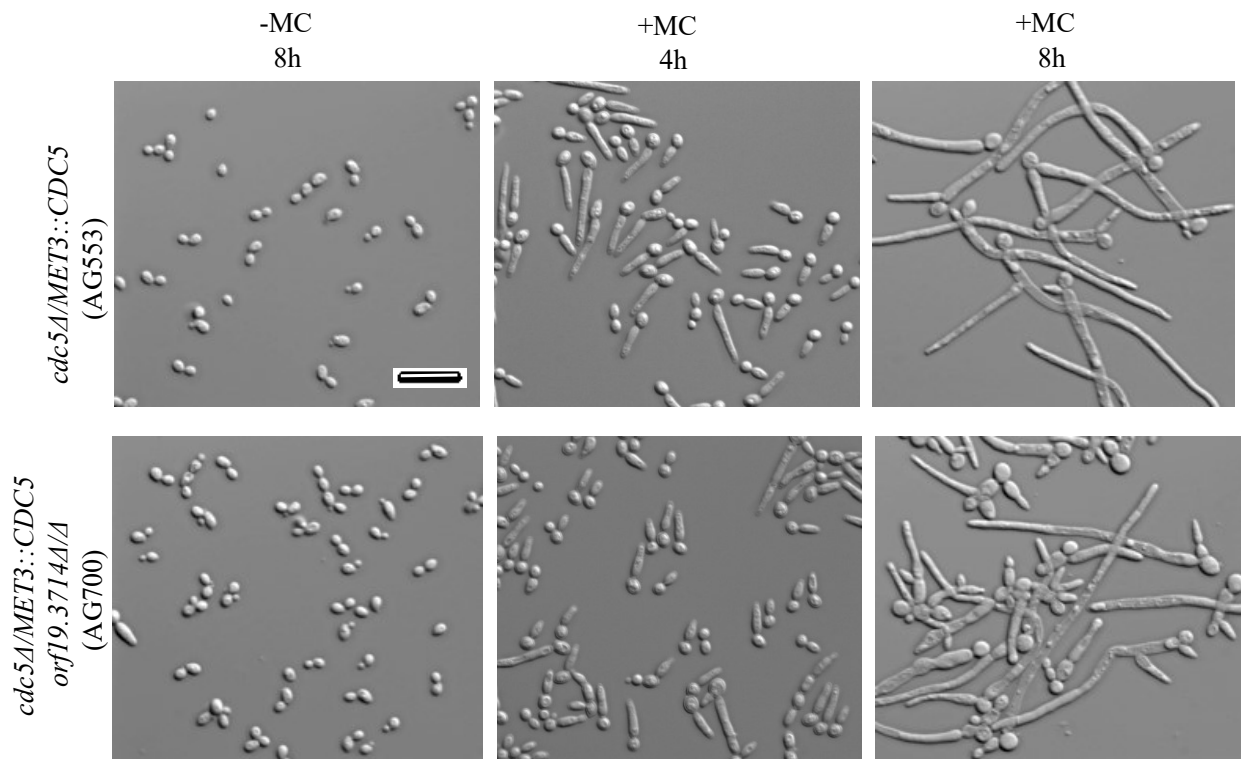
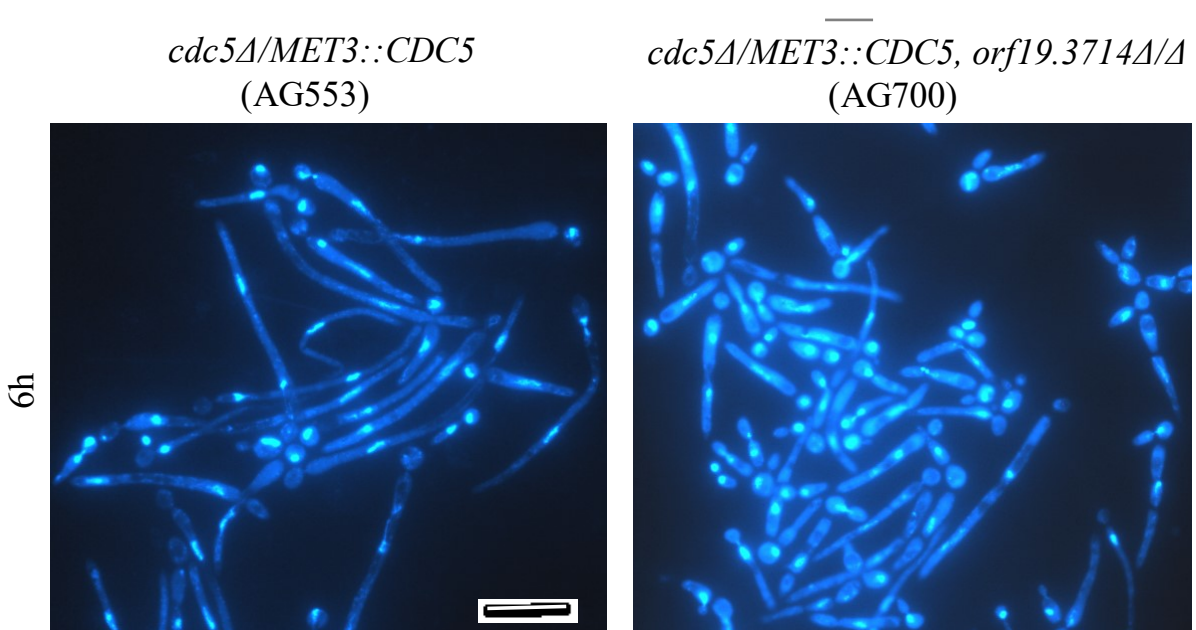


Figure 4.15: Orf19.3714p is not required for hyphal development under a variety of hyphae-inducing conditions. (A) Overnight cultures of strains BH420 (*URA3*+ *HIS1*+ *ARG4*+), AG721, 722 (*orf19.3714Δ::URA3/orf19.3714Δ::HIS1* + pBS-*ORF19.3714-ARG4*), and AG727, 728 (*orf19.3714Δ::URA3/orf19.3714Δ::HIS1* + pBS-*ARG4*) in YEPD medium were diluted to an O.D_{600nm} of 0.005 in sterile water, 1.5 μ l was combined with 3.5 μ l of water, and the 5 μ l volume was plated on 10% serum, Spider, or SLAD plates and incubated at 37°C for 5 days. (B) Overnight cultures of strains from (A) were diluted to an O.D_{600nm} of 0.2 in either pre-warmed YEPD supplemented with 10% fetal bovine serum and incubated at 37°C for 2 h. Cells were fixed in 70% ethanol and processed for microscopy. Bars: 10 μ m.

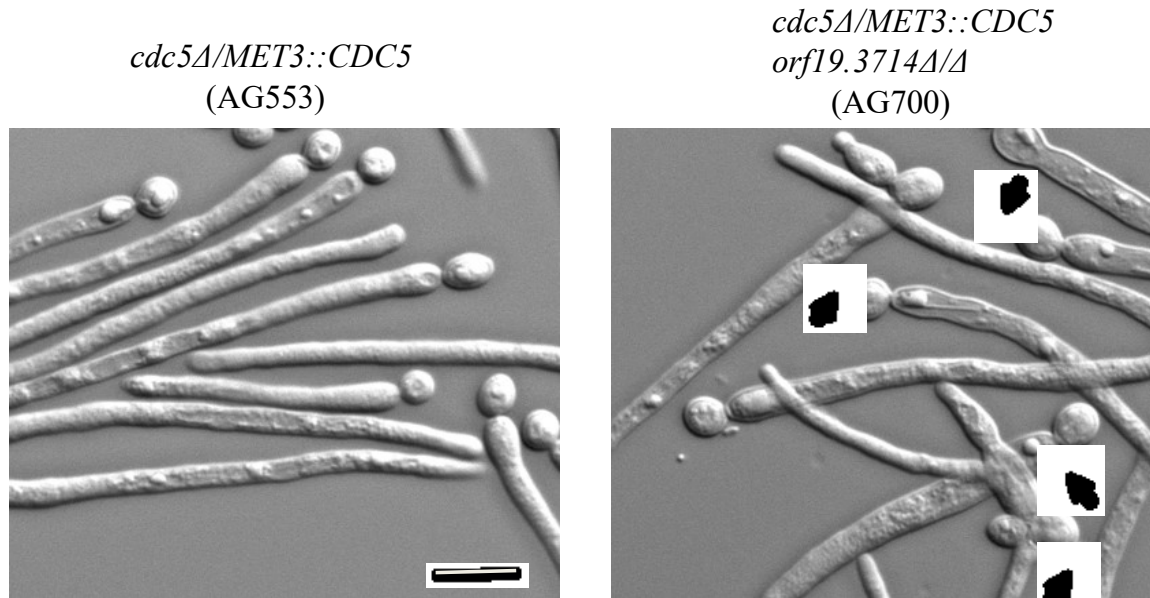
A



B



C



D

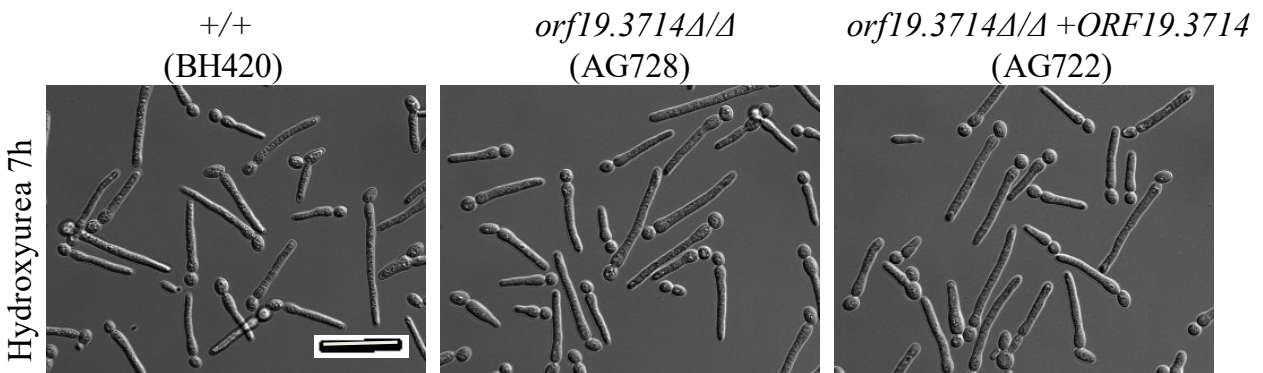


Figure 4.16: Orf19.3714p is required for maintaining filamentous growth in mitotic-arrested cells depleted of Cdc5p, but not S-phase arrested cells treated with hydroxyurea. (A, B, C) Overnight cultures of strains AG553 (*cdc5Δ::hisG/MET3::CDC5-ARG4, URA3+ HIS1+*) and AG700 (*cdc5Δ::hisG/MET3::CDC5-ARG4, orf19.3714Δ::URA3/orf19.3714Δ::HIS1*) were diluted into either +MC or -MC medium and incubated for 4 h or 8 h at 30°C. Cells were collected at indicated time points, fixed in 70% ethanol and (B) stained with DAPI. (C) Strains AG553 and AG700 from (A) at 6 h in +MC. Arrows indicate daughter cells budding from the mother cell. (D) Strains BH420 (*ORF19.3714/ORF19.3714, URA3+ HIS1+ ARG4+*), AG722 (*orf19.3714Δ::URA3/orf19.3714Δ::HIS1 + pBS-ORF19.3714-ARG4*), and AG728 (*orf19.3714Δ::URA3/orf19.3714Δ::HIS1 + pBS-ARG4*) were incubated in YEPD medium supplemented with 200 mM hydroxyurea (HU) for 7 h at 30°C. Cells were fixed in 70% ethanol and processed for microscopy. Bars: 10 μm

4.3.6 Identification of Orf19.3714p-interacting factors through affinity purification and mass spectrometry reveals spliceosome complex proteins

In order to gain more information on the function of Orf19.3714p, we identified its interacting proteins using two-step affinity purification followed by mass spectrometry with strains AG707 (*orf19.3714::URA3/ORF19.3714-TAP-ARG4*) and control strain BH415 (*URA3+ARG4+*). The most abundant co-purifying peptides corresponded to Cdc5p, providing additional support for an interaction between the two proteins (Table 4.8). Gene Ontology (GO) Term analysis (<http://www.candidagenome.org/>) of the 44 co-purifying peptides (Table 4.9) demonstrated that they were significantly enriched in functions associated with RNA splicing and ribonucleoprotein complex assembly and subunit organization. Specific factors included Orf19.3098p, a homologue of the RNA-dependent ATPase RNA helicase Brr2p that is required for spliceosome activation via disrupting U4/U6 base-pairing in native snRNPs (121, 122), Orf19.6740p, a homologue of Prp19p that is also involved in activation of the spliceosome (123, 124), and other splicing-associated and RNA helicase factors such as Prp8p, and Ded1p, for example. Additional peptides corresponded to ribosomal-associated proteins, a putative karyopherin β that is involved in nuclear import of ribosomal and histone proteins (Orf19.2489) and Hsp70p, all of which also co-purified with Cdc5p (Tables 4.4, 4.5). Intriguingly, the hyphal regulator Efg1p, the Mitogen-Activated Protein Kinase (MAPK) Pbs2p, and several uncharacterized factors were also present (Table 4.8).

The fact that Orf19.3714p bound many spliceosome factors suggests that it may be a component or regulator of this complex. The spliceosome is a large ribonucleoprotein (RNP) complex required for splicing introns from precursor mRNA (125). The most common type consists of U1, U2, U4/U6, and U5 small nuclear RNPs (snRNPs) and more than 100 non-snRNP proteins. The spliceosome is well conserved but its composition and function have not been extensively investigated in *C. albicans*. In order to construct a preliminary framework, the *C. albicans* genome was screened for homologues of spliceosome and associated proteins in *S. cerevisiae* (Table S4.1). Homologues for most factors were identified, except for two NineTeen Complex (NTC) proteins, including *SNT309* and *NTC20*, as well as the U1 snRNP protein Snu56p, the Retention and Splicing (RES) complex protein Pml1p, the disassembly protein Ntr2p, the U2 snRNP protein Ysf3p and the U4/U6.U5 snRNP protein Spp381p. Thus, *C. albicans*

shows strong conservation in the spliceosome composition, including homologues of core complex factors, although a few differences exist.

To test whether the presence of Cdc5p impacted the putative protein interactions of Orf19.3714p, we repeated the affinity purification under conditions of Cdc5p depletion. Cultures of strains AG713 (*cdc5::hisG/MET3::CDC5::ARG4*, *orf19.3714::URA3/ORF19.3714-TAP-HISI*) and the control strain BH420 (*URA3+ HISI+*, *ARG4+*) were diluted into +MC medium for 4 h to deplete Cdc5p, and processed for affinity purification followed by mass spectrometry analysis. While some factors were still present, including proteins associated with the ribosome (*ORF19.3504*, *ORF19.7217*), the nuclear pore complex (*ORF19.4683*, *ORF19.4627*), Hsp70p, and an uncharacterized protein, Orf19.928p, the majority of factors previously identified were absent (Table 4.10). Thus, the association between Orf19.3714p and proteins involved in the spliceosome may be Cdc5p dependent, although we cannot rule out that this is due to a mitotic block. The results suggest for the first time that a Plk function may extend to RNA splicing, in part through interacting with the novel protein Orf19.3714p in *C. albicans*.

Table 4.8: Orbitrap LC/MS analysis of putative Orf19.3714p-interacting proteins in exponentially growing cells¹

Protein ID	Gene name⁴	Present in control²	Number of peptides³	Protein description⁴
CAL0001101	<i>ORF19.3714</i>	No	53	Uncharacterized
CAL0005042	<i>CDC5/ORF19.6010</i>	No	28	Polo-like kinase; member of conserved Mcm1 regulon, depletion causes defects in spindle elongation and Cdc35-dependent filamentation
CAL0001532	<i>ORF19.3098</i>	No	20	Uncharacterized, Predicted RNA-dependent ATPase RNA helicase
CAL0004852	<i>ORF19.6740</i>	No	17	Uncharacterized, Ortholog(s) have ubiquitin-protein ligase activity and role in generation of catalytic spliceosome for first transesterification step fractions, at hyphal surface, not yeast cells
CAL0003115	<i>SNU114/ORF19.144</i>	No	14	Uncharacterized, Protein similar to <i>S. cerevisiae</i> Snu114p, which is an RNA helicase involved in pre-mRNA splicing; likely to be essential for growth
CAL0001639	<i>ORF19.2489</i>	No	12	Uncharacterized, Putative karyopherin beta
CAL0004832	<i>DED1/ORF19.7392</i>	No	11	Uncharacterized, Predicted ATP-dependent RNA helicase; RNA strand annealing activity
CAL0002209	<i>PRP8/ORF19.6442</i>	No	10	Uncharacterized, Protein similar to <i>S. cerevisiae</i> Prp8, a component of the snRNP complex
CAL0001259	<i>RPS3/ORF19.6312</i>	No	8	Uncharacterized, Ribosomal protein, Hog1 induced
CAL0005977	<i>CDC19/ORF19.3575</i>	No	8	Pyruvate kinase at yeast cell surface; hyphal growth role
CAL0004402	<i>PMA1/ORF19.5383</i>	No	7	Plasma membrane protein
CAL0001392	<i>ORF19.3037</i>	No	7	Uncharacterized, Putative poly(A)-binding protein
CAL0004426	<i>ORF19.5391</i>	No	7	Uncharacterized, Predicted RNA splicing and ER to

CAL0004009	<i>VMA2/ORF19.6634</i>	No	6	Golgi transport protein
CAL0005101	<i>TUB2/ORF19.6034</i>	No	6	Vacuolar protein
CAL0001367	<i>SSB1/ORF19.6367</i>	No	5	Beta-tubulin
CAL0001348	<i>ARX1/ORF19.3015</i>	No	5	Hsp70 family heat shock protein
CAL0004351	<i>HGT6/ORF19.2020</i>	No	5	Uncharacterized, Putative ribosomal large subunit biogenesis protein
CAL0000146	<i>TFP1/ORF19.1680</i>	No	5	Glucose transporter, stress response
CAL0006304	<i>RPL3/ORF19.1601</i>	No	4	Uncharacterized, Subunit of vacuolar H ⁺ -ATPase
CAL0000561	<i>ORF19.6271</i>	No	4	Ribosomal protein, large subunit
CAL0000906	<i>EFG1/ORF19.610</i>	No	3	Uncharacterized, Ortholog(s) have role in mRNA splicing, via spliceosome and nucleus
CAL0002245	<i>RNR21/ORF19.5801</i>	No	3	Required for hyphal growth, cell-wall gene regulation; roles in adhesion, virulence
CAL0006335	<i>ILV2/ORF19.1613</i>	No	3	Uncharacterized, Ribonucleosidediphosphate reductase
CAL0003655	<i>PET9/ORF19.930</i>	No	3	Putative acetolactate synthase, induced by amino acid starvation
CAL0001161	<i>GPD2/ORF19.691</i>	No	3	Mitochondrial ADP/ATP carrier protein involved in ATP biosynthesis
CAL0000928	<i>CWC22/ORF19.1771</i>	No	3	Surface protein, core stress response, oxidative stress
CAL0003731	<i>ORF19.4659</i>	No	3	Spliceosome-associated protein
CAL0006116	<i>ORF19.5525</i>	No	3	Ortholog(s) have RNA binding activity, role in mRNA splicing, via spliceosome
CAL0000006	<i>HSP70/ORF19.4980</i>	No	2	Putative oxidoreductase
CAL0006022	<i>RPT6/ORF19.3593</i>	No	2	Putative hsp70 chaperone; role in entry into host cells; heat-shock
CAL0006026	<i>TIF4631/ORF19.3599</i>	No	2	Putative ATPase of the 19S regulatory particle of the 26S proteasome
CAL0004814	<i>PBS2/ORF19.7388</i>	No	2	Uncharacterized, Putative translation initiation factor
CAL0003677	<i>PDB1/ORF19.5294</i>	No	2	MAPK kinase; role in osmotic and oxidative stress responses Hog1 stress
				Uncharacterized, Putative pyru-

CAL0005454	<i>OAC1/ORF19.7411</i>	No	2	vate dehydrogenase Uncharacterized, Putative mitochondrial inner membrane transporter
CAL0005689	<i>RPT1/ORF19.441</i>	No	2	Uncharacterized, Putative 26S proteasome regulatory subunit
CAL0001034	<i>SAM2/ORF19.657</i>	No	2	S-adenosylmethionine synthetase; localizes to surface of hyphae not yeast cells, Hog1-induced
CAL0000250	<i>GUT1/ORF19.558</i>	No	2	Uncharacterized, Putative glycerol kinase
CAL0003304	<i>ORF19.6583</i>	No	2	Uncharacterized
CAL0001665	<i>ORF19.5040</i>	No	2	Uncharacterized, Ortholog(s) have nucleocytoplasmic transporter activity
CAL0004080	<i>ORF19.6660</i>	No	2	Uncharacterized
CAL0001339	<i>ORF19.6354</i>	No	2	Uncharacterized
CAL0003634	<i>ORF19.928</i>	No	2	Uncharacterized

¹Approximately 159 mg protein extracts from 2 L cultures of AG707 (*orf19.3714::URA3/ORF19.3714-TAP-ARG4*) and BH415 (*URA3+ ARG4+*) strains were subjected to tandem affinity purification (Rigaut *et al.* 1999, Lui *et al.*, 2010). Elutions were TCA-precipitated and run just into the resolving portion of an SDS PAGE gel (Lui *et al.*, 2010). The compressed bands were stained with Coomassie blue, cut from the gel, and analyzed using an LTQ-OrbitrapElite with nano-ESI.

²Peptides identified in both the tagged and the untagged control strains were excluded from the results.

³Peptides at a frequency of 1 were excluded from the results.

⁴Gene names and descriptions were obtained from the Candida Genome Database (<http://www.candidagenome.org/>).

Table 4.9: Enriched functional categories of proteins that interact with Orf19.3714p¹

Gene Ontology term	Cluster Freq ²	Backgd Freq ³	Corrected P-value	FD rate (%)	Genes
mRNA splicing via spliceosome	8/44 (18.2%)	100/6517 (1.5%)	0.00011	0	<i>CWC22, PRP8, SNU114, ORF19.3098, ORF19.4659, ORF19.5319, ORF19.6271, ORF19.6740</i>
RNA splicing, via transesterification reactions with bulged adenosine as nucleophile	8/44 (18.2%)	101/6517 (1.5%)	0.00012	0	<i>SNU114, CWC22, PRP8, ORF19.3098, ORF19.4659, ORF19.6271, ORF19.6740, ORF19.5391</i>
RNA splicing, via transesterification reactions	8/44 (18.2%)	105/6517 (1.6%)	0.00017	0	<i>SNU114, CWC22, PRP8, ORF19.3098, ORF19.4659, ORF19.5391, ORF19.6271, ORF19.6740</i>
RNA splicing	8/44 (18.2%)	115/6517 (1.8%)	0.00034	0	<i>SNU114, CWC22, PRP8, ORF19.3098, ORF19.4659, ORF19.5391, ORF19.6271, ORF19.6740</i>
Organic substance metabolic process	34/44 (77.3%)	2892/6517 (44.4%)	0.00381	0	<i>SSA2, SNU114, RPL3, ILV2, TFP1, CWC22, ORF19.3098, CDC19, RPT6, TIF4631, RPT1, SSB1, HSP70, PDB1, PMA1, PBS2, DED1, PET9, GPD2, GUT1, RNR21, CDC5, TUB2, orf19.6271, RPS3, PRP8, SAM2, VMA2, ORF19.6740, ORF19.5040, ORF19.3037, ORF19.5525, ORF19.5391, ORF19.4659</i>
Ribonucleoprotein complex assembly	7/44 (15.9%)	117/6517 (1.8%)	0.00497	0	<i>SNU114, RPL3, PRP8, TIF4631, ORF19.3098, ORF19.5391, ORF19.6740</i>

mRNA processing	8/44 (18.2%)	166/6517 (2.5%)	0.00544	0	<i>ORF19.6271, ORF19.4659, SNU114, CWC22, PRP8, ORF19.3098, ORF19.6740, ORF19.5391,</i>
Spliceosomal conformational changes to generate catalytic conformation	4/44 (9.1%)	23/6517 (0.4%)	0.00653	0	<i>SNU114, PRP8, ORF19.3098, ORF19.6740</i>
Ribonucleoprotein complex subunit organization	7/44 (15.9%)	123/6517 (1.9%)	0.00691	0	<i>SNU114, RPL3, ORF19.3098, TIF4631, ORF19.5391, PRP8, ORF19.6740</i>
Macromolecular complex subunit organization	13/44 (29.5%)	540/6517 (8.3%)	0.01581	0	<i>SNU114, RPL3, ORF19.3098, RPT6, TIF4631, RPT1, ORF19.5040, ORF19.5391, CDC5, TUB2, PRP8, ORF19.6740, PBS2</i>
Primary metabolic process	32/44 (72.7%)	2758/6517 (42.3%)	0.01828	0	<i>SSA2, SNU114, RPL3, ILV2, TFP1, CWC22, ORF19.3098, CDC19, RPT6, TIF4631, RPT1, ORF19.4659, PET9, HSP70, PDB1, PMA1, ORF19.5391, ORF19.5525, GUT1, RNR21, CDC5, TUB2, ORF19.6271, RPS3, DED1, SSB1, PRP8, SAM2, VMA2, ORF19.6740, GPD2, PBS2</i>
Nucleocytoplasmic transport	7/44 (15.9%)	145/6517 (2.2%)	0.02011	0.17	<i>ORF19.2489, ARX1, ORF19.3037, ORF19.5040, RPS3, SSB1, PBS2</i>
Nuclear transport	7/44 (15.9%)	146/6517 (2.2%)	0.02102	0.15	<i>ORF19.2489, ARX1, ORF19.3037, ORF19.5040, RPS3, SSB1, PBS2</i>

Macromolecular complex assembly	11/44 (25.0%)	402/6517 (6.2%)	0.0231	0.14	<i>SNU114, RPL3, ORF19.3098, RPT6, TIF4631, RPT1, ORF19.5391, CDC5, TUB2,</i>
Interaction with host	5/44 (11.4%)	62/6517 (1.0%)	0.0242	0.13	<i>SSA2, CDC19, HSP70, EFG1, SSB1</i>
Cellular macromolecular complex assembly	10/44 (22.7%)	355/6517 (5.4%)	0.04163	0.12	<i>SNU114, RPL3, ORF19.3098, RPT6, TIF4631, RPT1, ORF19.5391, TUB2, PRP8, ORF19.6740</i>
Cellular metabolic process	32/44 (72.7%)	2856/6517 (43.8%)	0.04181	0.12	<i>SSA2, SNU114, RPL3, ILV2, TFP1, CWC22, ORF19.6740, GPD2, PBS2, DED1, PET9, ORF19.3098, CDC19, RPT6, TIF4631, RPT1, SAM2, VMA2, ORF19.4659, HSP70, PDB1, PMA1, ORF19.5391, PRP8, ORF19.5525, GUT1, RNR21, CDC5, TUB2, RPS3, SSB1, ORF19.6271</i>
Ribonucleoprotein complex biogenesis	10/44 (22.7%)	355/6517 (5.4%)	0.04262	0.11	<i>SNU114, RPL3, ARX1, ORF19.3098, TIF4631, RPS3, SSB1, PRP8, ORF19.6740, ORF19.5391</i>
Metabolic process	34/44 (77.3%)	3187/6517 (48.9%)	0.04771	0.11	<i>SSA2, SNU114, RPL3, ILV2, TFP1, CWC22, ORF19.3037, ORF19.3098, CDC19, RPT6, TIF4631, RPT1, ORF19.4659, HSP70, ORF19.5040, PDB1, PMA1, ORF19.5391, PET9, , GUT1, RNR21, CDC5, TUB2, ORF19.6271, RPS3, GPD2, SSB1, PRP8, SAM2, VMA2, ORF19.6740, PBS2, DED1, , ORF19.5525,</i>
mRNA metabolic process	8/44 (18.2%)	225/6517 (3.5%)	0.0483	0.1	<i>SNU114, CWC22, PRP8, ORF19.3098, ORF19.4659, ORF19.5391, ORF19.6271, ORF19.6740</i>

Positive regulation of response to stimulus	6/44 (13.6%)	118/6517 (1.8%)	0.05593	0.1	<i>CDC19, HSP70, CDC5, EFG1, SSB1, PBS2</i>
Response to host defenses	4/44 (9.1%)	43/6517 (0.7%)	0.0825	0.09	<i>CDC19, HSP70, EFG1, SSB1</i>
Nucleobase-containing compound metabolic process	19/44 (43.2%)	1246/6517 (0.7%)	0.09272	0.25	<i>SNU114, TFP1, CWC22, ORF19.3098, RPT6, SAM2, VMA2, ORF19.6740, TIF4631, ORF19.4659, PMA1, ORF19.5391, ORF19.5525, RNR21, CDC5, TUB2, ORF19.6271, SSB1, PRP8</i>

¹The 44 peptides identified in Table 9 were subjected to Gene Ontology (GO) term finder in CGD (<http://www.candidagenome.org/>) for all process function.

²The number of genes belonging to GO term out of the total number of genes subjected to the search engine.

³The numbers of genes belonging to *C. albicans* genome in that GO term out of the total number of genes in *C. albicans* genome.

Freq= Frequency; Backgd= Background; FD= False discovery

Table 4.10: Orbitrap LC/MS analysis of putative Orf19.3714p-interacting proteins in cells blocked in mitosis¹

Protein ID	Gene name⁴	Presence in control²	Number of Peptides³	Protein description⁴
CAL0001101	<i>ORF19.3714</i>	No	55	Uncharacterized
CAL0005657	<i>TDH3/ORF19.6814</i>	No	10	NAD-linked glyceraldehyde-3-phosphate dehydrogenase
CAL0005202	<i>PDC11/ORF19.2877</i>	No	9	Pyruvate decarboxylase; on hyphal not yeast cell surface
CAL0004558	<i>TEF1/ORF19.1435</i>	No	5	Translation elongation factor 1-alpha; at cell surface
CAL0000006	<i>HSP70/ORF19.4980</i>	No	4	Putative hsp70 chaperone; role in entry into host cells; heat-shock
CAL0001571	<i>ACT1/ORF19.5007</i>	No	4	Actin; at polarized growth site in budding and hyphal cells
CAL0000516	<i>GLT1/ORF19.6257</i>	No	4	Putative glutamate synthase
CAL0005977	<i>CDC19/ORF19.3575</i>	No	4	Pyruvate kinase at yeast cell surface, hyphal growth role
CAL0001178	<i>CIT1/ORF19.4393</i>	No	2	Citrate synthase, Efg1-regulated under yeast, not hyphal growth
CAL0003522	<i>PKH2/ORF19.5224</i>	No	2	Putative serine/threonine protein kinase
CAL0005101	<i>TUB2/ORF19.6034</i>	No	2	Beta-tubulin; functional ScTub2 homolog
CAL0005346	<i>CDC46/ORF19.5487</i>	No	2	Uncharacterized, Putative hexameric MCM complex subunit
CAL0003820	<i>MLP1/ORF19.4683</i>	No	2	Uncharacterized, Ortholog(s) have ribo-nucleoprotein complex binding activity
CAL0005770	<i>RPL23A/ORF19.3504</i>	No	2	Uncharacterized, Ribosomal protein
CAL0003773	<i>RPL4B/ORF19.7217</i>	No	2	Ribosomal protein
CAL0003646	<i>ORF19.4627</i>	No	2	Uncharacterized, Ortholog(s) have structural constituent of nuclear pore activity
CAL0006178	<i>ORF19.5552</i>	No	2	Uncharacterized, Putative transcriptional regulator of reductase genes ribonucleotide
CAL0003634	<i>ORF19.928</i>	No	2	Uncharacterized

¹Approximately 99 mg protein extracts from 2 L cultures of AG713 (*cdc5::hisG/MET3::CDC5-ARG4, orf19.3714::URA3/ORF19.3714-TAP-HIS1*) and BH420 (*URA3+*, *HIS1+*, *ARG4+*) strains were subjected to tandem affinity purification (Rigaut *et al.* 1999, Lui *et al.*, 2010). Elutions were TCA-precipitated and run just into the resolving portion of an SDS PAGE gel (Lui *et al.*, 2010). The compressed bands were stained with Coomassie blue, cut from the gel, and analysed using an LTQ-OrbitrapElite with nano-ESI.

²Peptides identified in both the tagged and the untagged control strains were excluded from the results.

³Peptides at a frequency of 1 were excluded from the results.

⁴Gene names and descriptions were obtained from the Candida Genome Database (<http://www.candidagenome.org/>).

4.4 DISCUSSION

Depletion of the Plk Cdc5p in *C. albicans* yeast cells impairs spindle elongation, resulting in a block in mitosis followed by initiation and maintenance of polarized growth from the yeast bud and induction of hyphal-specific virulence genes (9). Although Plks are conserved and have multiple cell cycle functions, not all substrates have been identified, and some species-specificity in function and sequence is emerging (10, 126, 127). In order to determine the mechanisms of action of Cdc5p in mitosis and morphogenesis in *C. albicans*, we identified its interacting proteins using affinity purification followed by mass spectrometry. Our work reveals a new interacting protein of the Plk family that is *Candida*-specific, and provides the first evidence for a possible link between Plk function and spliceosome activity.

4.4.1 Orf19.3714p is a novel interacting protein of Cdc5p

Plks have many functions and, accordingly, many interacting factors (33, 58, 128). In *S. cerevisiae*, a variety of approaches revealed 103 proteins that physically bind Cdc5p (30, 87, 129-132). Although not many binding partners were identified in a given single screen (104), 41 Cdc5p-interacting proteins were identified in cells blocked in meiosis, including the kinase Cdc7p, its regulatory unit Dbf4p, various cohesins, APC/C, and 26S proteasomes subunits (105). Although few proteins co-purified with Cdc5p from *C. albicans*, even in cells blocked in mitosis, Orf19.3714p was one of the most highly abundant factor. An interaction with Cdc5p was confirmed by co-immunoprecipitation and through affinity purification of Orf19.3714p. Orf19.3714p may be a substrate of Cdc5p due to the fact that it contains several consensus PBD and Plk phosphorylation sites (15, 17, 108), and was required in part to maintain the Cdc5p-depleted phenotype. However, Plks can bind proteins via non-canonical sequences, and phosphorylation of substrates is not always required for an interaction (133). It remains to be seen whether Cdc5p phosphorylates Orf19.3714p. Co-precipitation of other factors with Cdc5p, including Cdc7p and Dbf4p, validates the experimental approach since these proteins bind Cdc5p in *S. cerevisiae* (134, 135). In addition to regulating DNA replication initiation, Cdc7p/Dbf4p repress Cdc5p to prevent premature activation of key substrates in the MEN (18). The functions of Cdc7p and Dbf4p are not fully characterized in *C. albicans*, but Dbf4p was reported to suppress hyphal growth (136), and absence of *CDC7* or *DBF4* resulted in filamentation (137). It remains unclear if the interaction between Cdc5p and Cdc7/Dbf4p in *C. albicans* reflects a

functional relationship similar to the situation in *S. cerevisiae*.

The only sequence homologues of Orf19.3714p exist in other *Candida* species. A notable exception is *C. glabrata*, which is in the clade of *S. cerevisiae* (138, 139). Since it is one of the most abundant binding partners of Cdc5p, and *C. albicans* contains divergent, functional homologues of some cell cycle factors, including the *SIC1* homologue, *SOLI* (140, 141), Orf19.3714p may be a divergent form of a known protein that binds Cdc5p in *S. cerevisiae*. *C. albicans* has sequence homologues to all Cdc5p-binding proteins in *S. cerevisiae*, except *NDD1*, a regulator of transcription at the G2/M transition (45), *PRM3*, a regulator of nuclear envelope fusion during karyogamy (142), and *YDL186W*, a protein of unknown function (Table S4.2). However, unlike Orf19.3714p, none of these proteins interact with spliceosome factors. Thus, we conclude that Orf19.3714p represents a novel interacting protein within the Plk family.

4.4.2 Orf19.3714p may be important for mitosis and mitotic checkpoints

Since Orf19.3714p does not share sequence homology with any characterized protein, and its absence did not affect yeast or hyphal growth, the function of this protein is elusive. However, it may be important for or during mitosis based on several lines of evidence. First, Orf19.3714p binds Cdc5p, an important mitotic regulator. Second, Orf19.3714p is hyperphosphorylated when mitosis is arrested through depletion of Cdc5p or Cdc20p. Third, Orf19.3714p abundance is modulated during a block in mitosis, where it is enriched in the absence of Cdc5p but reduced when Cdc20p is depleted, suggesting regulation at the level of protein stability. Fourth, absence of Orf19.3714p in Cdc5p-depleted cells resulted in re-budding of the mother yeast cell, a characteristic of cells escaping from a mitotic block (83, 143, 144). Similar results were observed in Cdc5p-depleted cells lacking a homologue of the spindle checkpoint factor *BUB2* (83). In contrast, absence of Orf19.3714p had no effect on cells that were blocked in S phase with HU. This suggests that Orf19.3714p may influence mitotic checkpoints. In *S. cerevisiae*, the spindle checkpoint pathway consists of *MPS1*, *BUB1*, *BUB3*, *MAD1*, *MAD2*, and *MAD3* (145). It responds to defects in spindle microtubule attachment to kinetochores, which in turn inhibit activity of APC/C-Cdc20 and the metaphase-anaphase transition (146). The spindle position checkpoint consists of *BFA1-BUB2*, *CDC5*, and *KIN4*, and is activated when the mitotic spindle fails to align along the mother-daughter axis (147). *S. cerevisiae* cells treated with

nocodazole show re-budding if *BUB2* is absent, due to precocious activation of mitotic exit (148). The mitotic checkpoint pathways are not well defined in *C. albicans* (82, 83) but homologues of all components exist except for *MAD3*, which is a paralog of *BUB1* that arose due to genome duplication in *S. cerevisiae* (149). Intriguingly, *MAD2* and another checkpoint factor in *C. albicans*, *SWE1*, are not essential for yeast or hyphal growth *in vitro*, similar to *ORF19.3714*, but are important for growth *in vivo* as strains lacking either of these genes are avirulent in mouse models of infection (82, 91). This suggests that checkpoint factors, and checkpoint-associated polarized growth demonstrated by *C. albicans* cells upon mitotic arrest, are important for growth and virulence in the host (9, 75, 88, 150). Thus, Orf19.3714p may be important for mitosis, possibly through influencing the mitotic checkpoints. It will be important to test whether Orf19.3714p is required for growth and virulence *in vivo*.

4.4.3 Orf19.3714p may be associated with the spliceosome and potentially link Plk function to spliceosome activity

The main interacting factors of Orf19.3714p included several spliceosome-associated proteins, suggesting that Orf19.3714p is a component or regulator of this complex. The spliceosome is a large RNP complex that is required for splicing introns from precursor mRNA (125). The most common type that processes U2-type introns consists of U1, U2, U4/U6, and U5 small nuclear RNPs (snRNPs) and over 100 non-snRNP proteins. The composition and structure of the spliceosome is dynamic, and several RNA helicases are involved in its assembly and disassembly (151). After Cdc5p, the most enriched co-purifying proteins of Orf19.3714p included Orf19.3098p, a homologue of the RNA-dependent ATPase RNA helicase Brr2p that is required for spliceosome activation via disrupting U4/U6 base-pairing in native snRNPs (121, 122), Orf19.6740p, a homologue of Prp19p that is in turn a component of the NTC required for activation of the spliceosome (123, 124), Snu114p, a GTPase that activates Brr1p (152), and other splicing-associated and RNA helicase factors such as Prp8p, for example. The spliceosome composition has not been systematically investigated in *C. albicans*, except for the snRNAs U1, U2, U4, U5 and U6, and only 6% of the *C. albicans* genome contains introns (153, 154). A comparison of the *C. albicans* genome with that of *S. cerevisiae* revealed homologues of most spliceosome proteins (Table S4.1), except for two NTC complex factors, including *SNT309* and *NTC20*, as well as the U1 snRNP protein Snu56p, the RES complex protein Pml1p, and the

disassembly protein Ntr2p. Thus, Orf19.3714p may be a novel component or regulator of the spliceosome, although we cannot rule out the possibility that it is a divergent form of a known spliceosome component. Intriguingly, when Orf19.3714p was purified from cells lacking Cdc5p, most spliceosome factors did not co-purify. This suggests that Cdc5p may influence the interaction between Orf19.3714p and the spliceosomal components, although this may alternatively be due to a block in mitosis. Identification of Orf19.3714p-interacting factors from Cdc20p-depleted cells may help clarify this issue.

Based on the data, we propose a model whereby Orf19.3714p is a spliceosome-associated protein regulated in part by Cdc5p that influences efficient splicing of factors that include regulators of the mitotic checkpoints and/or mitotic exit. In agreement with this, depletion of various spliceosome proteins in other organisms can influence mitotic progression through deregulating splicing of messages encoding for spindle, kinetochore and M phase proteins, for example (155, 156). Intriguingly, HeLa cells treated with taxol can escape mitotic arrest when specific spliceosome components are down-regulated, and absence of the individual factors without taxol treatment results in cell cycle delays (157). Importantly, absence of spliceosome factors can differentially affect splicing of transcripts (158-160). The few *C. albicans* genes containing introns fall within the functional categories of microtubules, ribosomes, meiosis, splicing, mitochondrial respiration and protein degradation (154, 161). Notably, specific genes include factors that influence mitotic progression, including *TUBI,2* and *4*, *CDC14*, *TEMI*, *FKH2*, *CDC28* and *PHO85*, for example (154). However, we can not rule out a splicing-independent role for Orf19.3714p, as has been demonstrated for other splicing components including the NTC/Prp19p complex (162), nor the possibility that Orf19.3714p is itself a mitotic regulator that in turn binds and regulates the spliceosome, as demonstrated for Bub3p in fibroblast cells (163). It is not clear if Orf19.3714p function is required prior to or during mitosis. Although transcription and splicing are generally down-regulated during mitosis, transcription can still occur as seen with RNA polymerase II-dependent transcription of centromere satellite transcripts that help regulate the mitotic kinetochore (164). However, the post-translational modifications of Orf19.3714p during a mitotic block suggest regulation during this stage that may be either positive or negative. One possibility is that phosphorylation normally occurs before or during mitosis to influence activity and/or stability via targeted

degradation. This may be carried out in part by Cdc5p but also other kinases such as CDK, due to the presence of 1 perfect (S/T-P-X-R/K) and 15 partial (S/T-P) consensus CDK sites (data not shown), several consensus PLK phosphorylation sites, and the fact that Orf19.3714p was hyperphosphorylated in the absence of Cdc5p or Cdc20p. If Cdc5p is required for the activation of the APC/C, similar to the situation in *S. cerevisiae* (165), this could explain the enrichment of Orf19.3714p in cells lacking Cdc5p. Alternatively, the decrease in abundance of Orf19.3714p when Cdc20p is depleted may be due to an active APC/C under control of other factors such as Cdh1p. Indeed, Cdh1p is active, albeit at a reduced level, during metaphase even in the absence of Cdc20p in *S. cerevisiae* (148, 166). It will be informative to determine the levels and phosphorylation of Orf19.3714p during a normal cell cycle, and identify the associated regulatory mechanisms.

Although numerous kinases are involved in regulating core spliceosome components and accessory proteins, often to repress their activity for mitosis (167), our data suggest for the first time that a Plk may be linked to the spliceosome. Intriguingly, transcription profiles of cells depleted of Cdc5p show modulation of several spliceosome components (88). Future experiments involving RNA sequencing on strains with or without *ORF19.3714* as well as *CDC5* will provide important insights on this model.

In summary, our results extend the current repertoire of putative substrates and functions of Plks, which comprise an important and conserved family of cell cycle regulators. The fact that Orf19.3714p is a novel, fungal-specific protein has critical implications for the development of new therapeutic strategies and controlling growth of the organism, particularly if it is found to be essential for growth *in vivo* like many other factors that influence cell cycle checkpoints in *C. albicans*. Our work also opens the doors for investigations of the spliceosome, its link to Plk function, and post-transcriptional regulation of processes affecting growth in *C. albicans*, which remain poorly explored areas.

4.5 ACKNOWLEDGEMENTS

We would like to thank Centre for Microscopy and Cell Imaging (CMCI) at Concordia University for their help in microscopic pictures and Éric Bonneil at the Proteomics Centre, Institute for Research in Immunology and Cancer, Université de Montréal for mass spectrometry analyses. This work was supported by NSERC Discovery Grant N00944 to CB and NSERC PGSD Graduate Student Scholarship to AG.

4.6 REFERENCES:

1. **Chase D, Golden A, Heidecker G, Ferris DK.** 2000. *Caenorhabditis elegans* contains a third polo-like kinase gene. *DNA Seq* **11**:327-334.
2. **Ouyang B, Wang Y, Wei D.** 1999. *Caenorhabditis elegans* contains structural homologs of human prk and plk. *DNA Seq* **10**:109-113.
3. **Duncan PI, Pollet N, Niehrs C, Nigg EA.** 2001. Cloning and characterization of Plx2 and Plx3, two additional Polo-like kinases from *Xenopus laevis*. *Exp Cell Res* **270**:78-87.
4. **Liu J, Maller JL.** 2005. *Xenopus* Polo-like kinase Plx1: a multifunctional mitotic kinase. *Oncogene* **24**:238-247.
5. **de Carcer G, Escobar B, Higuero AM, Garcia L, Anson A, Perez G, Mollejo M, Manning G, Melendez B, Abad-Rodriguez J, Malumbres M.** 2011. Plk5, a polo box domain-only protein with specific roles in neuron differentiation and glioblastoma suppression. *Mol Cell Biol* **31**:1225-1239.
6. **de Carcer G, Manning G, Malumbres M.** 2011. From Plk1 to Plk5: functional evolution of polo-like kinases. *Cell Cycle* **10**:2255-2262.
7. **Kitada K, Johnson AL, Johnston LH, Sugino A.** 1993. A multicopy suppressor gene of the *Saccharomyces cerevisiae* G1 cell cycle mutant gene *dbf4* encodes a protein kinase and is identified as *CDC5*. *Mol Cell Biol* **13**:4445-4457.
8. **Ohkura H, Hagan IM, Glover DM.** 1995. The conserved *Schizosaccharomyces pombe* kinase *plk1*, required to form a bipolar spindle, the actin ring, and septum, can drive septum formation in G1 and G2 cells. *Genes Dev* **9**:1059-1073.
9. **Bachewich C, Thomas DY, Whiteway M.** 2003. Depletion of a polo-like kinase in *Candida albicans* activates cyclase-dependent hyphal-like growth. *Mol Biol Cell* **14**:2163-2180.
10. **Mogilevsky K, Glory A, Bachewich C.** 2012. The Polo-like kinase *PLKA* in *Aspergillus nidulans* is not essential but plays important roles during vegetative growth and development. *Eukaryot Cell* **11**:194-205.
11. **Graham TM, Tait A, Hide G.** 1998. Characterisation of a polo-like protein kinase gene homologue from an evolutionary divergent eukaryote, *Trypanosoma brucei*. *Gene* **207**:71-77.
12. **Archambault V, Glover DM.** 2009. Polo-like kinases: conservation and divergence in their functions and regulation. *Nat Rev Mol Cell Biol* **10**:265-275.

13. **Lowery DM, Lim D, Yaffe MB.** 2005. Structure and function of Polo-like kinases. *Oncogene* **24**:248-259.
14. **Park JE, Soung NK, Johmura Y, Kang YH, Liao C, Lee KH, Park CH, Nicklaus MC, Lee KS.** 2010. Polo-box domain: a versatile mediator of polo-like kinase function. *Cell Mol Life Sci* **67**:1957-1970.
15. **Elia AE, Cantley LC, Yaffe MB.** 2003. Proteomic screen finds pSer/pThr-binding domain localizing Plk1 to mitotic substrates. *Science* **299**:1228-1231.
16. **Elia AE, Rellos P, Haire LF, Chao JW, Ivins FJ, Hoepker K, Mohammad D, Cantley LC, Smerdon SJ, Yaffe MB.** 2003. The molecular basis for phosphodependent substrate targeting and regulation of Plks by the Polo-box domain. *Cell* **115**:83-95.
17. **Nakajima H, Toyoshima-Morimoto F, Taniguchi E, Nishida E.** 2003. Identification of a consensus motif for Plk (Polo-like kinase) phosphorylation reveals Myt1 as a Plk1 substrate. *J Biol Chem* **278**:25277-25280.
18. **Miller CT, Gabrielse C, Chen YC, Weinreich M.** 2009. Cdc7p-Dbf4p regulates mitotic exit by inhibiting Polo kinase. *PLoS Genet* **5**:e1000498.
19. **Garcia-Alvarez B, de Carcer G, Ibanez S, Bragado-Nilsson E, Montoya G.** 2007. Molecular and structural basis of polo-like kinase 1 substrate recognition: Implications in centrosomal localization. *Proc Natl Acad Sci U S A* **104**:3107-3112.
20. **Petersen J, Hagan IM.** 2005. Polo kinase links the stress pathway to cell cycle control and tip growth in fission yeast. *Nature* **435**:507-512.
21. **Glover DM, Hagan IM, Tavares AA.** 1998. Polo-like kinases: a team that plays throughout mitosis. *Genes Dev* **12**:3777-3787.
22. **Nigg EA.** 1998. Polo-like kinases: positive regulators of cell division from start to finish. *Curr Opin Cell Biol* **10**:776-783.
23. **Walters AD, May CK, Dauster ES, Cinquin BP, Smith EA, Robellet X, D'Amours D, Larabell CA, Cohen-Fix O.** 2014. The yeast polo kinase Cdc5 regulates the shape of the mitotic nucleus. *Curr Biol* **24**:2861-2867.
24. **Toyoshima-Morimoto F, Taniguchi E, Nishida E.** 2002. Plk1 promotes nuclear translocation of human Cdc25C during prophase. *EMBO Rep* **3**:341-348.
25. **Sakchaisri K, Asano S, Yu LR, Shulewitz MJ, Park CJ, Park JE, Cho YW, Veenstra TD, Thorner J, Lee KS.** 2004. Coupling morphogenesis to mitotic entry. *Proc Natl Acad Sci U S A* **101**:4124-4129.
26. **do Carmo Avides M, Tavares A, Glover DM.** 2001. Polo kinase and Asp are needed to promote the mitotic organizing activity of centrosomes. *Nat Cell Biol* **3**:421-424.
27. **Elowe S, Hummer S, Uldschmid A, Li X, Nigg EA.** 2007. Tension-sensitive Plk1 phosphorylation on BubR1 regulates the stability of kinetochore microtubule interactions. *Genes Dev* **21**:2205-2219.
28. **Lenart P, Petronczki M, Steegmaier M, Di Fiore B, Lipp JJ, Hoffmann M, Rettig WJ, Kraut N, Peters JM.** 2007. The small-molecule inhibitor BI 2536 reveals novel insights into mitotic roles of polo-like kinase 1. *Curr Biol* **17**:304-315.
29. **Park CJ, Park JE, Karpova TS, Soung NK, Yu LR, Song S, Lee KH, Xia X, Kang E, Dabanoglu I, Oh DY, Zhang JY, Kang YH, Wincovitch S, Huffaker TC, Veenstra TD, McNally JG, Lee KS.** 2008. Requirement for the budding yeast polo kinase Cdc5 in proper microtubule growth and dynamics. *Eukaryot Cell* **7**:444-453.
30. **Snead JL, Sullivan M, Lowery DM, Cohen MS, Zhang C, Randle DH, Taunton J, Yaffe MB, Morgan DO, Shokat KM.** 2007. A coupled chemical-genetic and

- bioinformatic approach to Polo-like kinase pathway exploration. *Chem Biol* **14**:1261-1272.
31. **Alexandru G, Uhlmann F, Mechtler K, Poupart MA, Nasmyth K.** 2001. Phosphorylation of the cohesin subunit Scc1 by Polo/Cdc5 kinase regulates sister chromatid separation in yeast. *Cell* **105**:459-472.
 32. **Sumara I, Vorlaufer E, Stukenberg PT, Kelm O, Redemann N, Nigg EA, Peters JM.** 2002. The dissociation of cohesin from chromosomes in prophase is regulated by Polo-like kinase. *Mol Cell* **9**:515-525.
 33. **Lee KS, Park JE, Asano S, Park CJ.** 2005. Yeast polo-like kinases: functionally conserved multitask mitotic regulators. *Oncogene* **24**:217-229.
 34. **Uhlmann F, Wernic D, Poupart MA, Koonin EV, Nasmyth K.** 2000. Cleavage of cohesin by the CD clan protease separin triggers anaphase in yeast. *Cell* **103**:375-386.
 35. **Hansen DV, Loktev AV, Ban KH, Jackson PK.** 2004. Plk1 regulates activation of the anaphase promoting complex by phosphorylating and triggering SCFbetaTrCP-dependent destruction of the APC Inhibitor Emi1. *Mol Biol Cell* **15**:5623-5634.
 36. **Moshe Y, Boulaire J, Pagano M, Hershko A.** 2004. Role of Polo-like kinase in the degradation of early mitotic inhibitor 1, a regulator of the anaphase promoting complex/cyclosome. *Proc Natl Acad Sci U S A* **101**:7937-7942.
 37. **Eckerdt F, Strebhardt K.** 2006. Polo-like kinase 1: target and regulator of anaphase-promoting complex/cyclosome-dependent proteolysis. *Cancer Res* **66**:6895-6898.
 38. **Rudner AD, Murray AW.** 2000. Phosphorylation by Cdc28 activates the Cdc20-dependent activity of the anaphase-promoting complex. *J Cell Biol* **149**:1377-1390.
 39. **Liang F, Jin F, Liu H, Wang Y.** 2009. The molecular function of the yeast polo-like kinase Cdc5 in Cdc14 release during early anaphase. *Mol Biol Cell* **20**:3671-3679.
 40. **Bardin AJ, Visintin R, Amon A.** 2000. A mechanism for coupling exit from mitosis to partitioning of the nucleus. *Cell* **102**:21-31.
 41. **Petronczki M, Lenart P, Peters JM.** 2008. Polo on the Rise-from Mitotic Entry to Cytokinesis with Plk1. *Dev Cell* **14**:646-659.
 42. **Yoshida S, Kono K, Lowery DM, Bartolini S, Yaffe MB, Ohya Y, Pellman D.** 2006. Polo-like kinase Cdc5 controls the local activation of Rho1 to promote cytokinesis. *Science* **313**:108-111.
 43. **Atkins BD, Yoshida S, Saito K, Wu CF, Lew DJ, Pellman D.** 2013. Inhibition of Cdc42 during mitotic exit is required for cytokinesis. *J Cell Biol* **202**:231-240.
 44. **Anderson M, Ng SS, Marchesi V, MacIver FH, Stevens FE, Riddell T, Glover DM, Hagan IM, McNerny CJ.** 2002. Plo1(+) regulates gene transcription at the M-G(1) interval during the fission yeast mitotic cell cycle. *EMBO J* **21**:5745-5755.
 45. **Darieva Z, Bulmer R, Pic-Taylor A, Doris KS, Geymonat M, Sedgwick SG, Morgan BA, Sharrocks AD.** 2006. Polo kinase controls cell-cycle-dependent transcription by targeting a coactivator protein. *Nature* **444**:494-498.
 46. **Fu Z, Malureanu L, Huang J, Wang W, Li H, van Deursen JM, Tindall DJ, Chen J.** 2008. Plk1-dependent phosphorylation of FoxM1 regulates a transcriptional programme required for mitotic progression. *Nat Cell Biol* **10**:1076-1082.
 47. **Murakami H, Aiba H, Nakanishi M, Murakami-Tonami Y.** 2010. Regulation of yeast forkhead transcription factors and FoxM1 by cyclin-dependent and polo-like kinases. *Cell Cycle* **9**:3233-3242.
 48. **Fairley JA, Mitchell LE, Berg T, Kenneth NS, von Schubert C, Sillje HH, Medema**

- RH, Nigg EA, White RJ.** 2012. Direct regulation of tRNA and 5S rRNA gene transcription by Polo-like kinase 1. *Mol Cell* **45**:541-552.
49. **Budirahardja Y, Gonczy P.** 2008. PLK-1 asymmetry contributes to asynchronous cell division of *C. elegans* embryos. *Development* **135**:1303-1313.
50. **Rivers DM, Moreno S, Abraham M, Ahringer J.** 2008. PAR proteins direct asymmetry of the cell cycle regulators Polo-like kinase and Cdc25. *J Cell Biol* **180**:877-885.
51. **Lu LY, Wood JL, Minter-Dykhouse K, Ye L, Saunders TL, Yu X, Chen J.** 2008. Polo-like kinase 1 is essential for early embryonic development and tumor suppression. *Mol Cell Biol* **28**:6870-6876.
52. **Zimmerman WC, Erikson RL.** 2007. Polo-like kinase 3 is required for entry into S phase. *Proc Natl Acad Sci U S A* **104**:1847-1852.
53. **Draghetti C, Salvat C, Zanoguera F, Curchod ML, Vignaud C, Peixoto H, Di Cara A, Fischer D, Dhanabal M, Andreas G, Abderrahim H, Rommel C, Camps M.** 2009. Functional whole-genome analysis identifies Polo-like kinase 2 and poliovirus receptor as essential for neuronal differentiation upstream of the negative regulator alphaB-crystallin. *J Biol Chem* **284**:32053-32065.
54. **Lui DY, Colaiacovo MP.** 2013. Meiotic development in *Caenorhabditis elegans*. *Adv Exp Med Biol* **757**:133-170.
55. **Mirouse V, Formstecher E, Couderc JL.** 2006. Interaction between Polo and BicD proteins links oocyte determination and meiosis control in *Drosophila*. *Development* **133**:4005-4013.
56. **George VT, Brooks G, Humphrey TC.** 2007. Regulation of cell cycle and stress responses to hydrostatic pressure in fission yeast. *Mol Biol Cell* **18**:4168-4179.
57. **Robertson AM, Hagan IM.** 2008. Stress-regulated kinase pathways in the recovery of tip growth and microtubule dynamics following osmotic stress in *S. pombe*. *J Cell Sci* **121**:4055-4068.
58. **Archambault V, Lepine G, Kachaner D.** 2015. Understanding the Polo Kinase machine. *Oncogene* **34**:4799-4807.
59. **Lee SY, Jang C, Lee KA.** 2014. Polo-like kinases (plks), a key regulator of cell cycle and new potential target for cancer therapy. *Balsaenggwa Saengsig* **18**:65-71.
60. **Ikeda KN, de Graffenried CL.** 2012. Polo-like kinase is necessary for flagellum inheritance in *Trypanosoma brucei*. *J Cell Sci* **125**:3173-3184.
61. **Zitouni S, Nabais C, Jana SC, Guerrero A, Bettencourt-Dias M.** 2014. Polo-like kinases: structural variations lead to multiple functions. *Nat Rev Mol Cell Biol* **15**:433-452.
62. **Miller LG, Hajjeh RA, Edwards JE, Jr.** 2001. Estimating the cost of nosocomial candidemia in the united states. *Clin Infect Dis* **32**:1110.
63. **Morschhauser J.** 2010. Regulation of multidrug resistance in pathogenic fungi. *Fungal Genet Biol* **47**:94-106.
64. **Orasch C, Marchetti O, Garbino J, Schrenzel J, Zimmerli S, Muhlethaler K, Pfyffer G, Ruef C, Fehr J, Zbinden R, Calandra T, Bille J.** 2014. *Candida* species distribution and antifungal susceptibility testing according to European Committee on Antimicrobial Susceptibility Testing and new vs. old Clinical and Laboratory Standards Institute clinical breakpoints: a 6-year prospective candidaemia survey from the fungal infection network of Switzerland. *Clin Microbiol Infect* **20**:698-705.
65. **Prasad R, Kapoor K.** 2005. Multidrug resistance in yeast *Candida*. *Int Rev Cytol* **242**:215-248.

66. **Pande K, Chen C, Noble SM.** 2013. Passage through the mammalian gut triggers a phenotypic switch that promotes *Candida albicans* commensalism. *Nat Genet* **45**:1088-1091.
67. **Vazquez-Torres A, Balish E.** 1997. Macrophages in resistance to candidiasis. *Microbiol Mol Biol Rev* **61**:170-192.
68. **Braun BR, Head WS, Wang MX, Johnson AD.** 2000. Identification and characterization of *TUPI*-regulated genes in *Candida albicans*. *Genetics* **156**:31-44.
69. **Braun BR, Johnson AD.** 1997. Control of filament formation in *Candida albicans* by the transcriptional repressor *TUPI*. *Science* **277**:105-109.
70. **Lo HJ, Kohler JR, DiDomenico B, Loebenberg D, Cacciapuoti A, Fink GR.** 1997. Nonfilamentous *C. albicans* mutants are avirulent. *Cell* **90**:939-949.
71. **Biswas S, Van Dijck P, Datta A.** 2007. Environmental sensing and signal transduction pathways regulating morphopathogenic determinants of *Candida albicans*. *Microbiol Mol Biol Rev* **71**:348-376.
72. **Sudbery PE.** 2011. Growth of *Candida albicans* hyphae. *Nat Rev Microbiol* **9**:737-748.
73. **Hazan I, Sepulveda-Becerra M, Liu H.** 2002. Hyphal elongation is regulated independently of cell cycle in *Candida albicans*. *Mol Biol Cell* **13**:134-145.
74. **Zheng X, Wang Y, Wang Y.** 2004. Hgc1, a novel hypha-specific G1 cyclin-related protein regulates *Candida albicans* hyphal morphogenesis. *EMBO J* **23**:1845-1856.
75. **Chou H, Glory A, Bachewich C.** 2011. Orthologues of the anaphase-promoting complex/cyclosome coactivators Cdc20p and Cdh1p are important for mitotic progression and morphogenesis in *Candida albicans*. *Eukaryot Cell* **10**:696-709.
76. **Senn H, Shapiro RS, Cowen LE.** 2012. Cdc28 provides a molecular link between Hsp90, morphogenesis, and cell cycle progression in *Candida albicans*. *Mol Biol Cell* **23**:268-283.
77. **Shapiro RS, Uppuluri P, Zaas AK, Collins C, Senn H, Perfect JR, Heitman J, Cowen LE.** 2009. Hsp90 orchestrates temperature-dependent *Candida albicans* morphogenesis via Ras1-PKA signaling. *Curr Biol* **19**:621-629.
78. **Milne SW, Cheetham J, Lloyd D, Shaw S, Moore K, Paszkiewicz KH, Aves SJ, Bates S.** 2014. Role of *Candida albicans* Tem1 in mitotic exit and cytokinesis. *Fungal Genet Biol* **69**:84-95.
79. **Shirayama M, Matsui Y, Toh EA.** 1994. The yeast TEM1 gene, which encodes a GTP-binding protein, is involved in termination of M phase. *Mol Cell Biol* **14**:7476-7482.
80. **Clemente-Blanco A, Gonzalez-Novo A, Machin F, Caballero-Lima D, Aragon L, Sanchez M, de Aldana CR, Jimenez J, Correa-Bordes J.** 2006. The Cdc14p phosphatase affects late cell-cycle events and morphogenesis in *Candida albicans*. *J Cell Sci* **119**:1130-1143.
81. **Gonzalez-Novo A, Labrador L, Pablo-Hernando ME, Correa-Bordes J, Sanchez M, Jimenez J, de Aldana CRV.** 2009. Dbf2 is essential for cytokinesis and correct mitotic spindle formation in *Candida albicans*. *Molecular Microbiology* **72**:1364-1378.
82. **Bai C, Ramanan N, Wang YM, Wang Y.** 2002. Spindle assembly checkpoint component CaMad2p is indispensable for *Candida albicans* survival and virulence in mice. *Mol Microbiol* **45**:31-44.
83. **Bachewich C, Nantel A, Whiteway M.** 2005. Cell cycle arrest during S or M phase generates polarized growth via distinct signals in *Candida albicans*. *Mol Microbiol* **57**:942-959.

84. **Cote P, Hogues H, Whiteway M.** 2009. Transcriptional analysis of the *Candida albicans* cell cycle. *Mol Biol Cell* **20**:3363-3373.
85. **Jaspersen SL, Charles JF, Tinker-Kulberg RL, Morgan DO.** 1998. A late mitotic regulatory network controlling cyclin destruction in *Saccharomyces cerevisiae*. *Mol Biol Cell* **9**:2803-2817.
86. **Jimenez J, Castelao BA, Gonzalez-Novo A, Sanchez-Perez M.** 2005. The role of MEN (mitosis exit network) proteins in the cytokinesis of *Saccharomyces cerevisiae*. *Int Microbiol* **8**:33-42.
87. **Song S, Lee KS.** 2001. A novel function of *Saccharomyces cerevisiae* CDC5 in cytokinesis. *J Cell Biol* **152**:451-469.
88. **Bachewich C, Whiteway M.** 2005. Cyclin Cln3p links G1 progression to hyphal and pseudohyphal development in *Candida albicans*. *Eukaryot Cell* **4**:95-102.
89. **Bensen ES, Clemente-Blanco A, Finley KR, Correa-Bordes J, Berman J.** 2005. The mitotic cyclins Clb2p and Clb4p affect morphogenesis in *Candida albicans*. *Mol Biol Cell* **16**:3387-3400.
90. **Chapa y Lazo B, Bates S, Sudbery P.** 2005. The G1 cyclin Cln3 regulates morphogenesis in *Candida albicans*. *Eukaryot Cell* **4**:90-94.
91. **Gale CA, Leonard MD, Finley KR, Christensen L, McClellan M, Abbey D, Kurischko C, Bensen E, Tzafrir I, Kauffman S, Becker J, Berman J.** 2009. *SLA2* mutations cause *SWE1*-mediated cell cycle phenotypes in *Candida albicans* and *Saccharomyces cerevisiae*. *Microbiology* **155**:3847-3859.
92. **Brown AJ, Barelle CJ, Budge S, Duncan J, Harris S, Lee PR, Leng P, Macaskill S, Abdul Murad AM, Ramsdale M, Wiltshire C, Wishart JA, Gow NA.** 2000. Gene regulation during morphogenesis in *Candida albicans*. *Contrib Microbiol* **5**:112-125.
93. **Leuker CE, Sonneborn A, Delbruck S, Ernst JF.** 1997. Sequence and promoter regulation of the *PCK1* gene encoding phosphoenolpyruvate carboxykinase of the fungal pathogen *Candida albicans*. *Gene* **192**:235-240.
94. **Care RS, Trevethick J, Binley KM, Sudbery PE.** 1999. The MET3 promoter: a new tool for *Candida albicans* molecular genetics. *Mol Microbiol* **34**:792-798.
95. **Homann OR, Dea J, Noble SM, Johnson AD.** 2009. A phenotypic profile of the *Candida albicans* regulatory network. *PLoS Genet* **5**:e1000783.
96. **Gimeno CJ, Fink GR.** 1992. The logic of cell division in the life cycle of yeast. *Science* **257**:626.
97. **Lavoie H, Sellam A, Askew C, Nantel A, Whiteway M.** 2008. A toolbox for epitope-tagging and genome-wide location analysis in *Candida albicans*. *BMC Genomics* **9**:578.
98. **Rose MD, Winston FM, Hieter P, Sherman F, Cold Spring Harbor Laboratory Press.** 1990. *Methods in yeast genetics : a laboratory course manual*. Cold Spring Harbor Laboratory Press, Cold Spring Harbor, N.Y.
99. **Liu HL, Osmani AH, Ukil L, Son S, Markossian S, Shen KF, Govindaraghavan M, Varadaraj A, Hashmi SB, De Souza CP, Osmani SA.** 2010. Single-step affinity purification for fungal proteomics. *Eukaryot Cell* **9**:831-833.
100. **Rigaut G, Shevchenko A, Rutz B, Wilm M, Mann M, Seraphin B.** 1999. A generic protein purification method for protein complex characterization and proteome exploration. *Nat Biotechnol* **17**:1030-1032.
101. **Bousset K, Diffley JF.** 1998. The Cdc7 protein kinase is required for origin firing during S phase. *Genes Dev* **12**:480-490.

102. **Donaldson AD, Fangman WL, Brewer BJ.** 1998. Cdc7 is required throughout the yeast S phase to activate replication origins. *Genes Dev* **12**:491-501.
103. **Hardy CF, Pautz A.** 1996. A novel role for Cdc5p in DNA replication. *Mol Cell Biol* **16**:6775-6782.
104. **Ho Y, Gruhler A, Heilbut A, Bader GD, Moore L, Adams SL, Millar A, Taylor P, Bennett K, Boutilier K, Yang L, Wolting C, Donaldson I, Schandorff S, Shewnarane J, Vo M, Taggart J, Goudreault M, Muskat B, Alfarano C, Dewar D, Lin Z, Michalickova K, Willems AR, Sassi H, Nielsen PA, Rasmussen KJ, Andersen JR, Johansen LE, Hansen LH, Jespersen H, Podtelejnikov A, Nielsen E, Crawford J, Poulsen V, Sorensen BD, Matthiesen J, Hendrickson RC, Gleeson F, Pawson T, Moran MF, Durocher D, Mann M, Hogue CW, Figeys D, Tyers M.** 2002. Systematic identification of protein complexes in *Saccharomyces cerevisiae* by mass spectrometry. *Nature* **415**:180-183.
105. **Matos J, Lipp JJ, Bogdanova A, Guillot S, Okaz E, Junqueira M, Shevchenko A, Zachariae W.** 2008. Dbf4-dependent *CDC7* kinase links DNA replication to the segregation of homologous chromosomes in meiosis I. *Cell* **135**:662-678.
106. **Willmund F, del Alamo M, Pechmann S, Chen T, Albanese V, Dammer EB, Peng J, Frydman J.** 2013. The cotranslational function of ribosome-associated Hsp70 in eukaryotic protein homeostasis. *Cell* **152**:196-209.
107. **Jackson AL, Pahl PM, Harrison K, Rosamond J, Sclafani RA.** 1993. Cell cycle regulation of the yeast Cdc7 protein kinase by association with the Dbf4 protein. *Mol Cell Biol* **13**:2899-2908.
108. **Burkard ME, Maciejowski J, Rodriguez-Bravo V, Repka M, Lowery DM, Clauser KR, Zhang C, Shokat KM, Carr SA, Yaffe MB, Jallepalli PV.** 2009. Plk1 self-organization and priming phosphorylation of HsCYK-4 at the spindle midzone regulate the onset of division in human cells. *PLoS Biol* **7**:e1000111.
109. **Kaplan MH, Zong RT, Herrscher RF, Scheuermann RH, Tucker PW.** 2001. Transcriptional activation by a matrix associating region-binding protein. contextual requirements for the function of bright. *J Biol Chem* **276**:21325-21330.
110. **Rajaiya J, Hatfield M, Nixon JC, Rawlings DJ, Webb CF.** 2005. Bruton's tyrosine kinase regulates immunoglobulin promoter activation in association with the transcription factor Bright. *Mol Cell Biol* **25**:2073-2084.
111. **Webb CF.** 2001. The transcription factor, Bright, and immunoglobulin heavy chain expression. *Immunol Res* **24**:149-161.
112. **Huh WK, Falvo JV, Gerke LC, Carroll AS, Howson RW, Weissman JS, O'Shea EK.** 2003. Global analysis of protein localization in budding yeast. *Nature* **425**:686-691.
113. **Goujon M, McWilliam H, Li W, Valentin F, Squizzato S, Paern J, Lopez R.** 2010. A new bioinformatics analysis tools framework at EMBL-EBI. *Nucleic Acids Res* **38**:W695-699.
114. **Urbina H, Schuster J, Blackwell M.** 2013. The gut of Guatemalan passalid beetles: a habitat colonized by cellobiose- and xylose-fermenting yeasts. *Fungal Ecology* **6**:339-355.
115. **Suh S-O, Nguyen NH, Blackwell M.** 2008. Yeasts isolated from plant-associated beetles and other insects: seven novel *Candida* species near *Candida albicans*. *FEMS Yeast Research* **8**:88-102.
116. **Schulze J, Sonnenborn U.** 2009. Yeasts in the gut: from commensals to infectious agents. *Dtsch Arztebl Int* **106**:837-842.

117. **Errico A, Deshmukh K, Tanaka Y, Pozniakovsky A, Hunt T.** 2010. Identification of substrates for cyclin dependent kinases. *Adv Enzyme Regul* **50**:375-399.
118. **Hammacott JE, Williams PH, Cashmore AM.** 2000. *Candida albicans CFL1* encodes a functional ferric reductase activity that can rescue a *Saccharomyces cerevisiae* *fre1* mutant. *Microbiology* **146 (Pt 4)**:869-876.
119. **Hu F, Elledge SJ.** 2002. Bub2 is a cell cycle regulated phospho-protein controlled by multiple checkpoints. *Cell Cycle* **1**:351-355.
120. **Hu F, Wang Y, Liu D, Li Y, Qin J, Elledge SJ.** 2001. Regulation of the Bub2/Bfa1 GAP complex by Cdc5 and cell cycle checkpoints. *Cell* **107**:655-665.
121. **Nottrott S, Urlaub H, Luhrmann R.** 2002. Hierarchical, clustered protein interactions with U4/U6 snRNA: a biochemical role for U4/U6 proteins. *EMBO J* **21**:5527-5538.
122. **Raghunathan PL, Guthrie C.** 1998. RNA unwinding in U4/U6 snRNPs requires ATP hydrolysis and the DEIH-box splicing factor Brr2. *Curr Biol* **8**:847-855.
123. **Chan SP, Kao DI, Tsai WY, Cheng SC.** 2003. The Prp19p-associated complex in spliceosome activation. *Science* **302**:279-282.
124. **Chanarat S, Strasser K.** 2013. Splicing and beyond: the many faces of the Prp19 complex. *Biochim Biophys Acta* **1833**:2126-2134.
125. **Will CL, Luhrmann R.** 2011. Spliceosome structure and function. *Cold Spring Harb Perspect Biol* **3**.
126. **de Graffenried CL, Ho HH, Warren G.** 2008. Polo-like kinase is required for Golgi and bilobe biogenesis in *Trypanosoma brucei*. *J Cell Biol* **181**:431-438.
127. **Vaid R, Sharma N, Chauhan S, Deshta A, Dev K, Sourirajan A.** 2016. Functions of Polo-Like Kinases: A Journey From Yeast To Humans. *Protein Pept Lett* **23**:185-197.
128. **Cullen CF, May KM, Hagan IM, Glover DM, Ohkura H.** 2000. A new genetic method for isolating functionally interacting genes: high *pl01(+)*-dependent mutants and their suppressors define genes in mitotic and septation pathways in fission yeast. *Genetics* **155**:1521-1534.
129. **Causier B.** 2004. Studying the interactome with the yeast two-hybrid system and mass spectrometry. *Mass Spectrom Rev* **23**:350-367.
130. **Fields S, Song O.** 1989. A novel genetic system to detect protein-protein interactions. *Nature* **340**:245-246.
131. **Williamson MP, Sutcliffe MJ.** 2010. Protein-protein interactions. *Biochem Soc Trans* **38**:875-878.
132. **Rahal R, Amon A.** 2008. The Polo-like kinase Cdc5 interacts with FEAR network components and Cdc14. *Cell Cycle* **7**:3262-3272.
133. **Chen YC, Weinreich M.** 2010. Dbf4 regulates the Cdc5 Polo-like kinase through a distinct non-canonical binding interaction. *J Biol Chem* **285**:41244-41254.
134. **Jares P, Donaldson A, Blow JJ.** 2000. The Cdc7/Dbf4 protein kinase: target of the S phase checkpoint? *EMBO Rep* **1**:319-322.
135. **Masai H, Arai K.** 2002. Cdc7 kinase complex: a key regulator in the initiation of DNA replication. *J Cell Physiol* **190**:287-296.
136. **Chien T, Tseng TL, Wang JY, Shen YT, Lin TH, Shieh JC.** 2015. *Candida albicans DBF4* gene inducibly duplicated by the mini-Ura-blaster is involved in hypha-suppression. *Mutat Res* **779**:78-85.
137. **O'Meara TR, Veri AO, Ketela T, Jiang B, Roemer T, Cowen LE.** 2015. Global analysis of fungal morphology exposes mechanisms of host cell escape. *Nat Commun* **6**:6741.

138. **Roetzer A, Gabaldon T, Schuller C.** 2011. From *Saccharomyces cerevisiae* to *Candida glabrata* in a few easy steps: important adaptations for an opportunistic pathogen. *FEMS Microbiol Lett* **314**:1-9.
139. **Marcet-Houben M, Gabaldon T.** 2009. The tree versus the forest: the fungal tree of life and the topological diversity within the yeast phylome. *PLoS One* **4**:e4357.
140. **Atir-Lande A, Gildor T, Kornitzer D.** 2005. Role for the SCFCDC4 ubiquitin ligase in *Candida albicans* morphogenesis. *Mol Biol Cell* **16**:2772-2785.
141. **Ofir A, Kornitzer D.** 2010. *Candida albicans* cyclin Clb4 carries S-phase cyclin activity. *Eukaryot Cell* **9**:1311-1319.
142. **Shen S, Tobery CE, Rose MD.** 2009. Prm3p is a pheromone-induced peripheral nuclear envelope protein required for yeast nuclear fusion. *Mol Biol Cell* **20**:2438-2450.
143. **Fraschini R, Formenti E, Lucchini G, Piatti S.** 1999. Budding yeast Bub2 is localized at spindle pole bodies and activates the mitotic checkpoint via a different pathway from Mad2. *J Cell Biol* **145**:979-991.
144. **Hoyt MA, Totis L, Roberts BT.** 1991. *S. cerevisiae* genes required for cell cycle arrest in response to loss of microtubule function. *Cell* **66**:507-517.
145. **Foley EA, Kapoor TM.** 2013. Microtubule attachment and spindle assembly checkpoint signalling at the kinetochore. *Nat Rev Mol Cell Biol* **14**:25-37.
146. **Zhou J, Yao J, Joshi HC.** 2002. Attachment and tension in the spindle assembly checkpoint. *J Cell Sci* **115**:3547-3555.
147. **Caydasi AK, Ibrahim B, Pereira G.** 2010. Monitoring spindle orientation: Spindle position checkpoint in charge. *Cell Div* **5**:28.
148. **Toda K, Naito K, Mase S, Ueno M, Uritani M, Yamamoto A, Ushimaru T.** 2012. APC/C-Cdh1-dependent anaphase and telophase progression during mitotic slippage. *Cell Div* **7**:4.
149. **Bolanos-Garcia VM, Blundell TL.** 2011. BUB1 and BUBR1: multifaceted kinases of the cell cycle. *Trends Biochem Sci* **36**:141-150.
150. **Gale CA, Berman J.** 2012. Cell Cycle and Growth Control in *Candida* Species, *Candida* and Candidiasis, Second Edition doi:doi:10.1128/9781555817176.ch8. American Society of Microbiology.
151. **Cordin O, Beggs JD.** 2013. RNA helicases in splicing. *RNA Biol* **10**:83-95.
152. **Small EC, Leggett SR, Winans AA, Staley JP.** 2006. The EF-G-like GTPase Snu114p regulates spliceosome dynamics mediated by Brr2p, a DExD/H box ATPase. *Mol Cell* **23**:389-399.
153. **Mitrovich QM, Tuch BB, De La Vega FM, Guthrie C, Johnson AD.** 2010. Evolution of yeast noncoding RNAs reveals an alternative mechanism for widespread intron loss. *Science* **330**:838-841.
154. **Mitrovich QM, Tuch BB, Guthrie C, Johnson AD.** 2007. Computational and experimental approaches double the number of known introns in the pathogenic yeast *Candida albicans*. *Genome Res* **17**:492-502.
155. **Maslon MM, Heras SR, Bellora N, Eyraas E, Caceres JF.** 2014. The translational landscape of the splicing factor SRSF1 and its role in mitosis. *Elife* doi:10.7554/eLife.02028:e02028.
156. **Mu R, Wang YB, Wu M, Yang Y, Song W, Li T, Zhang WN, Tan B, Li AL, Wang N, Xia Q, Gong WL, Wang CG, Zhou T, Guo N, Sang ZH, Li HY.** 2014. Depletion of pre-mRNA splicing factor Cdc5L inhibits mitotic progression and triggers mitotic catastrophe. *Cell Death Dis* **5**:e1151.

157. **Karamysheva Z, Diaz-Martinez LA, Warrington R, Yu H.** 2015. Graded requirement for the spliceosome in cell cycle progression. *Cell Cycle* **14**:1873-1883.
158. **Habara Y, Urushiyama S, Shibuya T, Ohshima Y, Tani T.** 2001. Mutation in the *prp12+* gene encoding a homolog of SAP130/SF3b130 causes differential inhibition of pre-mRNA splicing and arrest of cell-cycle progression in *Schizosaccharomyces pombe*. *RNA* **7**:671-681.
159. **Sundaramoorthy S, Vazquez-Novelle MD, Lekomtsev S, Howell M, Petronczki M.** 2014. Functional genomics identifies a requirement of pre-mRNA splicing factors for sister chromatid cohesion. *EMBO J* **33**:2623-2642.
160. **van der Lelij P, Stocsits RR, Ladurner R, Petzold G, Kreidl E, Koch B, Schmitz J, Neumann B, Ellenberg J, Peters JM.** 2014. SNW1 enables sister chromatid cohesion by mediating the splicing of sororin and APC2 pre-mRNAs. *EMBO J* **33**:2643-2658.
161. **Bruno VM, Wang Z, Marjani SL, Euskirchen GM, Martin J, Sherlock G, Snyder M.** 2010. Comprehensive annotation of the transcriptome of the human fungal pathogen *Candida albicans* using RNA-seq. *Genome Res* **20**:1451-1458.
162. **Hofmann JC, Husedzinovic A, Gruss OJ.** 2010. The function of spliceosome components in open mitosis. *Nucleus* **1**:447-459.
163. **Wan Y, Zheng X, Chen H, Guo Y, Jiang H, He X, Zhu X, Zheng Y.** 2015. Splicing function of mitotic regulators links R-loop-mediated DNA damage to tumor cell killing. *J Cell Biol* **209**:235-246.
164. **Chan FL, Marshall OJ, Saffery R, Kim BW, Earle E, Choo KH, Wong LH.** 2012. Active transcription and essential role of RNA polymerase II at the centromere during mitosis. *Proc Natl Acad Sci U S A* **109**:1979-1984.
165. **Cheng L, Hunke L, Hardy CF.** 1998. Cell cycle regulation of the *Saccharomyces cerevisiae* polo-like kinase *cdc5p*. *Mol Cell Biol* **18**:7360-7370.
166. **Nagai M, Ushimaru T.** 2014. Cdh1 is an antagonist of the spindle assembly checkpoint. *Cell Signal* **26**:2217-2222.
167. **Naro C, Sette C.** 2013. Phosphorylation-mediated regulation of alternative splicing in cancer. *Int J Cell Biol* **2013**:151839.
168. **Fabrizio P1, Dannenberg J, Dube P, Kastner B, Stark H, Urlaub H, Lührmann R.** 2009. The evolutionarily conserved core design of the catalytic activation step of the yeast spliceosome. *Mol Cell* **36**(4):593-608.

4.7 SUPPLEMENTARY DATA

Table S4.1: Spliceosomal proteins in *S. cerevisiae* and orthologs in *C. albicans*¹

<i>S. cerevisiae</i>		<i>C. albicans</i>	
Systemic name	Standard name	Assembly Identifier	Systemic name
Sm proteins			
YER029C	<i>SMB1</i>	<i>ORF19.2621</i>	Uncharacterized
YGR074W	<i>SMD1</i>	<i>ORF19.7673</i>	Uncharacterized (SMD1)
YLR275W	<i>SMD2</i>	<i>ORF19.5486.1</i>	SMD2
YLR147C	<i>SMD3</i>	<i>ORF19.4146</i>	SMD3
YOR159C	<i>SME1</i>	<i>ORF19.4205.1</i>	SME1
YPR182W	<i>SMX3</i>	<i>ORF19.4340</i>	Uncharacterized
YFL017W-A	<i>SMX2</i>	<i>ORF19.836.1</i>	Uncharacterized
U1 snRNP proteins			
YML046W	<i>PRP39</i>	<i>OR19.1492</i>	PRP39
YGR013W	<i>SNU71</i>	<i>OR19.1491</i>	Uncharacterized (SNU71)
YKL012W	<i>PRP40</i>	<i>OR19.3250</i>	Uncharacterized (PRP40)
YDR235W	<i>PRP42</i>	<i>OR19.4374</i>	PRP42
YHR086W	<i>NAM8</i>	<i>OR19.1876</i>	Uncharacterized (NAM8)
YDR240C	<i>SNU56</i>	NO HIT	
YIL061C	<i>SNP1</i>	<i>OR19.6866</i>	Uncharacterized (U1-70K)
YBR119W	<i>MUD1</i>	<i>OR19.7375</i>	Uncharacterized (USA1)
YDL087C	<i>LUC7</i>	<i>OR19.3116</i>	EXM2 (LUC7)
YLR298C	<i>YHC1</i>	<i>OR19.5492</i>	Uncharacterized (YHC1)
U2 snRNP proteins			
YML049C	<i>RSE1</i>	<i>ORF19.5391</i>	Uncharacterized (SAP130)
YMR288W	<i>HSH155</i>	<i>ORF19.2675</i>	Uncharacterized (HSH155)
YDL030W	<i>PRP9</i>	<i>ORF19.3178</i>	Uncharacterized (PRP9)
YMR240C	<i>CUS1</i>	<i>ORF19.7581</i>	Uncharacterized (CUS1)
YJL203W	<i>PRP21</i>	<i>ORF19.4659</i>	Uncharacterized (SAP114)
YDL043C	<i>PRP11</i>	<i>ORF19.4724</i>	Uncharacterized (SAP62)
YPL213W	<i>LEA1</i>	<i>ORF19.1260</i>	LEA1
YOR319W	<i>HSH49</i>	<i>ORF19.2261</i>	Uncharacterized (SAP49, HSH49)
YIR009W	<i>MSL1</i>	<i>ORF19.4748</i>	Uncharacterized (MSL1)
YPR094W	<i>RDS3</i>	<i>ORF19.2230</i>	Uncharacterized
YNL138W-A	<i>YSF3</i>	NO HIT	

U5 snRNP proteins

YHR165C	<i>PRP8</i>	<i>ORF19.6442</i>	PRP8
YER172C	<i>BRR2</i>	<i>ORF19.3098</i>	Uncharacterized (BRR2)
YKL173W	<i>SNU114</i>	<i>ORF19.144</i>	SNU114
YBR055C	<i>PRP6</i>	<i>ORF19.6356</i>	Uncharacterized (PRP6)
YDR243C	<i>PRP28</i>	<i>ORF19.672</i>	Uncharacterized (PRP28)
YHR156C	<i>LIN1</i>	<i>ORF19.2368</i>	Uncharacterized (LIN1)
YPR082C	<i>DIB1</i>	<i>ORF19.1975</i>	Uncharacterized (DIB1)

U4/U6 snRNP proteins

YGR091W	<i>PRP31</i>	<i>ORF19.1296</i>	Uncharacterized (PRP31)
YDR473C	<i>PRP3</i>	<i>ORF19.910</i>	PRP3
YPR178W	<i>PRP4</i>	<i>ORF19.7343</i>	Uncharacterized (PRP4)
YEL026W	<i>SNU13</i>	<i>ORF19.5885</i>	Uncharacterized (SNU13)

U4/U6.U5 snRNP proteins

YOR308C	<i>SNU66</i>	<i>ORF19.4326</i>	Uncharacterized (SNU66)
YFR005C	<i>SAD1</i>	<i>ORF19.2608</i>	ADH5 (SAD1)
YBR152W	<i>SPP381</i>	NO HIT	
YGR075C	<i>PRP38</i>	<i>ORF19.2303</i>	FGR16 (PRP38)
YDL098C	<i>SNU23</i>	<i>ORF19.1548</i>	SNU23

Lsm proteins

YER112W	<i>LSM4</i>	<i>ORF19.6458.1</i>	Uncharacterized
YNL147W	<i>LSM7</i>	<i>ORF19.2639.1</i>	Uncharacterized
YJR022W	<i>LSM8</i>	<i>ORF19.4305.1</i>	Uncharacterized
YBL026W	<i>LSM2</i>	<i>ORF19.514</i>	SNP3
YER146W	<i>LSM5</i>	<i>ORF19.7256</i>	Uncharacterized (LSM5)
YLR438C-A	<i>LSM3</i>	<i>ORF19.6135.1</i>	SMX4
YDR378C	<i>LSM6</i>	<i>ORF19.7509.2</i>	LSM6

RES complex

YGL174W	<i>BUD13</i>	<i>ORF19.4964</i>	Uncharacterized
YLR016C	<i>PML1</i>	NO HIT	
YIR005W	<i>IST3 (SNU17)</i>	<i>ORF19.1045</i>	Uncharacterized (IST3)

NTC/Prp19 complex

YDR416W	<i>SYF1</i>	<i>ORF19.2893</i>	Uncharacterized (SYF1)
YLR117C	<i>CLF1</i>	<i>ORF19.332</i>	Uncharacterized (CLF1)
YMR213W	<i>CEF1</i>	<i>ORF19.4799</i>	CEF1
YLL036C	<i>PRP19</i>	<i>ORF19.6740</i>	Uncharacterized (PRP19)
YJR050W	<i>ISY1</i>	<i>ORF19.6685</i>	ISY1
YGR129W	<i>SYF2</i>	<i>ORF19.7139</i>	Uncharacterized

YPR101W	<i>SNT309</i>	NO HIT	
YBR188C	<i>NTC20</i>	NO HIT	
NTC-Related Proteins			
YPL151C	<i>PRP46</i>	<i>ORF19.5413</i>	Uncharacterized (PRP46)
YAL032C	<i>PRP45</i>	<i>ORF19.5513</i>	PRP45
YBR065C	<i>ECM2</i>	<i>ORF19.5364</i>	Uncharacterized (ECM2)
YDL209C	<i>CWC2</i>	<i>ORF19.674</i>	Uncharacterized (CWC2)
YDR163W	<i>CWC15</i>	<i>ORF19.6360</i>	Uncharacterized (CWC15)
YCR063W	<i>BUD31</i>	<i>ORF19.4855</i>	BUD31
Early Splicing Factors			
YBR237W	<i>PRP5</i>	<i>ORF19.6831</i>	PRP5
YPR152C		<i>ORF19.5976</i>	Uncharacterized
Known Splicing Factors			
YNR011C	<i>PRP2</i>	<i>ORF19.5865</i>	Uncharacterized (PRP2)
YOR148C	<i>SPP2</i>	<i>ORF19.7620</i>	Uncharacterized
YKL095W	<i>YJU2</i>	<i>ORF19.5465</i>	Uncharacterized (YJU2)
YDR482C	<i>CWC21</i>	<i>ORF19.4875</i>	Uncharacterized (CWC21)
YGR278W	<i>CWC22</i>	<i>ORF19.1771</i>	CWC22
YLR323C	<i>CWC24</i>	<i>ORF19.2105</i>	Uncharacterized (CWC24)
YPL064C	<i>CWC27</i>	<i>ORF19.1735</i>	Uncharacterized
YGL128C	<i>CWC23</i>	<i>ORF19.3785</i>	Uncharacterized
YNL245C	<i>CWC25</i>	<i>ORF19.1281</i>	Uncharacterized (CWC25)
Step 2 Proteins			
YDR364C	<i>CDC40 (PRP17)</i>	<i>ORF19.6347</i>	Uncharacterized (CDC40)
YER013W	<i>PRP22</i>	<i>ORF19.4033</i>	PRP22
YKR086W	<i>PRP16</i>	<i>ORF19.2818</i>	Uncharacterized (PRP16)
YDR088C	<i>SLU7</i>	<i>ORF19.6827</i>	SLU7
YGR006W	<i>PRP18</i>	<i>ORF19.2112</i>	Uncharacterized (PRP18)
Disassembly proteins			
YGL120C	<i>PRP43</i>	<i>ORF19.1687</i>	Uncharacterized (PRP43)
YLR424W	<i>SPP382</i>	<i>ORF19.2980</i>	Uncharacterized (TIP39)
YKR022C	<i>NTR2</i>	NO HIT	
CBP Proteins			
YMR125W	<i>STO1</i>	<i>Orf19.387</i>	GCR3
YPL178W	<i>CBC2</i>	<i>ORF19.763</i>	Uncharacterized (CBC2)

¹Systemic names of Spliceosomal proteins from Fabrizio *et al.*, 2009 (168) in *S. cerevisiae* were plugged in SGD (<http://www.yeastgenome.org/>) to obtain the standard name, which was then plugged in CGD (<http://www.candidagenome.org/>) to obtain orthologs in *C. albicans*. Aliases are shown in brackets.

Table S4.2: Cdc5p interacting proteins in *S. cerevisiae* and orthologs in *C. albicans*¹.

<i>S. cerevisiae</i>		<i>C. albicans</i>	
Gene Systematic Name	Gene Name	Assembly identifier number	Standard name
YNL172W	<i>APC1</i>	<i>ORF19.6046</i>	<i>APC1</i>
YDL008W	<i>APC11</i>	<i>ORF19.7644</i>	Uncharacterized (APC11)
YLR127C	<i>APC2</i>	<i>ORF19.6821</i>	Uncharacterized (APC2)
YDR118W	<i>APC4</i>	<i>ORF19.5692</i>	Uncharacterized
YLR102C	<i>APC9</i>	<i>ORF19.5804</i>	<i>HYU1</i>
YPL255W	<i>BBP1</i>	<i>ORF19.6027</i>	Uncharacterized
YJR053W	<i>BFA1</i>	<i>ORF19.6080</i>	<i>BFA1</i>
YMR055C	<i>BUB2</i>	<i>ORF19.5827</i>	<i>BUB2</i>
YJR076C	<i>CDC11</i>	<i>ORF19.5691</i>	<i>CDC11</i>
YHR107C	<i>CDC12</i>	<i>ORF19.3013</i>	<i>CDC12</i>
YFR028C	<i>CDC14</i>	<i>ORF19.4192</i>	<i>CDC14</i>
YAR019C	<i>CDC15</i>	<i>ORF19.3545</i>	<i>CDC15</i>
YKL022C	<i>CDC16</i>	<i>ORF19.1792</i>	Uncharacterized (CDC16)
YFR036W	<i>CDC26</i>	<i>ORF19.5617</i>	Uncharacterized
YBL084C	<i>CDC27</i>	<i>ORF19.3231</i>	<i>CDC27</i>
YBR160W	<i>CDC28</i>	<i>ORF19.3856</i>	<i>CDC28</i>
YDL126C	<i>CDC48</i>	<i>ORF19.2340</i>	<i>CDC48</i>
YDL017W	<i>CDC7</i>	<i>ORF19.3561</i>	<i>CDC7</i>
YGL003C	<i>CDH1</i>	<i>ORF19.2084</i>	<i>CDH1</i>
YMR012W	<i>CLU1</i>	<i>ORF19.51</i>	Uncharacterized (CLU1)
YPR013C	<i>CMR3</i>	<i>ORF19.217</i>	Uncharacterized
YNL225C	<i>CNM67</i>	<i>ORF19.6213</i>	<i>SUI2</i>
YKL049C	<i>CSE4</i>	<i>ORF19.6163</i>	<i>CSE1</i>
YGR092W	<i>DBF2</i>	<i>ORF19.1223</i>	<i>DBF2</i>
YDR052C	<i>DBF4</i>	<i>ORF19.5166</i>	<i>DBF4</i>
YDR273W	<i>DON1</i>	<i>ORF19.448</i>	<i>CUE5</i>
YAL026C	<i>DRS2</i>	<i>ORF19.6778</i>	Uncharacterized (DRS2)
YGR098C	<i>ESP1</i>	<i>ORF19.3356</i>	<i>ESP1</i>
YNL068C	<i>FKH2</i>	<i>ORF19.5389</i>	<i>FKH2</i>
YBR045C	<i>GIP1</i>	<i>ORF19.3109</i>	Uncharacterized
YER133W	<i>GLC7</i>	<i>ORF19.6285</i>	<i>GLC7</i>
YEL017W	<i>GTT3</i>	<i>ORF19.3430</i>	Uncharacterized (BUD21)

YDL223C	<i>HBT1</i>	<i>ORF19.4072</i>	<i>IFF6</i>
YMR032W	<i>HOF1</i>	<i>ORF19.5664</i>	<i>HOF1</i>
YJL057C	<i>IKS1</i>	<i>ORF19.428</i>	Uncharacterized (IKS1)
YJL106W	<i>IME2</i>	<i>ORF19.2395</i>	<i>IME2</i>
YJL051W	<i>IRC8</i>	<i>ORF19.1334</i>	Uncharacterized
YIL026C	<i>IRR1</i>	<i>ORF19.7232</i>	<i>IRR1</i>
YPR067W	<i>ISA2</i>	<i>ORF19.6811</i>	<i>ISA2</i>
YDR229W	<i>IVY1</i>	<i>ORF19.6152</i>	Uncharacterized
YLR347C	<i>KAP95</i>	<i>ORF19.3681</i>	Uncharacterized (KAP95)
YAL018C	<i>LDS1</i>	<i>ORF19.6405</i>	Uncharacterized
YDR439W	<i>LRS4</i>	<i>ORF19.5373</i>	Uncharacterized (POL98, POL0)
YHR121W	<i>LSM12</i>	<i>ORF19.3698</i>	Uncharacterized
YER106W	<i>MAM1</i>	<i>ORF19.7440</i>	<i>HST6</i>
YDL003W	<i>MCD1</i>	<i>ORF19.7634</i>	<i>MCD1</i>
YMR036C	<i>MIH1</i>	<i>ORF19.3071</i>	<i>MIH1</i>
YHR015W	<i>MIP6</i>	<i>ORF19.3037</i>	Uncharacterized (PAB1)
YBR098W	<i>MMS4</i>	<i>ORF19.3648</i>	Uncharacterized
YDL028C	<i>MPS1</i>	<i>ORF19.7293</i>	<i>MPS1</i>
YJL019W	<i>MPS3</i>	<i>ORF19.2763</i>	Uncharacterized
YDR386W	<i>MUS81</i>	<i>ORF19.4206</i>	Uncharacterized (MUS81)
YLR457C	<i>NBP1</i>	<i>ORF19.3387</i>	Uncharacterized (POL90)
YIL144W	<i>NDC80</i>	<i>ORF19.2827</i>	Uncharacterized (TID3)
YOR372C	<i>NDD1</i>	<i>NO HIT</i>	
YJL076W	<i>NET1</i>	<i>ORF19.267</i>	Uncharacterized
YNL175C	<i>NOP13</i>	<i>ORF19.6766</i>	<i>NOP13</i>
YDR432W	<i>NPL3</i>	<i>ORF19.7238</i>	<i>NPL3</i>
YOR373W	<i>NUD1</i>	<i>ORF19.6789</i>	Uncharacterized (NUD1)
YMR076C	<i>PDS5</i>	<i>ORF19.2216</i>	<i>PDS5</i>
YPL154C	<i>PEP4</i>	<i>ORF19.1891</i>	<i>APR1 (PEP4)</i>
YNL102W	<i>POL1</i>	<i>ORF19.5873</i>	<i>POL1</i>
YPL192C	<i>PRM3</i>	<i>NO HIT</i>	
YDL006W	<i>PTC1</i>	<i>ORF19.4785</i>	<i>PTC1</i>
YPL153C	<i>RAD53</i>	<i>ORF19.6936</i>	<i>RAD53</i>
YDR217C	<i>RAD9</i>	<i>ORF19.4275</i>	<i>RAD9</i>
YPR007C	<i>REC8</i>	<i>ORF19.776</i>	Uncharacterized (SPO69)
YPR115W	<i>RGC1</i>	<i>ORF19.3505</i>	Uncharacterized
YHR027C	<i>RPN1</i>	<i>ORF19.4956</i>	<i>RPN1</i>
YIL075C	<i>RPN2</i>	<i>ORF19.5260</i>	<i>RPN2</i>
YKL145W	<i>RPT1</i>	<i>ORF19.441</i>	<i>RPT1</i>
YDR394W	<i>RPT3</i>	<i>ORF19.5793</i>	<i>PR26</i>

YOR259C	<i>RPT4</i>	<i>ORF19.482</i>	<i>RPT4</i>
YOR117W	<i>RPT5</i>	<i>ORF19.3123</i>	<i>RPT5</i>
YGL048C	<i>RPT6</i>	<i>ORF19.3593</i>	<i>RPT6</i>
YLR357W	<i>RSC2</i>	<i>ORF19.2964</i>	Uncharacterized (<i>RSC2</i>)
YGL175C	<i>SAE2</i>	<i>ORF19.4988</i>	Uncharacterized
YOR195W	<i>SLK19</i>	<i>ORF19.6763</i>	<i>SLK19</i>
YFL008W	<i>SMC1</i>	<i>ORF19.4367</i>	<i>SMC1</i>
YJL074C	<i>SMC3</i>	<i>ORF19.262</i>	<i>SMC3</i>
YDR477W	<i>SNF1</i>	<i>ORF19.1936</i>	<i>SNF1</i>
YGL115W	<i>SNF4</i>	<i>ORF19.5768</i>	<i>SNF4</i>
YDR356W	<i>SPC110</i>	<i>ORF19.2629</i>	<i>USO1</i>
YAL047C	<i>SPC72</i>	<i>ORF19.6583</i>	Uncharacterized
YHR172W	<i>SPC97</i>	<i>ORF19.708</i>	Uncharacterized (<i>SPC97</i>)
YHR014W	<i>SPO13</i>	<i>ORF19.3877</i>	Uncharacterized
YNL189W	<i>SRP1</i>	<i>ORF19.5682</i>	Uncharacterized (<i>SRP1</i>)
YNL209W	<i>SSB2</i>	<i>ORF19.6367</i>	<i>SSB1</i>
YHR184W	<i>SSP1</i>	<i>ORF19.3173</i>	Uncharacterized (<i>SSP120</i>)
YLR045C	<i>STU2</i>	<i>ORF19.6610</i>	Uncharacterized (<i>STU2</i>)
YBR231C	<i>SWC5</i>	<i>ORF19.5772</i>	Uncharacterized (<i>AOR1</i>)
YJL187C	<i>SWE1</i>	<i>ORF19.4867</i>	<i>SWE1</i>
YML064C	<i>TEM1</i>	<i>ORF19.3001</i>	<i>TEM1</i>
YML085C	<i>TUB1</i>	<i>ORF19.7308</i>	<i>TUB1</i>
YLR425W	<i>TUS1</i>	<i>ORF19.6842</i>	<i>TUS1</i>
YLL039C	<i>UBI4</i>	<i>ORF19.6771</i>	<i>UBI4</i>
YIL031W	<i>ULP2</i>	<i>ORF19.4353</i>	<i>ULP2</i>
YDL186W	<i>YDL186W</i>	NO HIT	
YHR097C	<i>YHR097C</i>	<i>ORF19.1658</i>	Uncharacterized
YPR058W	<i>YMC1</i>	<i>ORF19.4447</i>	<i>YMC1</i>
YOR192C-A	<i>YOR192C-A</i>	<i>ORF19.2538</i>	<i>PTC2</i>
YPL150W	<i>YPL150W</i>	<i>ORF19.4518</i>	Uncharacterized
YPR174C	<i>YPR174C</i>	<i>ORF19.4713</i>	Uncharacterized

¹A list of 103 Cdc5p physical interactors were obtained from SGD (<http://www.yeastgenome.org/>). Each gene name was plugged in CGD (<http://www.candidagenome.org/>) to obtain orthologs in *C. albicans*. For genes, where no hit was obtained in CGD, protein sequence was retrieved from SGD and plugged in CGD Blast (http://www.candidagenome.org/cgi-bin/compute/blast_clade.pl). Aliases are shown in brackets.

CHAPTER 5

Ch. 5: Discussion

Candida albicans is a leading human fungal pathogen that can cause systemic infections associated with high mortality rates (1). In order to enhance the small repertoire of therapeutic treatments, there is a strong need to identify new drug targets. This in turn requires comprehensive knowledge of the regulation of fungal cell proliferation in the host and virulence determinants. My work aimed to further our understanding of the networks governing mitosis in *C. albicans*, with a focus on the roles of a conserved mitotic regulator, the Plk Cdc5p, as well as to elucidate how mitosis is linked to a novel form of polar growth and expression of virulence genes. Previous work showed that depletion of Cdc5p in *C. albicans* yeast cells impaired spindle elongation and blocked mitosis, but cells subsequently formed filaments that expressed hyphal-specific virulence genes under yeast growth conditions (2). In contrast, cells of most other organisms cease growth and proliferation upon mitotic arrest. The results in *C. albicans* demonstrated a novel link between mitosis and morphogenesis. However, we knew very little about the regulation of these processes and the mechanisms of Cdc5p action in *C. albicans*. Further, the nature of the filaments that formed in response to a mitotic block and the mechanisms driving their formation and virulence gene expression were elusive. My work addressed these questions and provided significant new insights on (a) the networks controlling mitotic progression in *C. albicans*; (b) the strategies that *C. albicans* can utilize to modulate growth mode and expression of virulence genes; and (c) the function and targets of Plks, including a fungal-specific factor.

5.1 The APC/C cofactors Cdc20p and Cdh1p employ conserved and novel mechanisms of action during mitosis and morphogenesis in *C. albicans*, and may mediate in part Cdc5p function.

The APC/C is a conserved regulator of mitosis that targets specific mitotic regulators for destruction (3) and is regulated in part by Plks (4). Based on this, we hypothesized that the APC/C may be important for mitosis in *C. albicans* and may mediate, in part, Cdc5p function. Through investigating homologues of APC/C cofactors Cdc20p and Cdh1p, we provided the first characterization of APC/C function in *C. albicans*. These factors showed some conservation in

function in targeting a mitotic cyclin for degradation, and in influencing the metaphase-to-anaphase transition and mitotic exit. However, the data suggested that these proteins also have novel functions or mechanisms of action. First, *C. albicans* lacks a sequence homologue of a securin, a target of Cdc20p in organisms ranging from yeast to humans that prevents the enzyme separase from cleaving cohesion, which in turn adheres sister chromatids. Cdc20p may thus target a different factor(s) in *C. albicans*, consistent with other modes of cell cycle re-wiring in this organism (5). Intriguingly, another student in the lab affinity-purified the *C. albicans* separase, and one interacting factor is a novel, *Candida*-specific protein with some characteristics of a securin (S. Sparapani, data unpublished). Second, cells lacking Cdh1p were enlarged. In contrast, *S. cerevisiae* Δ *cdh1* cells were significantly reduced in size, implying a role in negatively regulating Start (6). The absence of human or mouse homologue of *CDH1*, *FZR1*, similarly resulted in a decrease in G1 phase (7). These results enhance our knowledge of the circuitry controlling mitosis in *C. albicans*, and suggest variations compared to other systems, including humans, which have important implications for controlling growth and therapeutic potential.

Our results also suggest that Cdc20p and Cdh1p may lie downstream of Cdc5p, and influence morphogenesis in *C. albicans*. For example, depletion of Cdc20p resulted in defects in mitosis and morphogenesis similar to those in Cdc5p-depleted cells, suggesting that the factors lie in a similar pathway governing mitotic progression and polarized growth. In support of this, Plks regulate Cdc20p directly or indirectly in other systems (8, 9). Plks also can act upstream of the Spindle Assembly Checkpoint (SAC) factor Mad2p, which binds and inactivates Cdc20p (10, 11). Cdh1p also lies downstream of Cdc5p function in *S. cerevisiae*, as Cdc5p is a component of the FEAR and MEN pathways that act to release Cdc14p from the nucleolus and ultimately activate Cdh1p (12, 13). Cdh1p then acts on Cdc5p by targeting it for degradation. The absence of Cdh1p did not phenocopy the absence of Cdc5p in *C. albicans* yeast cells. However, the high proportion of filamentous cells in the former, coupled with the absence of synergistic effects when *CDH1* was deleted from Cdc5p-depleted cells, suggests that Cdh1p may lie downstream of Cdc5p function in *C. albicans*, albeit not as a direct target. Future investigations will involve elucidating the mechanisms of action of Cdc20p and Cdh1p by identifying their targets, screening these for potential cell cycle and polarity regulatory functions, and defining the relationships

between Cdc5p, Cdc20p and Cdh1p.

5.2 Cdc5p-depleted filaments are elongated buds that transition to the hyphal fate over time in a Ume6p-dependent manner.

The nature and physiological significance of the filaments that formed in response to Cdc5p depletion, or by blocking mitosis through other means including depletion of Cdc20p, have been controversial (14, 15). Further, the mechanisms underlying the formation and expression of hyphal virulence genes, in the absence of normal environmental cues, were unclear. One study demonstrated that filament formation and expression of some hyphal-specific genes in response to Hsp90p depletion and a block in mitosis were mediated by a novel signaling pathway involving the transcription factor, Hms1p (16). However, Hsp90p has multiple targets. Further, these and other studies that characterized mitotic arrest-induced filaments were performed at a single time point, sometimes as late as 24 h after the initial gene shut-off or treatment (17-19). Based on previous results obtained from Cdc5p-depleted filaments (2, 20), we proposed that due to defects in the yeast bud switching from polar to isometric growth in early mitosis, mitotic-arrested filaments were initially elongated buds but adapted the hyphal fate later in time due to maintenance of polarized growth. This in turn could provide an advantage for the organism in terms of survival in the host and being able to escape environments that were imposing a mitotic stress. I tested this hypothesis by conducting the first time-course based analysis of the polar growth machinery and requirement for specific hyphal regulatory factors in mitotic-arrested cells. My findings indicated that hyphal-specific features emerged at only later stages of growth, supporting the hypothesis. For example, I detected hyphal-specific organization of the myosin light chain Mlc1p, hyperphosphorylation of the Cdc42p GAP Rga2p, and expression of hyphal-specific genes including the transcription factors *UME6* and *HGC1*, and the cell wall protein *HWPI*, in only later stage Cdc5p-depleted filaments, with the latter being dependent on the presence of Ume6p. Further, absence of Ume6p or Hgc1p influenced filament integrity and morphology only after an extended period of Cdc5p depletion. Finally, I demonstrated that polarized growth and *UME6* expression in Cdc5p-depleted cells were independent of the transcription factor Hms1p. We suggest that induction of *UME6*, a core hyphal regulator, may occur in response to maintenance of polarized growth and enhanced actin polymerization at the

polar tip. Consistent with this, previous work demonstrated that cellular actin can influence cAMP production, which is important for hyphal gene expression, via a sensor/effector apparatus including G actin and adenylyl cyclase components (21). Further, actin dynamics can influence expression of hyphal-specific genes, such as *HWPI* (22).

An important question stemming from these results is how the yeast bud may maintain polarized growth to initiate filament formation and allow the subsequent transition to the hyphal fate. In *S. cerevisiae*, yeast buds grow in a polar manner from G1/S to late G2 phase of the cell cycle, and then switch to isometric growth (23). The switch is regulated in part by the CDK Cdc28p falling under the control of the B-type cyclin Clb2p, which in turn causes disassembly of the Cdc24p-Bem1p-Cla4p complex, a decrease in Cdc42p-GTP, and depolarization of actin patches (23, 24). In *C. albicans*, yeast buds show similar growth patterns but the precise timing and mechanisms underlying the depolarizing switch are not yet known (25, 26). Our results provide new insights in this area and suggest that Cdc5p may influence the yeast bud growth pattern. A direct role is possible based on the fact that Plks can regulate cytoskeletal and polarity-regulating factors in other organisms including *S. cerevisiae* (27, 28). Polarity-regulatory factors were not uncovered in our Cdc5p protein interaction screen for *C. albicans*, but this does not rule out direct effects, as the screen was likely not saturated. Alternatively, Cdc5p's influence on yeast bud growth may be indirect. Indeed, depletion of Cdc20p similarly influenced the bud growth pattern. In this case, perhaps Cdc20p targets factor(s) that are important for the yeast bud transitioning from polar to isometric growth. If Cdc5p helps to activate Cdc20p, this could explain the similar effect on yeast bud growth in the absence of either factor.

Collectively our results clarify the nature of the cells produced through depletion of Cdc5p, underscore the concept that not all filamentous growth forms in *C. albicans* are created equal, and thus expand on the multiple strategies *C. albicans* can utilize for modulating growth mode and expression of virulence determinants. The ability of yeast cells to grow in a polarized fashion when experiencing a stress in mitosis, as opposed to arresting as a large doublet like non-pathogenic yeasts including *S. cerevisiae* do, coupled with a transition to the hyphal fate that includes strong expression of many virulence genes, would clearly provide an advantage for the organism to escape a stressful environment and enhance survival in the host. This is underscored

by the fact that the response requires mitotic checkpoints, and checkpoint factors such as Mad2p and Swe1p are required for growth *in vivo* and for virulence (29, 30). In this way, mitotic progression can be coupled to a polarized growth mode and the hyphal program. Future work will focus on elucidating the regulation of the polar-to-isometric growth switch in yeast buds, which has not been defined in *C. albicans*, exploring the potential contributions of Cdc5p and Cdc20p in this process, and clarifying the mechanisms by which maintenance of polarized growth of the yeast bud leads to induction of a core hyphal regulator, *UME6*.

5.3 Orf19.3714p is a novel, *Candida*-specific Plk-interacting factor that may be important for mitotic checkpoints in *C. albicans*.

Our results extend the repertoire of Plk substrates, and demonstrate that one is specific to *Candida* species and may be important for the mitotic checkpoints, which has strong therapeutic potential. Orf19.3714p was one of the most abundant proteins co-purifying with Cdc5p. Genetic approaches demonstrated that *ORF19.3714* was not essential for yeast or hyphal growth, but cells depleted of Cdc5p and lacking Orf19.3714p showed rebudding, suggesting an escape from the mitotic block. Similar results were obtained with the absence of the spindle factor checkpoint Bub2p (20). Further, Orf19.3714p was post-translationally modified in cells blocked in mitosis. Coupled with the fact that Orf.19.3714p is a predominant interacting factor of a mitotic Plk, the data suggest that Orf19.3714p may contribute to the maintenance of the mitotic checkpoints. Orf19.3714p may be a substrate of Cdc5p due to the fact that it contains several consensus PBD and Plk phosphorylation sites (31, 32), and was required in part to maintain the Cdc5p-depleted phenotype. Plks bind mitotic checkpoint pathway components in other systems (33, 34). However, Orf19.3714p is not likely to be a divergent form of a known checkpoint component, since *C. albicans* contains homologues of all mitotic checkpoint pathway components in the related *S. cerevisiae*. Novel, organism-specific binding proteins of Plks have been reported previously in other systems. For example, the Plk TbPLK in the trypanosome *T. brucei* binds trypanosome-specific proteins that associate with the cytoskeleton (35) and the basal body (36). However, TbPLK lacks conserved Plk residues involved in substrate binding, and strictly functions during cytokinesis, not mitosis. We thus propose that Orf19.3714p represents a novel Plk-interacting protein that influences the mitotic checkpoints.

The fact that Orf19.3714p is novel, fungal-specific and influences the mitotic checkpoint has critical implications for the development of new therapeutic strategies, particularly if it is found to be essential for growth *in vivo* like many other factors that influence cell cycle checkpoints in *C. albicans* (29, 30). The identification of new therapeutic drugs involves screening small compounds that may target virulence-determining traits, such as the yeast-to-hyphal transition, cell proliferation or other processes (37, 38), or proteins that are important for these processes. Future work will involve testing the importance of Orf19.3714p for growth and virulence *in vivo* using deletion strains in an *in vivo* model of mouse infection, and initiating screens for small molecule interactions.

5.4 Orf19.3714p is associated with the spliceosome and potentially links Plk function to RNA splicing.

Our finding that Orf19.3714p also co-precipitated with numerous proteins of the spliceosome complex suggests that Orf19.3714p may play a role in RNA splicing. Orf19.3714p may be a novel component or regulator of the spliceosome, although we cannot rule out the possibility that it is a divergent form of a known spliceosome component. Spliceosome function and post-transcriptional regulation of mitosis and other processes in *C. albicans* remain poorly explored areas. Our first systematic analysis of putative spliceosome composition in *C. albicans* demonstrates strong conservation compared to the model yeast *S. cerevisiae* and humans (data not shown). However, differences including absence of some factors and the involvement of at least one novel protein, Orf19.3714p, suggest organism-specific features in this important regulatory complex. Since the majority of the interactions between Orf19.3714p and spliceosome proteins were lost in the absence of Cdc5p, the data suggest for the first time that Plk function may extend to regulation of RNA splicing. This provides yet another example of potential variation in cell cycle factor function in *C. albicans*.

Based on the data, we propose a model whereby Orf19.3714p is a spliceosome-associated protein regulated in part by Cdc5p, which influences efficient splicing of factors including regulators of the mitotic checkpoints and/or mitotic exit. In agreement with this, depletion of various spliceosome proteins in other organisms can influence mitotic progression through

deregulating splicing of messages encoding for spindle, kinetochore and M phase proteins, for example (39) and absence of spliceosome factors can differentially affect splicing of transcripts (40, 41). Further, *C. albicans* genes containing introns have functions associated with microtubules, ribosomes, meiosis, splicing, mitochondrial respiration, protein degradation (42) and mitotic progression (43). Another possibility is that Orf19.3714p itself functions as a mitotic regulator, perhaps in the mitotic checkpoint pathway, but also can bind to and regulate the spliceosome, comparable to the situation with Bub3p in fibroblasts (44).

Future work will involve confirming interactions between Orf19.3714p and various spliceosome proteins using co-immunoprecipitation, repeating the affinity purification of Orf19.3714p in cells depleted of Cdc20p vs Cdc5p, sequencing RNA for strains with or without Orf19.3714p and Cdc5p to obtain evidence for an influence on splicing, localizing Orf19.3714p to help further deduce its function, conducting *in vivo* growth and virulence assays using mouse models for infection, and analyzing the levels and phosphorylation status of Orf19.3714p during the course of a normal cell cycle and under different growth and stress conditions to glean information on its regulation.

5.5 Summary

In summary, my investigations provide the first characterization of APC/C co-factors Cdc20p and Cdh1p in *C. albicans*, and suggest that they are important for mitotic progression, influence morphogenesis and may lie downstream of Cdc5p. I also clarify the nature of the polarized cells that form in response to Cdc5p depletion and uncover a new mechanism by which yeast cell mitosis may be linked to the hyphal regulatory program and expression of virulence genes. Finally, I provide new insights on Plk function and mechanisms of action by identifying a novel, fungal-specific interacting protein of Cdc5p, Orf19.3714p, which may contribute to spliceosome function. This work further underscores the emerging theme of variation in cell cycle factor function and circuitry in *C. albicans* (2, 45-49), broadens our understanding of how basic growth and cell division are controlled in this organism, reveals new factors and pathways that could be targeted for the purposes of controlling growth of the pathogen, and sets the stage for future investigations of post-transcriptional regulation at the level of RNA splicing, which

remains a poorly explored area in *C. albicans* biology.

5.6 References

1. **Miller LG, Hajjeh RA, Edwards JE, Jr.** 2001. Estimating the cost of nosocomial candidemia in the united states. *Clin Infect Dis* **32**:1110.
2. **Bachewich C, Thomas DY, Whiteway M.** 2003. Depletion of a polo-like kinase in *Candida albicans* activates cyclase-dependent hyphal-like growth. *Mol Biol Cell* **14**:2163-2180.
3. **Castro A, Bernis C, Vigneron S, Labbe JC, Lorca T.** 2005. The anaphase-promoting complex: a key factor in the regulation of cell cycle. *Oncogene* **24**:314-325.
4. **Hansen DV, Loktev AV, Ban KH, Jackson PK.** 2004. Plk1 regulates activation of the anaphase promoting complex by phosphorylating and triggering SCFbetaTrCP-dependent destruction of the APC Inhibitor Emi1. *Mol Biol Cell* **15**:5623-5634.
5. **Atir-Lande A, Gildor T, Kornitzer D.** 2005. Role for the SCFCDC4 ubiquitin ligase in *Candida albicans* morphogenesis. *Mol Biol Cell* **16**:2772-2785.
6. **Jorgensen P, Nishikawa JL, Bretkreutz BJ, Tyers M.** 2002. Systematic identification of pathways that couple cell growth and division in yeast. *Science* **297**:395-400.
7. **Sigl R, Wandke C, Rauch V, Kirk J, Hunt T, Geley S.** 2009. Loss of the mammalian APC/C activator *FZR1* shortens G1 and lengthens S phase but has little effect on exit from mitosis. *J Cell Sci* **122**:4208-4217.
8. **Reimann JD, Freed E, Hsu JY, Kramer ER, Peters JM, Jackson PK.** 2001. Emi1 is a mitotic regulator that interacts with Cdc20 and inhibits the anaphase promoting complex. *Cell* **105**:645-655.
9. **Moshe Y, Boulaire J, Pagano M, Hershko A.** 2004. Role of Polo-like kinase in the degradation of early mitotic inhibitor 1, a regulator of the anaphase promoting complex/cyclosome. *Proc Natl Acad Sci U S A* **101**:7937-7942.
10. **Lara-Gonzalez P, Westhorpe FG, Taylor SS.** 2012. The spindle assembly checkpoint. *Curr Biol* **22**:R966-980.
11. **van Vugt MA, Medema RH.** 2005. Getting in and out of mitosis with Polo-like kinase-1. *Oncogene* **24**:2844-2859.
12. **Liang F, Jin F, Liu H, Wang Y.** 2009. The molecular function of the yeast polo-like kinase Cdc5 in Cdc14 release during early anaphase. *Mol Biol Cell* **20**:3671-3679.
13. **Visintin R, Stegmeier F, Amon A.** 2003. The role of the polo kinase Cdc5 in controlling Cdc14 localization. *Mol Biol Cell* **14**:4486-4498.
14. **Berman J.** 2006. Morphogenesis and cell cycle progression in *Candida albicans*. *Curr Opin Microbiol* **9**:595-601.
15. **Gale CA, Berman J.** 2012. Cell Cycle and Growth Control in *Candida* Species, *Candida* and Candidiasis, Second Edition doi:doi:10.1128/9781555817176.ch8. American Society of Microbiology.
16. **Shapiro RS, Sellam A, Tebbji F, Whiteway M, Nantel A, Cowen LE.** 2012. Pho85, Pcl1, and Hms1 signaling governs *Candida albicans* morphogenesis induced by high temperature or Hsp90 compromise. *Curr Biol* **22**:461-470.

17. **Andaluz E, Ciudad T, Gomez-Raja J, Calderone R, Larriba G.** 2006. Rad52 depletion in *Candida albicans* triggers both the DNA-damage checkpoint and filamentation accompanied by but independent of expression of hypha-specific genes. *Mol Microbiol* **59**:1452-1472.
18. **Shapiro RS, Uppuluri P, Zaas AK, Collins C, Senn H, Perfect JR, Heitman J, Cowen LE.** 2009. Hsp90 orchestrates temperature-dependent *Candida albicans* morphogenesis via Ras1-PKA signaling. *Curr Biol* **19**:621-629.
19. **Umeyama T, Kaneko A, Niimi M, Uehara Y.** 2006. Repression of *CDC28* reduces the expression of the morphology-related transcription factors, Efg1p, Nrg1p, Rbf1p, Rim101p, Fkh2p and Tec1p and induces cell elongation in *Candida albicans*. *Yeast* **23**:537-552.
20. **Bachewich C, Nantel A, Whiteway M.** 2005. Cell cycle arrest during S or M phase generates polarized growth via distinct signals in *Candida albicans*. *Mol Microbiol* **57**:942-959.
21. **Zou H, Fang HM, Zhu Y, Wang Y.** 2010. *Candida albicans* Cyr1, Cap1 and G-actin form a sensor/effector apparatus for activating cAMP synthesis in hyphal growth. *Mol Microbiol* **75**:579-591.
22. **Wolyniak MJ, Sundstrom P.** 2007. Role of actin cytoskeletal dynamics in activation of the cyclic AMP pathway and *HWPI* gene expression in *Candida albicans*. *Eukaryot Cell* **6**:1824-1840.
23. **Pruyne D, Bretscher A.** 2000. Polarization of cell growth in yeast. I. Establishment and maintenance of polarity states. *J Cell Sci* **113 (Pt 3)**:365-375.
24. **Howell AS, Lew DJ.** 2012. Morphogenesis and the cell cycle. *Genetics* **190**:51-77.
25. **Crampin H, Finley K, Gerami-Nejad M, Court H, Gale C, Berman J, Sudbery P.** 2005. *Candida albicans* hyphae have a Spitzenkorper that is distinct from the polarisome found in yeast and pseudohyphae. *J Cell Sci* **118**:2935-2947.
26. **Sudbery P, Gow N, Berman J.** 2004. The distinct morphogenic states of *Candida albicans*. *Trends Microbiol* **12**:317-324.
27. **Atkins BD, Yoshida S, Saito K, Wu CF, Lew DJ, Pellman D.** 2013. Inhibition of Cdc42 during mitotic exit is required for cytokinesis. *J Cell Biol* **202**:231-240.
28. **Yoshida S, Kono K, Lowery DM, Bartolini S, Yaffe MB, Ohya Y, Pellman D.** 2006. Polo-like kinase Cdc5 controls the local activation of Rho1 to promote cytokinesis. *Science* **313**:108-111.
29. **Bai C, Ramanan N, Wang YM, Wang Y.** 2002. Spindle assembly checkpoint component CaMad2p is indispensable for *Candida albicans* survival and virulence in mice. *Mol Microbiol* **45**:31-44.
30. **Gale CA, Leonard MD, Finley KR, Christensen L, McClellan M, Abbey D, Kurischko C, Bensen E, Tzafrir I, Kauffman S, Becker J, Berman J.** 2009. *SLA2* mutations cause *SWE1*-mediated cell cycle phenotypes in *Candida albicans* and *Saccharomyces cerevisiae*. *Microbiology* **155**:3847-3859.
31. **Elia AE, Cantley LC, Yaffe MB.** 2003. Proteomic screen finds pSer/pThr-binding domain localizing Plk1 to mitotic substrates. *Science* **299**:1228-1231.
32. **Nakajima H, Toyoshima-Morimoto F, Taniguchi E, Nishida E.** 2003. Identification of a consensus motif for Plk (Polo-like kinase) phosphorylation reveals Myt1 as a Plk1 substrate. *J Biol Chem* **278**:25277-25280.
33. **Lee KS, Park JE, Asano S, Park CJ.** 2005. Yeast polo-like kinases: functionally conserved multitask mitotic regulators. *Oncogene* **24**:217-229.

34. **Xie S, Xie B, Lee MY, Dai W.** 2005. Regulation of cell cycle checkpoints by polo-like kinases. *Oncogene* **24**:277-286.
35. **McAllaster MR, Ikeda KN, Lozano-Nunez A, Anrather D, Unterwurzacher V, Gossenreiter T, Perry JA, Crickley R, Mercadante CJ, Vaughan S, de Graffenried CL.** 2015. Proteomic identification of novel cytoskeletal proteins associated with TbPLK, an essential regulator of cell morphogenesis in *Trypanosoma brucei*. *Mol Biol Cell* **26**:3013-3029.
36. **Hu H, Zhou Q, Li Z.** 2015. A Novel Basal Body Protein That Is a Polo-like Kinase Substrate Is Required for Basal Body Segregation and Flagellum Adhesion in *Trypanosoma brucei*. *J Biol Chem* **290**:25012-25022.
37. **Pierce CG, Chaturvedi AK, Lazzell AL, Powell AT, Saville SP, McHardy SF, Lopez-Ribot JL.** 2015. A Novel Small Molecule Inhibitor of Biofilm Formation, Filamentation and Virulence with Low Potential for the Development of Resistance. *NPJ Biofilms Microbiomes* **1**. pii: 15012.
38. **Siles SA, Srinivasan A, Pierce CG, Lopez-Ribot JL, Ramasubramanian AK.** 2013. High-throughput screening of a collection of known pharmacologically active small compounds for identification of *Candida albicans* biofilm inhibitors. *Antimicrob Agents Chemother* **57**:3681-3687.
39. **Mu R, Wang YB, Wu M, Yang Y, Song W, Li T, Zhang WN, Tan B, Li AL, Wang N, Xia Q, Gong WL, Wang CG, Zhou T, Guo N, Sang ZH, Li HY.** 2014. Depletion of pre-mRNA splicing factor Cdc5L inhibits mitotic progression and triggers mitotic catastrophe. *Cell Death Dis* **5**:e1151.
40. **Habara Y, Urushiyama S, Shibuya T, Ohshima Y, Tani T.** 2001. Mutation in the *prp12+* gene encoding a homolog of SAP130/SF3b130 causes differential inhibition of pre-mRNA splicing and arrest of cell-cycle progression in *Schizosaccharomyces pombe*. *RNA* **7**:671-681.
41. **Sundaramoorthy S, Vazquez-Novelle MD, Lekomtsev S, Howell M, Petronczki M.** 2014. Functional genomics identifies a requirement of pre-mRNA splicing factors for sister chromatid cohesion. *EMBO J* **33**:2623-2642.
42. **Bruno VM, Wang Z, Marjani SL, Euskirchen GM, Martin J, Sherlock G, Snyder M.** 2010. Comprehensive annotation of the transcriptome of the human fungal pathogen *Candida albicans* using RNA-seq. *Genome Res* **20**:1451-1458.
43. **Mitrovich QM, Tuch BB, Guthrie C, Johnson AD.** 2007. Computational and experimental approaches double the number of known introns in the pathogenic yeast *Candida albicans*. *Genome Res* **17**:492-502.
44. **Wan Y, Zheng X, Chen H, Guo Y, Jiang H, He X, Zhu X, Zheng Y.** 2015. Splicing function of mitotic regulators links R-loop-mediated DNA damage to tumor cell killing. *J Cell Biol* **209**:235-246.
45. **Cote P, Hogues H, Whiteway M.** 2009. Transcriptional analysis of the *Candida albicans* cell cycle. *Mol Biol Cell* **20**:3363-3373.
46. **Bensen ES, Clemente-Blanco A, Finley KR, Correa-Bordes J, Berman J.** 2005. The mitotic cyclins Clb2p and Clb4p affect morphogenesis in *Candida albicans*. *Mol Biol Cell* **16**:3387-3400.
47. **Chou H, Glory A, Bachewich C.** 2011. Orthologues of the anaphase-promoting complex/cyclosome coactivators Cdc20p and Cdh1p are important for mitotic progression and morphogenesis in *Candida albicans*. *Eukaryot Cell* **10**:696-709.

48. **Clemente-Blanco A, Gonzalez-Novo A, Machin F, Caballero-Lima D, Aragon L, Sanchez M, de Aldana CR, Jimenez J, Correa-Bordes J.** 2006. The Cdc14p phosphatase affects late cell-cycle events and morphogenesis in *Candida albicans*. *J Cell Sci* **119**:1130-1143.
49. **Gonzalez-Novo A, Labrador L, Pablo-Hernando ME, Correa-Bordes J, Sanchez M, Jimenez J, de Aldana CRV.** 2009. Dbf2 is essential for cytokinesis and correct mitotic spindle formation in *Candida albicans*. *Molecular Microbiology* **72**:1364-1378.